ICE-MARGINAL PROCESSES AND RETREAT DYNAMICS OF NORWEGIAN PLATEAU ICEFIELDS

PAUL WEBER

The thesis is submitted in partial fulfilment of the requirements for the award of the degree of Doctor of Philosophy of the University of Portsmouth.

October 2020

Portsmouth
Glaciology

Whilst registered as a candidate for the above degree, I have not been registered for any other research award. The results and conclusions embodied in this thesis are the work of the named candidate and have not been submitted for any other academic award.

Title page image: Oblique aerial photograph of the plateau icefields Langfjordjøkelen (Bártnatvuonjiehkki) and Øksfjordjøkelen (Ákšovuonjiehkki) (in the background) in the northernmost part of Arctic mainland Norway, taken between 1936 and 1939 by Widerøes Flyveselskap AS (Owner: Nasjonalbiblioteket).

A sharp crack and a low muttering roar told those of us who were familiar with the ways of ice that we were nearing the glacier, who was giving utterance to his just complaints against the tyranny of the summer sun.

—John F. Hardy, *The Jökuls glacier* (1862)

Abstract

A significant portion of Norwegian glaciers are plateau icefields. These are highly sensitive to changes in climate because of their top-heavy hypsometry. A small rise in the equilibrium line altitude may cause the ablation area to expand significantly, leading to rapid icefield recession. This behaviour deserves particular research attention in light of the current warming of the Earth's climate system. This doctoral thesis examines the response of the icefields Hardangerjøkulen in southern Norway, Svartisen just within the Arctic Circle, and Langfjordjøkelen in Arctic mainland Norway to climate warming since the Little Ice Age (LIA). These ice masses have been in retreat since they reached their maximum LIA positions between ~1750-1925. The glacial landform record of these icefields is used to reconstruct their maximum LIA extent. In addition, historical maps are used to reconstruct their ~1900 extent. These data sets are compared with data from available Norwegian glacier inventories of the present-day glacier extent, revealing substantial changes in icefield size. The greatest percentage decline occurred at Langfjordjøkelen in Arctic Norway, with an area reduction of 57 % between 1925 and 2018. Hardangerjøkulen in southern Norway lost 37 % of its original LIA area between 1750 and 2013, and the Vestre and Østre Svartisen icefields in northern Norway had lost 16 % and 23 % of their ~1900 areas by 2000, respectively. This research demonstrates how the LIA glacier extent can be employed as a valuable baseline to assess long-term glacier change.

Acknowledgements

First and foremost, I want to thank my brilliant main supervisors, Harold Lovell and Clare Boston, for guiding me so expertly through this project.

Thank you also to Liss Andreassen for welcoming me at NVE, introducing me to the beautiful historical glacier maps of Norway, and joining my supervision team.

My thanks also go to the NVE Glacier Group for sharing their knowledge on Norwegian glaciers, and particularly Miriam Jackson for her valuable advice along the way.

Martin Schaefer is thanked for providing his GIS expertise whenever needed.

To my fellow PhD comrades Cornelia 'Kim' van Diepen, Margarita Tsakiridou and Lauren Knight. Without your friendship, I would not have been able to complete this project.

Tusen takk til kjæresten min, Emil Kojedal, som har bistått med tålmodighet og kjærlighet gjennom hele prosessen.

Mein besonderer Dank gilt der grenzenlosen Unterstützung meiner Eltern, ohne die dieses Vorhaben nicht möglich gewesen wäre.

Contents

Chapter 1

Introduction

The current warming of the Earth's climate system is an indisputable fact (e.g. IPCC, 2014). Since the pre-industrial period (1850-1900), the global mean temperature has risen by 1.1 ± 0.1°C (WMO, 2020), nearly all of which is attributable to human activities (Allen et al., 2018; WMO, 2020). The rate of warming averaged 0.07°C per decade ($10a^{-1}$) in the period 1880-1980 and has more than doubled to 0.18°C $10a^{-1}$ since 1981 (NOAA National Centers for Environmental Information, 2020). The ten warmest years in the period 1880-2019 have all been recorded since 1998, and the five warmest years have all occurred since 2015 (NOAA National Centers for Environmental Information, 2020).

One of the most visible signs of climate warming is the dramatic decline of glaciers worldwide. Records of glacier front positions extending back to the late 1800s show that all monitored glaciers reached a historical minimum length in the early 21st century (Zemp et al., 2015). The global data coverage of glaciological and geodetic mass balance measurements recorded since the 1940s document the highest rates of mass loss on record in the period 2001-10 (glaciological and geodetic balances of -0.54 and -0.81 m water equivalent (w.e.) per year (a^{-1}), respectively) (Zemp et al., 2015). The glaciological mass balance can be compared to rates of surface mass loss of -0.40 m w.e. a^{-1} in the 1940s-60s, a reduced loss of -0.20 m w.e. a^{-1} in the 1970s-80s, and the beginning of an accelerated decrease in the 1990s of -0.47 m w.e. a^{-1} (Zemp et al., 2015). The latest IPCC *Special Report on the Ocean and Cryosphere in a Changing Climate* concluded that the rate of glacier mass loss in the period 2006-15 amounted to -123 ± 24 Gt a^{-1} for all glaciated mountain regions outside the Arctic (Hock et al., 2019), -143 ± 50 Gt a^{-1} for all Arctic glaciers (including the Greenland periphery), -278 ± 11 Gt a^{-1} for the Greenland Ice Sheet (GrIS), and -155 ± 19 Gt a^{-1} for all Antarctic ice masses combined (Meredith et al., 2019). Zemp et al. (2019) calculated a global cumulative mass loss of -9625 ± 7975 Gt in the period 1961-2016, equating to a sea-level contribution of 27 ± 22 mm. Glacier and ice sheet melting (with glaciers and ice caps being the largest sub-component) is currently the dominant contributor to sea-level rise (Oppenheimer et al., 2019). Glacier and ice cap decline (excluding GrIS and Antarctic ice masses) is projected to continue unabated over the course of the 21st century, further contributing to sea-level rise, with many small glaciers destined to disappear completely by the end of the century (Hock et al., 2019).

Of all glacier types, plateau icefields are particularly susceptible to climate warming because a large proportion of their surface area is concentrated in a comparatively narrow elevation band (cf. Furbish & Andrews, 1984; Oerlemans, 2012). Plateau icefields comprise a low-gradient source (accumulation) area on the plateau summit, which is drained by outlet

glaciers that typically extend radially into surrounding valleys. Therefore, if climate warming raises the equilibrium line altitude (ELA) to the height of the plateau summit, any further warming will cause the ablation area to expand significantly, whilst the accumulation area shrinks, leading to outlet glacier and overall icefield recession. This climate sensitivity has been modelled (as past reconstructions and future projections) and demonstrated by case studies for a number of Northern Hemisphere plateau icefields (e.g. Oerlemans, 1997; Nesje et al., 2008a; Jiskoot et al., 2009; Giesen & Oerlemans, 2010; Andreassen et al., 2012a; Åkesson et al., 2017; McGrath et al., 2017; Zekollari et al., 2017). For example, at the Clemenceau Icefield and Chaba Group icefield in the Canadian Rocky Mountains, Jiskoot et al. (2009) examined the effect of a hypothetical rise in ELA on the size of the accumulation area of glaciers with either top-heavy or bottom-heavy hypsometries (area-altitude distribution). An ELA increase of 100 m relative to two reference ELAs (one corresponding to an accumulation-area ratio (AAR) of 0.5 and the other to an AAR of 0.65) led to a reduction in accumulation area that was 2.6 and 2.1 times greater, respectively, at the top-heavy glaciers than at the bottom-heavy ice masses. This difference was even more pronounced for an ELA increase of 200 m (relative to the same reference ELAs), resulting in a reduction in accumulation area that was 3.3 and 2.6 times greater, respectively, at the top-heavy glaciers. In light of current climate warming, the sensitivity and response of plateau icefields to changes in climate deserve further research attention.

In Norway, much of the glacier ice is contained within plateau icefields (Andreassen et al., 2012b). These have undergone marked changes since the Little Ice Age (LIA), a period of relative cold conditions between ~1460 and ~1920 (Nesje et al., 2008b). Increased winter precipitation during the LIA caused most Norwegian glaciers and plateau icefields to expand significantly (Nesje et al., 2008b), reaching their maximum (Neoglacial) extent between the mid-18th and early 20th century (e.g. Grove, 2004). Following this advance, glaciers with an early LIA maximum experienced minor net retreat, punctuated by short-term readvances, that lasted until the end of the 19th century (Nesje et al., 2008a; Nussbaumer et al., 2011). In the 20th century, maritime glaciers had small-scale readvances in the 1900s and 1920s. This was followed by a period of pronounced recession of all glaciers in the middle of the century (Andreassen et al., 2005). In the 1990s, the outlet glaciers of many maritime icefields readvanced significantly in response to several preceding years of increased winter precipitation (Andreassen et al., 2005; Nesje et al., 2008a). The average rate of glacier retreat slowed from -16 m a^{-1} in the period 1960s-1982 to -2 m a^{-1} in the period 1982-2000 (Andreassen et al., 2020). Between 1947-85 and 1999-2006, Norwegian glaciers decreased in total area and average length by 326 km^2 (11 %) and 240 m, respectively (Winsvold et al., 2014). Since the beginning of the 21st century, virtually all Norwegian ice masses have been in rapid retreat because of climate warming, with an average retreat rate of -20 m a^{-1} (Andreassen et al., 2005,

2020). Investigating a subset of 137 Norwegian glaciers, including most of Norway's major plateau icefields, Andreassen et al. (2020) found a geodetic mass balance loss of -0.27 ± 0.05 m w.e. a^{-1} on average between ~1960 and ~2010.

In this doctoral thesis, the changes that have occurred in the plateau icefields of Norway since the LIA glacier maximum set the context for examining icefield evolution in response to changing climatic conditions. The research questions and knowledge gaps that this thesis aims to address are:

First, at many plateau icefields in Norway neither the geomorphological imprint of the LIA glacier maximum nor the patterns of recession since then have been fully recorded. However, a more detailed understanding of the landform record associated with plateau icefield recession is important for predicting the retreat dynamics of these ice masses under future climate change. This understanding will also be useful in reconstructions of the recessional dynamics of palaeo-icefields and their response to former changes in climate (e.g. McDougall, 2001; Benn & Ballantyne, 2005; Lukas & Bradwell, 2010; Finlayson et al., 2011; Boston et al., 2015).

Second, the spatial distribution of moraines, associated with the retreat of plateau icefields, is generally assumed to reflect climatic variations over time (e.g. Bickerton & Matthews, 1993). However, when examined in detail, the patterns of glacier recession derived from moraines may also reflect glacier response to local, non-climatic factors such as slope gradient or shading (Barr & Lovell, 2014; Boston & Lukas, 2019). Because the influence of these factors is still relatively underexplored, this may lead to difficulty in extracting a detailed climate signal from moraine spacing in palaeo-icefield reconstructions (cf. Lukas & Benn, 2006).

Third, only a few studies (e.g. Baumann et al., 2009; Stokes et al., 2018) have used landform evidence to produce digital GIS outlines of the LIA extent of Norwegian ice masses. However, these are needed to carry out quantitative glacier change assessments and to validate numerical icefield models.

Fourth, the limited availability of digital outlines of the historical glacier extent in Norway, including the LIA maximum, has also restricted the number of studies examining rates of glacier area and length change on a centennial timescale. Winsvold et al. (2014) have demonstrated the potential of historical maps to be an important source for defining glacier outlines to quantify long-term glacier change. However, historical maps have yet to be employed on a larger, regional scale. Long-term assessments of glacier change since the LIA (i.e. the pre-industrial era) are particularly important for placing the high rates of late-20th- and early-21st-century glacier decline in a broader temporal context.

Fig. 1-1. Distribution of glaciers (in dark blue) in Scandinavia and location of Norwegian ice masses mentioned in this chapter. The plateau icefields studied in this doctoral thesis are in italics. Ff: Folgefonna icefields (Søndre, Midtre and Nordre Folgefonna); ***H****: Hardangerjøkulen icefield*; JG: Jotunheimen glaciers; JB: Jostedalsbreen icefield; Å: Ålfotbreen; O: Okstindbreen; ***S****: Svartisen (Vestre and Østre Svartisen)* and Høgtuvbreen icefields; Fi: Frostisen (Ruostajiekŋa) icefield; L: Glaciers on the Lyngen Peninsula; ***LØ****: Langfjordjøkelen (Bártnatvuonjiehkki)* and Øksfjordjøkelen (Ákšovuonjiehkki) icefields. Glacier inventory data from RGI Consortium (2017). Topographic base map from ArcGIS Pro.

In light of the knowledge gaps outlined above, this doctoral thesis will:

(1) Map and assess the geomorphological evidence for the maximum LIA extent and subsequent recession stages of three Norwegian plateau icefields, where no systematic LIA mapping across the whole of each icefield has been carried out to date. The icefields were selected to provide sites covering a south-to-north transect across mainland Norway (Fig. 1-1; see Section 1.5 below for details on site selection).

(2) Use the mapped landform evidence to examine the extent to which the recession dynamics of each icefield's outlet glaciers and the formation of ice-marginal moraines are influenced by topographic factors.

(3) Produce full reconstructions of each icefield's maximum LIA extent in the form of digital GIS outlines, including an assessment of confidence.

(4) Compile additional digital outlines of the selected icefields tied to known time periods, with a major focus on digitising historical glacier outlines from old maps. Icefield extents for different time periods throughout the 20th and 21st century will also be derived from aerial photographs, satellite images, and contemporary mapping. Comparing these outlines will allow icefield area and length change to be quantified on a centennial timescale.

1.1. Number and geographical distribution of Norwegian glaciers

The latest complete inventory of Norwegian glaciers, compiled by Andreassen et al. (2012b) from 1999 to 2006 Landsat satellite imagery, lists a total of 2,534 ice bodies with a combined area of 2,692 ± 81 km^2. Just over half of this area is contained within the eleven largest ice masses in Norway, of which Jostedalsbreen is by far the largest with a size of ~474 km^2 (Andreassen et al., 2012b). Altogether, Norwegian glaciers cover ~0.8 % of mainland Norway's land area. They typically take the form of plateau icefields and small mountain glaciers, including cirque and valley glaciers (Andreassen et al., 2012b). Many ice masses, particularly icefields, can be subdivided into discrete glacier units along drainage (ice flow) divides. Andreassen et al. (2012b) defined 3,143 glacier units in total, with an average size of 0.86 km^2. The majority of these units (73 %; n = 2,284) are smaller than 0.5 km^2 (Andreassen et al., 2012b).

The glaciers of mainland Norway reside in the Scandinavian Mountains, a ~1,700 km-long and up to ~2,500 m-high mountain range that runs along the entire length of the Scandinavian Peninsula from southwestern Norway to the northernmost part of the peninsula in Arctic Norway. About half of all glaciers (n = 1,252), and glacier units (n = 1,575), lie in southern Norway between 59°44′ and 62°54′ N latitude, whilst the other half (1,282 glaciers; 1,568 units) is spread over northern Norway between ~65°9′ and ~70°27′ N latitude (Fig. 1-1).

However, southern Norwegian glaciers account for 57 % (1,523 km^2) of the total glacier area (northern Norway: 1,169 km^2) (Andreassen et al., 2012b). There also is a marked difference in the area-altitude distribution between southern and northern Norwegian glaciers (Fig. 1-2). Whilst a major portion of the glacier area in the south is situated at altitudes between 1,400 and 1,600 m a.s.l., the glaciers in the north can generally be found at lower altitudes, with the bulk of the glacier area located between 1,000 and 1,300 m a.s.l. (Andreassen et al., 2012b). Of all Norwegian (and Scandinavian) ice masses, the glaciers in Jotunheimen (Fig. 1-1), southern Norway, are located furthest inland (~190 km). The favoured slope aspect of small glaciers in Scandinavia is the northeast (Evans, 2006), reflecting the prevailing climatic conditions outlined in Section 1.2.

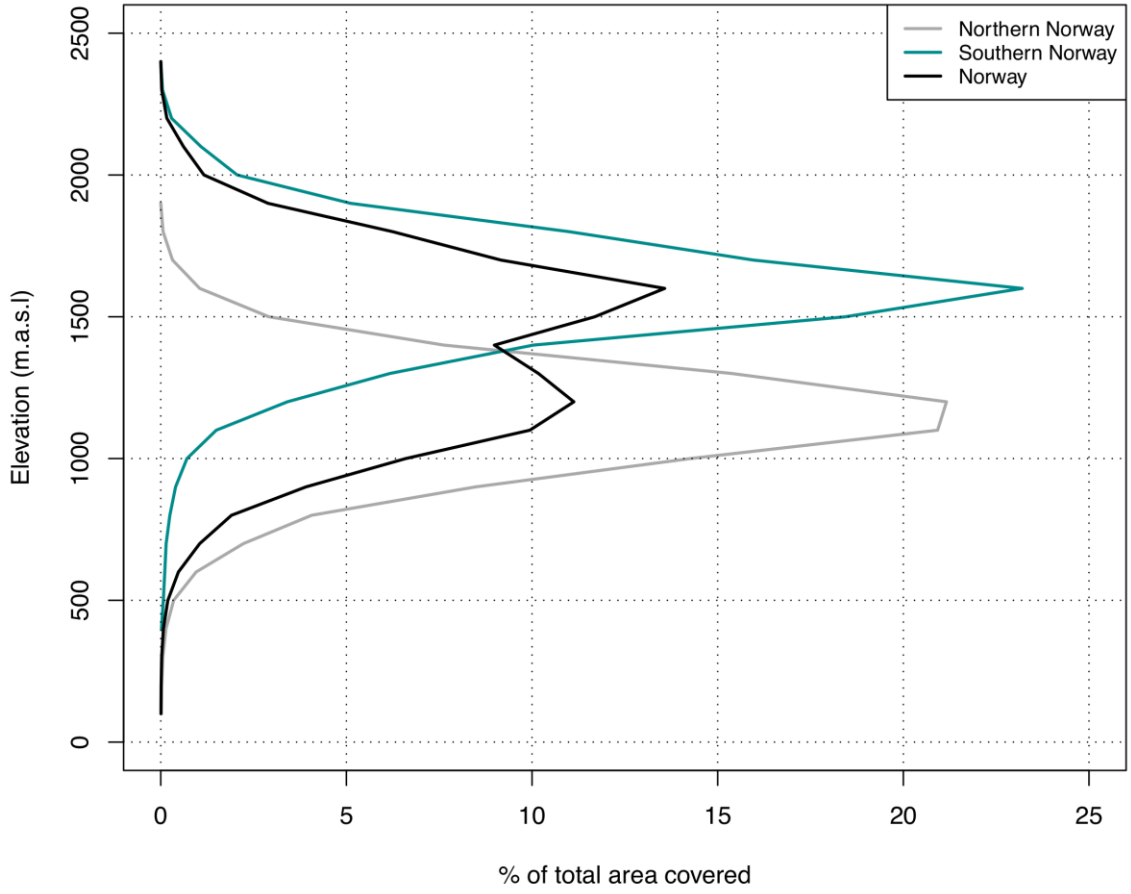

Fig. 1-2. Bimodal area-altitude distribution (hypsometry) of Norwegian glaciers showing a clear difference in the altitudinal range between the glacier area in southern and northern Norway. Taken from Andreassen et al. (2012b).

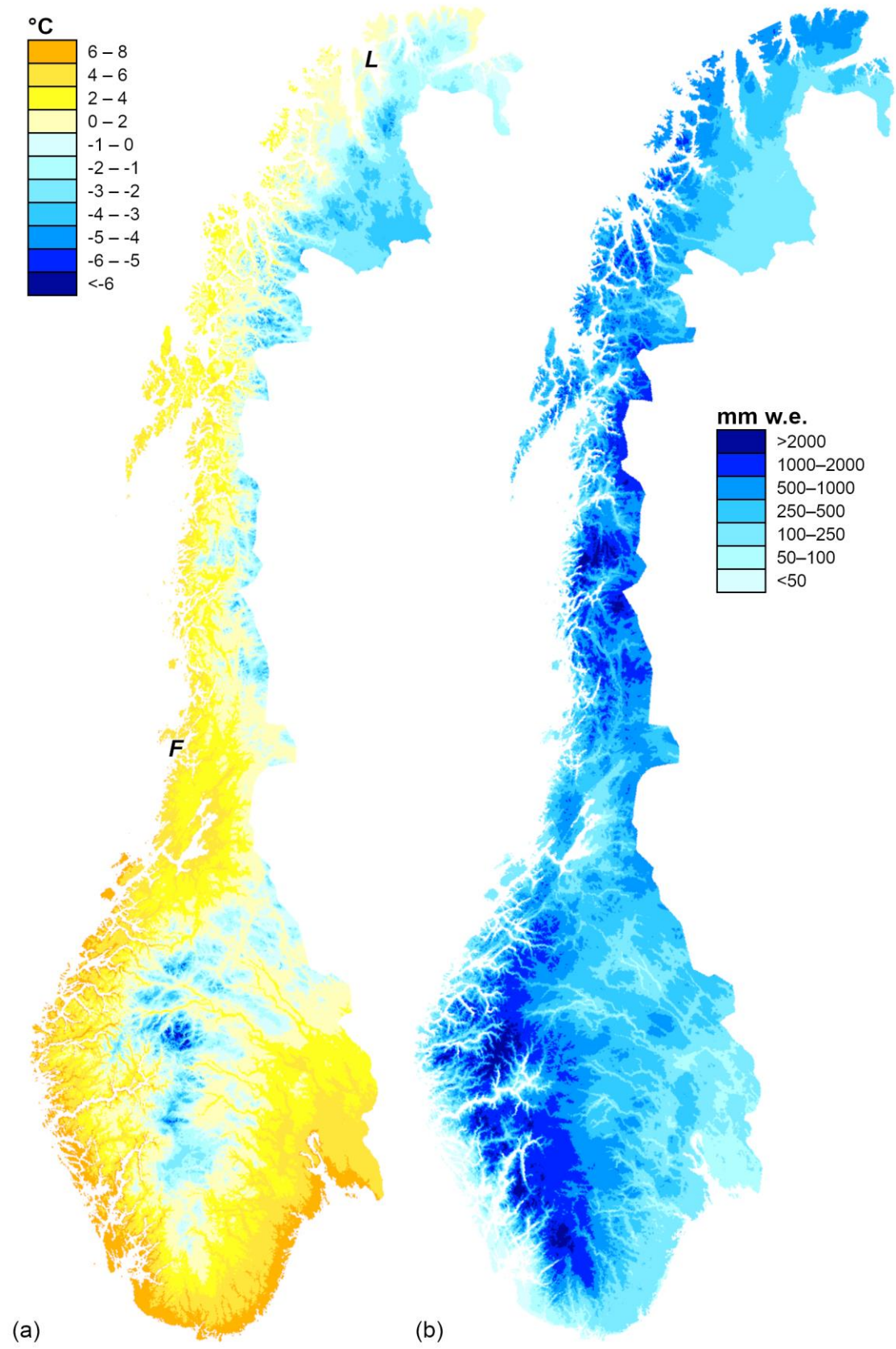

Fig. 1-3. (a) Average annual air temperature (in °C) across Norway in the normal period 1971-2000. Fjords: F: Folda; L: Laksefjorden (Lágesvuotna). (b) Average annual maximum amount in snowfall (in mm water equivalent) across Norway in the normal period 1971-2000. Acquired from http://www.senorge.no/.

1.2. Climatic context

The state of a glacier and whether it will grow or shrink depends primarily on two climatic parameters: (summer) air temperature, leading to mass loss, and solid (winter) precipitation, leading to mass gain. Norway lies in the west-wind belt and receives mild, moist air masses from the Atlantic Ocean, resulting in a maritime climate with heavy precipitation and relatively small intra-annual temperature variations (10-15°C) in coastal areas (Hanssen-Bauer et al., 2015). Further inland, in the lee of the Scandinavian Mountains, the climate becomes drier and more continental, with comparatively large intra-annual fluctuations in temperature (20-30°C) (Hanssen-Bauer et al., 2015).

The annual temperature in Norway averaged 1.3°C in the period 1971-2000, but can vary greatly depending on both altitude and latitude (Fig. 1-3a) (Hanssen-Bauer et al., 2015). Annual temperatures are lowest in the highest mountain areas, reaching less than -4°C. The average summer (June to August) temperature in the maritime coastal areas of southern and central Norway ranges from 12 to 14°C, and may exceed 10°C in some parts of the inner fjords and valleys of northern Norway (Hanssen-Bauer et al., 2015). Average summertime temperatures in the high mountain areas typically vary around 2 to 4°C. In the period 1900-2014, mean annual temperatures rose by 0.09°C $10a^{-1}$, with a distinct warming of +0.32°C $10a^{-1}$ between 1900 and 1938 (the Early Twentieth Century Warming episode; cf. Hanssen-Bauer, 2005; Hegerl et al., 2018), a period of cooling (-0.04°C $10a^{-1}$) between 1938 and 1976, and a more extreme warming of +0.50°C $10a^{-1}$ between 1976 and 2014 (Hanssen-Bauer et al., 2015). Warming since 1900 has been greatest (0.11°C $10a^{-1}$) in the maritime areas in the north of Norway between the Folda fjord (~64°38′ N latitude) and Laksefjorden (Lágesvuotna) (~70°40′ N latitude) (see Fig. 1-3a for location). Warming has also varied seasonally, having been greatest during spring (0.13°C $10a^{-1}$) (Hanssen-Bauer et al., 2015).

The mean annual precipitation in Norway was approximately 1600 mm in the period 1971-2000, ranging from well above 2500 mm along the coast (typical mean values in the west of southern Norway are as high as 3500-4000 mm, and exceed 5000 mm in coastal mountain areas at the westernmost glaciers) to less than 500 mm in the most continental parts of inner Norway (Hanssen-Bauer et al., 2015). This spatial pattern is also reflected in the maximum annual snowfall amount (Fig. 1-3b), reaching values in excess of 2000 mm w.e. in coastal mountain areas. Between 1900 and 2014, annual precipitation across Norway increased by more than 18 % (Hanssen-Bauer et al., 2015). In southern Norway, there was also a positive trend in snowfall (as measured in snow water equivalent) at elevations above 850 m a.s.l. between 1931 and 2009 (Skaugen et al., 2012).

Weather and climate conditions in Norway, especially in winter, are strongly influenced by atmospheric pressure patterns over the mid-to-high latitudes of the Northern Hemisphere,

namely the hemisphere-wide Arctic Oscillation (AO) and its regional-scale subset, the North Atlantic Oscillation (NAO) (NSIDC, n.d.; Dahlman, 2009a, b; Lindsey, 2011; Kennedy & Lindsey, 2014). When air pressure is lower than average over the Arctic (NAO: over Iceland) and higher than average over the mid-latitudes (NAO: over the Azores; i.e. a stronger-than-average Icelandic Low and Azores High) (positive mode of the AO/NAO), the jet stream shifts to the north of its average position, steering the storms that follow it on a more northerly track too. This results in increased storminess and precipitation over northern Europe, along with warmer-than-average temperatures brought by mild air masses from lower latitudes. When conditions are reversed, i.e. above-average air pressure over the Arctic/Iceland and below-average air pressure over the mid-latitudes/Azores (negative phase of the AO/NAO), the jet stream is located further south. Northern Europe experiences relatively dry and cold conditions, as the Atlantic jet stream and weaker ocean storms bring moist air masses into the Mediterranean (NSIDC, n.d.).

1.3. Surface mass balance of Norwegian glaciers

Glacier mass gain (accumulation) and mass loss (ablation) across the glacier surface can be quantified together in the glacier mass balance. There are currently ten Norwegian glaciers with active, long-term mass balance programmes (Fig. 1-4) (Kjøllmoen et al., 2019). The longest running monitoring programme is that at Storbreen (Storbrean), Jotunheimen, where the first measurements were carried out in 1949. To date, these measurements have produced a continuous, 70-year record of annually resolved surface mass balance observations (NVE, 2019). In the early 1960s (1962/63), continuous mass balance measurements started at the southern Norwegian glaciers Ålfotbreen (its northern glacier unit), Rembesdalskåka (an outlet glacier of Hardangerjøkulen), Nigardsbreen (outlet of Jostedalsbreen), Gråsubreen, and Hellstugubreen. This was followed in the late 1980s (1986/88) by the addition of Hansebreen (a northeastern glacier unit of Ålfotbreen) and Austdalsbreen (outlet of Jostedalsbreen) (NVE, 2019). Together, these glaciers represent an east-to-west transect from the continental Jotunheimen glaciers (Storbreen, Hellstugubreen, Gråsubreen) to Ålfotbreen (with Hansebreen), one of the most westerly and maritime ice masses in Norway (Kjøllmoen et al., 2019). By contrast, there are only two active, long-term mass balance programmes in northern Norway, where continuous monitoring commenced in 1970 at Engabreen (outlet of Vestre Svartisen) and in 1989 at Langfjordjøkelen (Bártnatvuonjiehkki) (only modelled values available for 1994/95; Andreassen et al., 2012a) (NVE, 2019). The mass balance series of all ten glaciers mentioned above have been homogenised (and calibrated where necessary) by Andreassen et al. (2016).

In the period prior to the late 1980s, the continental Jotunheimen glaciers (Storbreen, Hellstugubreen, Gråsubreen) experienced a gradual decline in cumulative mass balance to between -8.5 and -11.7 m w.e., whilst Rembesdalskåka was approximately in balance, and the maritime glaciers Nigardsbreen, Ålfotbreen and Engabreen recorded positive cumulative balances (highest cumulative value: 5.3 m w.e. at Ålfotbreen in 1987) (Fig. 1-4) (NVE, 2019). Heavy-snow winters in the late 1980s and early 1990s resulted in mass balance gains at all ice masses but Langfjordjøkelen in the 1990s (Fig. 1-4) (Andreassen et al., 2005; Nesje et al., 2008a). This volume increase was particularly pronounced at the maritime glaciers, with a peak in cumulative balance of 13.7 and 7.0 m w.e. in 1995 at Ålfotbreen and Rembesdalskåka, respectively, and a double peak of 8.4 and 8.7 m w.e. in 1995 and 2000, respectively, at Nigardsbreen (NVE, 2019). By contrast, there was only a small volume increase of 1.3 to 3.3 m w.e. at the continental Jotunheimen glaciers (NVE, 2019). The mean annual gain in mass balance of all ten glaciers was 0.24 m w.e. a^{-1} between 1989 and 2000 (Andreassen et al., 2020). Since the beginning of the 21st century, the cumulative balance of all glaciers has been in decline (Fig. 1-4). The greatest volume loss occurred at Hansebreen, which decreased by 28.0 m w.e. between 2000 and 2019, followed by Langfjordjøkelen with a decrease of 22.4 m w.e. in the same period (NVE, 2019). The three Jotunheimen glaciers had lost between 13.9 and 16.3 m w.e. by autumn 2018 (NVE, 2019). Nigardsbreen is the only glacier still maintaining a positive cumulative balance (5.1 m w.e. in autumn 2019), whilst Engabreen's cumulative balance had shrunk to 0.0 m w.e. in autumn 2019 (NVE, 2019). The mean annual change in mass balance of all glaciers was -0.83 m w.e. a^{-1} in the period 2001-18 (Andreassen et al., 2020). Overall, Langfjordjøkelen in northernmost Norway shows the greatest total decline in cumulative balance of all ten mass balance series, amounting to -27.9 m w.e. over the measurement period 1989-2019 (NVE, 2019). Large total mass balance losses in excess of -20 m w.e. also occurred at the three Jotunheimen glaciers (-23.9 to -26.3 m w.e. by 2018) and Hansebreen (-25.1 m w.e. by 2019) (NVE, 2019).

There is a positive correlation between the winter (Bw) and annual (Ba) balance of Norwegian glaciers and the NAO and/or AO (Nesje et al., 2000; Rasmussen, 2007; Marzeion & Nesje, 2012; Andreassen et al., 2020). A strongly positive wintertime NAO/AO phase is associated with heavy winter accumulation and positive balance years, most prominently represented by the period of increased winter precipitation and glacier readvances in the late-1980s/1990s (e.g. Nesje et al., 2000). The five maritime glaciers in southern Norway with available long-term balance series correlate strongly with both the NAO and AO (Rasmussen, 2007; Andreassen et al., 2020). Here, the mean correlation coefficient between the 1989-2018 winter balance Bw and both the December to March (Dec-Mar) NAO and AO is 0.80, whilst the correlation coefficient between the 1989-2018 annual balance Ba and $NAO_{Dec\text{-}Mar}$/$AO_{Dec\text{-}Mar}$ averages 0.75 and 0.74, respectively (based on data provided by Andreassen et al., 2020). This

relationship is weaker at the three continental Jotunheimen glaciers, where $Bw/NAO_{Dec-Mar}$ and $Bw/AO_{Dec-Mar}$ is 0.68 and 0.62 on average, respectively; and $Ba/NAO_{Dec-Mar}$ and $Ba/AO_{Dec-Mar}$ is 0.55 and 0.57 on average, respectively (based on data provided by Andreassen et al., 2020). By contrast, Engabreen and Langfjordjøkelen in northern Norway are better correlated with the AO, with $Bw/AO_{Dec-Mar}$ of 0.51 comparing to $Bw/NAO_{Dec-Mar}$ of 0.33; and $Ba/AO_{Dec-Mar}$ of 0.62 comparing to $Ba/NAO_{Dec-Mar}$ of 0.51 (based on data provided by Andreassen et al., 2020).

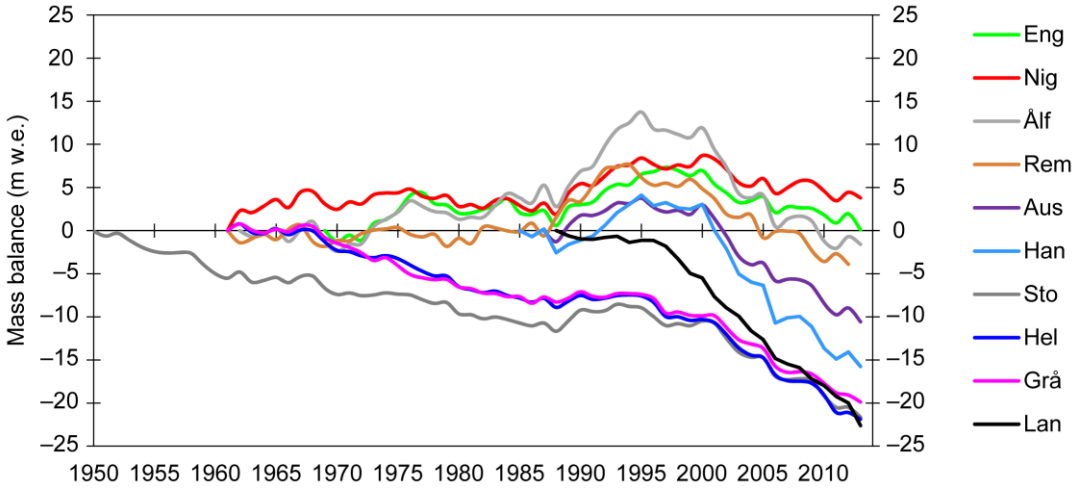

Fig 1-4. Cumulative mass balance of the ten Norwegian glaciers with available long-term observations up to and including data for 2013. Mass balance series are homogenised, and calibrated where necessary; see Andreassen et al. (2016) for details. Taken from Andreassen et al. (2016).

1.4. Norwegian glacier change since the LIA

1.4.1. Timing of the maximum LIA glacier extent

The timing of the maximum LIA glacier extent varies spatially across Norway, and even across outlet glaciers of the same ice mass. In this section, the existing published data is summarised, proceeding from south to north across Norway.

At the Søndre Folgefonna icefield, historical evidence compiled by Nussbaumer et al. (2011) shows that the maximum LIA extent of the outlet glaciers Bondhusbrea and Buarbreen occurred in the late 19th century. The icefield's western outlet Bondhusbrea reached its maximum LIA position in 1875, followed by a second advance in 1889/90 that ended close to the first LIA limit (see also Tvede, 1973). The eastern outlet Buarbreen advanced to its maximum LIA position in 1878/79, producing a terminal moraine, and remained at this position until 1892/93. By contrast, the south-southeastern outlet Blomstølsskardbreen (informal name)

experienced its maximum LIA extent in the 1930s (Tvede, 1973). At Nordre Folgefonna, lichenometric dating of ice-marginal moraines along the north-northwestern glacier flank (area to the south of the Dravladalsvatnet lake) by Bakke et al. (2005a, b) indicates LIA glacier advances in ~1750, ~1870 and ~1930.

Approximately 60 km to the northeast at the Hardangerjøkulen icefield, Andersen & Sollid (1971) lichenometrically dated the maximum LIA position of the northeastern outlets Midtdalsbreen and Blåisen to ~1750.

In Jotunheimen, Storbreen stood approximately at its maximum LIA position in the late 18th century (~1790 by inference), according to a historical eyewitness account recorded by Øyen (1893). Matthews (2005) lichenometrically dated ice-marginal moraine sequences on the forelands of 16 Jotunheimen glaciers, including Storbreen. The dates obtained from the outermost (presumed LIA) moraines range from 1699 to 1790 (discarding dates from two glaciers) (with a calculated mean of 1753).

At the Jostedalsbreen icefield, a wealth of historical evidence documents both the period of LIA glacier advance (1680s to 1743-50) and the subsequent recession (Grove, 2004 and historical sources cited therein; Nussbaumer et al., 2011 and historical sources cited therein). Reliable written sources pinpoint the maximum LIA extent of the eastern outlet Nigardsbreen in the Mjølverdalen valley to 1748. In the neighbouring valley to the south, Krundalen, the LIA advance of the outlet Bergsetbreen (and Tuftebreen) was reported to have culminated slightly earlier in 1743. An early- to mid-18th-century LIA glacier maximum has been presumed for Bøyabreen in the far south of the icefield (Nussbaumer et al., 2011 and historical sources cited therein). The western outlet Brenndalsbreen had a mid-18th-century LIA maximum (Grove, 2004 and historical sources cited therein; Nussbaumer et al., 2011 and historical sources cited therein). The available historical evidence suggests relative synchronicity in the timing of the maximum LIA extent across Jostedalsbreen (cf. Grove, 2004). Additional, lichenometric LIA dates from seven outlet glacier forelands have been collected by Bickerton & Matthews (1993). On methodological grounds, the authors judge maximum LIA dates of ~1750 at the western outlet Bødalsbreen, ~1705 at Fåbergstølsbreen and ~1863 at Stigaholtbreen (both eastern outlets) to be sound, but discarded the LIA dates obtained from the eastern outlets Austerdalsbreen, Bergsetbreen, Tuftebreen and Lodalsbreen. In particular, the Bergsetbreen and Lodalsbreen dates are inconsistent with available historical evidence (Bickerton & Matthews, 1993 and historical sources cited therein; Grove, 2004 and historical sources cited therein; Nussbaumer et al., 2011 and historical sources cited therein).

Approximately 600 km to the northeast at the Okstindbreen icefield in northern Norway, Winkler (2003) carried out lichenometric dating at the major northern outlet glacier Austre Okstindbreen and at a presently ice-free cirque basin (today occupied by the

Mørkbekktjønna lake) abutting the icefield's western outlet Vestisen. This work suggests LIA dates of between 1713 and 1757 at Austre Okstindbreen and a LIA date of 1761 at the cirque.

In the Svartisen area, different lines of evidence point to a mid-18th-century LIA glacier maximum. Lichenometric dating at Høgtuvbreen by Jansen et al. (2016) produced a LIA date of 1773 ± 29 a. At Østre Svartisen's southern outlet glacier Austerdalsisen, Winkler (2003) lichenometrically dated the maximum LIA glacier extent to between 1718 and 1755. An 18th-century LIA glacier maximum of Austerdalsisen is supported by radiocarbon dating by Jansen et al. (2018), which yielded a calibrated maximum date of 1736-1805. Vestre Svartisen's western outlet glacier Engabreen destroyed a farm in the 1720s to advance to its mid-18th-century maximum LIA extent (Rekstad, 1892, 1893, 1900). At a small valley glacier below the Spidstinden massif immediately to the north of Østre Svartisen, Winkler (2003) also found a mid-18th-century LIA date of 1746 based on lichenometry.

On the Lyngen Peninsula in northern Norway, Ballantyne (1990) used lichenometry and dendrochronology along with historical evidence (see historical sources cited therein) to establish the timing of four distinct LIA advances at 21 ice masses. The most recent of these advances dates to 1910-20 at 15 glaciers, and to 1920-30 at five glaciers situated at higher altitudes (>550 m a.s.l.) (weighted average of the medians: 1918). At nine of these glaciers (all <1.9 km^2 in size at the time of the study), this early-20th-century advance represents the most extensive LIA glacier expansion. At the other eleven (larger) glaciers, the most extensive LIA advance occurred in the mid-18th century. Ballantyne (1990) also identified two intervening mid-19th-century LIA advances, one depositing moraines in 1865-80 at three of the studied glaciers and the other in 1825-45 at one glacier. Bakke et al. (2005c) obtained a lichenometric date of 1890-1928 from a moraine of presumed LIA age at one additional Lyngen glacier. To the east of the Lyngen (Ivguvuotna) fjord in the Rotsunddalen (Cohkolatvággi) valley, Leigh et al. (2020) lichenometrically dated the moraines of presumed LIA age at four glaciers to between 1814 ± 41 a and 1877 ± 34 a (with a calculated mean of 1846 ± 69 a).

In northernmost Norway, sparse historical evidence suggests that the outlet glaciers of the Øksfjordjøkelen (Ákšovuonjiehkki) icefield were at extended positions throughout the second half of the 19th century (Hoel & Werenskiold, 1962 and references therein; Whalley & Kjøllmoen, 2000 and references therein). At the neighbouring Langfjordjøkelen icefield, Wittmeier et al. (2015) dated the LIA glacier maximum to 1925 ± 20 a based on an analysis and age-depth modelling of lacustrine sediments from a chain of lakes downstream of the icefield.

1.4.2. Post-LIA glacier change assessed from ice-front position records

After the LIA glacier maximum, southern Norwegian glaciers entered a period of minor net retreat until the early 20th century, as shown by Nesje et al. (2008a) who examined length variations of selected glaciers at Folgefonna, Hardangerjøkulen, Jostedalsbreen and in Jotunheimen. Historical evidence from the Jostedalsbreen outlets Bøyabreen, Bergsetbreen and Nigardsbreen shows that this retreat was punctuated by small-scale glacier advances in the 19th century (Nussbaumer et al., 2011 and historical sources cited therein). In Nordland, the non-calving Svartisen glaciers had retreated only a short distance from their maximum LIA positions by the end of the 19th century (Theakstone, 1965 and references therein). The glaciers in the Okstindbreen and Frostisen areas also stood close to their LIA limits at the end of the 19th century after an advance in the latter part of the century (Hoel & Werenskiold, 1962 and references therein).

In 1899, systematic glacier front position measurements started in Norway (Andreassen et al., 2005; NVE, 2019). Both the total number of glaciers measured in any one year and the continuity of individual measurement series have varied through time. Over 40 Norwegian glaciers have more than 20 years of observations, and eleven glaciers have continuous or near-continuous measurement series since the beginning of the 20th century (1899-1905) (Andreassen et al., 2005; NVE, 2019).

These observations document an episode of frontal advance (up to ~180 m) in the 1900s and into the early 1910s at the measured outlet glaciers of Søndre Folgefonna, Jostedalsbreen (except for two outlets) and Vestre Svartisen as well as of the measured glaciers in the Okstindbreen and Frostisen areas. Another, slightly more extensive glacier advance (up to ~240 m; no data available for the Okstindbreen and Frostisen areas) occurred in the 1920s and into the early 1930s. No such advances were recorded in Jotunheimen, where a period of general net retreat was punctuated by a few individual years with small-scale (<10 m) frontal advance. In the mid-part of the 20th century, the measured outlet glaciers of the maritime icefields (now also including Hardangerjøkulen) retreated substantially (~0.3-~2.3 km) between the 1930s and the 1950s-70s, followed in general by minor net retreat until the 1980s. A distinct frontal readvance (up to ~280 m) of the maritime outlets occurred between the late 1980s/early 1990s and ~2000. The short response time of Jostedalsbreen's western outlet Briksdalsbreen (Nesje et al., 2008a) had already initiated a stepwise readvance in the early 1970s, which continued until the late 1990s and produced a net advance of 465 m (NVE, 2019). By contrast, 20th-century glacier change in continental Jotunheimen since ~1930 was characterised by a more or less steady retreat (~380-~850 m), although a period of reduced retreat or even frontal standstill can be observed between the 1970s/80s and the 1990s. Since the beginning of the 21st century, virtually all measured glaciers have entered a state of substantial frontal retreat (up to

~925 m by 2019). Of the eleven glaciers with available long-term measurements since 1899-1905, maritime outlet glaciers have experienced a total cumulative retreat of between ~0.7 and ~2.9 km, whilst glaciers in Jotunheimen have retreated between ~0.6 and ~1.2 km (NVE, 2019).

1.5. Study areas – A latitudinal transect

This thesis examines three Norwegian plateau icefields in detail: the Hardangerjøkulen icefield in southwestern Norway, the double icefield Vestre and Østre Svartisen in northern Norway just above the Arctic Circle, and the Langfjordjøkelen (Bártnatvuonjiehkki) icefield in the northernmost part of Arctic mainland Norway (Fig. 1-1). These icefields were chosen to form a latitudinal transect extending from southern to northernmost mainland Norway. This takes into account that (1) the bulk of the glacier area in northern Norway is located in a lower elevation band (1,000-1,300 m a.s.l.) than the area of southern Norwegian glaciers (1,400-1,600 m a.s.l.) (Andreassen et al., 2012b; see Section 1.1), and (2) climate warming since 1900 has been greater in the coastal areas of Arctic mainland Norway (0.11°C $10a^{-1}$) than in the rest of the Norwegian mainland (0.09°C $10a^{-1}$) (Hanssen-Bauer et al., 2015; see Section 1.2). All three icefields have long-term in situ data (both mass balance and glacier front position measurements) for individual outlets that can be compared to the observations and results of this thesis.

Hardangerjøkulen was selected as the ice mass representing southern Norway because previous modelling studies have demonstrated the icefield's climate sensitivity associated with its top-heavy geometry (Giesen & Oerlemans, 2010; Åkesson et al., 2017). This provides the opportunity to compare empirical reconstructions with modelled outputs. The relatively simple geometry of the (almost) circular icefield also allows interesting assessments of the relative response of individual outlet glaciers of Hardangerjøkulen to be made in the context of topographic factors. A secondary reason was that the icefield is easily accessible by train, minimising fieldwork costs and logistics considerably.

The reason for selecting Vestre and Østre Svartisen was that they are by far the largest and most prominent icefields in northern Norway, and their behaviour has regional-scale implications for hydropower supply (cf. NVE, n.d., 2015). Because of their importance for hydropower, Svartisen was examined as part of a wider study of the long-term evolution (since ~1899) of all ice masses in Nordland county (where this icefield is located).

The selection of Langfjordjøkelen for northernmost mainland Norway was based on its surface mass balance history, which shows the greatest cumulative balance loss of all monitored glaciers in Norway (Andreassen et al., 2012a; see Section 1.4), providing an interesting starting

point for comparing long-term icefield change since the LIA maximum to the changes observed at other Norwegian ice masses.

1.6. Thesis outline

This work is organised as a series of three scientific journal manuscripts, followed by a discussion that links the three papers and draws out the key findings of the thesis.

Chapter 2 (Paper I) presents the first icefield-wide assessment of the maximum LIA extent and subsequent recession of the Hardangerjøkulen icefield. A close version of this chapter is published in the journal *The Holocene* (Weber et al., 2019), available at https://doi.org/10.1177/0959683619865601. Previous studies have investigated only a limited number of individual outlet glaciers of the icefield. The presented LIA reconstruction of the entire icefield allows Hardangerjøkulen's recession from the LIA maximum in around ~1750 to present to be quantified as well as a relative chronology of the recession to be established. It is shown that ~41 km^2 (~37 %) of the icefield area was lost between the LIA and 2010, and that periods of moraine formation were asynchronous across the icefield, controlled by topography of individual outlet valleys. The results of this study can be used by glacier modellers to calibrate and validate model simulations of Hardangerjøkulen's evolution. The chapter is accompanied by a large-format, 1:20,000 scale map of the glacial geomorphology and surficial geology of the icefield, which can be found in the Appendix and online (https://journals.sagepub.com/doi/suppl/10.1177/0959683619865601). The map, along with the glacial geomorphological/geological descriptions in the chapter, can be used by other researchers as a basis to design and plan future field-based studies on the Holocene history of Hardangerjøkulen, e.g. lake core studies.

Chapter 3 (Paper II) extracts the ~1899 (covering the period 1882-1916) glacier extent in Nordland county, northern Norway, from historical maps. A close version of this chapter is published in the *Journal of Glaciology* (Weber et al., 2020a), available at https://doi.org/10.1017/jog.2020.3. A particular focus of the chapter is on assessing the accuracy of the map-derived glacier inventory data, which has not always been done thoroughly in previous glacier inventories from historical maps. To that end, the map-based 1899 glacier outlines were extensively validated against written descriptions and landscape photos produced during the original map surveys as well as against independent geomorphological evidence and old air photos. This allows a realistic picture of the uncertainties associated with the 1899 glacier area to be gained. The new data set reveals that substantial changes in the extent of Nordland's glaciers have occurred since the end of the 19th century, with a total reduction in glacier cover of 47 % (807 ± 137 km^2) between 1899 and 2000. The chapter demonstrates the

value of historical maps for extending existing inventories further back in time, improving understanding of 20th-century glacier change. The inventory can be used as a baseline data set for glacier change assessments in future studies.

The plateau icefield Langfjordjøkelen in the northernmost part of Arctic mainland Norway has experienced the most dramatic decline of all Norwegian ice masses in recent decades. **Chapter 4 (Paper III)** reconstructs the icefield's ~1925 maximum LIA extent from the glacial landform record. This reconstruction is employed in an assessment of centennial-scale icefield change in order to place Langfjordjøkelen's recent rapid decline in a long-term (~100-year) context. A revised version of this chapter is published in the journal *Polar Research* (Weber et al., 2020b), available at https://doi.org/10.33265/polar.v39.4304. The results of this work show that Langfjordjøkelen reduced in total area and average length by 57 % and 42 %, respectively, between the LIA and 2018. This is the most severe recession of any Norwegian ice mass with available and comparable long-term glacier change data.

References

Allen, MR, Dube, OP, Solecki, W, Aragón-Durand, F, Cramer, W, Humphreys, S, Kainuma, M, Kala, J, Mahowald, N, Mulugetta, Y, Perez, R, Wairiu, M & Zickfeld, K (2018): Framing and Context. In: Masson-Delmotte, V, Zhai, P, Pörtner, H-O, Roberts, D, Skea, J, Shukla, PR, Pirani, A, Moufouma-Okia, W, Péan, C, Pidcock, R, Connors, S, Matthews, JBR, Chen, Y, Zhou, X, Gomis, MI, Lonnoy, E, Maycock, T, Tignor, M & Waterfield, T (eds.): *Global Warming of 1.5°C. An IPCC Special Report on the impacts of global warming of 1.5°C above pre-industrial levels and related global greenhouse gas emission pathways, in the context of strengthening the global response to the threat of climate change, sustainable development, and efforts to eradicate poverty.* IPCC, Geneva, pp. 49–91.

Andersen, JL & Sollid, JL (1971): Glacial chronology and glacial geomorphology in the marginal zones of the glaciers, Midtdalsbreen and Nigardsbreen, south Norway. *Norsk Geografisk Tidsskrift - Norwegian Journal of Geography* 25, 1–38.

Andreassen, LM, Elvehøy, H, Kjøllmoen, B, Engeset, R & Haakensen, N (2005): Glacier mass-balance and length variation in Norway. *Annals of Glaciology* 42, 317–325.

Andreassen, LM, Kjøllmoen, B, Rasmussen, A, Melvold, K & Nordli, Ø (2012a): Langfjordjøkelen, a rapidly shrinking glacier in northern Norway. *Journal of Glaciology* 58, 581–593.

Andreassen, LM, Winsvold, SH, Paul, F & Hausberg, JE (2012b): *Inventory of Norwegian Glaciers*. NVE Rapport 38. Norwegian Water Resources and Energy Directorate (NVE), Oslo, pp. 236.

Andreassen, LM, Elvehøy, H, Kjøllmoen, B. & Engeset, RV (2016): Reanalysis of long-term series of glaciological and geodetic mass balance for 10 Norwegian glaciers. *The Cryosphere* 10, 535–552.

Andreassen, LM, Elvehøy, H, Kjøllmoen, B & Belart, J (2020): Glacier change in Norway since the 1960s – an overview of mass balance, area, length and surface elevation changes. *Journal of Glaciology* 66, 313–328.

Bakke, J, Dahl, SO, Nesje, A (2005a): Lateglacial and early Holocene palaeoclimatic reconstruction based on glacier fluctuations and equilibrium-line altitudes at northern Folgefonna, Hardanger, western Norway. *Journal of Quaternary Science* 20, 179–198.

Bakke, J, Lie, Ø, Nesje, A, Dahl, SO & Paasche, Ø (2005b): Utilizing physical sediment variability in glacier-fed lakes for continuous glacier reconstructions during the Holocene, northern Folgefonna, western Norway. *The Holocene* 15, 161–176.

Bakke, J, Dahl, SO, Paasche, Ø, Løvlie, R & Nesje, A (2005c): Glacier fluctuations, equilibrium-line altitudes and palaeoclimate in Lyngen, northern Norway, during the Lateglacial and Holocene. *The Holocene* 15, 518–540.

Ballantyne, CK (1990): The Holocene glacial history of Lyngshalvöya, northern Norway: chronology and climatic implications. *Boreas* 19, 93–117.

Barr, ID & Lovell, H (2014): A review of topographic controls on moraine distribution. *Geomorphology* 226, 44–64.

Baumann, S, Winkler, S & Andreassen, LM (2009): Mapping glaciers in Jotunheimen, South-Norway, during the "Little Ice Age" maximum. *The Cryosphere* 3, 231–243.

Benn, DI & Ballantyne, CK (2005): Palaeoclimatic reconstruction from Loch Lomond Readvance glaciers in the West Drumochter Hills, Scotland. *Journal of Quaternary Science* 20, 577–592.

Bickerton, RW & Matthews, JA (1993): 'Little ice age' variations of outlet glaciers from the Jostedalsbreen ice-cap, Southern Norway: A regional lichenometric-dating study of ice-marginal moraine sequences and their climatic significance. *Journal of Quaternary Science* 8, 45–66.

Boston, CM, Lukas, S & Carr, SJ (2015): A Younger Dryas plateau icefield in the Monadhliath, Scotland, and implications for regional palaeoclimate. *Quaternary Science Reviews* 108, 139–162.

Boston, CM & Lukas, S (2019): Topographic controls on plateau icefield recession: insights from the Younger Dryas Monadhliath Icefield, Scotland. *Journal of Quaternary Science* 34, 433–451.

Dahlman, L (2009a): *Climate Variability: Arctic Oscillation*. Retrieved from the NOAA Climate.gov website: https://www.climate.gov/news-features/understanding-climate/climate-variability-arctic-oscillation.

Dahlman, L (2009b): *Climate Variability: North Atlantic Oscillation*. Retrieved from the NOAA Climate.gov website: https://www.climate.gov/news-features/understanding-climate/climate-variability-arctic-oscillation.

Evans, IS (2006): Local aspect asymmetry of mountain glaciation: a global survey of consistency of favoured directions for glacier numbers and altitudes. *Geomorphology* 73, 166–184.

Finlayson, A, Golledge, N, Bradwell, T & Fabel, D (2011): Evolution of a Lateglacial mountain icecap in northern Scotland. *Boreas* 40, 536–554.

Furbish, D & Andrews, J (1984): The Use of Hypsometry to Indicate Long-Term Stability and Response of Valley Glaciers to Changes in Mass Transfer. *Journal of Glaciology* 30, 199–211.

Giesen, RH & Oerlemans, J (2010): Response of the ice cap Hardangerjøkulen in southern Norway to the 20th and 21st century climates. *The Cryosphere* 4, 191–213.

Grove, JM (2004): *The Little Ice Age: Ancient and Modern.* 2nd edition. Routledge Studies in Physical Geography and Environment. Routledge, London, New York, 760 pp.

Hanssen-Bauer, I (2005): *Regional temperature and precipitation series for Norway: analyses of time-series updated to 2004*. MET Report 15/2005. Meteorological Institute, Oslo, 34 pp.

Hanssen-Bauer, I, Førland, EJ, Haddeland, I, Hisdal, H, Mayer, S, Nesje, A, Nilsen, JEØ, Sandven, S, Sandø, AB, Sorteberg, A & Ådlandsvik, B (eds.) (2015): *Klima i Norge 2100*. NCCS report 2/2015. Miljødirektoratet, Oslo, 203 pp.

Hegerl, GC, Brönnimann, S, Schurer, A & Cowan, T (2018): The early 20th century warming: Anomalies, causes, and consequences. *WIREs Climate Change* 9, e522.

Hock, R, Rasul, G, Adler, C, Cáceres, B, Gruber, S, Hirabayashi, Y, Jackson, M, Kääb, A, Kang, S, Kutuzov, S, Milner, A, Molau, U, Morin, S, Orlove, B & Steltzer, H (2019): High Mountain Areas. In: Pörtner, H-O, Roberts, DC, Masson-Delmotte, V, Zhai, P, Tignor, M, Poloczanska, E, Mintenbeck, K, Alegría, A, Nicolai, M, Okem, A, Petzold, J, Rama, B & Weyer, NM (eds.): *IPCC Special Report on the Ocean and Cryosphere in a Changing Climate*. IPCC, Geneva, pp. 131–202.

Hoel, A & Werenskiold, W (1962): Glaciers and Snowfields in Norway. *Norsk Polarinstitutt skrifter* 114.

IPCC (2014): *Climate Change 2014: Synthesis Report. Contribution of Working Groups I, II and III to the Fifth Assessment Report of the Intergovernmental Panel on Climate*

Change [Core Writing Team, Pachauri, R. K. & Meyer, L. A. (eds.)]. IPCC, Geneva, 151 pp.

Jansen, HL, Simonsen, JR, Dahl, SO, Bakke, J & Nielsen, PR (2016): Holocene glacier and climate fluctuations of the maritime ice cap Høgtuvbreen, northern Norway. *The Holocene* 26, 736–755.

Jansen, HL, Dahl, SO & Nielsen, PR (2018): An inverse approach to the course of the 'Little Ice Age' glacier advance and the following deglaciation at Austerdalsisen, eastern Svartisen, northern Norway. *The Holocene* 28, 1041–1056.

Jiskoot, H, Curran, CJ, Tessler, DL & Shenton, L (2009): Changes in Clemenceau Icefield and Chaba Group glaciers, Canada, related to hypsometry, tributary detachment, length–slope and area–aspect relations. *Annals of Glaciology* 50, 133–143.

Kennedy, C & Lindsey, R (2014): *How is the polar vortex related to the Arctic Oscillation?* Retrieved from the NOAA Climate.gov website: https://www.climate.gov/news-features/event-tracker/how-polar-vortex-related-arctic-oscillation.

Kjøllmoen, B, Andreassen, LM, Elvehøy, H. & Jackson, M (2019): *Glaciological investigations in Norway 2018*. NVE Rapport 2019:46. Norwegian Water Resources and Energy Directorate (NVE), Oslo, 84 pp.

Leigh, JR, Stokes, CR, Evans, DJA, Carr, RJ & Andreassen, LM (2020): Timing of Little Ice Age maxima and subsequent glacier retreat in northern Troms and western Finnmark, northern Norway. *Arctic, Antarctic, and Alpine Research* 52, 281–311.

Lindsey, R (2011): *Long Distance Relationships: the Arctic and North Atlantic Oscillations*. Retrieved from the NOAA Climate.gov website: https://www.climate.gov/news-features/understanding-climate/long-distance-relationships-arctic-and-north-atlantic.

Lukas, S & Benn, DI (2006): Retreat dynamics of Younger Dryas glaciers in the far NW Scottish Highlands reconstructed from moraine sequences. *Scottish Geographical Journal* 122, 308–325.

Lukas, S & Bradwell, T (2010): Reconstruction of a Lateglacial (Younger Dryas) mountain ice field in Sutherland, northwestern Scotland, and its palaeoclimatic implications. *Journal of Quaternary Science* 25, 567–580.

Marzeion, B & Nesje, A (2012): Spatial patterns of North Atlantic Oscillation influence on mass balance variability of European glaciers. *The Cryosphere* 6, 661–673.

Matthews, JA (2005): 'Little Ice Age' glacier variations in Jotunheimen, southern Norway: A study in regionally controlled lichenometric dating of recessional moraines with implications for climate and lichen growth rates. *The Holocene* 15, 1–19.

McDougall, DA (2001): The geomorphological impact of Loch Lomond (Younger Dryas) Stadial plateau icefields in the central Lake District, northwest England. *Journal of Quaternary Science* 16, 531–543.

McGrath, D, Sass, L, O'Neel, S, Arendt, A & Kienholz, C (2017): Hypsometric control on glacier mass balance sensitivity in Alaska and northwest Canada. *Earth's Future* 5, 324–336.

Meredith, M, Sommerkorn, M, Cassotta, S, Derksen, C, Ekaykin, A, Hollowed, A, Kofinas, G, Mackintosh, A, Melbourne-Thomas, J, Muelbert, MMC, Ottersen, G, Pritchard, H & Schuur, EAG (2019): Polar Regions. In: Pörtner, H-O, Roberts, DC, Masson-Delmotte, V, Zhai, P, Tignor, M, Poloczanska, E, Mintenbeck, K, Alegría, A, Nicolai, M, Okem, A, Petzold, J, Rama, B & Weyer, NM (eds.): *IPCC Special Report on the Ocean and Cryosphere in a Changing Climate*. IPCC, Geneva, pp. 203–320.

Nesje, A, Lie, Ø & Dahl, SO (2000): Is the North Atlantic Oscillation reflected in Scandinavian glacier mass balance records? *Journal of Quaternary Science* 15, 587–601.

Nesje, A, Bakke, J, Dahl, SO, Lie, Ø & Matthews, JA (2008a): Norwegian mountain glaciers in the past, present and future. *Global and Planetary Change* 60, 10–27.

Nesje, A, Dahl, SO, Thun, T & Nordli, Ø (2008b): The 'Little Ice Age' glacial expansion in western Scandinavia: summer temperature or winter precipitation? *Climate Dynamics* 30, 789–801.

NOAA National Centers for Environmental Information (2020): *State of the Climate: Global Climate Report for Annual 2019*. Retrieved from https://www.ncdc.noaa.gov/sotc/global/201913.

NSIDC (n.d.): *Patterns in Arctic Weather and Climate*. Retrieved from the National Snow and Ice Data Center website: https://nsidc.org/cryosphere/arctic-meteorology/weather_climate_patterns.html.

Nussbaumer, SU, Nesje, A & Zumbühl, HJ (2011): Historical glacier fluctuations of Jostedalsbreen and Folgefonna (southern Norway) reassessed by new pictorial and written evidence. *The Holocene* 21, 455–471.

NVE (n.d.): *Vannkraftdatabase*. Retrieved from the Norwegian Water Resources and Energy Directorate (NVE) website: https://www.nve.no/energiforsyning/kraftproduksjon/vannkraft/vannkraftdatabase/.

NVE (2015): *Svartisen.* Retrieved from the Norwegian Water Resources and Energy Directorate (NVE) website: https://www.nve.no/vann-vassdrag-og-miljo/nves-utvalgte-kulturminner/kraftverk/svartisen/.

NVE (2019): *Climate indicator products*. Retrieved from the Norwegian Water Resources and Energy Directorate (NVE) website: http://glacier.nve.no/glacier/viewer/ci/en/.

Oerlemans, J (1997): A flowline model for Nigardsbreen, Norway: projection of future glacier length based on dynamic calibration with the historic record. *Annals of Glaciology* 24, 382–389.

Oerlemans, J (2012): Linear modelling of glacier length fluctuations. *Geografiska Annaler: Series A, Physical Geography* 94, 183–194.

Oppenheimer, M, Glavovic, BC, Hinkel, J, van de Wal, R, Magnan, AK, Abd-Elgawad, A, Cai, R, Cifuentes-Jara, M, DeConto, RM, Ghosh, T, Hay, J, Isla, F, Marzeion, B, Meyssignac, B & Sebesvari, Z (2019): Sea Level Rise and Implications for Low-Lying Islands, Coasts and Communities. In: Pörtner, H-O, Roberts, DC, Masson-Delmotte, V, Zhai, P, Tignor, M, Poloczanska, E, Mintenbeck, K, Alegría, A, Nicolai, M, Okem, A, Petzold, J, Rama, B & Weyer, NM (eds.): *IPCC Special Report on the Ocean and Cryosphere in a Changing Climate*. IPCC, Geneva, pp. 321–445.

Øyen, PA (1893): Isbræstudier i Jotunheimen. *Nyt magazin for naturvidenskaberne* 34, 12–72.

Rasmussen, LA (2007): Spatial extent of influence on glacier mass balance of North Atlantic circulation indices. *Terra Glacialis* 10, 43–58.

Rekstad, J (1892): Om Svartisen og dens gletschere. *Det Norske Geografiske Selskabs Årbog* 3, 1891–1892, 71–86.

Rekstad, J (1893): Beretning om en undersøgelse af Svartisen, foretagen i somrene 1890 og 1891. *Archiv for Mathematik og Naturvidenskab* 16, 266–321.

Rekstad, J (1900): Om periodiske forandringer hos norske bræer. In: Reusch, H (ed.): *Aarbog for 1896 til 99. Norges Geologiske Undersøgelse 28*. I kommission hos H. Aschehoug & Co., Kristiania, pp. 1–15.

RGI Consortium (2017): Randolph Glacier Inventory – A Dataset of Global Glacier Outlines: Version 6.0: Technical Report, Global Land Ice Measurements from Space, Colorado, USA. Digital Media.

Skaugen, T, Bache Stranden, H, Saloranta, T (2012): Trends in snow water equivalent in Norway (1931–2009). *Hydrology Research* 43, 489–499.

Stokes, CR, Andreassen, LM, Champion, MR & Corner, GD (2018): Widespread and accelerating glacier retreat on the Lyngen Peninsula, northern Norway, since their 'Little Ice Age' maximum. *Journal of Glaciology* 64, 100–118.

Theakstone, WH (1965): Recent Changes in the Glaciers of Svartisen. *Journal of Glaciology* 5, 411–431.

Tvede, AM (1973): Folgefonni – en glasiologisk avviker. *Naturen* 97, 11–16.

Weber, P, Boston, CM, Lovell, H & Andreassen, LM (2019): Evolution of the Norwegian plateau icefield Hardangerjøkulen since the 'Little Ice Age'. *The Holocene* 29, 1885–1905.

Weber, P, Andreassen, LM, Boston, CM, Lovell, H & Kvarteig, S (2020a): An ~1899 glacier inventory for Nordland, northern Norway, produced from historical maps. *Journal of Glaciology* 66, 259–277.

Weber, P, Lovell, H, Andreassen, LM & Boston, CM (2020b): Reconstructing the Little Ice Age extent of Langfjordjøkelen, Arctic mainland Norway, as a baseline for assessing centennial-scale icefield recession. *Polar Research* 39, 4304.

Whalley, WB & Kjøllmoen, B (2000): Øksfjord and Seiland. In: Andreassen, LM (ed.): *Regional change of glaciers in northern Norway*. NVE Report 2000:1. Norwegian Water Resources and Energy Directorate (NVE), Oslo, pp. 96–113.

Winkler, S (2003): A new interpretation of the date of the 'Little Ice Age' glacier maximum at Svartisen and Okstindan, northern Norway. *The Holocene* 13, 83–95.

Winsvold, SH, Andreassen, LM & Kienholz, C (2014): Glacier area and length changes in Norway from repeat inventories. *The Cryosphere* 8, 1885–1903.

Wittmeier, HE, Bakke, J, Vasskog, K & Trachseld, M (2015): Reconstructing Holocene glacier activity at Langfjordjøkelen, Arctic Norway, using multi-proxy fingerprinting of distal glacier-fed lake sediments. *Quaternary Science Reviews* 114, 78–99.

WMO 2020. WMO Statement on the State of the Global Climate in 2019. Geneva: WMO.

Zekollari, H, Huybrechts, P, Noël, B, van de Berg, WJ & van den Broeke, MR (2017): Sensitivity, stability and future evolution of the world's northernmost ice cap, Hans Tausen Iskappe (Greenland). *The Cryosphere* 11: 805–825.

Zemp, M, Frey, H, Gärtner-Roer, I, Nussbaumer, SU, Hoelzle, M, Paul, F, Haeberli, W, Denzinger, F, Ahlstrøm, AP, Anderson, B, Bajracharya, S, Baroni, C, Braun, LN, Cáceres, BE, Casassa, G, Cobos, G, Dávila, LR, Granados, HD, Demuth, MN, Espizua, L, Fischer, A, Fujita, K, Gadek, B, Ghazanfar, A, Hagen, JO, Holmlund, P, Karimi, N, Li, Z, Pelto, M, Pitte, P, Popovnin, VV, Portocarrero, CA, Prinz, R, Sangewar CV, Severskiy, I, Sigurđsson, O, Soruco, A, Usubaliev, R & Vincent, C (2015): Historically unprecedented global glacier decline in the early 21st century. *Journal of Glaciology* 61, 745–762.

Zemp, M, Huss, M, Thibert, E, Eckert, N, McNabb, R, Huber, J, Barandun, M, Machguth, H, Nussbaumer, SU, Gärtner-Roer, I, Thomson, L, Paul, F, Maussion, F, Kutuzov, S & Cogley, JG (2019): Global glacier mass changes and their contributions to sea-level rise from 1961 to 2016. *Nature* 568, 382–386.

Åkesson, H, Nisancioglu, KH, Giesen, RH & Morlighem, M (2017): Simulating the evolution of Hardangerjøkulen ice cap in southern Norway since the mid-Holocene and its sensitivity to climate change. *The Cryosphere* 11, 281–302.

Chapter 2

Paper I – Published in The Holocene, ***29****(12), 2019, 1885–1905*
https://doi.org/10.1177%2F0959683619865601

The following version of the published manuscript has been slightly amended according to the examiners' comments. All external readers should refer to the published version.

Evolution of the Norwegian plateau icefield Hardangerjøkulen since the 'Little Ice Age'

Paul Weber[1,*], Clare M. Boston[1], Harold Lovell[1], Liss M. Andreassen[2]

[1]University of Portsmouth, Department of Geography, Buckingham Building, Lion Terrace, Portsmouth, PO1 3HE, United Kingdom, *paul.weber@port.ac.uk
[2]Norwegian Water Resources and Energy Directorate (NVE)

Abstract

The maximum Little Ice Age (LIA) glacier extent provides a significant baseline to assess long-term glacier change and to place currently observed rates of glacier recession in a broader temporal context. To that end, we examine the evolution of the plateau icefield Hardangerjøkulen since the LIA. Firstly, we reconstruct Hardangerjøkulen's maximum LIA extent (~AD 1750) and subsequent recession based on the glacial landform record and aided by historical map interpretation. Ice-marginal moraines, glacial drift limits, trimlines, and identifiable erosion and weathering boundaries provide evidence of a LIA icefield with an area of 110 km^2. Existing LIA model simulations of Hardangerjøkulen are not yet fully able to reproduce our reconstructed extent. Secondly, we compile a set of remotely-sensed icefield outlines from successive time points in the 20th and 21st century to calculate icefield area and length change since the LIA. This reveals a substantial reduction in icefield size, with a total area loss of 41 km^2 (37 %; 2 % $10a^{-1}$) by 2010, and a cumulative frontal retreat averaging 1.3 km (29 %; 5 m a^{-1}) by 2013. Icefield recession has been greatest since the end of the 20th century, when rates of areal shrinkage increased to 6.5-10 % $10a^{-1}$ in 1995-2010, and the rate of average terminus retreat accelerated to 17 m a^{-1} in 2003-2010. Thirdly, we present a relative dating approach, based on the known age of the different icefield outlines, that allows bracketing ages to be assigned to all ice-marginal landforms between any two outlines. This approach shows that episodes of moraine formation vary temporally between individual outlet

glaciers of Hardangerjøkulen, suggesting that the moraine record of a single outlet glacier alone may not be sufficient to derive an icefield-wide picture of past ice advances, and thereby climate fluctuations.

Keywords: Hardangerjøkulen, plateau icefield, Norway, Little Ice Age (LIA), glacier reconstruction, glacier change

2.1. Introduction

Since the end of the 20th century, worldwide recession of glaciers and ice caps due to climate warming is occurring at the highest recorded rates and contributing significantly to sea-level rise (Vaughan et al., 2013; IPCC, 2014; Zemp et al., 2015, 2019). Global records of glacier length fluctuations and mass balance extend back to the end of the 19th century and late 1940s, respectively, and measurements of glacier area changes have become widespread since the 1980s following the availability of satellite remote sensing (Zemp et al., 2014, 2015). These observational records can be reconstructed back into pre-industrial times using historical documents, old maps, paintings, aerial and terrestrial photographs, as well as glacial landform evidence (e.g. Nussbaumer et al., 2011; Leclercq et al., 2014). Long-term data series are important in order to allow the magnitude of contemporary glacier (and thereby climate) change to be placed into a centennial-scale context.

Norway has one of the longest length change (since 1899) and mass balance (since 1949) records in the world (Norges vassdrags- og energidirektorat (NVE) – Norwegian Water Resources and Energy Directorate; Andreassen et al., 2005), and complete inventories of the spatial extent of Norwegian glaciers have been compiled for several time points since ~1950 (Andreassen et al., 2012a; Winsvold et al., 2014). Reconstructions of glacier fluctuations go back to the Little Ice Age (LIA), when Norwegian glaciers experienced their last major expansion (Grove, 2004). The timing of the LIA maximum differs widely across Norway, ranging from the early 18th century to the early 20th century (e.g. Winkler, 2003; Grove, 2004; Matthews, 2005; Wittmeier et al., 2015), and also varies across outlet glaciers of the same ice mass (Tvede, 1973; Bickerton and Matthews, 1993; Bakke et al., 2005a, b). Nevertheless, the maximum LIA glacier extent provides an ideal baseline for assessing long-term glacier change. For this purpose, glacier area is a crucial variable because unlike glacier length it is not based on localised point data with limited spatial coverage (cf. Zemp et al., 2014). To date, however, LIA glacier area has only been quantified for very few regions in Norway (e.g. Baumann et al., 2009; Stokes et al., 2018), resulting in a lack of digitally-available glacier outlines for long-term change analyses. Reconstructions of glacier fluctuations since the LIA are typically biased

towards length changes of individual mountain and outlet glaciers (Grove, 2004; Nesje et al., 2008; Nussbaumer et al., 2011), often only indirectly expressed through the mapping of moraine patterns (e.g. Erikstad and Sollid, 1986).

Monitoring long-term glacier change through multi-temporal inventories of glacier area is of high importance for plateau icefields, which make up a significant portion of Norwegian glaciers. These ice masses are particularly sensitive to climate variations because of their top-heavy hypsometry. A rise of the equilibrium line altitude (ELA) to the plateau, where the bulk of these low-gradient ice masses is situated, can lead to a substantial expansion of the ablation area, triggering rapid outlet glacier and icefield recession (cf. Oerlemans, 2012). This sensitivity has been demonstrated by case studies and model simulations at plateau icefields in Norway (e.g. Oerlemans, 1997; Nesje et al., 2008; Giesen and Oerlemans, 2010; Andreassen et al., 2012b; Åkesson et al., 2017) and elsewhere in the Northern Hemisphere (e.g. Jiskoot et al., 2009; Zekollari et al., 2017). In particular, Åkesson et al. (2017) simulated the Late Holocene evolution of the southern Norwegian Hardangerjøkulen icefield (Fig. 2-1) and found that a rise in ELA of 100 m will result in a ~17 % area reduction of the present-day icefield, compared to ~10 % at Nigardsbreen (southern Norway), ~6 % at the Vatnajökull ice cap (Iceland) and ~1.5 % at Franz Josef Glacier (New Zealand). Giesen and Oerlemans (2010) modelled the future evolution of Hardangerjøkulen and projected that, under a temperature increase of 3°C between 1961-1990 and 2071-2100, the icefield will have almost entirely disappeared by the year 2100. Predicting the future of these ice masses requires detailed knowledge of their past and present behaviour.

Against this backdrop, we use geomorphological mapping and historical maps to examine rates of area and length change at Hardangerjøkulen since the LIA maximum, in order to further understanding of the icefield's post-LIA evolution. The specific aims are (1) to reconstruct Hardangerjøkulen's maximum LIA extent and subsequent recession using the glacial landform record, with additional guidance provided by historical maps; (2) to quantify icefield area and length change since the LIA maximum; and (3) to establish a relative age chronology for the glacial landforms and recession patterns.

2.2. Study area

Hardangerjøkulen is the sixth largest ice mass in Norway (Andreassen et al., 2012a), covering an area of ~69.2 km^2 and ranging in altitude from 1,856 m a.s.l. on the icefield summit to 1,066 m a.s.l. at the terminus of the Rembesdalskåka outlet glacier (Fig. 2-1). Other key outlets are Ramnabergbreen in the north of the icefield, Bukkaskinnsbreen (informal name), Midtdalsbreen and Blåisen in the northeast, Torsteinsfonna in the east, and Austra and Vestra

Leirebottsskåka in the south (Fig. 2-1). The icefield lies in the southern Scandinavian Mountains on the boundary between the maritime west coast climate and the more continental climate of southeastern Norway. After ice-free conditions in the Mid-Holocene, glacier activity on the plateau restarted by ~4.8-3.4 ka BP and reached its peak during the LIA (Dahl and Nesje, 1994, 1996; Nesje et al., 1994). The maximum LIA position of Midtdalsbreen and Blåisen has been mapped and lichenometrically dated to ~AD 1750 by Andersen and Sollid (1971). Nesje and Dahl (1991) calculated a LIA ELA of 1,560 +40/-45 m a.s.l. for Midtdalsbreen, which is approximately 130 m below the modern-day ELA of Rembesdalskåka at 1,689 m a.s.l. (mean ELA value for the period 1963-2017 calculated from direct mass balance measurements at Rembesdalskåka using data published in Kjøllmoen et al., 2017). Following the LIA maximum, the glacial landform record of Midtdalsbreen and Blåisen (Andersen and Sollid, 1971) indicates that Hardangerjøkulen, in parallel with other glaciers in southern Norway, entered a phase of slow net retreat, which continued into the 1930s-40s (Nesje et al., 2008). Frontal position measurements at Rembesdalskåka since 1917 show that icefield recession intensified after 1940 (Andreassen et al., 2005). However, in the 1990s, the icefield outlets, along with many maritime glaciers in western Norway, readvanced in response to a period of increased winter precipitation (Andreassen et al., 2005; Nesje et al., 2008). Since the culmination of this advance around 1995, Hardangerjøkulen's outlet glaciers have undergone rapid 21st-century retreat (Andreassen et al., 2005).

2.3. Methods and data

Mapping of glacial landforms and surficial deposits was carried out remotely in ArcGIS from digital colour aerial photographs and verified during extensive field campaigns, following methods outlined in Chandler et al. (2018). The aerial photographs have a spatial resolution of 0.25 m and were captured on 20.-22.07.2013 (acquired fromhttp://norgeibilder.no/). All references in this paper to the 'current' glacier margin or the 'present day' therefore refer to the icefield dimensions in July 2013. Field mapping took place at all key outlet glaciers and along the southwestern plateau flank in July and August of 2016 and 2017 using a handheld GPS device with a maximum accuracy of 3-4 m. The landform features mapped around the icefield include ice-marginal moraines, glacial drift limits, trimlines, and identifiable erosion and weathering boundaries (Table 2-1). Typically, the surficial deposits and landforms relating to the LIA and later are comparatively fresh-looking, characterised by limited vegetation and lichen cover and unweathered surfaces. In addition, visual analysis of historical maps from the mid-19th to the early 20th century was employed to help identify Hardangerjøkulen's LIA dimensions. Once the maximum LIA extent of Hardangerjøkulen was reconstructed, remotely-

sensed icefield outlines from different time points in the 20th and 21st century were used to estimate glacier change and to date glacial landforms. The former icefield outlines are based on published glacier inventories (Andreassen et al., 2012a; Winsvold et al., 2014) or were extracted from topographic maps and vertical aerial photographs (Table 2-2). The methods for these assessments, including the separation of the outlines into glacier units and the generation of individual centrelines, are covered in detail in the respective sections of the paper.

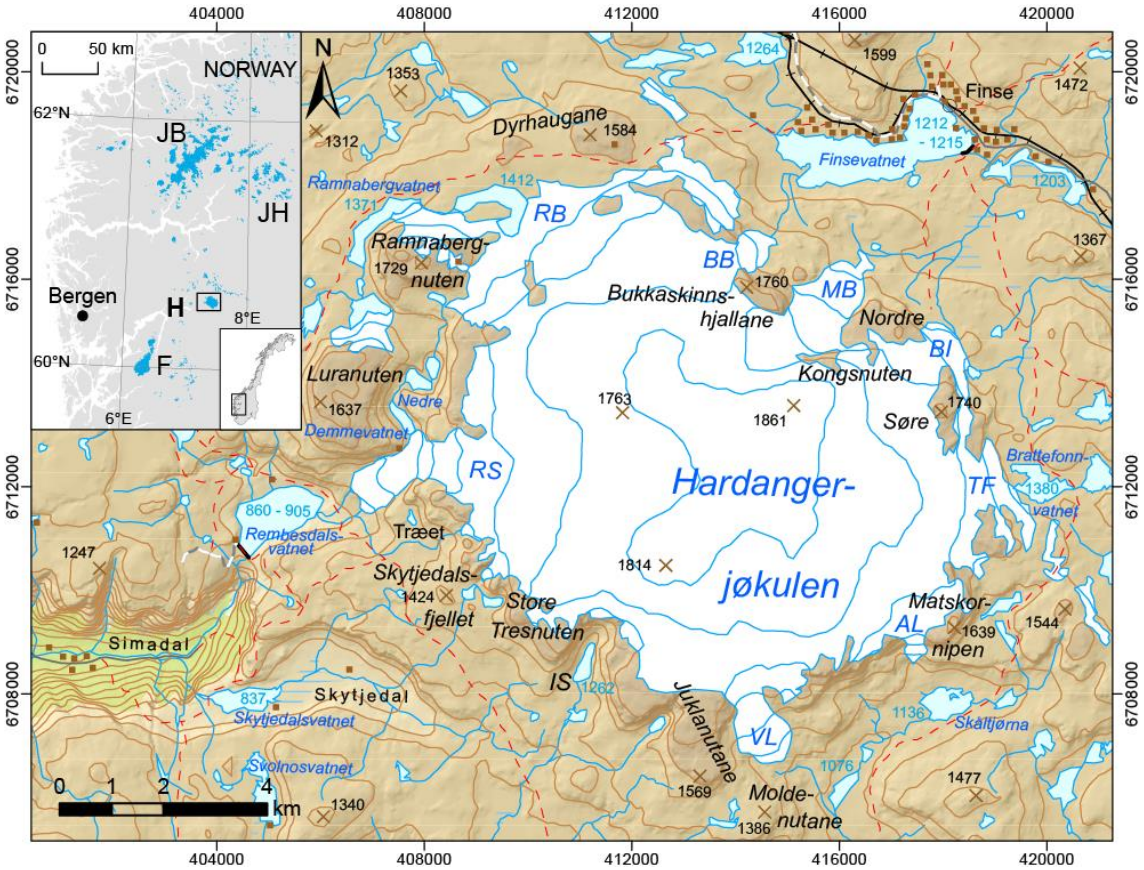

Fig. 2-1. Topographic map of the Hardangerjøkulen icefield and its outlet glaciers (1:130 000; Coordinate System: ETRS 1989 UTM Zone 32N; Projection: Transverse Mercator; Map data from Kartverket – Norwegian Mapping Authority). RB: Ramnabergbreen; BB: Bukkaskinnsbreen (informal name); MB: Midtdalsbreen; BI: Blåisen; TF: Torsteinsfonna; AL: Austra Leirebottsskåka; VL: Vestra Leirebottsskåka; IS: Isdøleskåka; RS: Rembesdalskåka. The inset shows the location of Hardangerjøkulen (H) along with other ice masses in southwestern Norway. F: Folgefonna; JB: Jostedalsbreen; JH: Jotunheimen glaciers (Glacier inventory data from Andreassen et al., 2012a).

Table 2-1. Glacial landforms mapped at the margins of Hardangerjøkulen.

Landform feature	Subform	Physical characteristics observed in the field
Ice-marginal moraine		Diamictic ridge deposited at the ice margin during a glacier advance or episode of standstill demarcating the glacier's former extent
	Frontal moraine	Ridge deposited at the glacier front
	Lateral moraine	Ridge deposited at the lateral glacier margin
	Latero-frontal moraine	Ridge consisting of lateral and frontal moraine sections
	Annual moraine	Ridge in a sequence of other ridges whose dense spacing suggests ridge formation on an annual basis
	Recessional moraine	Ridge deposited in any of the above positions during a stage of overall glacier retreat from an ice advance
Controlled moraine		Ridge originating from englacial or supraglacial debris concentrations that form a (occasionally ice-cored) moraine upon separation from the glacier (cf. Evans, 2009)
Glacial drift		Cover of glacially transported material; can be in the form of sheets of diamictic sediment (till) with variable thickness and continuity, or in the form of boulders strewn across a surface
Glacial drift limit		Boundary between the edge of a glacial drift cover and a surface of different composition beyond
Weathering/ erosional boundary		Boundary between freshly glacially eroded (ice-moulded) and often striated (assumed LIA) bedrock and more weathered and vegetated (assumed older) bedrock
Trimline		Boundary between areas where vegetation is absent or sparse, indicating recent (assumed LIA) ice retreat, and areas with well-established, stable vegetation (assumed older)
Esker		Sinuous ridge of glaciofluvial sediment deposited by meltwater in ice-walled conduits during glacier retreat
Fluting		Ice flow parallel lineations on glacier forelands composed of diamictic sediment (till)

Table 2-2. Overview of remotely-sensed icefield outlines of Hardangerjøkulen. These were used to assess icefield change since the LIA and assign relative ages to the ice-marginal moraines formed at the margins of Hardangerjøkulen.

Date/Year	Source	Scale/ resolution	Produced/ published by	Reference/Comment
1923-29	Topographic map (*gradteigskart*) based on ground surveys carried out in the 1920s; published in 1932	1:100 000	Norwegian Mapping Authority (Norges Geografiske Oppmåling)	Map georectified (15 control points; total RMSE: 19.2; 2nd Order Polynomial Transformation) and outline digitised on-screen by main author
31.08.1961	Topographic map based on vertical aerial photographs; unpublished (NVE)	1:20 000	Widerøes Flyveselskap (aerial photographs and map)	Map georectified (17 control points; total RMSE: 2.7; 1st Order Polynomial Transformation) and outline digitised on-screen by main author
1973 (1964)	Topographic maps (N50, three map sheets) based on vertical aerial photographs; published in 1982; map sheet showing Vestra Leirebottsskåka area based on aerial photographs from 1964; published in 1970	1:50 000	Norwegian Mapping Authority (Norges Geografiske Oppmåling)	Winsvold et al. (2014); missing glacier unit with ID 2967 was added by main author from a 1974 vertical aerial photograph
06.08.1988	Landsat 5 TM	30 m	Landsat	Winsvold et al. (2014)
31.08.1995	Updated topographic map (N50) based on vertical aerial photographs; published in 2001	1:50 000	Norwegian Mapping Authority (Kartverket)	Digital outline provided by Kartverket
09.08.2003	Landsat 5 TM	30 m	Landsat	Andreassen et al. (2012a)
29.09.2010	Digital vertical aerial photographs; unpublished (NVE)	0.2 m	Terratec	Outline digitised on-screen by NVE
20.-22.07.2013	Digital vertical aerial photographs	0.25 m	Terratec; available from http://norgeibilder.no/	Outline digitised on-screen by main author

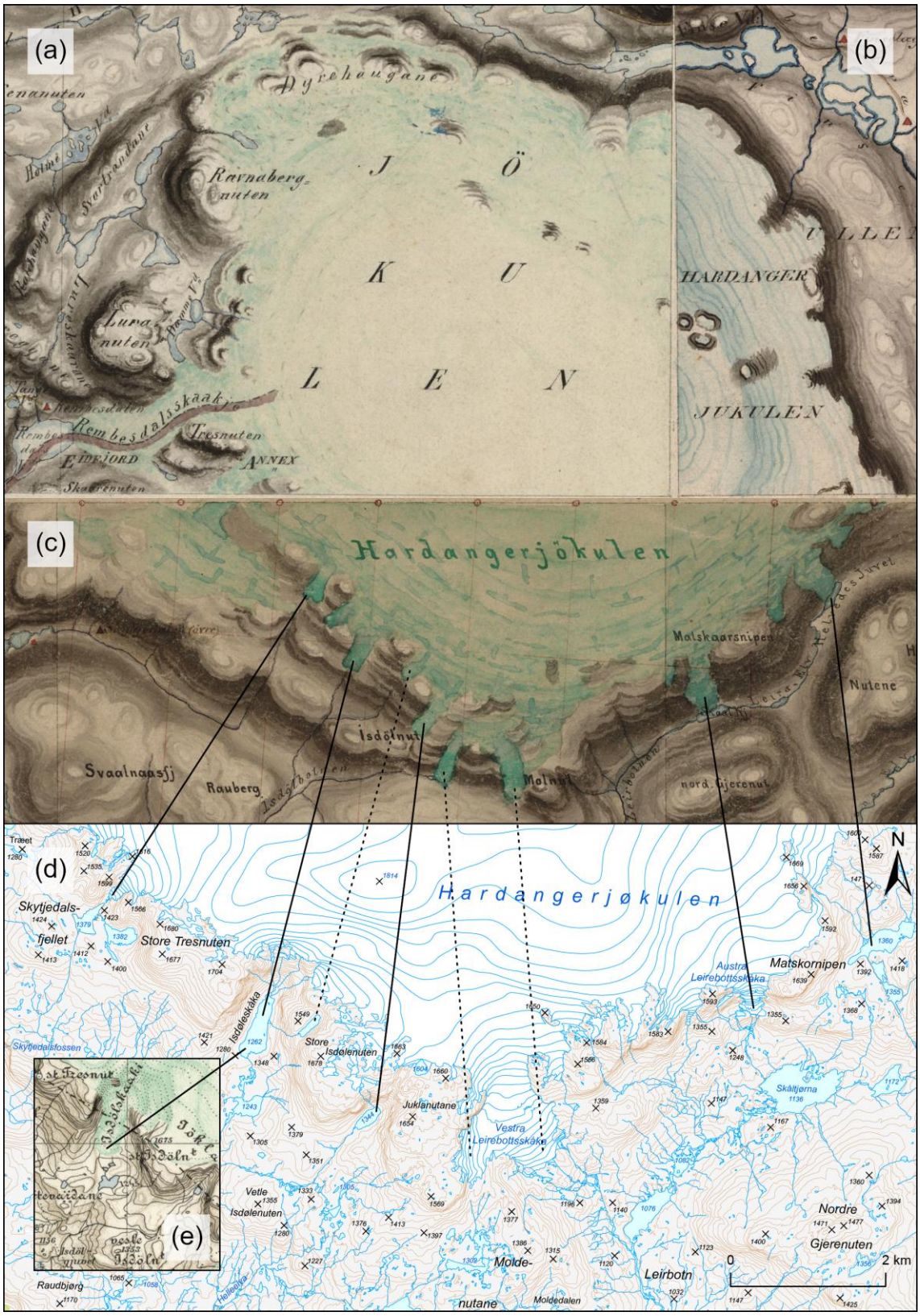

Fig. 2-2. (a) Northwestern quadrant of Hardangerjøkulen between Rembesdalskåka in the west and the Finsevatnet lake (1,212-1,215 m a.s.l.) in the northeast, as shown on *rektangelmålingen* 23B 3, 4, 7, 8 (1:100 000; mapped by F. Lowzow; 1864; published by Norges Geografiske Oppmåling; available from Kartverket). (b) Northeastern quadrant of Hardangerjøkulen between Finsevatnet in the north and Torsteinsfonna in the east, as depicted on *rektangelmålingen* 24A 1 (1:100 000; mapped by L. Broch; 1848; published by Norges Geografiske Oppmåling; available

from Kartverket). (c) Southern half of Hardangerjøkulen between Matskornipen (1,639 m a.s.l.) in the southeast and Skytjedalsfjellet (1,424 m a.s.l.) in the southwest, as shown on *porteføljen* no. 28 (1:100 000; produced by E. Lund and F. Sejersted; 1860; published by Norges Geografiske Oppmåling; available from Kartverket). (d) Outlet glaciers indicated in C and E are related to a modern-day topographic map of the same area (1:70 000; Map data from Kartverket); solid lines: certain agreement; dotted lines: inferred. (e) The glacier-filled Isdøleskåka cirque, as depicted on *gradteigskartet* D33 Vest Hardangerjökulen (1:100 000; unknown cartographer; 1932; published by Norges Geografiske Oppmåling; available from Kartverket).

2.4. Mid-19th to early-20th-century dimensions of Hardangerjøkulen based on historical maps

Historical maps can provide valuable information on former glacier extents (e.g. Tennant et al., 2012; Cullen et al., 2013; Winsvold et al., 2014). Hardangerjøkulen first appears in large scale (1:100 000) on hand-drawn mid-19th-century *rektangelmålinger* ('rectangle survey maps') and *porteføljekart* ('portfolio maps') (Fig. 2-2), published by Norges Geografiske Oppmåling (Norwegian Geographical Survey; now: Kartverket) (Harsson and Aanrud, 2016). These maps depict the northern half of the icefield as a uniform, quasi-circular ice cap covering the plateau, without distinguishable outlet glaciers (Fig. 2-2a and b). One interesting detail to note, however, is that the northern icefield margin seems to impinge on and partly envelop the Dyrhaugane massif (1,584 m a.s.l.) (Fig. 2-2a). By contrast, the southern half of Hardangerjøkulen is shown in more detail with a number of outlet glaciers extending from the icefield, including Austra Leirebottsskåka (Fig. 2-2c). Many of these outlets are in locations that today are free of glacier ice (Fig. 2-2d), indicating substantial glacier retreat since the mid-19th century. Curiously, the cartographers appear to have erroneously placed Vestra Leirebottsskåka on the western instead of the eastern side of the Moldenutane massif (1,386 m a.s.l.); and the nameless lake that today fills the valley bottom in front of this outlet (1,076 m a.s.l.) does not appear to have existed at the time (Fig. 2-2c).

Between 1923 and 1929, the Hardangerjøkulen area was re-surveyed for the 1:100 000 scale *gradteigskartene* ('quadrangle maps') (Harsson and Aanrud, 2016). As part of the field mapping campaign around Hardangerjøkulen, the surveyors produced detailed written descriptions and photographs of the landscape, against which the mapping can be checked and verified. These records demonstrate that the icefield and its extent was mapped with high accuracy. The Hardangerjøkulen *gradteigskartet* shows that the Isdøleskåka cirque at the southwestern flank of the plateau was still filled by a sizeable outlet glacier in the 1920s (Fig. 2-2d and e). The icefield outline depicted on this map was used for the glacier change assessment and relative landform dating presented in Sections 2.7. and 2.8., respectively (Table 2-2).

2.5. Geomorphological evidence and identification of LIA limit

Here, we describe the geomorphological record exposed during glacier recession since the LIA for each outlet glacier and the plateau summit, starting with Midtdalsbreen in the northeast and proceeding in a clockwise fashion around the icefield (Fig. 2-1). The results of our mapping are presented online in the supplementary materials of the published paper as a large-format 1:20 000 scale map of the glacial geomorphology and surficial geology of Hardangerjøkulen (see Appendix). Sections of this map, illustrating the glacial geomorphology of Hardangerjøkulen's key outlet glaciers, are presented in Fig. 2-3.

2.5.1. Midtdalsbreen

Midtdalsbreen (Fig. 2-3a) extends down from the plateau to an altitude of 1,403 m a.s.l. The glacial geomorphology of the outlet has previously been mapped at a scale of 1:5 000 by Sollid and Bjørkenes (1977), with the position of the glacier margin shown in 1975. Their mapping was re-examined and the majority incorporated into our work. The focus of the field mapping undertaken as part of this study was primarily on the immediate glacier foreland. Midtdalsbreen's maximum LIA extent is delimited by a cover of fresh-looking, sparsely vegetated glacial drift that stretches down to the southern slope of the 1,397 m-high foothill between Finsevatnet and the plateau. Along its margin, the drift sheet attains its greatest thickness and is bordered by moraine ridges. The ridges are particularly pronounced in the east, where a belt of bouldery moraines runs along the lateral drift margin (Fig. S2-1). These vary in morphology from well-defined, single-crested and sinuous ridges to hummocks and mounds. Many inactive meltwater channels occur along the ice-proximal side of the moraine belt. Towards the centre of the glacier foreland, scattered moraines have a semicircular arrangement around a bowl-shaped depression containing glaciofluvial deposits, ice-moulded bedrock and extensively fluted glacial drift. The radial arrangement of the flutings reflects divergent ice flow towards the margin during the LIA. The area around the current glacier front exhibits two distinct landform types. Firstly, an assemblage of sandy-gravelly deposits and ice margin parallel ridges lies at the southeastern end of the ice front, where the glacier margin is mantled in debris. The features result from differential melting of the glacier beneath the debris cover, leading to ice-cored ridges of sorted sands and gravels, which eventually become detached from the glacier ('controlled moraine'; cf. Evans, 2009; see also Reinardy et al., 2019). These were described by Andersen and Sollid (1971) under the term 'stratified moraine'. By contrast, the area in front of the northwestern ice margin is dominated by densely-spaced moraine ridges, between which flutings are abundant. The close spacing of the ridges points to an annual

formation rate, which is supported by observations made by Andersen and Sollid (1971). Building on these observations, Reinardy et al. (2013) link annual moraine development to a process operating on a seasonal cycle: In winter, sediments become frozen to the base of Midtdalsbreen and are transported with the advancing ice front. This is followed by sediment melt-out and deposition in spring/summer.

2.5.2. Blåisen

Blåisen (Fig. 2-3a) is located between Nordre (1,620 m a.s.l.) and Søre (1,740 m a.s.l.) Kongsnuten and flows down the plateau flank to 1,424 m a.s.l. An expansive, radially fluted drift sheet with a relatively fresh appearance surrounds the outlet glacier. The drift sheet is separated from that of Midtdalsbreen by a narrow corridor of weathered bedrock terrain. It extends northwards across an undulating area of higher ground to the edge of a prominent escarpment, eastwards to the nameless lake at 1,321 m a.s.l., and southwards to the 1,407 m-high plateau foothill. We interpret this drift sheet to represent the maximum LIA extent, which accords with the mapping of Andersen and Sollid (1971). The northern part is densely covered with moraine ridges, which generally decrease in size towards the glacier margin. The outermost moraine along the bedrock corridor stands up to 8 m high and transitions from a sinuous, single-crested ridge at the base of Nordre Kongsnuten (Fig. S2-2) into a broad, multi-crested moraine belt with numerous intervening depressions and hollows away from the plateau. Subangular boulders up to 6 m wide litter the moraine belt surface. Inside this LIA moraine limit lies a series of smaller recessional moraines (up to 4 m high) that are clearly defined and continuous (Fig. S2-2). These ridges are sinuous and have smooth, flat to rounded crests with a large number of well-embedded boulders. Near Blåisen's main meltwater stream they become fragmentary and hummocky. By contrast, the moraine ridges east of the meltwater stream, along the edge of the escarpment and on the central glacier foreland, are often relatively subdued and difficult to distinguish from sediment draped over rolling bedrock humps. Sequences of very small, less than 1 m high moraines, presumed annual in origin, are nested around the northern half of the current glacier margin. Blåisen's easternmost LIA position is marked by an area of frontal moraines on the far side of the lake situated at 1,321 m a.s.l. (Fig. S2-3). The moraines have a highly variable morphology and height, occurring as flat morainic bands, distinct ridges with well-defined, round-topped crests, and as areas of ridged hummocks. Boulders of up to 4 m in diameter are strewn over the otherwise finer-grained and smoother surfaces of the moraines. To the southeast of Blåisen, arcuate recessional moraines are grouped around a proglacial lake

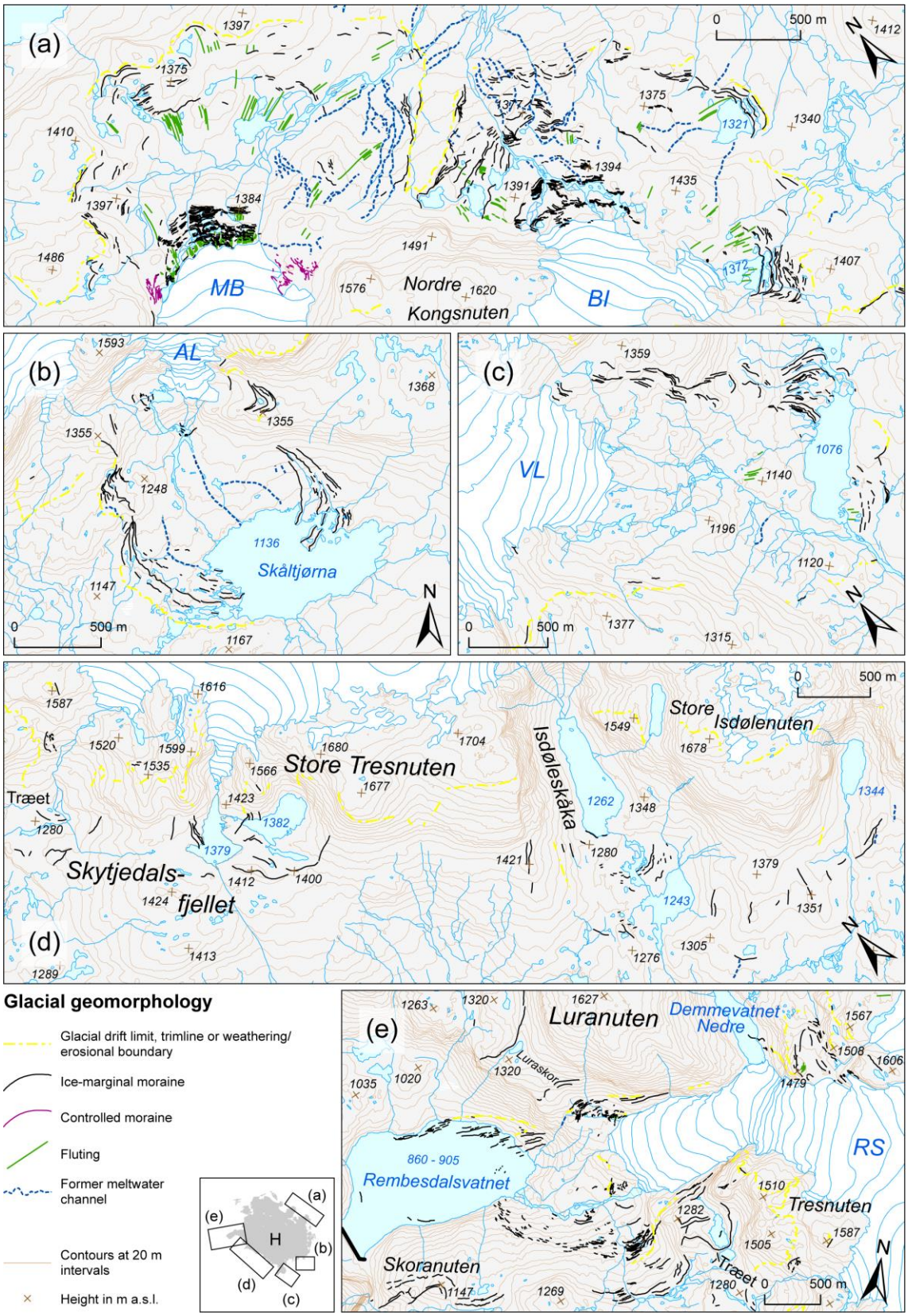

Fig. 2-3. Summary geomorphological maps of key outlet glaciers of Hardangerjøkulen (Data for base maps, including icefield outline, from Kartverket). (a) Midtdalsbreen and Blåisen (1:32 000). (b) Austra Leirebottsskåka (1:31 000). (c) Vestra Leirebottsskåka (1:34 000). (d) Former cirque outlet glaciers along the southwestern plateau flank (1:37 000). (e) Rembesdalskåka (1:48 000). The inset shows the location of the outlet glacier forelands.

(1,372 m a.s.l.) in front of a small, southeast-oriented ice apron that is attached to the northeast-facing present-day glacier front (Fig. S2-4). The ridges are short and fragmented around the LIA limit, but become progressively longer and more continuous towards the modern margin. Overall, the moraines inside Blåisen's LIA limit, which often occur in compact sequences, delimit successive ice positions retreating towards the plateau. Beyond the LIA limit, Andersen and Sollid (1971) mapped a pre-LIA moraine (based on lichenometry) to the northeast of the drift sheet; however, we interpret this feature to be one of several colluvial boulder deposits along the foot of the escarpment.

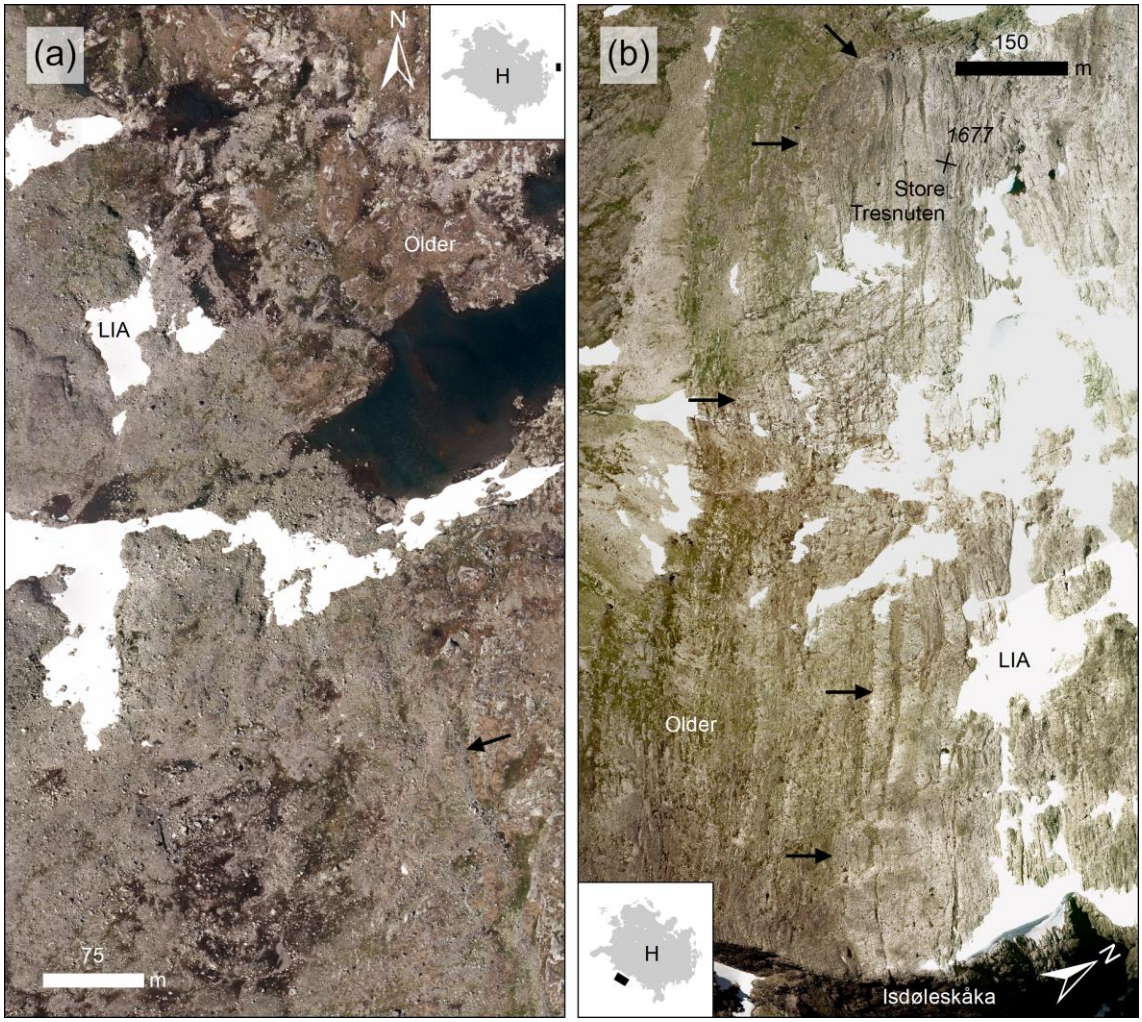

Fig. 2-4. (a) Glacial drift sheet with distinct LIA drift limit (indicated by arrow) at Torsteinsfonna. (b) Black arrows indicate the (assumed LIA) erosional/weathering boundary on the plateau summit between Isdøleskåka and Store Tresnuten (1,677 m a.s.l.). The insets show the location of the photographed areas around the present-day icefield (July 2013 vertical aerial photographs acquired from http://norgeibilder.no/).

2.5.3. Torsteinsfonna and the eastern plateau flank

Torsteinsfonna in the east of Hardangerjøkulen is a wide, apron-shaped outlet presently covering the upper plateau flank. Numerous nunataks fragment the glacier snout. A sweeping, semi-elliptical sheet of fluted glacial drift extends over the flat foreland of the plateau up to the eastern shore of the Brattefonnvatnet lake (1,381 m a.s.l.). The boundary of this drift cover is very sharp (Fig. 2-4a) and also delineated by moraine ridges, recording Torsteinsfonna's maximum LIA extent. To the northeast of Matskornipen (1,639 m a.s.l.), the outline of another former LIA outlet is imprinted on the eastern plateau flank in the form of ice-moulded bedrock and a thin blanket of fluted glacial drift.

2.5.4. Austra Leirebottsskåka

Austra Leirebottsskåka (Fig. 2-3b) is an icefall in the southeast of Hardangerjøkulen. At present, this outlet terminates at 1,312 m a.s.l. on a bedrock terrace midway down the steep flank of the plateau. On the eastern side of the terrace, a group of tightly-curved moraines is emplaced onto a lobate sheet of fresh-looking, unvegetated glacial drift, outlining a very small former ice lobe that is inferred to have protruded from Austra Leirebottsskåka during the LIA. On the western end of the terrace, a lateral moraine extends down into a cluster of nested latero-frontal moraine ridges, which were deposited on thick glacial drift on the higher ground to the west of the 1,248 m-high foothill of the plateau. This landform assemblage defines a localised lobe in the former LIA glacier margin. The moraine cluster links up with arcuate moraine ridges in the valley below. These valley-floor moraines form a series of loops that set off from two points at the foot of the plateau and curve towards the Skåltjørna lake (1,136 m a.s.l.) (Fig. S2-5). Many of these ridges are discontinuous and fragmented, or occur as disjointed mounds, which are particularly pronounced around Skåltjørna where they form ridged islets in the lake. The valley-floor moraines to the west of Skåltjørna sit on a sheet of thick glacial drift deposits, which forms a sharp boundary to the weathered and vegetated bedrock beyond. We interpret the moraine loops and the glacial drift limit to represent the maximum LIA position of Austra Leirebottsskåka and ice front fluctuations immediately following the LIA maximum (cf. Evans and Twigg, 2002; Evans, 2003). During the LIA, Austra Leirebottsskåka extended from the plateau all the way down to the valley bottom, where it spread out into a piedmont lobe. The glacier foreland between the moraine loops and the present-day ice margin is dominated by exposed, ice-moulded bedrock (Fig. S2-5). Only isolated patches of drift and very few moraine fragments are present here, most prominently below the current ice margin. To the west of Austra Leirebottsskåka, ice-moulded bedrock and glacial drift limits demarcate the extent of

another, smaller, LIA icefall, before the LIA drift limit rises and continues westwards along the plateau edge towards Vestra Leirebottsskåka.

2.5.5. Vestra Leirebottsskåka

Vestra Leirebottsskåka (Fig. 2-3c), Hardangerjøkulen's major southern outlet, flows from the plateau as an icefall onto a relatively gentle, U-shaped bedrock slope, terminating at 1,275 m a.s.l. The ice-marginal landform record preserved on this slope is highly asymmetrical, with a complex system of lateral moraines descending the eastern flank of the slope, while the western flank and central part of the slope are largely devoid of ice-marginal landforms. On the lower part of the eastern slope, short frontal moraine segments are also present (Fig. S2-6). In the valley below, the lateral moraines fan out into four major morainic belts, each consisting of numerous fragmented and often mound-like ridges. These latero-frontal belts curve towards the lake that fills the valley bottom in front of Vestra Leirebottsskåka (Fig. S2-6). The southeastern side of the lake is characterised by an ice-moulded and striated bedrock plain, which in places is draped with extensive boulder blankets or thin veneers of drift (Fig. S2-6). Frontal moraine segments and mounds are developed on these surface layers. The ice-polished bedrock, partially covered by sheets of glacial drift, marks the maximum LIA extent of Vestra Leirebottsskåka, while the morainic belts around the lake are evidence for minor readvances or episodes of glacier standstill (cf. Evans and Twigg, 2002; Evans, 2003) in the time immediately following the LIA maximum.

2.5.6. Former cirque outlet glaciers along the southwestern plateau flank

Steep-sided cirques with overdeepened, lake-filled floors are cut into the southwestern flank of the plateau (Fig. 2-3d). The four deepest and most pronounced of these cirques are, from east to west, Juklanutane (informal name), Isdøleskåka (official name), Skytjedalsfjellet–Store Tresnuten and Træet (both informal names). Ice-marginal moraines relating to more than one glacial episode exist here (cf. Liestøl, 1963), of which pre-LIA landforms are typically surrounded by blankets of grey-whitish boulders. Most of the cirques are presently ice-free, but historical maps and old aerial and terrestrial photographs show that they all hosted minor outlet glaciers in the 19th century up until the early 20th century (Fig. 2-2). Between the cirques, the LIA icefield margin follows the edge of the plateau summit, as evidenced by distinct erosional boundaries on bedrock (Fig. 2-4b) and glacial drift limits.

The dominant landform feature of the Juklanutane cirque is an enormous multi-crested lateral moraine ridge (up to 80 m high) on the eastern side of the cirque mouth (Fig. S2-7). Its highest crest peaks at 1,418 m a.s.l. A ~200 m-long trimline is clearly visible along the western side of the cirque mouth at elevations of between ~1,350 and ~1,380 m a.s.l. (Fig. S2-7). This is at a lower elevation than the top crest of the lateral moraine on the opposite side, suggesting that the two features are not contemporaneous. The bedrock on the cirque floor below the trimline appears to be ice-moulded, onto which a small pile of relatively sorted, presumed glaciofluvial, material was deposited. Beyond the cirque, hummocks and patches of glacial drift occur on the gently-sloping plateau foreland (Fig. S2-7). The area between the hummocks is paved with grey-whitish boulders. Bounding the entire zone is a frontal and a lateral moraine ridge approximately 900 m to the west of the cirque mouth. We interpret the trimline and glacially eroded bedrock within the cirque basin to document the extent of the former LIA outlet. All other glacial landforms likely demarcate a more extensive ice advance predating the LIA (cf. Liestøl, 1963) because the reconstructed glacier would have been out of proportion to the LIA dimensions of Hardangerjøkulen's other outlets.

At Isdøleskåka, arcuate bedrock ridges around the cirque mouth create a more or less closed, elongated basin. This depression is occupied by three lakes, which are separated from each other by bedrock sills. The rock floor within the cirque basin has a gently undulating topography and is draped with patches of sediment of varying thickness, making it often difficult to judge whether moraine ridges are present here or whether bedrock hillocks are blanketed by sediment. Sequences of curved latero-frontal moraines are developed to the west of the outer lake (1,243 m a.s.l.) as well as on the bedrock sill between outer and middle lake. These moraines often consist of only piles and short fragments. More pronounced, bouldery lateral moraines occur to the east of the outer lake (Fig. S2-8) as well as to the west of the inner lake (1,262 m a.s.l.). A clearly defined, but fragmented, frontal moraine runs along the shoreline of the inner lake. The 1932 *gradteigskartet* (Fig. 2-2e) and a historical photograph of Isdøleskåka taken in 1928 during the *gradteigskartene* land surveys show that the ice margin terminated on the bedrock sill between the inner and middle lake. This suggests that the frontal moraine around the inner lake was formed during the retreat of the LIA outlet around, or not long after, this time. Consequently, the outer moraines on the cirque floor may reflect the pre-1928 LIA extent and subsequent recession of Isdøleskåka. The bedrock ridge bounding the cirque mouth in the northwest is topped at 1,421 m a.s.l. by a distinct double lateral moraine (Fig. S2-8). The considerable elevation of the moraine indicates the margin of an outlet glacier that must have extended well beyond the confines of the cirque basin (cf. Liestøl, 1963), and is therefore assumed to be of pre-LIA age.

The Skytjedalsfjellet–Store Tresnuten double cirque opens towards a confined upland basin between the Store Tresnuten summit (1,677 m a.s.l.) and the Skytjedalsfjellet foothill. A

small icefall is currently occupying the headwall of the northwestern cirque. The floor of the basin is filled by two lakes, which are enclosed by a semicircular ridge system of fragmented latero-frontal moraines (Fig. S2-9). The moraine complex has a mature appearance, often with flat-topped crests and massive, up to 10-15 m wide clasts incorporated, and is surrounded by grey-whitish boulder blankets. This is taken as evidence for a pre-LIA age (cf. Liestøl, 1963). A sequence of densely-spaced latero-frontal recessional moraines curves around the sides of the northwestern lake (1,380 m a.s.l.) and the northwestern tip of the southeastern lake (1,383 m a.s.l.) (Fig. S2-9). The ridges are only sparsely vegetated, revealing a sedimentary composition that changes from mainly openwork bouldery at the foot of the plateau flank to finer grained and matrix-supported towards the middle of the basin. This landform assemblage delineates the maximum LIA extent of the northwestern cirque outlet. By contrast, evidence for a LIA outlet in the southeastern cirque is sparse. The shore of the southeastern lake below the cirque headwall is flanked by colluvium. A lateral moraine ridge at the edge of the plateau summit above the cirque as well as ice-moulded bedrock and fresh-looking, unvegetated glacial drift in the upper part of the cirque headwall are indicators of a small hanging glacier during the LIA.

In the Træet cirque, a lobate sheet of sparsely vegetated glacial drift comes down the side of the plateau. This drift cover is bounded by a small number of subtle frontal moraine ridges at the plateau base (Fig. S2-10), which mark the maximum LIA extent of this former outlet lobe. In the upper part of the plateau flank, sets of recessional moraines represent stages in the retreat of the LIA cirque outlet. On the flat area of higher ground in front of the cirque, bouldery moraines can be found beyond the LIA drift sheet, ranging from well-defined, round-crested ridges to openwork bands of boulders (Fig. S2-10). These ridges are surrounded by blankets of grey-whitish boulders and interpreted to be of pre-LIA age.

2.5.7. Rembesdalskåka

Rembesdalskåka (Fig. 2-3e) is the icefield's largest glacier unit (Andreassen et al., 2012a). The outlet glacier dams a northern side valley to form the Nedre Demmevatnet lake (~1,240 m a.s.l.), from which frequent jökulhlaups have been recorded since before ~AD 1800 (Liestøl, 1956; Kjøllmoen et al., 2017). Rembesdalskåka's terminus lies on the plateau flank above a deep upland basin containing the Rembesdalsvatnet lake (Fig. 2-5a). Rembesdalsvatnet was dammed for hydropower generation in the late 1970s (lowest and highest regulated water level: 860 m and 905 m a.s.l., respectively), submerging much of the landform evidence relating to the glacier's maximum LIA position. Low water levels in early summer 2017 allowed a frontal moraine segment and suites of lateral moraines to be mapped on the lake bottom (Fig. 2-5b), which can also be identified on old aerial photographs (Fig. 2-5a). The lateral moraines in the

northeastern part of the lake basin can be seen to climb from the lake bed onto the bedrock slope between Rembesdalsvatnet and the present-day glacier terminus. This slope is highly eroded by glacier action, contrasting with the weathered and vegetated terrain around it (Fig. 2-5a and c). We interpret the ice-moulding to be the result of LIA glacier erosion and the lake-bed moraines to represent LIA recessional moraines, indicating that Rembesdalskåka covered the entire lake basin at its LIA maximum.

The lateral margins of the ice-moulded bedrock slope are fringed by pronounced trimlines and erosional boundaries (Fig, 2-5c), and groups of moraines (mainly lateral) that are often located on thick deposits of glacial drift. The greatest concentration of moraines occurs on the southeastern side of the upland basin, where an intricate network of discontinuous, meandering lateral moraine ridges was deposited down the slope. The ridges are very closely-spaced, often pushed into each other's flanks to form multi-crested ridge complexes. Whilst the moraines become fresher-looking and more sharp-crested downvalley, their height and sedimentary composition vary considerably both along the length of individual ridges and between ridges. The moraines record successive post-LIA retreat positions of Rembesdalskåka.

Around the present-day ice margin, a ~50-200 m wide zone of extremely shiny, freshly ice-moulded and striated bedrock documents the 1990s glacier readvance (Fig. 2-5d). The maximum extent of this readvance is delimited by moraine ridges on the central glacier foreland around Rembesdalskåka's main meltwater stream as well as on a reverse bed slope to the northwest of the current ice front (Fig. 2-5d). The moraine on the southern side of the stream is a single-crested ridge, primarily made up of an openwork framework of large boulders, whereas those on the northern side of the stream and the reverse bed slope are finer-grained, matrix-supported ridges with multiple crests. On their ice-proximal side, these ridges are adjoined by a multitude of tightly-spaced moraines, which are often very small, short and sinuous. The compact spacing of both LIA and recent moraines may suggest that they might be annual in origin.

Further up-glacier, lateral moraines run parallel to the glacier tongue. The moraines above the northern ice margin are often constructed of huge, angular boulders that have been arranged by the glacier into linear bands along the southern flank of Luranuten (1,649 m a.s.l.) (Fig. 2-5d). By contrast, those above the southern ice margin are coarse-grained, bouldery sediment ridges along the steep valley side, each pushed into the proximal flank of the next higher moraine, with only the topmost ridge exhibiting a pronounced distal flank. In the Nedre Demmevatnet basin, glacial drift limits and a handful of moraine ridges, one of which is submerged, define a former ice lobe that extended into the side valley at the LIA maximum (Fig. 2-5e). Another LIA ice lobe of Rembesdalskåka existed on a flat terrace area of the plateau flank above Nedre Demmevatnet, as shown by a lobate sheet of unvegetated glacial drift with numerous moraine ridges.

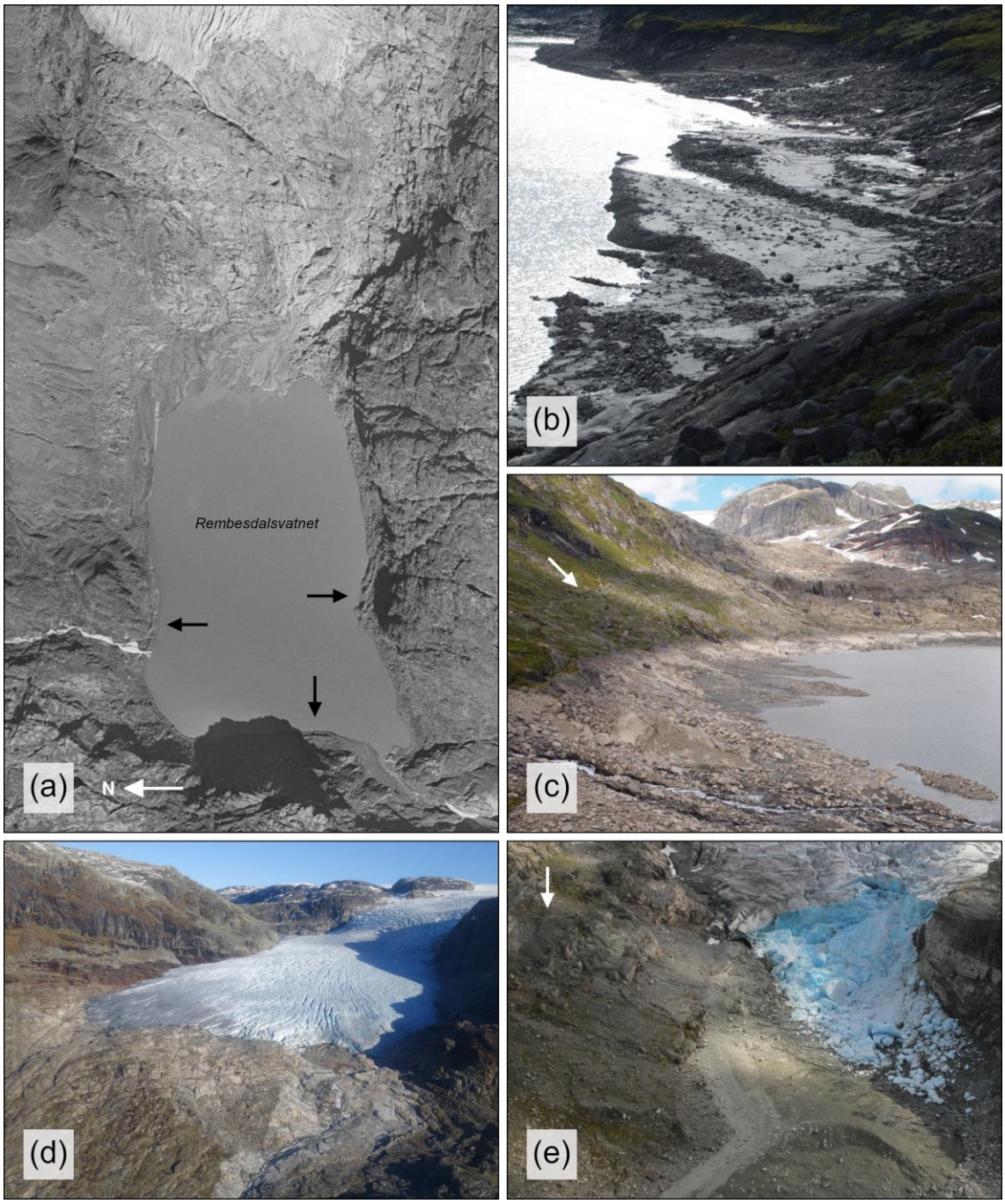

Fig. 2-5. Glacial geomorphology at Rembesdalskåka. (a) Vertical aerial photograph of Rembesdalsvatnet and Rembesdalskåka from 19.09.1961 (Sortie: WF-1237; Owner: Kartverket) showing the lake before the dam was constructed. Black arrows indicate major moraine ridges that are associated with the maximum LIA advance and are today submerged. Note the bright, ice-moulded bedrock between the lake and the 1961 glacier margin. (b) Westward view across the northeastern part of the lake basin, showing post-LIA recessional moraines exposed on the bottom of Rembesdalsvatnet. (c) Eastward view towards the ice-moulded foreland of Rembesdalskåka, showing the LIA trimline above Rembesdalsvatnet (indicated by white arrow) and the same post-LIA recessional moraines as in (b). (d) Rembesdalskåka in October 2017 (Photo: Hallgeir Elvehøy, NVE). The freshly ice-moulded zone in front of the ice margin marks the 1990s glacier readvance, which is clearly delineated by pronounced moraine ridges on either side of the meltwater stream. Also note the LIA lateral moraines above the lateral glacier margin in the distance to the left. (e) Exposed lake bottom of Nedre Demmevatnet in August 2014 after a jökulhlaup event (Photo: Hallgeir Elvehøy, NVE). Frontal moraines are clearly visible in the

foreground of the photo. A lateral moraine ridge can be seen on a bedrock terrace in the distance to the left (indicated by white arrow). Together, the ridges outline a small LIA ice lobe that extended into the side valley. Note the distinctly ice-moulded bedrock of the valley sides.

Pre-LIA moraines are also preserved around Rembesdalskåka (cf. Liestøl, 1963), which can be differentiated from LIA moraines by their very large size and extent. A prominent latero-frontal moraine ridge (up to ~40 m high) curves along the western flank of Luranuten towards the edge of the cliff overlooking Rembesdalsvatnet, indicating a glacier advance of pre-LIA age from the north, not sourced from the plateau. A pre-LIA, more extensive position of Rembesdalskåka is recorded along the northern side of the upland basin by a set of latero-frontal moraines on the slope of the Luraskor mountain gap; and along the southern rim of the upland basin by a system of meandering, lobed moraines that stretches from the foot of the Tresnuten ridge (Fig. S2-10) across the summit area of Skoranuten (1,147 m a.s.l.) to the head of the Simadal valley. On the opposite side of the valley, the moraines continue further northwestwards for another 9 km or so (cf. Fig. 1 in Liestøl, 1963), presumably outlining a past ice sheet margin. Two other systems of pre-LIA moraines are developed in the Skytjedal valley and around the Svolnosvatnet lake (1,075 m a.s.l.).

2.5.8. Ramnabergbreen and the northwestern plateau flank

From Rembesdalskåka, the LIA drift limit trends northwards along the western edge of the plateau towards Ramnabergnuten (1,729 m a.s.l.). Two small ice bodies on Ramnabergnuten's northern flank were likely confluent with the icefield during the LIA maximum, as still seen on the 1932 *gradteigskartet* and evidenced by a continuous cover of fluted drift between the mountain and the plateau summit. The northern LIA maximum limit over Ramnabergnuten is denoted by a densely fluted drift sheet around the northeastern end of the Ramnabergvatnet lake (1,371 m a.s.l.). The radial pattern of the flutings on this foreland points to divergent LIA ice flow from a local ice dispersal area centred on Ramnabergnuten. There are also what seem to be curved segments of subaqueous moraine ridges in the lake, which can be seen on the July 2013 aerial imagery. The Ramnabergnuten drift sheet vanishes at the northwestern arm of the large, unnamed ice-marginal lake (1,412 m a.s.l.) abutting Ramnabergbreen. Instead, a raised shoreline runs along the northern lake side, indicating a previously higher lake level. The drift cover reappears south of the Dyrhaugane massif, where it is extensively fluted and interspersed with short recessional moraines. Its northern boundary is demarcated by glacial drift limits and a prominent elongated boulder blanket, which places the maximum LIA extent of the outlet glacier halfway between the present-day ice front and the Dyrhaugane ridge. The terrain beyond

the drift sheet is weathered bedrock, and there is no geomorphological evidence that Ramnabergbreen advanced further northwards, up the slope and around Dyrhaugane, during the LIA, as depicted on the 1864 *rektangelmålingen* (Fig. 2-2a). An assemblage of short, linear ridges was laid down on the lower northern flank of the 1,585 m-high plateau foothill between two detached ice bodies. The ridges are aligned downhill, perpendicular to the contours of the foothill, and have an ice flow parallel to transverse orientation in alignment with the flutings that occur on the glacier foreland below. They appear (based on aerial photograph interpretation) to be made up of homogeneous fine-grained sediment. Based on these characteristics, the features are interpreted as short eskers (cf. Benn and Evans, 2010).

2.5.9. The north-northeastern plateau flank

Hardangerjøkulen's north-northeastern sector comprises the midsized outlet glacier Bukkaskinnsbreen between the mountains Bukkaskinnsryggen (1,690 m a.s.l.) and Bukkaskinnshjallane (1,760 m a.s.l.), and a separate apron glacier on the northeastern mountainside of Bukkaskinnsryggen. On the 1932 *gradteigskartet*, the apron glacier and the icefield can still be seen as a contiguous ice mass. A relatively thin LIA drift sheet with glacial flutings extends in front of the glaciers. Its lower end forms a thick tongue of glacial drift that stretches down the plateau slope towards an outwash plain around the western shore of Finsevatnet. Latero-frontal moraines at the downslope end of the sediment tongue mark the maximum LIA position. There are only a few other moraines on the glacier foreland, with two small groups of subdued moraine ridges present in the distal part of the drift sheet, and another concentration of moraines around the current ice front of Bukkaskinnsbreen. On the eastern side of the immediate glacier foreland, ice margin parallel ridges of sorted glaciofluvial sediment are present, resulting from drainage guided by the ice margin. Bukkaskinnsbreen's foreland is connected to that of Midtdalsbreen by a densely fluted drift cover at the base of Bukkaskinnshjallane.

2.5.10. Confidence assessment of the presented LIA reconstruction

Hardangerjøkulen's reconstructed LIA outline has a total area of 109.7 km^2. The length of this outline is 82.4 km, of which we categorised individual segments into three classes of confidence (Fig. 2-6): Approximately 49.2 km (59.7 %) of the outline is classed as certain based on unambiguous geomorphological evidence described in the previous sections. Approximately 26.0 km (31.5 %) is interpolated over short distances between segments of unambiguous LIA

outline and is thus defined as fairly certain, whilst 7.3 km (8.8 %) of the outline is less certain and only inferred from the topography of the terrain. The LIA outline of most outlet glaciers falls into the first two categories, being clearly delineated almost throughout by ice-marginal moraines and glacial drift limits. Exceptions are the former cirque outlets Isdøleskåka and Juklanutane, where LIA moraines are sparse or entirely absent, respectively. These outlets were reconstructed by connecting the outermost LIA ice margin indicators (i.e. the trimline in the Juklanutane cirque and the outer cirque-floor moraines at Isdøleskåka) with those nearest on the plateau summit above the cirques. Their lateral margins were drawn to rise relatively symmetrically along the contour lines of each cirque.

Along the edges of the plateau summit, the maximum LIA extent of Hardangerjøkulen is often clearly delineated by distinct glacial drift limits and marked erosional/weathering boundaries (Fig. 2-4). Although currently pronounced, these surface features will become obscured with increasing time after deglaciation by vegetation growth and surface processes (e.g. rainwater and snow meltwater run-off, weathering, etc.). This low preservation potential means that former warm-based or polythermal plateau icefields in ancient landscapes could either be not recognised through absence of evidence or misinterpreted as cold-based (cf. Rea and Evans, 2003).

An area where the exact position of the LIA margin is less clear is the plateau summit between the 1,654 m and 1,569 m peaks of the Juklanutane massif. Here, the LIA reconstruction is based on boundaries between areas of bright (inferred ice-moulded) and darker, rougher looking bedrock surfaces. An alternative possibility is that these boundaries could have been created by patches of perennial snow, which can presently be found in this area. However, the perennial snow patches demonstrate that snow and ice can accumulate and persist here, making it equally feasible that this area hosted LIA ice. Also, the relatively gentle, outwards-sloping summit topography of Juklanutane would have feasibly allowed LIA ice to expand to the plateau edge, as consequently mapped by this study. Applying a negative 100-m buffer to the LIA outline between Isdøleskåka and Juklanutane (Fig. 2-6) reduces the outline area by only 1.0 km^2 (0.9 %).

Hardangerjøkulen's LIA outline has been reconstructed without nunataks. The present-day nunataks in the centre of the icefield each project less than 6 m above the surrounding ice surface (2010 DEM; NVE; unpublished) and are likely to have been ice-covered during the LIA. No nunataks appear in the icefield's centre on the 1932 *gradteigskartet*, where the highest elevation of the ice surface was at 1,876 m a.s.l. (2010 DEM: 1,856 m a.s.l.; 20 m of vertical thinning over an ~80-year period). Potential candidates for LIA nunataks are the summits of the two highest mountain peaks Bukkaskinnshjallane and Søre Kongsnuten along the northeastern plateau edge (Fig. 2-6), which are currently 55 m and 75 m above the surrounding ice surface (2010 DEM), respectively. On the 1932 *gradteigskartet*, this height difference was less than

21 m at Bukkaskinnshjallane and less than 58 m at Søre Kongsnuten (34 m and 17 m of vertical thinning in ~80 years, respectively). Given the proximity of the early-20th-century icefield surface to the two mountaintops, and the flat-topped nature of the summit areas, we speculate that they were ice-covered during the LIA. However, any parts of the summits that did emerge from the LIA icefield would have had a negligible effect on its area (cf. Section 2.7.1.). A nunatak-free LIA icefield is tentatively supported by signs of ice moulding and thin glacial drift on these mountain peaks, as visible on the July 2013 aerial imagery.

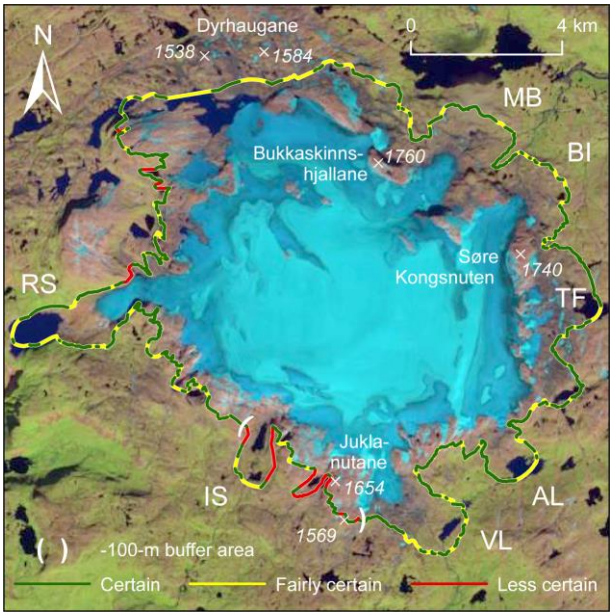

Fig. 2-6. Reconstructed outline of Hardangerjøkulen at its maximum LIA extent, classified into different levels of confidence and overlayed onto a LandsatLook Natural Color image from 03.09.2018 (acquired from https://earthexplorer.usgs.gov/).

2.6. Comparison to modelled LIA extents

The reconstructed LIA icefield was compared to existing LIA model simulations of Hardangerjøkulen (Giesen, 2009; Åkesson et al., 2017). Both studies employ a two-dimensional, vertically integrated shallow ice approximation (SIA), but Åkesson et al. (2017), building on the work of Giesen (2009), use a more up-to-date ice thickness data set as input.

The Åkesson et al. (2017) model (Fig. 2-7) produced a simulation of the icefield's LIA geometry at a resolution of between 200 and 500 m, which varied spatially based on modelled ice velocities. This places the positional accuracy of the modelled LIA outline shown in Fig. 2-7 to ±100-250 m, with additional uncertainties relating to how well the model represents parameters such as subglacial topography, glacier dynamics and past surface mass balance.

Åkesson et al.'s (2017) LIA model matches the geomorphological record presented here reasonably well in general, but underestimates ice cover in the northwest over Ramnabergnuten (by ~970 m), in the northeast around glacier unit 2959 (~750 m), as well as the extent of the outlet glaciers Blåisen (~370 m) and particularly Rembesdalskåka (~1060 m) and Vestra Leirebottsskåka (~900 m). By contrast, the model corresponds very closely to the mapped extent of the cirque outlets Isdøleskåka and Juklanutane, an area for which our proposed LIA limit is based on limited landform evidence. No LIA nunataks are predicted by the model. Our reconstructed LIA area of 109.7 km^2 can be compared to the modelled area of 99.3 km^2. An important factor to consider in this comparison is that the maximum LIA extent identified from the geomorphological record is time-independent, whilst Åkesson et al.'s (2017) model is a snapshot of the icefield at a specific point in time, i.e. AD 1750. As the simulation demonstrates, Hardangerjøkulen and its outlet glaciers likely grew in a nonlinear and asynchronous fashion, so it is possible that the AD 1750 snapshot does not capture the maximum LIA extent of some outlets, which may have been reached earlier or later in time. The Giesen (2009) model overestimates the reconstructed LIA icefield extent, particularly in the north of Hardangerjøkulen.

For the Åkesson et al. (2017) model, only the LIA extent of Midtdalsbreen and Rembesdalskåka was available for model calibration and validation. Our icefield-wide, empirically-constrained LIA reconstruction is a robust data set for improving future models of the Hardangerjøkulen icefield evolution. Comparable modelling studies by Aðalgeirsdóttir et al. (2011) of Hoffellsjökull, an outlet glacier of Vatnajökull, and by Zekollari et al. (2014) of the Vadret da Morteratsch glacier (Switzerland) have successfully used detailed LIA reconstructions to accurately match their models to. However, unlike Hardangerjøkulen these examples are single glacier units, and Åkesson et al.'s (2017) study shows that simulating the evolution of a highly dynamic ice mass with multiple glacier units and outlet glaciers remains a challenge. Future work on dating Hardangerjøkulen's LIA extent, which has so far only been done for the northeastern part (Andersen and Sollid, 1971), would also be useful to icefield modellers.

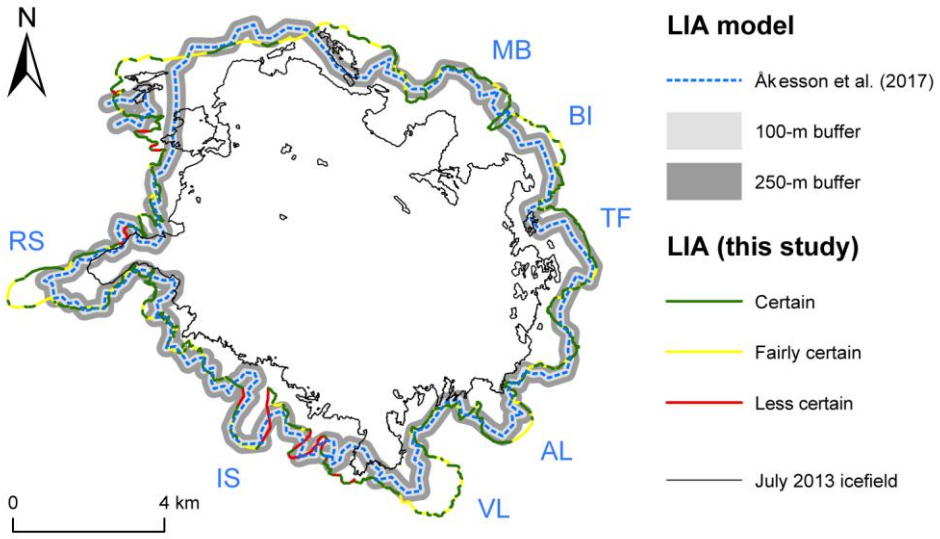

Fig. 2-7. Comparison between geomorphological (this study; shown in classes of confidence) and modelled (Åkesson et al., 2017) LIA reconstruction. The model accuracy of ±100-250 m stated by Åkesson et al. (2017) is illustrated in the form of two buffer zones around the modelled LIA outline.

2.7. Glacier change assessment

In conjunction with former icefield outlines from successive time points since the mid-1920s (Table 2-2), we used Hardangerjøkulen's reconstructed LIA geometry as a benchmark to quantify glacier area and length change up to the present day. One of the greatest sources of uncertainty in relation to remotely-sensed glacier outlines is the inclusion of seasonal snow or snowfields as part of a glacier area (e.g. Racoviteanu et al., 2009). The possible error introduced by this is estimated by Paul and Andreassen (2009) to be 5-10 % for glaciers with an area of > 5 km^2 and up to 25 % for glaciers < 1 km^2 in size. We regard these estimates as an indicator of the possible error range associated with our area change analysis (i.e. 5-10 % for the icefield and its outlet glaciers; up to 25 % for small detached ice bodies), although we did not perform separate error calculations.

All icefield outlines were split into individual glacier units using the hydrological drainage divides from Andreassen et al. (2012a) and the same glacier ID numbers (Fig. 2-8a). The drainage basins had to be manually extended in order to accommodate the pre-1973 icefield dimensions (Fig. 2-8b). Also, since glacier units 2958 and 2967 were originally confluent with Ramnabergbreen (2962) and Blåisen (2966), respectively, their drainage basins were merged into their parent units in the early icefield outlines. Once the two glacier units had become detached from their parent outlets, they were treated as separate entities and glacier area change was assessed independently. Where small ice patches other than glacier units 2958 and 2967

became separated from the icefield from one outline to the next, their area was still included in that of their parent units. This may introduce a low degree of uncertainty because the inclusion of these ice patches can vary between outlines, depending on their source and creator. For instance, all previous glacier inventories generally exclude ice bodies smaller than 0.01 km^2 (Andreassen et al., 2012a; Winsvold et al., 2014).

Absolute and relative glacier area change was calculated stepwise as differences per time interval (A_{t0}-A_{t1}; A_{t1}-A_{t2}; and so on), both for the icefield as a whole and for each individual glacier unit (Fig. 2-8c and d; Table 2-3 and 2-4). Decadal rates of area change were computed in the same fashion using compound interest calculation (Fig. 2-8d) (Andreassen et al., 2008; Zemp et al., 2014), and assuming AD 1750 as the timing of the icefield-wide LIA maximum.

Glacier centrelines were used to assess cumulative glacier length change at 13 icefield units (Table 2-5), excluding four units with extreme changes in glacier geometry through time due to ice-marginal snow (2958; 2959; 2967; and 2970). Average rates of length change were calculated in Table 2-6. Winsvold et al. (2014) employed a DEM-based least-cost path algorithm to generate centrelines for the 1973, 1988 and 2003 glacier inventories of Hardangerjøkulen. Using these as a basis, we manually re-digitised one centreline per glacier unit that was applicable to all time points (Fig. 2-8c). The centrelines were drawn so that they followed the middle of each glacier unit between the glacier head and terminus in the least costly way, whilst still coinciding with the most downvalley part of the glacier front in all time points (Fig. 2-8c).

We compared the findings of our change analysis to surface mass balance data from Rembesdalskåka (continuous data series since measurements began in 1963; Kjøllmoen et al., 2017), and *in situ* length change data based on field measurements of glacier front positions of Rembesdalskåka (since 1917, but with gaps) and Midtdalsbreen (continuous series since 1982), available from NVE.

2.7.1. Areal change

From an original LIA area of 109.7 km^2, Hardangerjøkulen had lost 15.3 km^2 (14.0 %; 0.9 % $10a^{-1}$) by the mid-1920s. Historical survey reports and photographs generally confirm the 1923-29 outline (based on historical mapping) to be accurate (cf. Section 2.4.), but the northern margin at Ramnabergbreen is shown to extend about 150 m beyond our reconstructed LIA limit (Fig. 2-8c). Since such an extended ice front position is not supported by the geomorphological evidence, the 1923-29 outline is regarded as slightly overestimated in this area, although the error is only minimal (0.5 km^2; 0.5 % of the total 1923-29 icefield area). An overestimation of

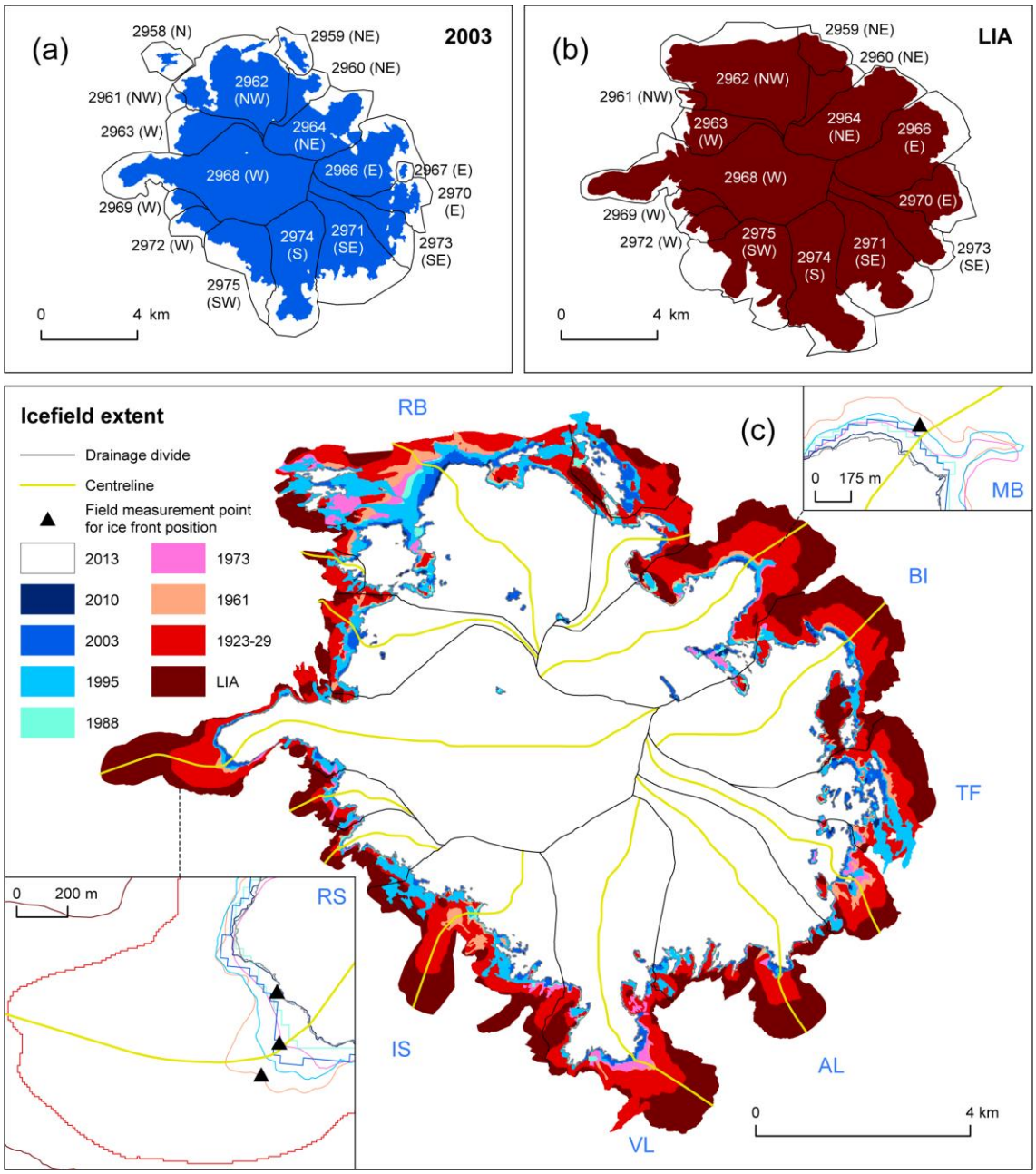

Fig. 2-8. (Continued)

the northern ice margin has already been noted on the 1864 *rektangelmålingen* (cf. Section 2.5.8. and Fig. 2-2). A possible reason for this error might be that the early surveyors and cartographers mapped snowfields attached to the ice margin as part of the glacier. Late-lying and perennial snow is more common on the high upland area in front of Ramnabergbreen than in many other areas of the plateau, as can be observed on multiple series of vertical aerial photographs.

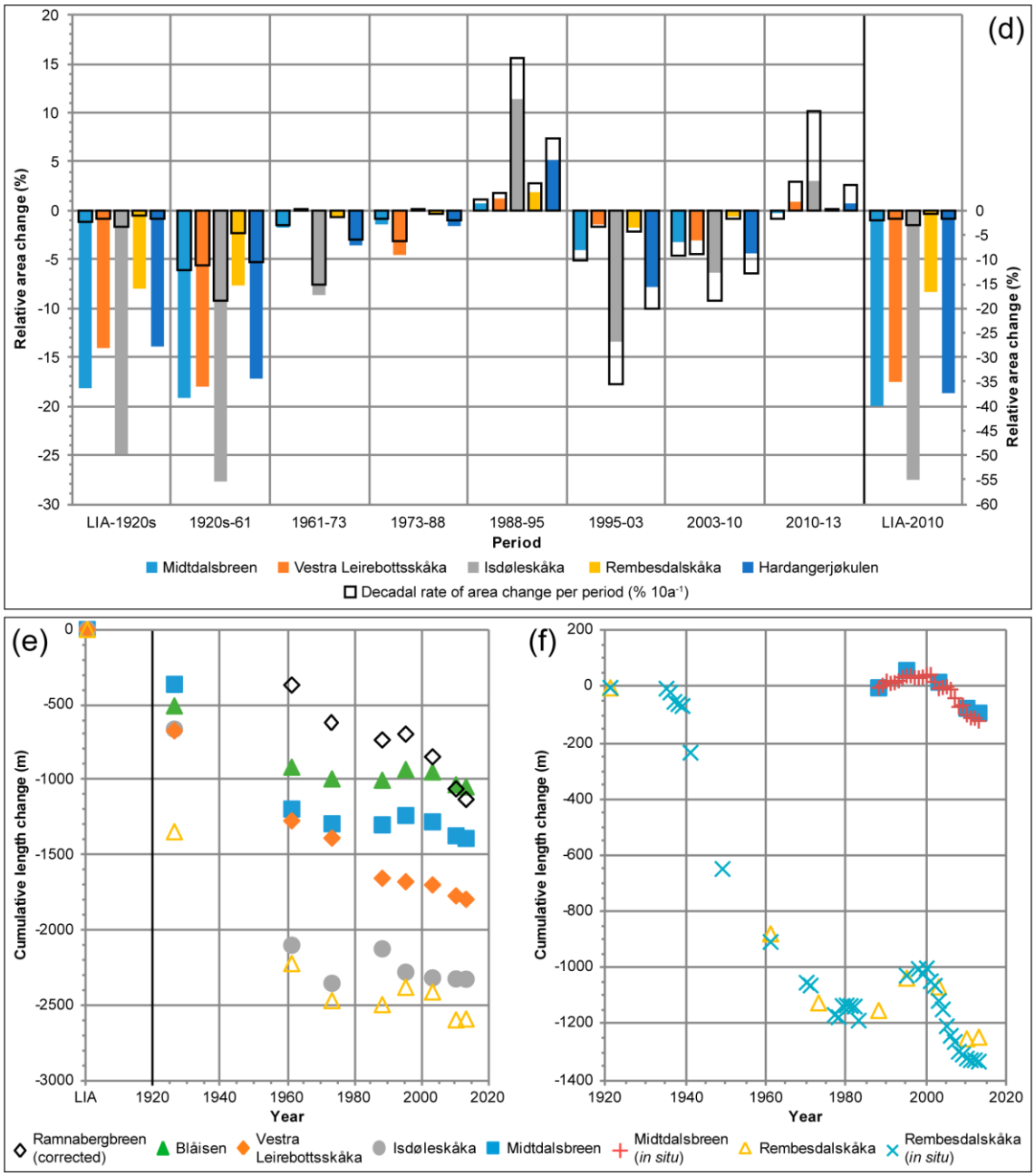

Fig. 2-8. Glacier area and length change at Hardangerjøkulen since the LIA maximum (~AD 1750). (a) 2003 icefield outline with individual drainage basins, glacier ID numbers and glacier aspect data from Andreassen et al. (2012a). (b) LIA icefield outline with extended drainage basins. Glacier ID numbers and glacier aspect information taken from Andreassen et al. (2012a). (c) Icefield recession from the LIA maximum to present using glacier outlines from successive time points. Glacier centrelines used for assessing glacier length change are shown for 13 icefield units. The insets show changes in the glacier front of Rembesdalskåka (RS) and Midtdalsbreen (MB) in greater detail, with triangles marking the locations from where *in situ* frontal position measurements have been or are currently carried out in the field (Data: NVE). (d) Relative glacier area change since the LIA maximum at selected outlet glaciers and at Hardangerjøkulen as a whole. Decadal rates of area change per period, based on compound interest calculation, are shown as open black bars. (e) Cumulative centreline length change since the LIA maximum at selected outlet glaciers of Hardangerjøkulen. (f) Comparison between cumulative centreline and *in situ* length changes at Rembesdalskåka and Midtdalsbreen (Data: NVE).

Icefield recession was most substantial between 1923-29 and 1961 when an area of 16.2 km^2 (17.1 %; 5.4 % $10a^{-1}$) was lost. The strong retreat might have been in response to the observed early-20th-century warming that culminated in the 1930s (cf. Hanssen-Bauer, 2005). In the periods 1961-1973 and 1973-1988, overall icefield recession was relatively minor, with a reduction of 2.8 km^2 (3.6 %; 3.0 % $10a^{-1}$) and 1.1 km^2 (1.5 %; 1.0 % $10a^{-1}$), respectively (note that the 1973 outline of Vestra Leirebottsskåka is based on 1964 aerial photographs; Table 2-2). This is in accordance with surface mass balance measurements at Rembesdalskåka (Andreassen et al., 2016; Kjøllmoen et al., 2016), which record a slightly negative cumulative mass balance of -1.25 m w.e. in the period 1963-1988 (Kjøllmoen et al., 2017). The prominent 1990s readvance that many glaciers along the west coast of Norway experienced in response to several preceding years of increased winter precipitation (Andreassen et al., 2005; Nesje et al., 2008) is recorded at Hardangerjøkulen in the form of an area gain of 3.9 km^2 (5.2 %; 7.3 % $10a^{-1}$) between 1988 and 1995. This is also reflected in Rembesdalskåka's cumulative mass balance, which peaked in 1995 at 6.97 m w.e. (Kjøllmoen et al., 2017). An analysis of icefield elevation change for the period 1961-1995 (Kjøllmoen et al., 2001) reveals that a broad zone from west to east across Hardangerjøkulen, comprising the drainage basins of Rembesdalskåka and Blåisen as well as the icefield centre, thickened by up to 20 m. By contrast, pronounced thinning occurred at the extremities of most other icefield sectors, including across the glacier tongues of Midtdalsbreen, Torsteinsfonna and Vestra Leirebottsskåka. Thinning was particularly severe in the south of the Isdøleskåka drainage basin (up to 35 m) and across the northwestern icefield sector, including the drainage basin of Ramnabergbreen (up to 55 m) (Kjøllmoen et al., 2001).

Since the end of the 20th century, the icefield has been in recession, with area losses of 6.1 km^2 (7.8 %) and 3.2 km^2 (4.5 %) in the periods 1995-2003 and 2003-2010, respectively. Again, this is mirrored in the cumulative mass balance of Rembesdalskåka, which decreased to -2.94 m w.e. by 2010 (Kjøllmoen et al., 2017). The two periods also exhibit the highest decadal rates of area change with -10.1 % $10a^{-1}$ and -6.5 % $10a^{-1}$, respectively (Fig. 2-8d), consistent with the global and regional trend of accelerated 21st-century glacier decline (Vaughan et al., 2013; Stokes et al., 2018). An updated ice thickness change analysis for the period 1961-2010 (NVE) shows almost icefield-wide thinning, which had increased to maximum values of 40-60 m and over 60 m across the drainage basins of Isdøleskåka and Ramnabergbreen, respectively. The 1961-1995 zone of ice thickening (Kjøllmoen et al., 2001) had reduced to a few isolated patches, located primarily in the icefield centre.

A slight area increase of 0.5 km^2 (0.8 %; 2.5 % $10a^{-1}$) is indicated for the final three-year period 2010-2013. However, rather than a true area gain, this is attributed to seasonal snow around the icefield margin being included in the 2013 outline, inflating the glacier extent. *In situ* front measurements at both Rembesdalskåka and Midtdalsbreen in the 2010-2013 period show a clear retreat. A true increase in area is also contradicted by Rembesdalskåka's mass balance,

with predominantly negative balance years in this period (Kjøllmoen et al., 2016) and an overall negative trend in the cumulative mass balance since 1995 (Andreassen et al., 2016; Kjøllmoen et al., 2017). Consequently, icefield-wide area change since the LIA was assessed using the 2010 outline, revealing a total loss of 40.8 km^2 or 37.2 % of the icefield area at the LIA, with a decadal rate of recession of 1.8 % $10a^{-1}$.

The changes in Hardangerjøkulen's area over the different time periods are generally mirrored across individual icefield units (Table 2-3 and 2-4; Fig. 2-8d). Exceptions are the two periods 1961-1973 and 1973-1988, which both show minor icefield-wide area loss, although a combination of area gain and loss can be seen across the individual glacier units (Table 2-3 and 2-4). Rembesdalskåka (westerly aspect) shows the smallest relative area change over the whole measurement period LIA-2010 (-16.6 %), whilst relative area change at Isdøleskåka (southwesterly aspect) is amongst the largest of all icefield units (-55.0 %) (Fig. 2-8d). Vestra Leirebottsskåka (southerly aspect) and Midtdalsbreen (northeasterly aspect) show moderately high relative area changes of -35.0 % and -40.1 %, respectively (Fig. 2-8d). This demonstrates that aspect is not a major control on icefield change. Instead, we speculate that relative area change amongst individual glacier units may be a function of hypsometric factors, specifically the area ratio between outlet- and plateau-based ice. Since changes in the area of a glacier unit can only occur in the outlets, but not on the plateau where the icefield units are joined along shared drainage divides, relative area change is expected to be smaller for glacier units with a large plateau-based area percentage, and vice versa. So Rembesdalskåka has experienced little relative change due to a large plateau area, whilst the opposite is true for Isdøleskåka. Very small icefield units, particularly the detached ice bodies, are subject to extremely high relative area fluctuations, which can be up to ~290 % and are likely caused by seasonal snow included in their outlines.

Our results compare well with other assessments of long-term glacier area change in southern Norway. Baumann et al. (2009) reconstructed the maximum LIA extent of glaciers in Jotunheimen, approximately 125 km to the north-northeast of Hardangerjøkulen (Fig. 2-1), and compared it to 2003 glacier inventory data from Andreassen et al. (2008). They found a total glacier area reduction of 35 % (~100 km^2) from the LIA to 2003, which equals relative area change at Hardangerjøkulen in the same period (-34.3 %; -37.6 km^2; area change calculated for the period LIA-2003). The timing of the LIA maximum in Jotunheimen is thought to have occurred around ~AD 1750, with LIA ages from individual glaciers varying throughout the 18th century (Matthews, 2005). Andreassen et al. (2008) assessed glacier area change in Jotunheimen between 1931-34 and 2003 and found that glacier size had decreased by 23 % (~30 km^2). This again matches relative area change at Hardangerjøkulen (-23.6 %; 22.3 km^2) area change calculated for the period from 1923-29 to 2003) and suggests synchronicity in the areal response of Hardangerjøkulen and glaciers in Jotunheimen to climate warming since the LIA.

Table 2-3. Glacier area of Hardangerjøkulen and its glacier units since the LIA (~AD 1750). Aspect data from Andreassen et al. (2012a). Note that where ice bodies detach to form separate glacier units (i.e. units 2958 and 2967 in 1961 and 1973, respectively), the parent glaciers (i.e. units 2962 and 2966, respectively) record an abrupt artificial area loss, even though this area is still present within the glacier region as a whole.

Glacier unit ID	Glacier unit name	Aspect	Area (km²)								
			LIA	1923-29	1961	1973	1988	1995	2003	2010	2013
2958	*Unnamed*	N			0.4	1.0	0.3	1.1	0.3	0.2	0.3
2959	*Unnamed*	NE	2.2	1.7	0.6	0.5	0.7	1.0	0.7	0.3	0.5
2960	*Unnamed*	NE	2.6	2.3	1.8	1.7	1.7	1.8	1.7	1.6	1.6
2961	*Unnamed*	NW	0.5	0.5	0.2	0.1	0.2	0.2	0.1	0.1	0.1
2962	Ramnabergbreen	NW	15.8	15.1	12.1	11.0	11.1	11.2	9.9	9.2	9.2
2963	*Unnamed*	W	4.0	3.7	3.2	3.0	3.0	3.2	2.9	2.8	2.8
2964	Midtdalsbreen	NE	10.9	8.9	7.2	7.1	7.0	7.1	6.8	6.6	6.5
2966	Blåisen	E	10.9	8.5	7.0	6.5	6.6	6.9	6.5	6.3	6.3
2967	*Unnamed*	E				0.1	0.1	0.2	0.1	0.1	0.1
2968	Rembesdalskåka	W	20.7	19.0	17.6	17.4	17.3	17.7	17.4	17.3	17.3
2969	*Unnamed*	W	1.5	1.0	0.8	0.9	0.8	0.8	0.7	0.7	0.7
2970	Torsteinsfonna	E	4.1	3.4	2.4	2.0	2.0	2.5	1.8	1.4	1.5
2971	Austra Leirebottsskåka	SE	9.5	7.7	6.9	6.8	6.7	7.0	6.7	6.5	6.6
2972	*Unnamed*	W	1.9	1.4	1.2	1.2	1.2	1.3	1.1	1.1	1.1
2973	*Unnamed*	SE	4.9	4.5	3.8	3.6	3.4	3.6	3.4	3.3	3.3
2974	Vestra Leirebottsskåka	S	11.9	10.2	8.4	8.4	8.0	8.1	8.0	7.7	7.8
2975	Isdøleskåka	SW	8.3	6.2	4.5	4.1	4.1	4.6	4.0	3.7	3.8
HAJ	**Hardangerjøkulen**		**109.7**	**94.4**	**78.2**	**75.4**	**74.3**	**78.2**	**72.1**	**68.9**	**69.4**

Table 2-4. Absolute area change per measurement interval and for the overall period LIA-2010.

Glacier unit ID	Glacier unit name	Area change (km²)								
		LIA-1920s	1920s-61	1961-73	1973-88	1988-95	1995-2003	2003-10	2010-13	LIA-2010
2958	*Unnamed*			+0.7	-0.8	+0.8	-0.8	-0.1	+0.1	
2959	*Unnamed*	-0.5	-1.1	-0.1	+0.2	+0.3	-0.3	-0.3	+0.1	-1.9
2960	*Unnamed*	-0.2	-0.5	-0.1	+0.1	+0.04	-0.1	-0.1	+0.005	-1.0
2961	*Unnamed*	-0.1	-0.3	-0.1	+0.1	+0.1	-0.1	-0.03	+0.01	-0.4
2962	Ramnabergbreen	-0.7	-3.0	-1.1	+0.1	+0.1	-1.2	-0.7	-0.01	-6.6
2963	*Unnamed*	-0.3	-0.5	-0.2	+0.005	+0.1	-0.3	-0.1	+0.01	-1.3
2964	Midtdalsbreen	-2.0	-1.7	-0.1	-0.1	+0.1	-0.3	-0.2	-0.02	-4.4
2966	Blåisen	-2.3	-1.5	-0.5	+0.2	+0.3	-0.4	-0.2	+0.03	-4.5
2967	*Unnamed*				+0.01	+0.1	-0.04	-0.04	+0.03	
2968	Rembesdalskåka	-1.7	-1.5	-0.1	-0.1	+0.3	-0.3	-0.1	+0.01	-3.4
2969	*Unnamed*	-0.5	-0.2	-0.03	-0.1	+0.1	-0.1	-0.03	+0.01	-0.8
2970	Torsteinsfonna	-0.7	-1.0	-0.4	-0.1	+0.5	-0.6	-0.4	+0.005	-2.7
2971	Austra Leirebottsskåka	-1.8	-0.8	-0.1	-0.1	+0.2	-0.3	-0.1	+0.04	-2.9
2972	*Unnamed*	-0.5	-0.2	+0.01	+0.05	+0.1	-0.2	-0.03	+0.03	-0.8
2973	*Unnamed*	-0.5	-0.6	-0.2	-0.2	+0.2	-0.2	-0.1	+0.005	-1.6
2974	Vestra Leirebottsskåka	-1.7	-1.8	+0.01	-0.4	+0.1	-0.1	-0.2	+0.1	-4.1
2975	Isdøleskåka	-2.1	-1.7	-0.4	+0.01	+0.5	-0.6	-0.3	+0.1	-4.6
HAJ	**Hardangerjøkulen**	**-15.3**	**-16.2**	**-2.8**	**-1.1**	**+3.9**	**-6.1**	**-3.2**	**+0.5**	**-40.8**

Table 2-5. Cumulative glacier length change at Hardangerjøkulen since the LIA (~AD 1750).

Glacier unit ID	Glacier unit name	LIA centreline length (m)	Cumulative length change (m)								Cumulative length change LIA-2013 (%)
			1923-29	1961	1973	1988	1995	2003	2010	2013	
2960	*Unnamed*	3351	-127	-426	-428	-476	-443	-436	-510	-537	-16.0
2961	*Unnamed*	1299	-504	-666	-1013	-735	-652	-766	-817	-803	-61.8
2962	Ramnabergbreen	4935	285	-84	-334	-449	-410	-561	-774	-844	-17.1
2962*	Ramnabergbreen*	4935		-369	-619	-734	-695	-846	-1059	-1129	-22.9
2963	*Unnamed*	4846	-97	-737	-830	-809	-741	-867	-1137	-1096	-22.6
2964	Midtdalsbreen	5971	-364	-1193	-1291	-1298	-1236	-1278	-1371	-1388	-23.2
2966	Blåisen	5384	-508	-915	-993	-1002	-931	-947	-1032	-1046	-19.4
2968	Rembesdalskåka	11027	-1344	-2220	-2466	-2493	-2378	-2409	-2594	-2588	-23.5
2969	*Unnamed*	2460	-431	-639	-675	-712	-667	-851	-880	-866	-35.2
2971	Austra Leirebottsskåka	6015	-667	-1126	-1359	-1247	-1152	-1212	-1330	-1365	-22.7
2972	*Unnamed*	2385	-226	-327	-368	-428	-399	-480	-472	-462	-19.4
2973	*Unnamed*	6185	-338	-768	-952	-1358	-1086	-1090	-1419	-1413	-22.8
2974	Vestra Leirebottsskåka	6929	-673	-1271	-1386	-1653	-1676	-1697	-1770	-1793	-25.9
2975	Isdøleskåka	4025	-662	-2098	-2351	-2122	-2277	-2315	-2322	-2324	-57.7
Mean[1]		4982	-457	-981	-1133	-1159	-1103	-1169	-1286	-1293	-28.7

* Corrected for overestimation; recalculated without the 1923-29 outline

[1] Excluding uncorrected values for Ramnabergbreen

2.7.2. Length change

Unlike icefield area, changes in glacier length were calculated up to 2013 despite the ice-marginal snow included in this outline, but which did not affect the lower-lying outlet glacier termini. The mean change in cumulative centreline length of the 13 investigated icefield units from the LIA to 2013 is -1.3 km (-28.7 %; -4.9 m a^{-1}). Rembesdalskåka, Vestra Leirebottsskåka and Midtdalsbreen decreased in cumulative length by 2.6 km (23.5 %), 1.8 km (25.9 %) and 1.4 km (23.2 %) from the LIA to 2013, respectively (Fig. 2-8e). At the lake-terminating outlet glacier Ramnabergbreen, calving does not seem to have been a factor in accelerating frontal retreat, even though the ice-marginal lake in front of the outlet already appears on the 1932 *gradteigskartet*. Here, a change in cumulative length of -1.1 km (-22.9 %) from the LIA to 2013 (corrected for overestimation) is below the icefield-wide average. Moreover, the post-1961 length changes at this outlet are probably a function of the observed strong thinning of the glacier unit (Kjøllmoen et al., 2001; NVE). By contrast, rapid terminus retreat by calving is inferred for Rembesdalskåka in the period between the LIA and 1923-29 as well as at Isdøleskåka between 1923-29 and 1961, when the two outlets receded through what is today Rembesdalsvatnet and the inner lake of the Isdøleskåka cirque, respectively, at three times their interval averages of ~0.5 km each (Table 2-6). Overall, frontal retreat at Hardangerjøkulen was

most rapid at the beginning of the 21st century, with length changes averaging -16.7 m a^{-1} in the period 2003-2010, reflecting the global trend (Vaughan et al., 2013; Zemp et al., 2015). Strong retreat can also be observed from the 1920s to 1973, when the investigated icefield units receded by 12.7-15.0 m a^{-1} on average, possibly in response to the early-20th-century warming episode (cf. Hanssen-Bauer, 2005). Glacier length change at Hardangerjøkulen since the LIA is broadly consistent with length change in Jotunheimen, where glaciers retreated by 34 % from the LIA to 2003 (Baumann et al., 2009), as compared to 23 % at Hardangerjøkulen (centreline length change calculated for the period LIA-2003).

Our findings agree well with *in situ* length change data (Fig. 2-8f), revealing only small differences between the two methods (cf. Winsvold et al., 2014). For Rembesdalskåka, cumulative *in situ* length change was calculated for the period 1921-2013 (-1,331 m) and compared to a change in cumulative *centreline* length for the period between 1923-29 and 2013 (-1,244 m), giving a difference of 87 m. For Midtdalsbreen, cumulative *in situ* length change was calculated for the period 1988-2013 (-118 m), whilst the calculated change in cumulative *centreline* length was -90 m in the same period, yielding a difference of 28 m. Both data sets also display the same general trends (Fig. 2-8f). The strong frontal retreat in the first half of the 20th century can be observed in both the *centreline* and *in situ* data from Rembesdalskåka, whilst the 1990s readvance can be seen in both the *centreline* and *in situ* data from Rembesdalskåka and Midtdalsbreen.

Table 2-6. Comparisons of mean length changes of the 13 investigated icefield units for each measurement period.

	LIA-1920s[1]	1920s-61	1961-73	1973-88	1988-95	1995-2003	2003-10	2010-13[2]	LIA-2013[3]
Mean total change (m)	-495	-524	-152	-26	+56	-66	-117	-7	-1293
Mean rate of change (m a^{-1})	-2.8	-15.0	-12.7	-1.7	+8.1	-8.3	-16.7	-2.5	-4.9

[1] Excluding Ramnabergbreen and assuming AD 1750 as the timing of the icefield-wide LIA maximum

[2] Values are likely too low due to ice-marginal snow at some glacier units

[3] Using the mean cumulative change (Table 4)

2.8. Relative chronology of moraine formation

Using the known age of the icefield outlines listed in Table 2-2 as time-markers, a relative chronology of moraine formation (Fig. 2-9) and recession patterns was established. The approach presented here can essentially be employed as a relative dating technique, that is to say, the ice-marginal landforms located between two glacier outlines of known age most likely stem from that interval (taking glacier readvances into account). This allows the relative age of

virtually all moraines developed since the LIA to be assessed in a comprehensive, icefield-wide and rapid manner. It is a time-efficient approach not dependent on laborious data collection in the field, as demanded by, for example, the most commonly applied dating method in LIA chronology, lichenometry (cf. Andersen and Sollid, 1971). The age control on the glacier outlines is excellent (cf. Table 2-2), except for the LIA outline, the age of which should be regarded as an approximation. This produces accurate, albeit only relative, dating results, which can be regarded as less prone to error or methodological weaknesses than lichenometric dating (cf. Osborn et al., 2015). The temporal resolution of the approach will likely increase where a higher frequency of sources for glacier outlines is available. We presume our dating approach to be even more effective in areas where the maximum LIA extent of glaciers occurred at or around the time of accurate topographic mapping campaigns. This might, for example, be the case in Finnmark, northernmost Norway, where the LIA glacier maximum was reached in ~1925 (Wittmeier et al., 2015), not long after the *gradteigskartene* surveys in this area (~1890s; Winsvold et al., 2014).

At Hardangerjøkulen, a substantial number of the moraines around the icefield were produced between the LIA maximum (~AD 1750) and 1923-29 (however, note the long time span between the two outlines, comprising ~180 years, i.e. almost 70 % of the total time). This reflects post-LIA active recession of the outlet glaciers with minor standstills and readvances that created suites of moraine ridges, potentially on an annual basis at Rembesdalskåka and Blåisen (cf. Evans and Twigg, 2002; Evans, 2003). Numerous moraine sequences formed between the LIA maximum and the early 20th century have also been reported from the Jostedalsbreen ice cap (Bickerton and Matthews, 1993), approximately 130 km to the north of Hardangerjøkulen (Fig. 2-1), and from Jotunheimen (Matthews, 2005), indicating very dynamic glacier behaviour across southern Norway in this period. It should be noted, however, that the timing of the LIA maximum at Hardangerjøkulen has only been dated for the northeastern sector of the icefield (Andersen and Sollid, 1971). Studies from other southern Norwegian icefields have shown that LIA ages can vary significantly across outlet glaciers of the same ice mass, e.g. outlet glaciers of Folgefonna (Fig. 2-1): ~AD 1750, ~AD 1870-90 and ~1930 (Tvede, 1973; Bakke et al., 2005a, b); outlet glaciers of Jostedalsbreen: ~AD 1705-1860 according to lichenometric dating by Bickerton and Matthews (1993).

The limit of the 1923-29 outline coincides with an arcuate line of dispersed moraine segments at Midtdalsbreen, but also with moraine ridges at other outlets of Hardangerjøkulen, providing a very narrow and precise age range for these landforms. This is in line with observations made by Fægri (1935) who documented a substantial 1920s advance of Rembesdalskåka, associated with the formation of a prominent frontal moraine. Moraine ridges dating from this time have also been identified at Jostedalsbreen (Bickerton and Matthews, 1993) and in Jotunheimen (Matthews, 2005), pointing towards a regional-scale event.

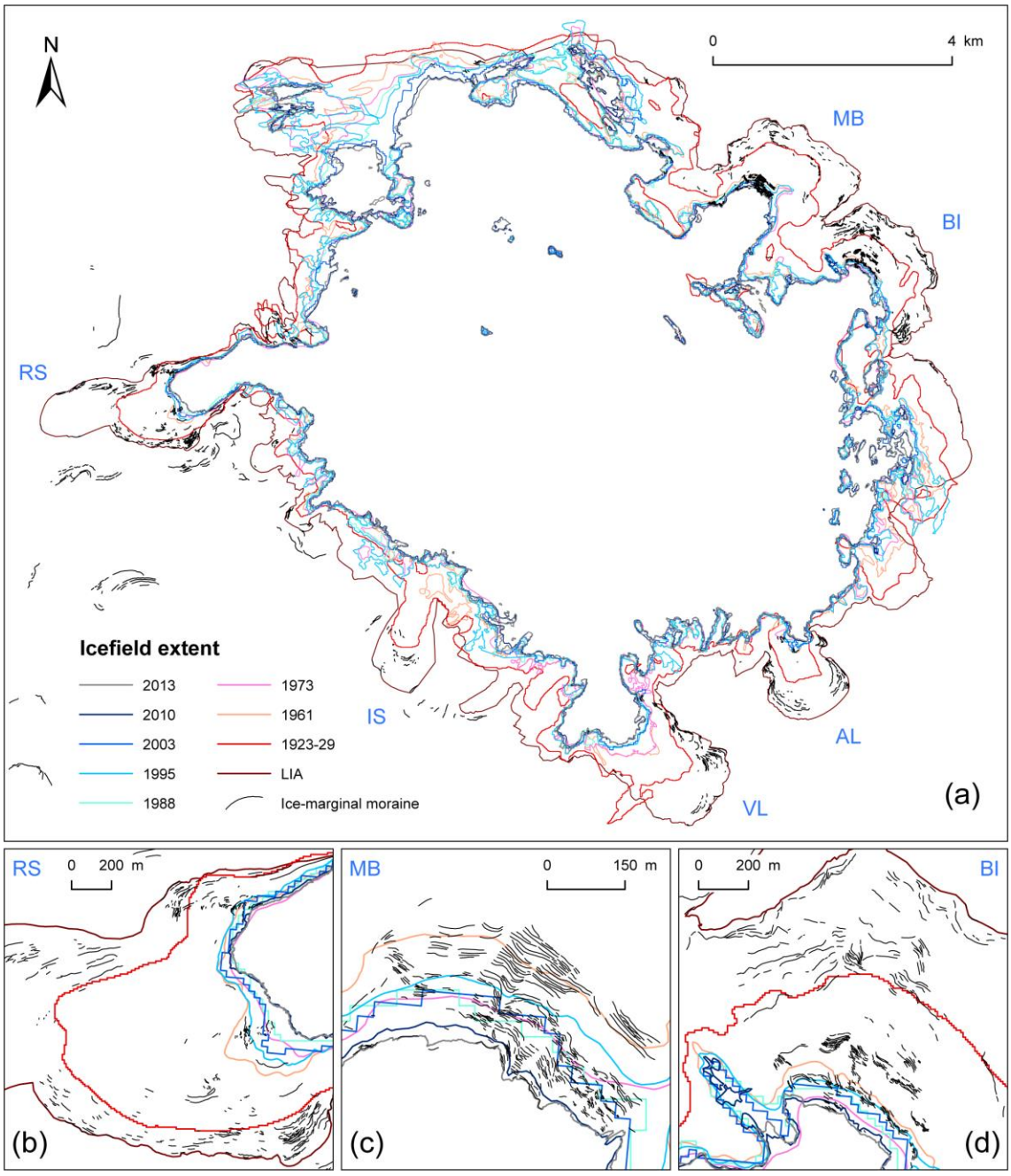

Fig. 2-9. (a) Icefield outlines of known age provide age brackets for the ice-marginal moraines at Hardangerjøkulen (1:100 000). Panels (b) to (d) show moraine formation through time in greater detail at (b) Rembesdalskåka (1:30 000); (c) Midtdalsbreen (1:11 500); and (d) Blåisen (1:24 000).

In the period of strong icefield recession between 1923-29 and 1961, moraine formation virtually ceased at all outlet glaciers, except at Blåisen and in a few lateral positions at Rembesdalskåka (Fig. 2-9b and d). Particularly at Blåisen, moraine ridges continued to develop in densely-spaced, assumed annual, sequences after 1923-29 and into the present day. We hypothesise that differences in the degree of coupling between the glacier margins and the glaciofluvial system may explain the contrasting behaviour of the outlet glaciers (cf. Benn et al., 2003). Rembesdalskåka, Vestra and Austra Leirebottsskåka were at this point beginning to retreat from the sediment- and lake-filled valley floors in front of them onto the bedrock slopes of the plateau flank. At Midtdalsbreen, the foreland exposed in the period between the two outlines is dominated by ice-moulded bedrock, fluted drift and glaciofluvial deposits, often with distinct terrace elements (Sollid and Bjørkenes, 1977). We suggest that strong icefield recession led to the development of highly competent, well-connected meltwater streams at these outlets which efficiently transported any sediments away from the glacier margins into the proglacial environment, inhibiting moraine production ('coupled ice margin'; cf. Benn et al., 2003). These sediments were deposited at Midtdalsbreen in the bowl-shaped depression on the central glacier foreland, whilst they were transferred from the other outlets into the proglacial lake basins and onwards. By contrast, the areas of the Blåisen and Rembesdalskåka forelands where moraines were deposited in this period are reverse bed slopes, and we speculate that the slope topography prevented an efficient proglacial drainage network from being established in these locations. Glacial sediments were not, or only partially, evacuated from the glacier margin, instead remaining around the ice front and becoming available for moraine formation during glacier advances ('decoupled ice margin'; cf. Benn et al., 2003).

After 1961 (or, more precisely, 1955 according to terrestrial photographs analysed by Andersen and Sollid, 1971), moraine formation resumed at Midtdalsbreen (Fig. 2-9c), which had then begun to retreat across a reverse bed slope. Until present, moraine ridges have been produced here on an annual basis during winter advances (Reinardy et al., 2013), signifying rapid outlet glacier response to seasonal changes. The 1990s readvance created ice-marginal moraines at all key outlet glaciers, although in highly varying quantities. At Rembesdalskåka, the readvance is seen predominantly in the form of the fresh zone of ice-moulding around the glacier margin (Fig. 2-5d), and ice retreat from this advance initiated a brief phase of annual moraine development. Since the beginning of the 21st century, Midtdalsbreen has been the only outlet where ice-marginal moraines are still being formed in large numbers.

Our analysis demonstrates that the timing of moraine-forming events can differ between individual outlet glaciers of Hardangerjøkulen. Furthermore, the findings suggest that moraine production and distribution at the landform scale is not solely a result of climate-driven glacier fluctuations, but is also determined by non-climatic, often topographic, factors (cf. Barr and Lovell, 2014; Boston and Lukas, in press). Specifically, here we argue that foreland topography

modulates proglacial drainage and sediment supply, which affects the formation and preservation potential of moraines. This raises an important question as to what extent individual moraine ridges are a reliable proxy for distinct climate signals (cf. Lukas, 2012), as utilised by other workers (e.g. Beedle et al., 2009). Our findings suggest that if moraine sequences are to be used as indicators of past icefield advances (and therefore favourable climatic conditions for icefield growth), the moraine record of a single outlet glacier alone may not be representative.

2.9. Conclusions

Geomorphological mapping of glacial landforms and surficial deposits enabled a reconstruction of the maximum LIA extent of Hardangerjøkulen. In general, the icefield reached the edges of the plateau summit, and its outlet glaciers exhibited extensive advances onto the plateau foreland, covering a total area of 109.7 km^2 at the LIA maximum. Nearly 60 % of the LIA outline was firmly established from ice-marginal moraines, glacial drift limits, trimlines, and identifiable and erosional/weathering boundaries. The remainder was reliably interpolated over short distances between the landform-based sections of the outline. A comparison of our LIA reconstruction to a model simulation of the LIA icefield by Åkesson et al. (2017) reveals that the model, taken at a single time-step of AD 1750, underestimates ice extent of Rembesdalskåka, Vestra Leirebottsskåka, Blåisen and in parts of the northern icefield sector by 0.8 km on average. This suggests that there are unresolved challenges in modelling dynamic icefields with multiple glacier units and outlets.

By using remotely-sensed outlines of the icefield from several time points in the last ~100 years, we were able to track changes in icefield area and length from the LIA to present. By 2010, Hardangerjøkulen had lost 40.8 km^2 (37.2 %; 1.8 % $10a^{-1}$) of its original LIA area; and by 2013, its icefield units had retreated by a cumulative average of 1.3 km (28.7 %; 4.9 m a^{-1}). 20^{th}-century icefield change was characterised by rapid recession in the mid-part of the century, when Hardangerjøkulen decreased in area by 5.4 % $10a^{-1}$ in ~1930-1960 and its termini retreated by 12.7-15.0 m a^{-1} in ~1930-1970, whilst the early 1990s saw a brief re-expansion of the icefield both in area (7.3 % $10a^{-1}$) and average length (8.1 m a^{-1}). Since the end of the 20^{th} century, icefield recession has reached its highest rates on record, with areal shrinkage of 6.5-10.1 % $10a^{-1}$ in 1995-2010 and icefield-wide terminus retreat of 16.7 m a^{-1} in 2003-2010. These results are consistent with the global trend of accelerated glacier decline in the 21^{st} century (Vaughan et al., 2013; Zemp et al., 2015).

The known age of the icefield outlines also allowed us to establish the relative age of virtually all ice-marginal landforms developed since the LIA. Most of the icefield's moraine

ridges date from the period between the LIA and 1923-29, after which moraine formation discontinued (Midtdalsbreen, Vestra and Austra Leirebottsskåka) or was much reduced (Rembesdalskåka) until the early-1990s icefield readvance. Exceptions are Blåisen, where moraines have been continuously produced since the LIA maximum; and Midtdalsbreen, where the mid-1950s marked the beginning of an ongoing and unequalled phase of annual moraine formation. The reason for this discrepancy may be related to the availability of sediment for moraine construction, which we suggest is a function of the capability of the glaciofluvial system to transport sediments away from the outlet glacier margins (cf. Benn et al., 2003). This clear evidence for temporal variations in moraine formation across Hardangerjøkulen's outlet glaciers has important ramifications for the use of moraine sequences as indicators of past icefield advances and attempts to link moraine spacing to changes in palaeo-climate. We therefore propose that the moraine record of a single outlet alone should not be used to make general inferences about past icefield (and climate) fluctuations.

Acknowledgements

We would like to thank Lauren Knight, Benedict Reinardy and Danni Pearce for field assistance. The Finse Alpine Research Centre kindly provided accommodation during part of the fieldwork. Thanks are also due to Henning Åkesson for sharing and discussing his modelled LIA outline of Hardangerjøkulen. PW gratefully acknowledges funding from the EU's Erasmus+ programme and the University of Portsmouth's Placement Scheme for Postgraduate Researchers, enabling invaluable research stays at NVE. Two anonymous referees are thanked for their constructive reviews that helped improve the paper. This work is also a contribution to the Norwegian Copernicus Glacier Service project (Contract NIT.06.15.5). Edited by Atle Nesje.

Funding statement

Fieldwork at Hardangerjøkulen was supported by a number of grants. CMB received INTERACT funding (project acronym PLATREAT) under the European Community's Seventh Framework Programme. PW received financial support from an RGS/IBG Dudley Stamp Memorial Award and a BSG Postgraduate Research Grant.

Author contributions

PW: Conceptualisation; methodology; investigation; writing – original draft; map preparation
CMB, HL, LMA: Conceptualisation; methodology (LMA); investigation (CMB); writing – review and editing; supervision

Data availability

The LIA, 1923-29 and 2013 icefield outlines produced by this study will be made available for download at https://www.nve.no/glacier/ and from *NVEs Breatlas* ('glacier atlas'), along with previously published icefield outlines.

Supplementary materials

Map: *Glacial geomorphology and surficial geology of the plateau icefield Hardangerjøkulen, southern Norway* (1:20 000)

References

Aðalgeirsdóttir G, Guðmundsson S, Björnsson H et al. (2011) Modelling the 20th and 21st century evolution of Hoffellsjökull glacier, SE-Vatnajökull, Iceland. *The Cryosphere* 5: 961-975.

Andersen JL and Sollid JL (1971) Glacial chronology and glacial geomorphology in the marginal zones of the glaciers, Midtdalsbreen and Nigardsbreen, south Norway. *Norsk Geografisk Tidsskrift - Norwegian Journal of Geography* 25(1): 1-38.

Andreassen LM, Elvehøy H, Kjøllmoen B et al. (2005) Glacier mass-balance and length variation in Norway. *Annals of Glaciology* 42: 317-325.

Andreassen LM, Paul F, Kääb A et al. (2008) Landsat-derived glacier inventory for Jotunheimen, Norway, and deduced glacier changes since the 1930s. *The Cryosphere* 2: 131-145.

Andreassen LM, Winsvold SH, Paul F et al. (2012a) *Inventory of Norwegian glaciers.* Oslo: NVE.

Andreassen LM, Nordli Ø, Rasmussen A et al. (2012b) Langfjordjøkelen, a rapidly shrinking glacier in northern Norway. *Journal of Glaciology* 58(209): 581-593.

Andreassen LM, Elvehøy H, Kjøllmoen B et al. (2016) Reanalysis of long-term series of glaciological and geodetic mass balance for 10 Norwegian glaciers. *The Cryosphere* 10: 535-552.

Bakke J, Dahl SO and Nesje A (2005a) Lateglacial and early Holocene palaeoclimatic reconstruction based on glacier fluctuations and equilibrium-line altitudes at northern Folgefonna, Hardanger, western Norway. *Journal of Quaternary Science* 20(2): 179-198.

Bakke J, Lie Ø, Nesje A et al. (2005b) Utilizing physical sediment variability in glacier-fed lakes for continuous glacier reconstructions during the Holocene, northern Folgefonna, western Norway. *The Holocene* 15(2): 161-176.

Barr ID and Lovell H (2014) A review of topographic controls on moraine distribution. *Geomorphology* 226: 44-64.

Baumann S, Winkler S and Andreassen LM (2009) Mapping glaciers in Jotunheimen, South-Norway, during the "Little Ice Age" maximum. *The Cryosphere* 3: 231-243.

Beedle MJ, Menounos B, Luckman BH et al. (2009) Annual push moraines as climate proxy. *Geophysical Research Letters* 36(20): L20501.

Benn DI and Evans DJA (2010) *Glaciers and Glaciation.* London: Hodder Education.

Benn DI, Kirkbride MP, Owen LA et al. (2003) Glaciated Valley Landsystems. In: Evans DJA (ed) *Glacial landsystems.* London: Hodder Arnold.

Bickerton RW and Matthews JA (1993) 'Little ice age' variations of outlet glaciers from the Jostedalsbreen ice-cap, Southern Norway: A regional lichenometric-dating study of ice-marginal moraine sequences and their climatic significance. *Journal of Quaternary Science* 8(1): 45-66.

Boston CM and Lukas S (in press) Topographic controls on plateau icefield recession: insights from the Younger Dryas Monadhliath Icefield, Scotland. *Journal of Quaternary Science*.

Chandler BMP, Lovell H, Boston CM et al. (2018) Glacial geomorphological mapping: A review of approaches and frameworks for best practice. *Earth-Science Reviews* 185: 806-846.

Cullen NJ, Sirguey P, Mölg T et al. (2013) A century of ice retreat on Kilimanjaro: the mapping reloaded. *The Cryosphere* 7: 419-431.

Dahl SO and Nesje A (1994) Holocene glacier fluctuations at Hardangerjøkulen, central-southern Norway: a high-resolution composite chronology from lacustrine and terrestrial deposits. *The Holocene* 4(3): 269-277.

Dahl SO and Nesje A (1996) A new approach to calculating Holocene winter precipitation by combining glacier equilibrium-line altitudes and pine-tree limits: a case study from Hardangerjokulen, central southern Norway. *The Holocene* 6(4): 381-398.

Erikstad L and Sollid JL (1986) Neoglaciation in South Norway using lichenometric methods. *Norsk Geografisk Tidsskrift - Norwegian Journal of Geography* 40(2): 85-105.

Evans DJA (2003) Ice-Marginal Terrestrial Landsystems: Active Temperate Glacier Margins. In: Evans DJA (ed) *Glacial landsystems.* London: Hodder Arnold.

Evans DJA (2009) Controlled moraines: origins, characteristics and palaeoglaciological implications. *Quaternary Science Reviews* 28(3-4): 183-208.

Evans DJA and Twigg DR (2002) The active temperate glacial landsystem: a model based on Breiðamerkurjökull and Fjallsjökull, Iceland. *Quaternary Science Reviews* 21(20-22): 2143-2177.

Fægri K (1935) *Forandringer ved norske breer 1934-35.* Bergens Museums Årbok 1935. Naturvidenskapelig rekke Nr. 6. Bergen: Bergens museum.

Giesen RH (2009) *The ice cap Hardangerjøkulen in the past, present and future climate.* PhD thesis, Utrecht University, Netherlands.

Giesen RH and Oerlemans J (2010) Response of the ice cap Hardangerjøkulen in southern Norway to the 20th and 21st century climates. *The Cryosphere* 4: 191-213.

Grove JM (2004) *Little Ice Ages: Ancient and Modern.* London, New York: Routledge.

Hanssen-Bauer I (2005) *Regional temperature and precipitation series for Norway: Analyses of time-series updated to 2004.* MET report no. 15/2005, 6 September. Oslo: Meteorologisk institutt.

Harsson BG and Aanrud R (2016) *Med kart skal landet bygges: oppmåling og kartlegging av Norge 1773-2016.* Ringerike: Kartverket.

IPCC (2014) *Climate Change 2014: Synthesis Report. Contribution of Working Groups I, II and III to the Fifth Assessment Report of the Intergovernmental Panel on Climate Change* [Core Writing Team, Pachauri RK and Meyer LA (eds)]. Geneva: IPCC.

Jiskoot H, Curran CJ, Tessler DL et al. (2009) Changes in Clemenceau Icefield and Chaba Group glaciers, Canada, related to hypsometry, tributary detachment, length–slope and area–aspect relations. *Annals of Glaciology* 50(53): 133-143.

Kjøllmoen B, Andreassen LM, Elvehøy H et al. (2001) *Glaciological investigations in Norway in 2000.* NVE Report 2 2001. Oslo: NVE.

Kjøllmoen B, Andreassen LM, Elvehøy H et al. (2016) *Glaciological investigations in Norway 2011-2015*. NVE Rapport 88 2016. Oslo: NVE.

Kjøllmoen B, Andreassen LM, Elvehøy H et al. (2017) *Glaciological investigations in Norway in 2016.* NVE Report 76 2017. Oslo: NVE.

Leclercq PW, Oerlemans J, Basagic HJ et al. (2014) A data set of worldwide glacier length fluctuations. *The Cryosphere* 8: 659-672.

Liestøl O (1956) Glacier dammed lakes in Norway. *Norsk Geografisk Tidsskrift - Norwegian Journal of Geography* 15(3-4): 122-149.

Liestøl O (1963) Et senglacialt breframstøt ved Hardangerjøkulen. *Norsk Polarinstitutt Årbok* 1962: 132-139.

Lukas S (2012) Processes of annual moraine formation at a temperate alpine valley glacier: insights into glacier dynamics and climatic controls. *Boreas* 41: 463-480.

Matthews JA (2005) 'Little Ice Age' glacier variations in Jotunheimen, southern Norway: a study in regionally controlled lichenometric dating of recessional moraines with implications for climate and lichen growth rates. *The Holocene* 15(1): 1-19.

Nesje A and Dahl SO (1991) Holocene glacier variations of Blåisen, Hardangerjøkulen, central southern Norway. *Quaternary Research* 35(1): 25-40.

Nesje A, Bakke J, Dahl SO et al. (2008) Norwegian mountain glaciers in the past, present and future. *Global and Planetary Change* 60(1-2): 10-27.

Nesje A, Dahl SO, Løvlie R et al. (1994) Holocene glacier activity at the southwestern part of Hardangerjøkulen, central-southern Norway: evidence from lacustrine sediments. *The Holocene* 4(4): 377-382.

Nussbaumer SU, Nesje A and Zumbühl HJ (2011) Historical glacier fluctuations of Jostedalsbreen and Folgefonna (southern Norway) reassessed by new pictorial and written evidence. *The Holocene* 21(3): 455-471.

Oerlemans J (1997) A flowline model for Nigardsbreen, Norway: projection of future glacier length based on dynamic calibration with the historic record. *Annals of Glaciology* 24: 382-389.

Oerlemans J (2012) Linear modelling of glacier length fluctuations. *Geografiska Annaler: Series A, Physical Geography* 94(2): 183-194.

Osborn G, McCarthy D, LaBrie A et al. (2015) Lichenometric dating: science or pseudo-science? *Quaternary Research* 83(1): 1-12.

Paul F and Andreassen LM (2009) A new glacier inventory for the Svartisen region, Norway, from Landsat ETM+ data: challenges and change assessment. *Journal of Glaciology* 55(192): 607-618.

Racoviteanu AE, Paul F, Raup B et al. (2009) Challenges and recommendations in mapping of glacier parameters from space: Results of the 2008 Global Land Ice Measurements from Space (GLIMS) workshop, Boulder, Colorado, USA. *Annals of Glaciology* 50(53): 53-69.

Rea BR and Evans DJA (2003) Plateau Icefield Landsystems. In: Evans DJA (ed) *Glacial landsystems.* London: Hodder Arnold.

Reinardy BTI, Leighton I and Marx PJ (2013) Glacier thermal regime linked to processes of annual moraine formation at Midtdalsbreen, southern Norway. *Boreas* 42(4): 896-911.

Reinardy BTI, Booth AD, Hughes ALC et al. (2019) Pervasive cold ice within a temperate glacier – implications for glacier thermal regimes, sediment transport and foreland geomorphology. *The Cryosphere* 13: 827-843.

Sollid JL and Bjørkenes A (1977) *Glacial Geology of Midtdalsbreen.* 1:5000. Oslo: Norges Geografiske Oppmåling.

Stokes CR, Andreassen LM, Champion MR et al. (2018) Widespread and accelerating glacier retreat on the Lyngen Peninsula, northern Norway, since their 'Little Ice Age' maximum. *Journal of Glaciology* 64(243): 100-118.

Tennant C, Menounos B, Wheate R et al. (2012) Area change of glaciers in the Canadian Rocky Mountains, 1919 to 2006. *The Cryosphere* 6: 1541-1552.

Tvede AM (1973) Folgefonni – en glasiologisk avviker. *Naturen* 97(1): 11-16.

Vaughan DG, Comiso JC, Allison I et al. (2013) Observations: Cryosphere. In: Stocker TF, Qin D, Plattner G-K et al. (eds) *Climate Change 2013: The Physical Science Basis. Contribution of Working Group I to the Fifth Assessment Report of the Intergovernmental Panel on Climate Change.* Cambridge, New York: Cambridge University Press, pp. 317-382.

Winkler S (2003) A new interpretation of the date of the 'Little Ice Age' glacier maximum at Svartisen and Okstindan, northern Norway. *The Holocene* 13(1): 83-95.

Winsvold SH, Andreassen LM and Kienholz C (2014) Glacier area and length changes in Norway from repeat inventories. *The Cryosphere* 8: 1885-1903.

Wittmeier HE, Bakke J, Vasskog K et al. (2015) Reconstructing Holocene glacier activity at Langfjordjøkelen, Arctic Norway, using multi-proxy fingerprinting of distal glacier-fed lake sediments. *Quaternary Science Reviews* 114: 78-99.

Zekollari H, Fürst J and Huybrechts P (2014) Modelling the evolution of Vadret da Morteratsch, Switzerland, since the Little Ice Age and into the future. *Journal of Glaciology* 60(224): 1155-1168.

Zekollari H, Huybrechts P, Noël B et al. (2017) Sensitivity, stability and future evolution of the world's northernmost ice cap, Hans Tausen Iskappe (Greenland). *The Cryosphere* 11: 805-825.

Zemp M, Armstrong R, Gärtner-Roer I et al. (2014) Introduction: Global Glacier Monitoring—a Long-Term Task Integrating in Situ Observations and Remote Sensing. In: Kargel J, Leonard G, Bishop M et al. (eds) *Global Land Ice Measurements from Space.* Berlin, Heidelberg: Springer, pp. 1-21.

Zemp M, Frey H, Gärtner-Roer I et al. (2015) Historically unprecedented global glacier decline in the early 21st century. *Journal of Glaciology* 61(228): 745-762.

Zemp M, Huss M, Thibert E et al. (2019) Global glacier mass changes and their contributions to sea-level rise from 1961 to 2016. *Nature* 568(7752): 382-386.

Åkesson H, Nisancioglu KH, Giesen RH et al. (2017) Simulating the evolution of Hardangerjøkulen ice cap in southern Norway since the mid-Holocene and its sensitivity to climate change. *The Cryosphere* 11: 281-302.

Chapter 2 – Supplementary figures

Fig. S2-1. Midtdalsbreen. Outermost moraine along the eastern margin of the LIA drift sheet. View towards the west.

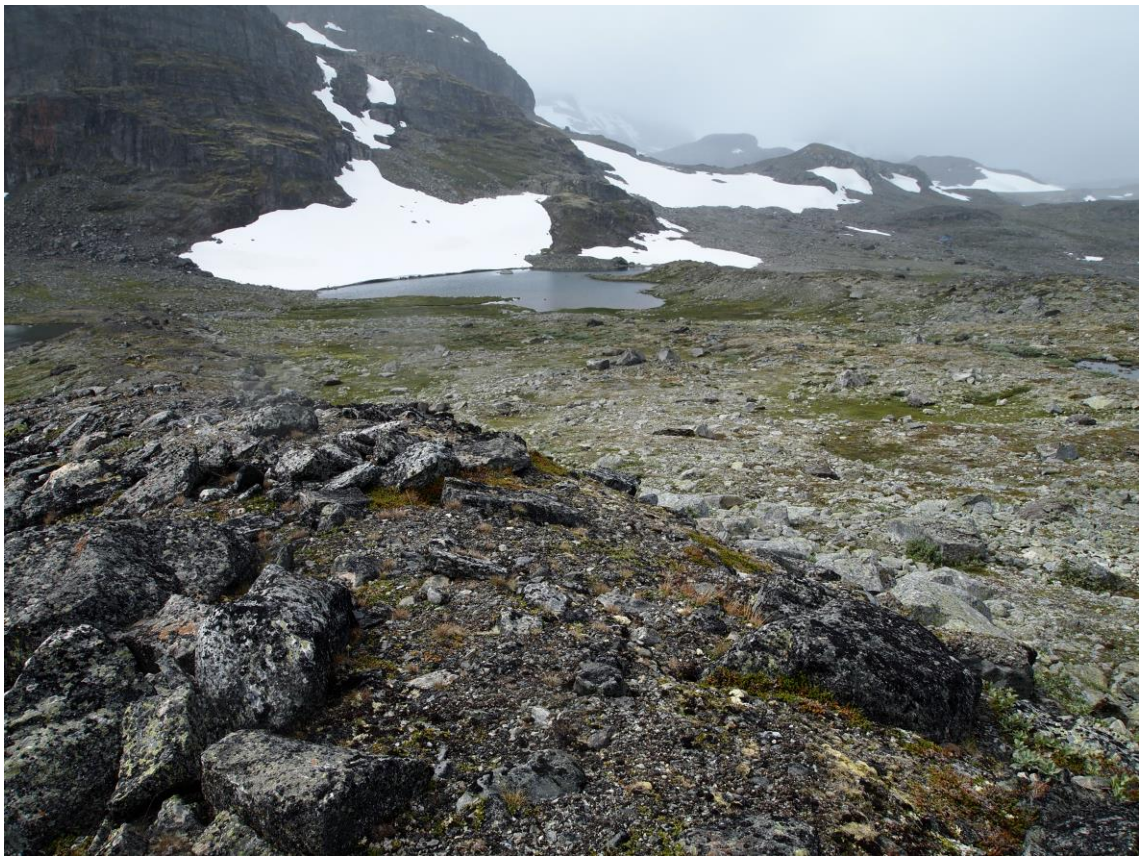

Fig. S2-2. Blåisen. Outermost LIA moraine in the west of the glacier foreland (in the distance to the right of the photograph) stretching towards and along the lake at the foot of the plateau. Photograph taken from the ridge crest of a continuous recessional moraine. View towards the southwest.

Fig. S2-3. Blåisen. Ice-marginal moraines on the far side of the lake mark Blåisen's maximum LIA extent. View towards the northeast.

Fig. S2-4. Blåisen. Suites of recessional moraines are nested around the proglacial lake in front of the small ice apron (in the distance of the photograph) attached to Blåisen's main glacier front (behind the bedrock ridge). View towards the northwest.

Fig. S2-5. Austra Leirebottsskåka. Moraine loops indicate the maximum extent and subsequent fluctuations of the LIA piedmont lobe. Preserved as ridged islets in the Skåltjørna lake. Note the distinctly ice-moulded bedrock inside the moraine loops. View towards the east-northeast.

Fig. S2-6. Vestra Leirebottsskåka. The outlet's maximum LIA extent is marked by an unvegetated area of ice-moulded bedrock, often draped by boulder blankets, on the far side of the lake. Latero-frontal moraine belts (indicated by black arrow) occupy the valley floor on the near side of the lake/river. White arrows indicate short frontal moraine segments on the lower part of the plateau flank. The lateral moraine in the right-hand foreground of the photograph demarcates Vestra Leirebottsskåka's maximum lateral LIA extent. View towards the south-southeast.

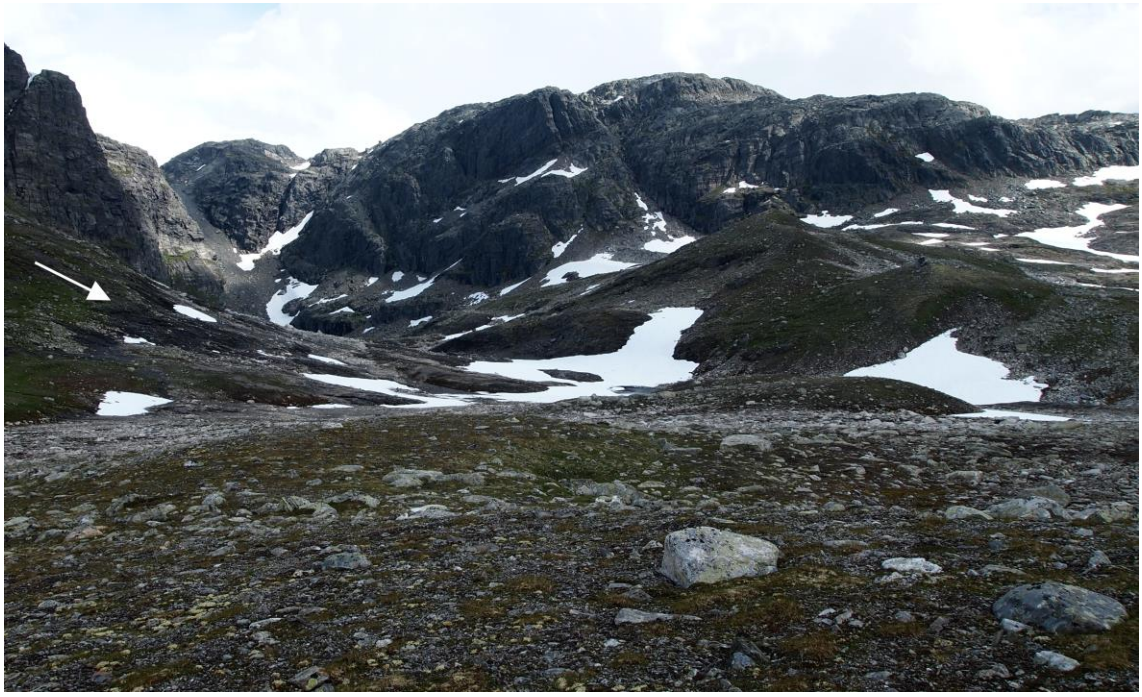

Fig. S2-7. Juklanutane cirque. The trimline along the western side of the cirque mouth (indicated by white arrow) is interpreted to mark the maximum LIA extent of the former cirque outlet glacier. The enormous lateral moraine (partly underlain by bedrock) on the opposite side of the cirque mouth is interpreted to document a pre-LIA glacier advance. In the foreground of the photograph, hummocky patches of glacial drift surrounded by blankets of grey-whitish boulders are visible, which are believed to relate to this pre-LIA glacial event. View towards the northeast.

Fig. S2-8. Isdøleskåka. The lateral moraine ridge on the near side of the outer lake in the left-hand foreground of the photograph is interpreted to delimit the maximum LIA extent of the former cirque outlet glacier. A pre-LIA lateral moraine can be seen on top of the bedrock rim enclosing the cirque basin (indicated by black arrow). View towards the northwest.

Fig. S2-9. Skytjedalsfjellet–Store Tresnuten cirque. The two lakes occupying the upland basin are surrounded by a semicircular system of prominent pre-LIA moraines (indicated by black arrows). The maximum LIA extent of the northwestern cirque outlet glacier is recorded by smaller moraine ridges on the strip of land between the two lakes (indicated by white arrows). Note the ice-moulded bedrock knob protruding into the lake in the foreground of the photograph. View towards the southeast.

Fig. S2-10. Træet cirque. An inconspicuous frontal moraine marks the maximum LIA extent of the former cirque outlet glacier (indicated by white arrow). Prominent ice-marginal landforms, in particular a continuous bouldery lateral moraine (visible in the foreground of the photograph), document a pre-LIA glacier advance. Note the pre-LIA moraines in the distance deposited by Rembesdalskåka. View towards the northwest.

Chapter 3

Paper II – Manuscript submitted to Journal of Glaciology

A peer-reviewed and revised version of this manuscript has been published in the
*Journal of Glaciology, **66**(256), 2020, 259–277*
https://doi.org/10.1017/jog.2020.3
All external readers should refer to the published version. The following version of the manuscript has been slightly amended according to the examiners' comments.

An ~1899 glacier inventory for Nordland, northern Norway, produced from historical maps

Paul Weber[1,*], Liss M. Andreassen[2], Clare M. Boston[1], Harold Lovell[1], Sidsel Kvarteig[3]

[1]University of Portsmouth, Department of Geography, Buckingham Building, Lion Terrace, Portsmouth, PO1 3HE, United Kingdom, *paul.weber@port.ac.uk
[2]Norwegian Water Resources and Energy Directorate (NVE)
[3]Norwegian Mapping Authority (Kartverket)

Abstract

Glaciers depicted on old maps reveal their historical extents, prior to the advent of aerial and satellite remote sensing. Digital glacier inventories produced from these maps can be employed in assessments of centennial-scale glacier change. This study reconstructs the ~1899 (covering the period 1882-1916) glacier extent in the northern Norwegian county of Nordland from historical gradteigskart maps, with an emphasis on examining the accuracy of the mapped glaciers. Glacier outlines were digitised from georectified scans of the analogue maps in a raster graphics editor and were subsequently inventoried in a GIS. The accuracy of the historical glacier extent was established from written descriptions and landscape photographs created during the original field surveys, and further validated against independent glacier outlines of (1) the maximum Little Ice Age (LIA) extent derived from geomorphological evidence, and (2) the 1945 extent derived from vertical aerial photographs. An overall uncertainty of ±17 % is associated with our inventory. Nordland's glaciers covered an area of 1,712 ± 291 km^2 in 1899. By 2000, total ice cover had decreased by 47 % (807 ± 137 km^2) at a rate of 6 % $10a^{-1}$ (80 ± 14 km^2 $10a^{-1}$). The approach presented in this research may serve as a blueprint for future studies intending to derive glacier inventories from historical maps.

Keywords: glacier change, glacier inventory, historical maps, map accuracy, Little Ice Age (LIA), Nordland, Norway

3.1. Introduction

Measurements of the area and extent of glaciers in the form of glacier inventories provide crucial input data for quantifying glacier volume (e.g. Bahr and others, 1997, 2009; Farinotti and others, 2009; Radić and Hock, 2010; Linsbauer and others, 2012; Vaughan and others, 2013) and modelling glacier mass change (e.g. Marzeion and others, 2012; Radić and others, 2014), both of which are needed for estimates of the glacier contribution to sea-level rise. Moreover, repeat glacier inventories provide an important way to monitor and measure changes to the cryosphere (e.g. Paul and others, 2011a; Nuth and others, 2013; Vaughan and others, 2013; Fischer and others, 2014; Gardent and others, 2014), and thereby to the climate system (e.g. IPCC, 2014).

For recent decades, glacier inventories can be compiled with relative ease and at chosen time intervals from satellite images that have been widely available since the 1970s (e.g. Rundquist and others, 1980; Howarth and Ommanney, 1986; Paul and others, 2011b; Pfeffer and others, 2014). Vertical aerial photographs, and topographic maps based on these, provide additional sources for glacier inventories that can also cover a few decades prior to the satellite era (e.g. Andreassen and others, 2008; Paul and Andreassen, 2009; Winsvold and others, 2014). Extending glacier inventories even further back in time typically relies on the availability of 19th- and early-20th-century maps, which can contain valuable information on the historical extent of glaciers and enable glacier change to be assessed on a centennial timescale (e.g. Georges, 2004; Andreassen and others, 2008; Tennant and others, 2012; Cullen and others, 2013; Winsvold and others, 2014; Rastner and others, 2016; Tielidze, 2016; Freudiger and others, 2018; Weber and others, 2019). This is particularly important for placing the rates of 21st-century glacier decline in a broader context. Inventories produced from old maps might also reveal 'disappeared' glaciers that have completely melted away over the course of the last century, which could then be included in improved estimates of 20th-century sea-level rise (cf. Parkes and Marzeion, 2018).

Glacier inventories from historical maps are, in a strict sense, a representation of what the cartographers at the time chose to draw in as glacier ice (this is a noteworthy difference to most satellite-derived inventories, where semi-automatic image classification selects all existing snow and ice bodies, and it is up to the inventory creators to decide which to include/exclude). Their reliability therefore depends on, first, the quality of the historical map source and the precision of the original glacier mapping, and second, how thoroughly map uncertainties were

assessed and taken into account by the inventory creators. The latter has been executed to varying degrees in previous work. For example, Tennant and others (2012) extracted early-20th-century (1903-1924) glacier outlines for the Canadian Rocky Mountains from Interprovincial Boundary Commission Survey maps and examined rates of glacier change into the 2000s. They visually identified mapping and printing inaccuracies and quantified the total inventory uncertainty by combining the root-mean-square error (RMSE) of the georeferenced maps and the error associated with the digitising process. Cullen and others (2013) used a historical map of the 1912 extent of the Kilimanjaro ice masses in eastern Africa as a baseline to track icefield changes into the 21st century. The map was georeferenced, and planimetric distortions corrected by employing a DEM-based approach. In addition, the position of the icefield's outlet glaciers was accurately determined from old photographs and geomorphological (moraine) evidence. The mapping and the digitised glacier outlines were also checked against other available historical observations. Freudiger and others (2018) digitised historical glacier outlines for the Swiss Alps from old Siegfried maps published in the periods 1878-1918 and 1917-1944. They described the history of the maps in detail and evaluated map accuracy in a qualitative manner. An error estimate was also provided for their digitising strategy. As an advance on previous historical map work, Freudiger and others (2018) devised a quantitative test for the validation of former glacier outlines. This involved assessing the degree to which the historical glacier extents fitted into a sequence of glacier outlines from other available inventories, particularly the maximum Little Ice Age (LIA) glacier extent.

This brief review demonstrates that the approaches towards establishing glacier inventories from historical maps have been as different and unique as the map series they were derived from. There is a tendency to presume the historical maps and their contents are essentially true, without further assessing the accuracy of the map source and the mapped glaciers beyond previously published material on the original surveys. It is also common for there to be little or no quantitative error assessments of the applied GIS routines, and/or no attempt to convert such error values into an overall inventory uncertainty (i.e. reporting glacier area without error terms). Occasionally, the publication date of the historical maps is confused with the date of the original map surveys, with the former erroneously taken as the timestamp of the reconstructed glacier extent.

In Norway, only a few attempts to produce early- or pre-20th-century glacier outlines from historical maps have been carried out, focussing on individual plateau icefields (Winsvold and others, 2014; Weber and others, 2019). These studies used the 1:100,000 scale gradteigskartene ('quadrangle maps'), which were Norway's main map series from the mid-1890s (Harsson and Aanrud, 2016). Here, this map series is employed to reconstruct the ~1899 (covering the period 1882-1916; hereafter 1899 inventory, using the median of the survey period) extent of glaciers in the county of Nordland, northern Norway. Nordland's glaciers

make up a third (34 %; 906 km^2) of the total ice-covered area in Norway (2,693 km^2) (Andreassen and others, 2012a). They play a central role in the county's hydropower generation (e.g. Kennett and others, 1997) and can cause jökulhlaups from glacier-dammed lakes with both destructive and beneficial consequences (Holmsen, 1948; Liestøl, 1956; Knudsen and Theakstone, 1988; Engeset and others, 2005; Jackson and Ragulina, 2014). Inventories of glacier change are important for Nordland, as they can be used to help quantify the contribution of glaciers to runoff (cf. Huss, 2011), with implications for hydropower supply, as well as helping to monitor the changing risks from glacier-related hazards.

The aims of our research are (1) to examine the history of the Nordland gradteigskartene maps and the accuracy of the mapped glaciers for their suitability as a glacier inventory; (2) to build a digital GIS inventory of the glacier outlines displayed on the old maps; (3) to independently evaluate the accuracy of the historical glacier extents from geomorphological data and early aerial photographs; (4) to compare the new data set with existing glacier inventories in order to quantify 20th-century glacier change in Nordland; and (5) to offer general recommendations for creating glacier inventories from historical map sources.

3.2. Study area and previous work

Nordland extends for approximately 500 km from 64° 56' N to 69° 19.5' N (Coordinate system: ETRS 1989 UTM Zone 33N), with the northern half located within the Arctic Circle (Fig. 3-1). The county is nearly 38,200 km^2 in area, which comprises around 12 % of mainland Norway's land area. In ~2000, just over 2 % of Nordland was covered by glacier ice, according to the inventory of Norwegian glaciers by Andreassen and others (2012a). This inventory was derived from 1999-2006 Landsat satellite imagery and shows the extent of Nordland's glaciers in 1999-2001 (created in part by Paul and Andreassen, 2009). Additional inventories of Nordland's glaciers are available for ~1976 (1967-1985; created in part by Paul and Andreassen, 2009) and 1988. These form part of the complete glacier inventories of Norway for ~1960 (1947-85; derived from topographic maps based on aerial photographs) and ~1990 (1988-97; derived from Landsat satellite imagery) by Winsvold and others (2014). Here, we use the dates 1976, 1988 and 2000 (the median of each acquisition time range) to refer to the respective Nordland subsets of the glacier inventories (Table 3-1). All glacier ID numbers used in this study to identify individual ice masses are taken from the Andreassen and others (2012a) inventory.

A significant portion of the glacier area in Nordland is contained within the large plateau icefields Vestre and Østre Svartisen, Blåmannsisen (Ålmåjalosjiegŋa) and Okstindbreen (Fig. 3-1). Nordland's glaciers experienced their last major expansion during the LIA (e.g. Grove, 2004). Historical records of a farm being destroyed by Vestre Svartisen's major outlet

glacier Engabreen in the early 1720s (Rekstad, 1892, 1893, 1900), along with radiocarbon (Jansen and others, 2018) and lichenometric (Winkler, 2003; Jansen and others, 2016) dates from the Svartisen area, Høgtuvbreen, and the glaciers in the Okstindan mountains, place the culmination of this glacier advance in the mid-18th century. Moraine evidence just outside the LIA limit of the Okstindan glaciers (Griffey, 1977; Griffey and Worsley, 1978; Winkler, 2003; Bakke and others, 2010) and Engabreen (Worsley and Alexander, 1976) demonstrates that the LIA advance of these ice masses was preceded by a slightly more extensive Neoglacial advance, dated to ~AD 700 at Austre Okstindbreen (Bakke and others, 2010). The first scientific observations on many of the glaciers of Svartisen and Okstindan were made by early explorers, geologists and glaciologists from the late 19th century (e.g. de Seue, 1876; Rekstad, 1892, 1893, 1900; Rabot, 1899; Marstrander, 1910, 1911; see also summaries in Hoel and Werenskiold, 1962 and Theakstone, 1965). The observations show that the glaciers in both the Svartisen and Okstindan areas terminated a short distance from their outer LIA limits at the end of the 19th century. However, whilst Svartisen's non-calving outlet glaciers had been in slow retreat up until the beginning of the 20th century, the Okstindan glaciers had advanced considerably since ~1875 (Hoel and Werenskiold, 1962; Theakstone, 1965, 1990, 2010, 2018; and references therein; Knudsen & Theakstone, 1984). Hoel (1907) also suggested a late-19th-century advance of the Frostisen (Ruostajiekŋa) icefield that ended close to the LIA limit.

More systematic glaciological monitoring, including glacier front position measurements, was initiated in the Svartisen, Okstindan and Frostisen areas in the first decade of the 20th century (e.g. Hoel, 1907; Rekstad, 1910, 1912, 1914; Hoel and Werenskiold, 1962; Andreassen and others, 2005). These investigations document an episode of outlet glacier advance in the 1900s (Hoel, 1907; Marstrander, 1910; Rekstad, 1910, 1912; Hoel and Werenskiold, 1962) and partly into the 1910s at some glaciers in the Okstindan and Frostisen areas (Hoel and Werenskiold, 1962), followed by rapid retreat in the period ~1930-60 (Fægri, 1935; Theakstone, 1965, 1990, 2010, 2018; Hoel and Werenskiold, 1962; Knudsen & Theakstone, 1984; Andreassen and others, 2005; Nesje and others, 2008). Glacier change in the last four decades of the 20th century was spatially more heterogeneous across Nordland (Andreassen and others, 2000). Høgtuvbreen and the glaciers in the Frostisen area continued to retreat, albeit at lower rates. A mixture of advances and retreats occurred in Okstindan and across the different outlet glaciers of Blåmannsisen. Variations in glacier behaviour were even more pronounced in the Svartisen area (Andreassen and others, 2000), where calving contributed to the recession of some outlets (Theakstone, 1990, 2010, 2018). Engabreen, in accordance with other maritime glaciers along the west coast of Norway, readvanced significantly in the 1990s after a period of increased winter precipitation in the late 1980s and early 1990s (Andreassen and others, 2000, 2005; Nesje and others, 2008; Theakstone, 2010). A comparison of the 1976 and 2000 inventory data for the Svartisen–Blåmannsisen region (Paul

and Andreassen, 2009) found no significant changes in either the area of the three plateau icefields or the total glacier area in the region, but saw that areal change became more variable in the smaller glacier size classes. Since the beginning of the 21st century, Vestre Svartisen's outlet glaciers have entered a state of rapid retreat (Andreassen and others, 2005; Nesje and others, 2008; Theakstone, 2018). Engabreen's recent behaviour is reflected in surface mass balance measurements, which have been performed annually at the outlet glacier since 1970. A volume increase of 6.4 m w.e. between 1988 and 2000 was cancelled out by a mass balance loss of 6.1 m w.e. in the period 2000-2017 (Kjøllmoen and others, 2018).

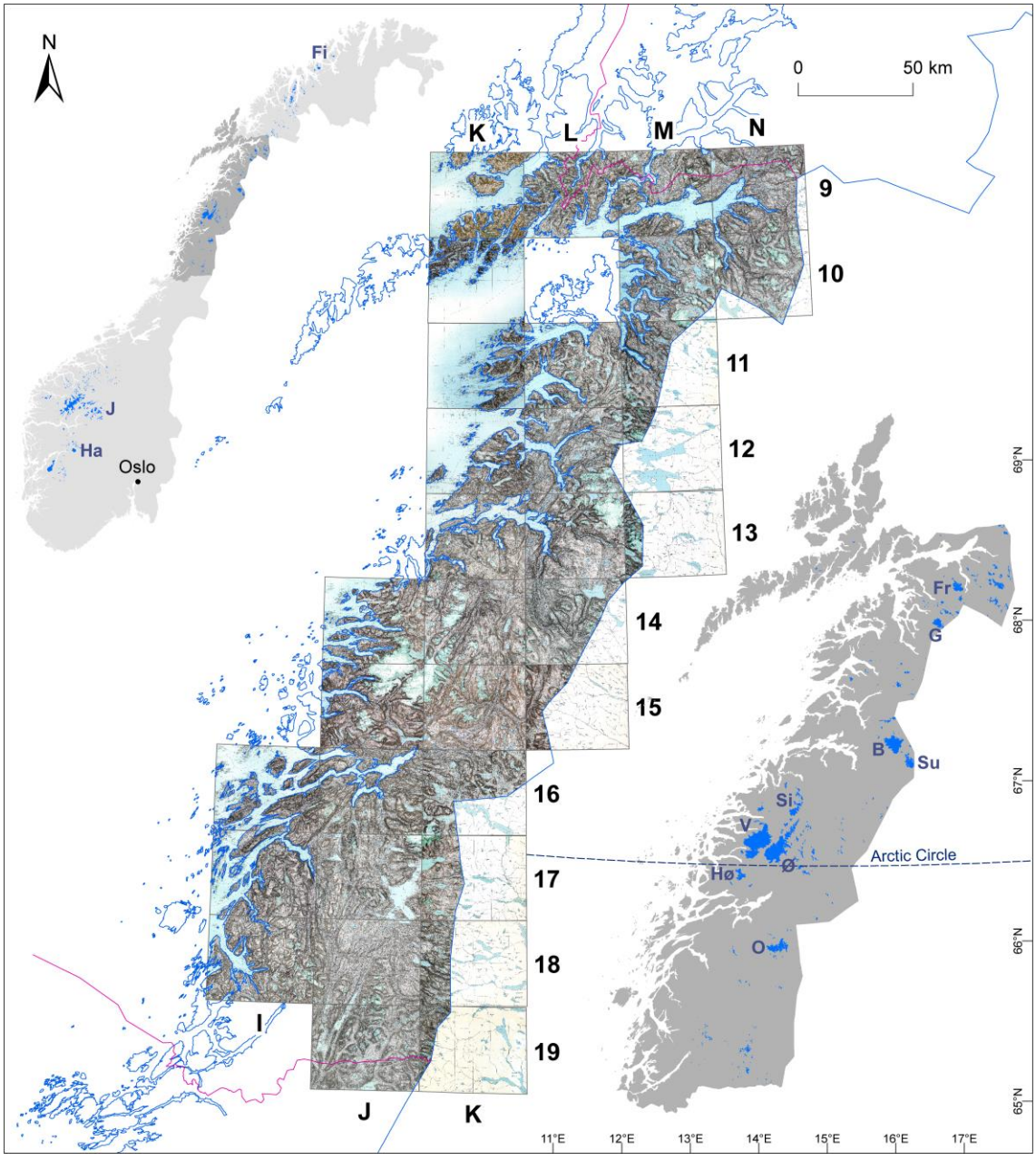

Fig. 3-1. Mosaic of all 33 historical Nordland gradteigskart maps containing glaciers and used in this study. The map sheets are arranged in an alphanumeric grid system. The inset maps show

the location of ice masses in Norway (top-left) and Nordland (bottom-right). Glacier inventory data from Andreassen and others (2012a). Ice masses mentioned in this study are marked. Norway: Ha: Hardangerjøkulen; J: Jotunheimen glaciers; Fi: Plateau icefields in Finnmark. Nordland: O: Okstindbreen; Hø: Høgtuvbreen; Ø: Østre Svartisen; V: Vestre Svartisen; Si: Simlebreen; Su: Sulitjelmaisen (Sallajiegŋa); B: Blåmannsisen (Ålmåjalosjiegŋa); G: Gihtsejiegŋa; Fr: Frostisen (Ruostajiekŋa).

Table 3-1. Published inventories of Norwegian glaciers with available digital outlines.

Glacier inventory	Area covered	Timestamp	Sub-inventory (area)	Sub-inventory (timestamp)	Source	Creator
Historical (LIA)	Jotunheimen, southern Norway	~1750			Geomorphological evidence	Baumann and others (2009)
	Lyngen Peninsula, northern Norway (18 glaciers)	~1750			Geomorphological evidence	Stokes and others (2018)
	Lyngen Peninsula, northern Norway (18 glaciers)	1915			Geomorphological evidence	Stokes and others (2018)
	Hardangerjøkulen, southern Norway	~1750			Geomorphological evidence	Weber and others (2019)
1900	Finnmark, northern Norway	1887-1902			Historical maps (gradteigskart)	Winsvold and others (2014)
	Hardangerjøkulen, southern Norway	1923-1929			Historical map (gradteigskart)	Weber and others (2019)
	Nordland, northern Norway	1882-1916			Historical maps (gradteigskart)	This study
1960	Norway (complete)	1947-1985			Topographic maps based on aerial photographs	Winsvold and others (2014)
			Jotunheimen, southern Norway	1966-1983	Topographic maps based on aerial photographs	Andreassen and others (2008)
			Svartisen–Blåmannsisen, northern Norway	1967-1985	Topographic maps based on aerial photographs	Paul and Andreassen (2009)
			Jostedalsbreen, southern Norway	1966	Topographic maps based on aerial photographs	Paul and others (2011a)
1990	Norway (complete)	1988-1997			Landsat satellite imagery	Winsvold and others (2014)
2003	Norway (complete)	1999-2006			Landsat satellite imagery	Andreassen and others (2012a)
			Jotunheimen, southern Norway	2003	Landsat satellite imagery	Andreassen and others (2008)
			Svartisen–Blåmannsisen, northern Norway	1999-2001	Landsat satellite imagery	Paul and Andreassen (2009)
			Jostedalsbreen, southern Norway	2006	Landsat satellite imagery	Paul and others (2011a)
2014	Lyngen Peninsula, northern Norway	2014			Landsat satellite imagery	Stokes and others (2018)
	Hardangerjøkulen, southern Norway	2013			Digital colour aerial photographs	Weber and others (2019)

3.3. Historical map production and assessment of glacier mapping accuracy

Nordland is covered by a total of 54 gradteigskart map sheets (hereafter referred to as 'maps' or 'map sheets'), of which 33 contain glaciers (Fig. 3-1, Table 3-2). The maps were produced from trigonometrical plane-table surveys that took place between 1882 and 1916. Harsson (2009) and Harsson and Aanrud (2016) provide an overview of the production of the maps, which is important to consider in order to assess their suitability for deriving a reliable glacier inventory (Fig. 3-2a and b).

According to Harsson (2009) and Harsson and Aanrud (2016), the plan for a new 100,000 scale main map series for Norway was set out by Norges geografiske oppmåling (NGO; Norwegian geographical survey; now: Kartverket – Norwegian Mapping Authority) in 1867. A crucial step in the development of this map series was the inclusion of contour lines as a standard map element in 1870. The mapping of northern Norway began at the beginning of the 1880s and introduced the gradteigskartene map format. These maps have a polyconic projection with a prime meridian that runs through the Astronomical Observatory in Oslo. Lines of latitude and longitude define the margins of each map sheet. Since the meridians converge towards the poles, the maps of northern Norway cover a whole degree of longitude (Harsson, 2009; Harsson and Aanrud, 2016). The map sheets are organised in an alphanumeric grid system. Each row of maps was given a number, starting with 1 in the north; and each column of maps was assigned a letter of the Norwegian alphabet in descending order from east to west. The 33 Nordland map sheets showing glaciers are located in rows 9-19 and columns I-N (Fig. 3-1, Table 3-2).

The mapping of Nordland was completed in only 34 years (Table 3-2), with the greatest activity taking place in the 1890s when up to 50 people were working across the county. Geodetic triangulation to supplement the thin network of already existing trigonometric points along the coast commenced in the south of Nordland in the late 1870s and reached the northern county border in 1904. The measurements were carried out with theodolites following instructions that required a high level of accuracy. The heights of the trigonometric points were also established by theodolite, using vertical angular measurements. From 1872 onwards, the coordinates of all surveyed trigonometric points were, as a standard, calculated by employing the least-squares method (Harsson, 2009; Harsson and Aanrud, 2016).

The triangulators were followed by the topographers, who arrived in Nordland in the early 1880s. Work began each season in spring with the snowmelt and continued until autumn when the snow returned. Field surveying took place by plane tabling, which as a method was at a high and refined stage of its development in Norway in the period of the Nordland surveys, as reflected in the skill level of the topographers, the technological standard of the survey instruments, and the availability of field and technical equipment (Harsson, 2009; Harsson and Aanrud, 2016). All aspects of the mapping were guided by detailed and frequently updated

Table 3-2. Overview of published Nordland gradteigskart maps and respective georeferencing details.

Map sheet	Gradteigskart title	Surveyed	Published	Revised in the field	Print version	Printed	Control points	Number of control points	Total RMSE (Forward; m)	Greatest residual error (m)	Polynomial transformation
G19	*Sklinden*	*1883-1897*	*1901*		*1901-3*						
H19	*Helgelandsflesa*	*1883-1889*	*1901*								
I19	*Bindalen*	*1884-1888*	*1901*	*1908*	*1908-2*	*04/1917*					
J19	Börgefjeld	1882-1889	1901				TP	7	14.1	20.0	1st order
K19	Ranseren	1885-1889	1899				TP, BM	6	47.1	61.3	1st order
H18	*Vega*	*1885-1909*	*1900*	*1908*		*10/1916*					
I18	Velfjorden	1885-1889	1894				TP	15	14.3	26.0	1st order
J18	Hatfjelldalen	1887-1892	1896				TP	7	12.7	14.9	1st order
K18	Skarmodalen	1889-1891	1895				TP, BM	5	19.1	28.1	1st order
H17	*Flovær*	*1886-1890*	*1895*	*1908*							
I17	Mosjöen	1886-1890	1895				TP, LH, SL	12	25.0	40.2	1st order
J17	Rösvand	1888-1893	1897				TP	10	18.7	41.1	1st order
K17	Krutfjeld	1891	1896				TP	5	9.9	14.0	1st order
H16	*Skibaasvær*	*1890-1892*	*1900*		*1900-2*						
I16	Dönna	1888-1893	1896				TP, LH, SL	11	7.1	15.1	2nd order
J16	Ranen	1890-1894	1900				TP	15	17.4	37.8	1st order
K16	Umbugten	1891-1894	1897				TP, BM	10	18.8	27.6	1st order
L16	*Virvand*	*1893-1894*	*1897*		*1897-3*						
H15	*Trænen*	*N/A*	*1903*		*1903-3*						
I15	*Lurö*	*1891-1896*	*1904*		*1904-2*						
J15	Svartisen	1895-1897	1901				TP	16	14.4	31.1	3rd order
K15	Dunderlandsdalen	1894-1899	1902		1902-2	*06/1919*	TP	7	1.6	3.3	2nd order
K15*	Dunderlandsdalen	1894-1899	1902		1902-1		TP	7	1.0	2.1	2nd order
L15	Nasa	1895	1898				TP, BM	8	12.5	19.0	1st order
I14	*Valvær*	*1895-1897*	*1904*		*1904-1*						

J14	Melöy	1896-1899	1902			TP, LH, SL	11	18.9	39.1	2nd order
K14	Beiardalen	1898-1905	1907			TP	10	18.9	31.1	1st order
L14	Junkerdalen	1908-1914	1916			TP, BM	8	7.0	12.6	2nd order
J13	*Gildeskaal*	*1897-1899*	*1903*		*1903-2*					
K13	Bodö	1899-1902	1906			TP, LH, SL	10	19.1	28.7	1st order
L13	Saltdalen	1904-1906	1910			TP, LH, SL	14	16.9	34.8	1st order
M13	Sulitelma	1906-1907	1909			TP, BM	4	8.6	13.0	1st order
H12/I12	*Röst*	*1898*	*1900*		*1900-4*					
J12	*Helligvær*	*1899*	*1903*		*1903-2*					
K12	Kjerringöy	1900-1903	1906			TP, LH, SL	8	19.1	28.3	1st order
L12	Sörfold	1906-1908	1914			TP	9	16.3	24.4	1st order
M12	Riddoalgge (Linnajavrre)	1908	1913			TP, BM	5	17.8	25.3	1st order
I11	*Lofotodden*	*1898-1899*	*1903*		*1903-2*					
K11	Steigen	1901-1902	1905			TP, LH, SL	11	22.3	38.4	1st order
L11	Nordfold	1904-1908	1911			TP	7	22.9	34.3	1st order
M11	Hellemobotn	1909-1915	1917			TP, BM	8	18.0	26.8	1st order
I10	*Moskenesöen*	*1898*	*1901*							
J10	*Vestvaagö*	*1894-1896*	*1902*	*1907*	*1907-2*					
K10	Svolvær	1894-1899	1902			TP, LH, SL	10	13.5	29.5	2nd order
L10	*Hamaröy*	*1895-1904*	*1909*							
M10	Tysfjord	1909-1916	1917			TP, BM	14	21.7	30.7	2nd order
N10	Skjomen	1915-1916	1919			TP, BM	14	13.3	26.0	1st order
J9	*Kvalnes*	*1896*	*1902*		*1902-2*					
K9	Hadsel	1896-1898	1904			TP, LH, SL	11	15.6	27.7	2nd order
L9	Lödingen	1899-1905	1907			TP, LH, SL	12	12.7	25.4	2nd order
M9	Ofoten	1900-1902	1905			TP, LH, SL	14	11.3	19.0	2nd order
N9	Narvik	1900-1901	1904			TP, BM	12	20.4	40.8	1st order

K8	*Öksnes*	*1899-1907*	*1908*	*1921*					
L8	*Kvæfjord*	*1909-1911*	*1914*						
L7	*Andöya*	*1907-1912*	*1914*						
		1882-1916	**1896-1919**			**9.9**			
Grad-teigs-måling K15 nv/4*		1894-1899			TP, MT	8	5.1	10.3	2nd order

***** Not inventoried; only used to estimate the map (re-)production error (e_{MR})

Control points: TP - Trigonometric point; BM - Boundary marker; LH - Lighthouse; SL - Sector light; MT - Mountaintop

Map sheets in italics do not contain ice masses and were not used in this study.

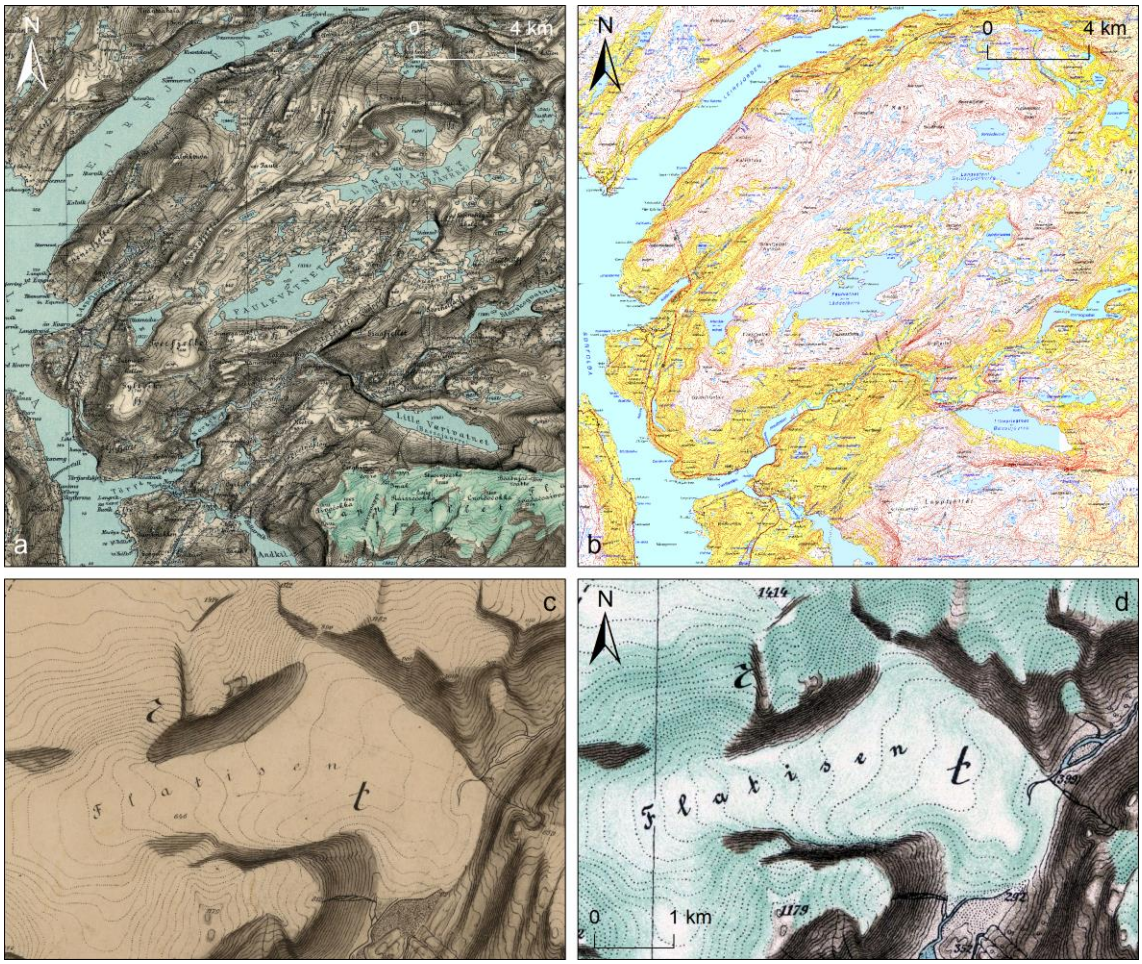

Fig. 3-2. (a) Section of gradteigskartet map sheet L12 Sörfold (1:100,000; produced by an unknown cartographer; published in 1914; Norges geografiske oppmåling; available from Kartverket), displayed at a scale of 1:250,000. An extensive plateau icefield appears to cover the Lappfjellet massif in the southeast of the map area. (b) Modern-day topographic map ('N50 Raster'; Kartverket) with the same extent as (a). Note how well the historical mapping matches the modern mapping, particularly the mapped shoreline of the Sørfolda–Leirfjorden and other water bodies, attesting to the high quality of the old Nordland maps. Also note the restricted ice cover on Lappfjellet, suggesting substantial glacier recession since the beginning of the 20th century. (c) Section of survey map (rektangelmålingen) J15 nö/4 (1:50,000; surveyed by Captain O. H. Paulsen; 1897; Norges geografiske oppmåling; available from Kartverket) showing Flatisen, an eastern outlet glacier of Vestre Svartisen. (d) Flatisen (1:80,000) as depicted on gradteigskartet map sheet J15 Svartisen (1:100,000; produced by T. Lundtvedt and O. Engh; published in 1901; Norges geografiske oppmåling; available from Kartverket).

survey instructions (e.g. Norges Geografiske Opmåling, 1905), which, for instance, stipulated the use of 30 m-intervals for contour lines (drawn as dotted lines over glaciers). Heights were measured by clinometer and aneroid barometer. An updated edition of the survey instructions from 1912 introduced obligatory glacier frontal position measurements (Harsson and Aanrud, 2016). However, this coincided with the final stages of the Nordland surveys and was only carried out at a handful of Nordland's glaciers on map sheets M10 Tysfjord and M11 Hellemobotn, including two outlet glaciers of Frostisen. The 1912 survey instructions and the

results of the frontal position measurements are detailed by Hoel and Werenskiold (1962). After each survey season, the plane-table maps produced in the field were transferred and compiled into clean and uniform survey maps. These are known as gradteigsmålinger ('quadrangle survey maps'; henceforth referred to as 'survey maps') and formed the basis for the final gradteigskartene maps (Kvarteig and others, 2009). However, the maps of southern Nordland in map rows 16-19, including Okstindbreen, were based on rektangelmålinger ('rectangle survey maps'), which would have normally provided the basis for the older, discontinued rektangelkart ('rectangle maps') map format (Kvarteig and others, 2009). All survey maps were hand-drawn, hill-shaded and display glaciers as white features (Fig. 3-2c).

The (re-)production and printing of the final map sheets was a highly complex process involving photogravure and lithography and could take an average of 1.8 years per map (Harsson and Aanrud, 2016). Photogravure was used to make an intaglio printing plate for each map sheet. An accurate drawing of the map was photographed and the negative transferred to a silver-coated copperplate and etched in. A lithographic printing plate was produced for the hill-shading (brown to beige) and the colouration of water bodies (blue) and ice masses (turquoise to beige). The production of the printing plates was carried out by different specialists. The final map was then printed from the two printing plates, with the map colour applied first (Harsson and Aanrud, 2016). In Section 3.4.2., we examine the implications of this multistep printing workflow for the accuracy of the mapped glaciers.

3.3.1. Topographic descriptions and landscape photography

In addition to the mapping, all topographers were required to produce detailed written descriptions of the surveyed areas and the natural landscape features within them (e.g. Norges Geografiske Opmåling, 1905; cf. Hoel and Werenskiold, 1962; Harsson and Aanrud, 2016). Only five of the handwritten descriptions were ever published in the 1920s (L10 Hamaröy, L11 Nordfold, M10 Tysfjord, M11 Hellemobotn, N10 Skjomen), with the bulk of the descriptions archived at Kartverket in Hønefoss, Norway. At the turn of the 19th century, NGO also started to equip topographers with cameras so they could supplement their field mapping with photographs of the surveyed landscape (Aasbø, 2016; Harsson and Aanrud, 2016). These photographs were often taken from the same location as where the mapping was carried out (Aasbø, 2016). Initially intended as an aid for drawing the survey maps after the field season was completed, the landscape photographs were ultimately used for illustrative purposes in the topographic descriptions (Harsson and Aanrud, 2016). Today, both the descriptions and the photographs are invaluable sources of independent evidence to validate the historical maps and, most importantly, the glacier extent displayed on them (Fig. 3-2 and 3-3).

In the context of producing glacier inventories from the maps, a critical question is to what degree the topographers differentiated between glacier ice and perennial/seasonal snow (cf. Racoviteanu and others, 2009). As shown by Paul and Andreassen (2009), seasonal snow attached to a glacier, or even blanketing small glaciers entirely, can conceal the ice margin and may result in the mapping of exaggerated glacier outlines. Perennial snowfields typically occur in locations with favourable topographic conditions (e.g. depression, gullies, etc.) and often exhibit little change over time; thus, including them in a glacier inventory can obscure the signal and magnitude of glacier change in a multi-temporal glacier change assessment (Paul and Andreassen, 2009).

Based on a sample of topographic descriptions and photographs, it appears that the mapping of valley and outlet glaciers was largely accurate. For example, Captain O. H. Paulsen, who surveyed the areas around Høgtuvbreen and the southern sector of Vestre Svartisen in 1895-97 (survey maps J15 sö/4, sv/4, nö/4; map sheet J15 Svartisen), provided an overview of the icefields' outlet glaciers, crevasse patterns and summit areas. He described Vestre Svartisen's former key outlet glacier Flatisen as being,

"formed by the coalescence of three glaciers, one along the valley and two from the northern side, with distinct boundaries, which probably indicates, that these three glaciers have a somewhat differing velocity, although Flatisen in its entire width looks like a continuous ice mass. Flatisen is the only of the glaciers, which stretches right across the valley [Vesterdalen]. It almost forms a natural bridge across the river [Glomåga]." (Paulsen, 1898) (Translated from Norwegian)

Paulsen's description is accurately reflected in his mapping and on the final map (Fig 3-2c and d).

To give another example, First Lieutenant K. M. Leewy, who surveyed the western sector of Blåmannsisen and the adjacent mountains and valleys to the west in 1905 (survey map L13 nö/4; map sheet L13 Saltdalen; Fig. 3-3a), observed that

"Everlasting ice and snow cover large parts of the terrain. Blaamanden [Blåmannsisen] is one of the largest glaciers north of Svartisen. Large areas of [the mountain summits of] Skoffedalsfjeld [Skoffedalsfjellet], Stortveraafjeld [Stortverråfjellet] and Lilletveraafjeld [Blåfjellet] are permanently covered by snow. Snow- and ice-glaciers appear to a certain extent to be of the same size from one year to the next. The size still varies a little in response to the amount of snow in the winter and the temperature in the summer. This year (1905), the amount of snow in the mountains was particularly great because of the heavy snowfall last winter." (Leewy, 1905, p. 170-34) (Translated from Norwegian)

A photograph taken during the 1905 survey (Fig. 3-3c) shows Blåmannsisen's largest western outlet glacier (glacier ID 957) south of the mountain Kjerringa. Much of the glacier and its crevassed surface are snow-free, providing ideal conditions for determining and mapping the exact glacier extent. Proglacial meltwater ponds and streams are visible in the foreground of the photograph. These features are reproduced in detail on the final map (Fig. 3-3a) and demonstrate that the outlet glacier along with its foreland and the position of the glacier margin were mapped with high accuracy. Another pair of photographs, one showing a topographer carrying out a plane-table survey on top of Blåmannsisen (Fig. 3-3d), and the other how equipment is transported on sledges across the icefield (Fig. 3-3e), attests that even the accumulation areas of glaciers and icefields were visited and mapped.

Less clear, however, is the nature of the features on Skoffedalsfjellet, Stortverråfjellet and Blåfjellet, which Leewy describes as perennial snowfields rather than glaciers (whilst also emphasising the substantial amount of snow from the previous winter). Further complicating matters, Leewy used the term 'snow-glacier' ("sne- og isbræerne"; sne = snow; is = ice; bræerne = definite plural form of glacier) in his description, which can either denote a glacier-like mass made up entirely of snow, i.e. a snowfield, or refer to the upper, snow-covered (accumulation) part of a glacier. The term appears to have been frequently used in the latter sense at the time (e.g. Rekstad, 1892, 1893). A survey photograph from the top of Stortverråfjellet (Fig. 3f) shows a wide, plateau-like expanse of snow with mountain peaks on the horizon, resembling a typical surface of a plateau icefield summit. The fragmented remnants of this feature were identified and mapped as small glaciers from the 1999 Landsat scene used for the 2000 inventory (Fig. 3-3b), which is why we lean towards interpreting all three features as glaciers rather than perennial snowfields.

An example of a mapping approach for small glaciers and ice bodies is the topographic description for survey map L12 sv/4 (map sheet L12 Sörfold). Captain O. G. Lund surveyed the coastal mountains south of the Sørfolda fjord in 1908 (Fig. 3-4a) and reported that

"There is no noteworthy everlasting ice or snow, although I have marked down some snow patches in Nordskaret and Sørskaret. In some other places, for instance at Korsviktind [Korsviktinden], I could not determine whether or not the snow will disappear over the course of the summer and have not marked down any glacier." (Lund, 1908, p. 92-1) (Translated from Norwegian)

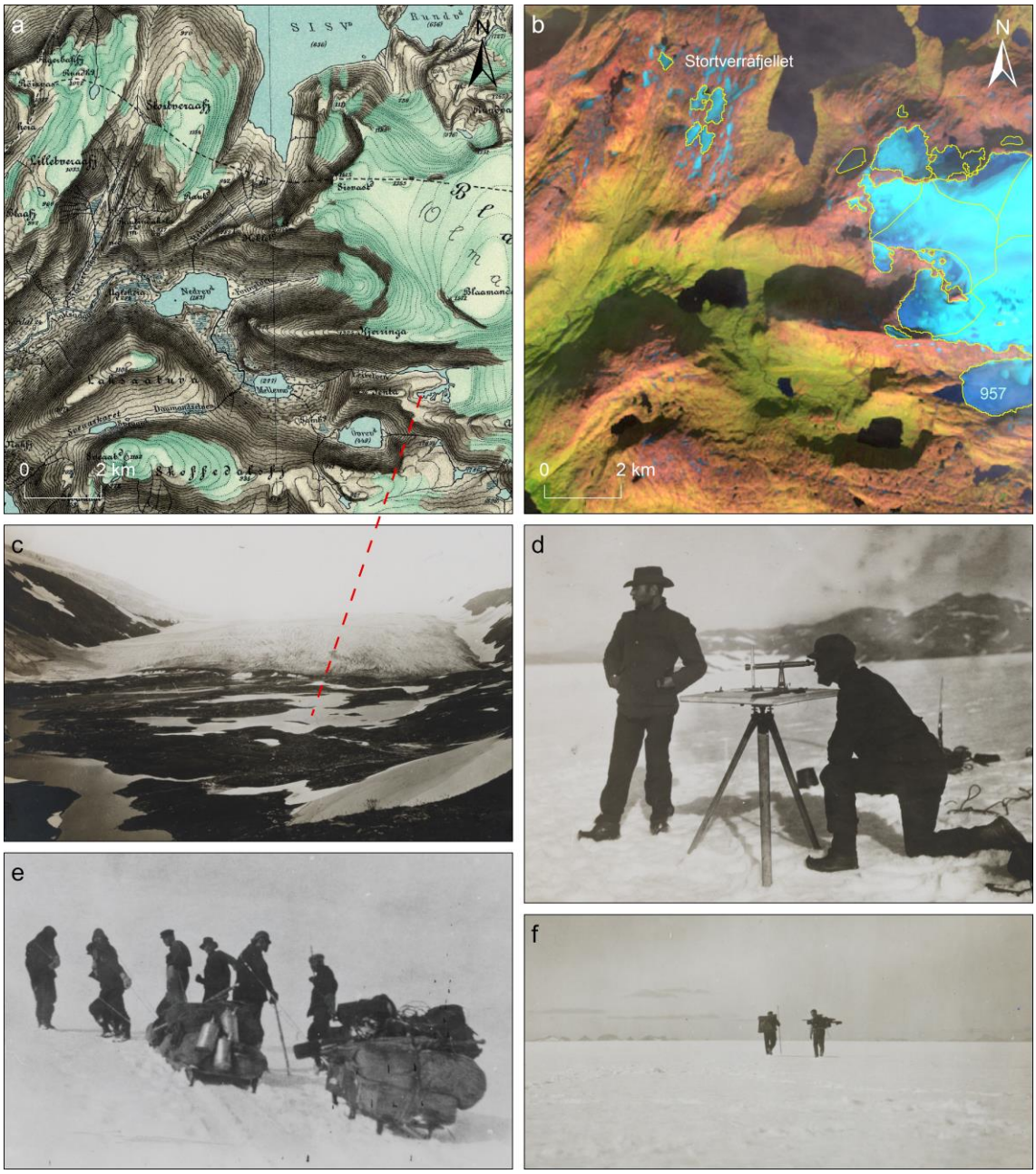

Fig. 3-3. (a) Section of map sheet L13 Saltdalen (1:100,000; produced by T. Lundtvedt and O. Engh; published in 1910; Norges geografiske oppmåling; available from Kartverket) showing the western Blåmannsisen area at a scale of 1:150,000. (b) Landsat-7 scene from 7 September 1999 (bands 5, 4, 3) with the same extent as (a) (Paul and Andreassen, 2009). The 1999 glacier extent, as delineated by Paul and Andreassen (2009), is outlined in yellow. A substantial reduction in ice cover is apparent between the historical map and the satellite image, particularly on the mountain summits to the west of Blåmannsisen. (c) Historical survey photograph of Blåmannsisen's western outlet glacier with ID 957 (Photo: Norges geografiske oppmåling, Nasjonalbiblioteket (National Library of Norway), SKM-S-L13-013). Note the proglacial meltwater system in front of the outlet that is mapped in some detail on the final L13 map. Dashed line shows location of the meltwater system in (a). (d) Plane tabling on top of Blåmannsisen (Photo: Norges geografiske oppmåling, Nasjonalbiblioteket, SKM-S-L13-011). (e) Survey equipment is transported on sledges across Blåmannsisen (Photo: Norges geografiske oppmåling, Nasjonalbiblioteket, SKM-S-L13-028). (f) Surveyors crossing Stortverråfjellet (Photo: Norges geografiske oppmåling, Nasjonalbiblioteket, SKM-S-L13-010). All photographs were taken during the original field surveys.

This account is convincing evidence that the surveyors differentiated between seasonal snow and ice masses, but probably not between glaciers and perennial snow. Yet it also suggests that mapping was conducted with great care and in a conservative manner; if the surveyor could not ascertain whether a feature was seasonal snow or a snow-covered glacier/perennial snow patch, the feature was not mapped in. This is documented by three field photographs from the surveyed area. Fig. 3-4c and d show the two adjacent valleys Midtiskaret and Sørskaret, respectively. Although the mountain flanks at the head of both valleys are draped with what appears to be patches of snow or snow-covered ice, only the most distinct feature in Sørskaret was ultimately mapped. The conservative mapping approach becomes even more evident at Korsviktinden, where no glaciers/perennial snow patches were mapped, despite the snowy mountain flanks visible in Fig. 3-4b.

Our analysis of selected historical survey reports and photographs demonstrates that the glaciers depicted on the Nordland map sheets were mapped carefully, with the omission of seasonal snow. Nonetheless, it is reasonable to expect that the exact mapping approach and quality probably varied (within the framework of the survey instructions) between the individual topographers and between regions (with the latter depending on their accessibility and local snow conditions). In regard to perennial snow, it is interesting to note that many of the topographers used the term 'everlasting' ("evig") snow. We believe that today's strict distinction between glaciers and perennial snowfields may have been more fluid at the time of the surveys, where the concept of permanent snow was also applied to the upper part of a glacier's accumulation area, which is snow-covered in all seasons. The renowned geologist J. Rekstad, for instance, wrote about Høgtuvbreen that

"This mountain ridge [Høgtuva massif] is in large part covered by everlasting snow, which does not have a considerable thickness though. This glacier area sends out some small ice-glaciers; the largest of these stretches eastwards down to 500 m a.s.l., and [the river] Leiraaen [in the Leirdalen valley] originates from it" (Rekstad, 1893, p. 268). (Translated from Norwegian)

This supports the impression that a number of the features described as perennial snowfields and included on the maps are, at least partly, genuine glaciers. Based on these descriptions and the available information on map production, we conclude that the maps are an acceptable data source for a glacier inventory.

On the other hand, a 'cryospheric' inventory that in addition to glaciers also includes all perennial and seasonal snow bodies could be a valuable data set for a range of climatological and hydrological research questions. For example, this would be very useful for assessments of the land area with increased albedo, or the amount of ice and snow available for melt (with implications for flood forecasting and hydropower generation).

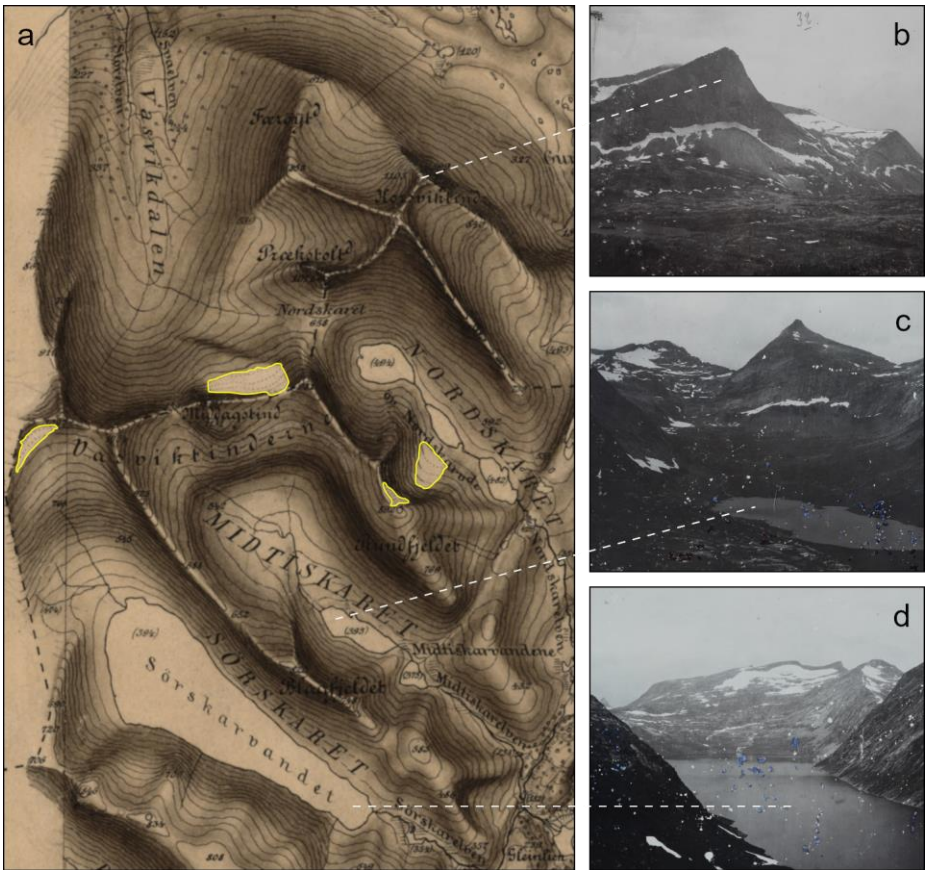

Fig. 3-4. (a) Section of survey map L12 sv/4 (1:50,000; surveyed by Captain E. Falch, First Lieutenant D. Ebbesen and Captain O. G. Lund; 1906-1908; Norges geografiske oppmåling; available from Kartverket) showing the Vassviktindan massif to the west of the Sjunkfjorden. Glaciers are outlined in yellow. Panels (b) to (d) show historical survey photographs of (b) the mountains Korsviktinden (in the foreground to the left) and Færøytinden (in the distance to the right); (c) the Midtiskaret valley and the Midtiskartinden mountain in the distance; and (d) the Sørskaret valley with the Sørskarvatnet lake in the foreground of the photo and the Sørskarfjellet mountain in the distance (Photos: Norges geografiske oppmåling, Nasjonalbiblioteket, SKM-S-L12-009 and SKM-S-L12-010). All photographs were taken during the original field surveys.

3.4. Creating the 1899 Nordland glacier inventory: Methods and error analysis

3.4.1. Georeferencing of map sheets

Digital scans of all 33 map sheets containing glaciers, along with the original survey maps, were downloaded at a resolution of 300 dpi from Kartverket's online database of historical maps (https://kartverket.no/Kart/Historiske-kart/). The map sheets were georeferenced in ArcGIS to the digital 1:50,000 raster map of Norway ('N50 Raster') from Kartverket (Coordinate system: ETRS 1989 UTM Zone 33N). For control points (CPs), we only used trigonometric points, boundary markers on the border with Sweden, lighthouses, and sector lights that were present in

the same location both on the historical map sheets and the N50 raster map. The rationale behind this approach was the assumption that the positions of these critical survey, territorial and navigational markers were measured with the highest possible accuracy for their time, using state of the art survey instruments and techniques (Harsson and Aanrud, 2016), and with the greatest possible care, thus constituting high-quality CPs. We have assumed that the positional accuracy of mapped features away from the trigonometric points may be lower, and that the location of some mapped features may been altered over time due to human activity or natural processes (e.g. the location of river bends, etc.). On average ten CPs were obtained per map sheet (Table 3-2), ranging from a maximum of 16 CPs to a minimum of 4-5 CPs for some of the map sheets covering the border region with Sweden, of which major portions show unmapped Swedish territory. We applied first- to third-order polynomial transformations depending on the best visual match to the reference data (Table 3-2). Two-thirds of the map sheets (n = 23) were transformed using a first-order polynomial, which yielded an average RMSE of 18 m, whilst a second-order polynomial was chosen for nine maps (average RMSE of 12 m), and a third-order polynomial for one map sheet (RMSE of 14 m). The georeferenced maps were permanently transformed (i.e. georectified) and saved as GeoTIFF raster images.

Tennant and others (2012) quantified the uncertainty associated with their historical glacier extent by using the RMSE as one part of a buffer around the digitised glacier polygons. A buffer created from the weighted average of our RMSE values (17 m) changes the glacier area of our inventory by ±6 %. However, our RMSE values are based on different polynomial transformations and so technically can not be combined into a single value. Moreover, we mainly employed first-order polynomial transformations, which essentially only shifted, scaled and rotated the rasters. Since these operations are unlikely to have influenced the area of the features shown on the maps, we do not regard the RMSE as a suitable measure of the uncertainty associated with the glacier extent.

3.4.2. Digitising of glacier outlines

Based on the turquoise to beige colouration of the mapped glaciers, we digitised their outlines on-screen in a raster graphics editor (GIMP) in a semi-automated manner, rather than by manual editing in a GIS. Since most raster editors, including GIMP, do not support GeoTIFF files and strip them off their geospatial information, we had to store this information in separate world (.tfw) files before beginning the digitising work. We used a raster editor tool within GIMP that automatically identifies and selects image pixels and areas of similar colour. A colour value threshold of 0 to 255 can be set to adjust the range of colour to be included in the selection. We found that thresholds of 10-15 colour values produced adequate outlines for many of the

glaciers. A major obstacle to our approach, however, was that the mapped glaciers were drawn and printed without clear boundary lines and often display a blurred transition from glacier ice to the surrounding terrain surface (Fig. 3-5a). This resulted in the automatic selection also including areas of similar colour beyond the glaciers (Fig. 3-5b). Additional and careful manual post-processing was therefore necessary to obtain the final glacier outlines, which we consider accurate to the pixel level (Fig. 3-5b). We compared the post-processed, pixel-accurate glacier outlines for map sheet J14 Melöy to automatic selections based on thresholds of 10 and 15 colour values and found that the threshold-only selections were 1 and 4 % larger in total area, respectively.

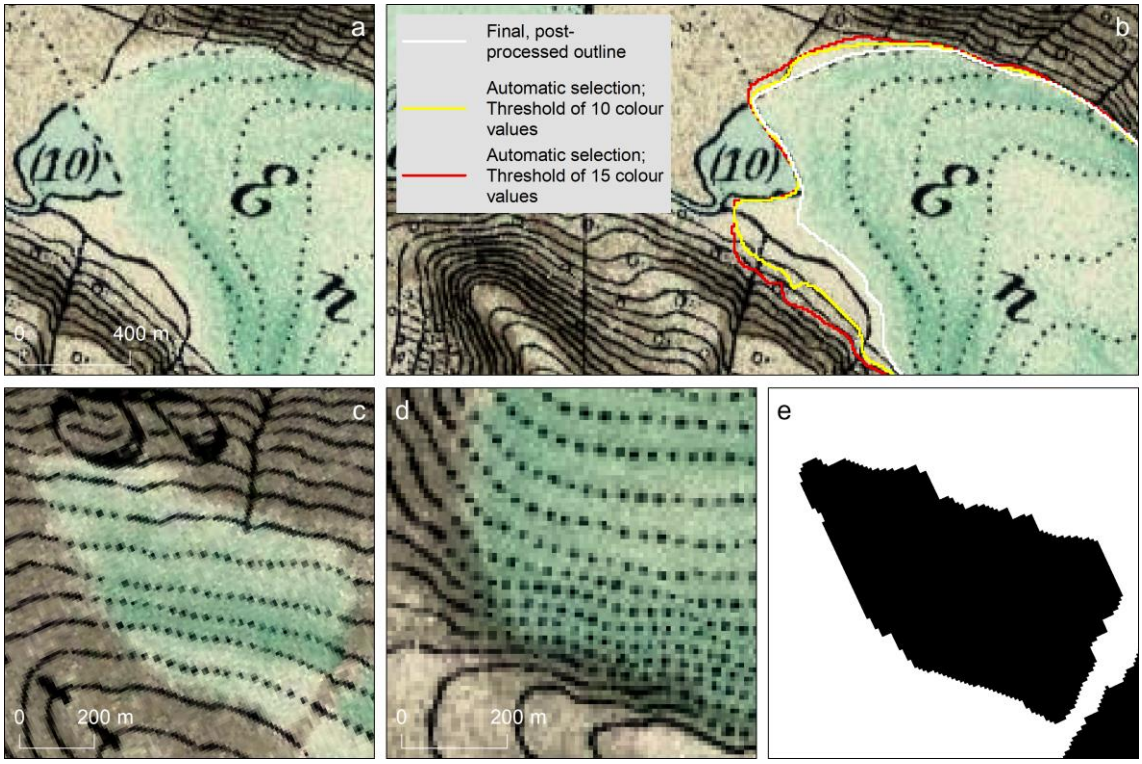

Fig. 3-5. (a) Tongue of Vestre Svartisen's major outlet glacier Engabreen (1:23,000), as depicted on map sheet J14 Melöy (1:100,000; produced by T. Lundtvedt and O. Engh; published in 1902; Norges geografiske oppmåling; available from Kartverket). Note the blurred transition between the ice front and the glacier foreland. (b) Digitised outlines of Engabreen's tongue based on (1) automatic selections using different colour value thresholds and (2) manual post-processing of the best-fit selection to derive the final glacier outline. Due to the poorly defined ice margin, the automatic selections also included areas of similar colour beyond the glacier. By contrast, note how accurately the automatic selections detect the glacier extent along the northern valley side where terrain contour lines and hill-shading provide a clear boundary line for the glacier. (c) Example of solid terrain contour lines extending into a glacier surface. (d) Example of dotted glacier contour lines outside a turquoise glacier surface. Faint traces of turquoise printing ink seem to be visible around some of the dots. (e) Black raster polygon of the glacier depicted in (c). This stencil-like black-and-white raster was imported into ArcGIS to generate the glacier polygons for the GIS inventory.

A few cases of small discrepancies occur on the maps where solid terrain contour lines extend into glacier surfaces (Fig. 3-5c); and conversely, where dotted glacier contour lines continue across hill-shaded terrain surfaces (Fig. 3-5d). A potential explanation for these mismatches may be that the complex, multistep map production process described in Section 3.3. resulted in small misalignments between the coloured glacier areas and the line features of the maps. Following our digitising approach, in many of these cases the glacier extent was determined based on the colour extent. Exceptions were made where faint traces of turquoise were visible on terrain surfaces with dotted glacier contour lines, suggesting that the glaciers' original printing ink did not properly adhere to the map paper during lithography, or may have faded over time. Such areas were included as part of a glacier. Overall, we estimate the digitising error (e_D) of the final, colour-based glacier outlines to be not more than one row of pixels around the polygons. With the sides of a pixel in the 300 dpi raster maps equalling a length of circa 9 x 9 m, applying a 9 m-buffer to the glacier polygons changes the area of our inventory by ±4 %.

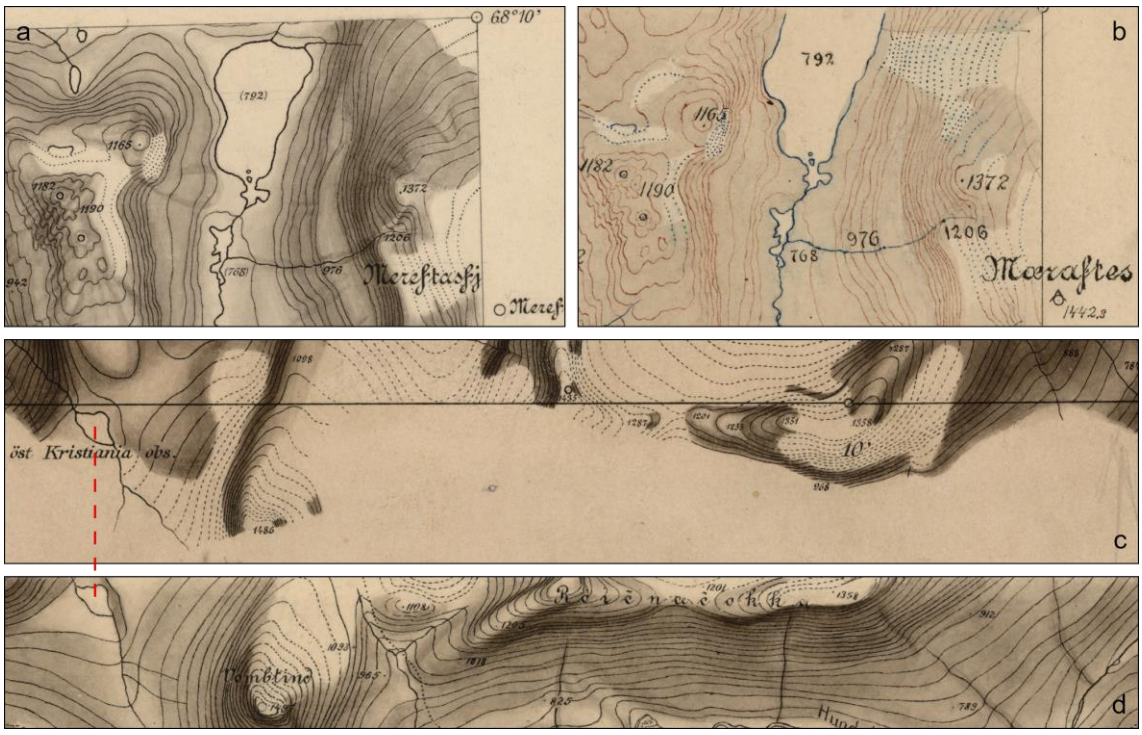

Fig. 3-6. In panels (a) and (b), two versions of survey map M10 sö/4 both depict the area around the Snøvatnet lake to the west of the Meraftesfjellet massif. (a) Classic version in the design of the 1905 survey instructions (1:50,000; surveyed by Captain O. B. Getz, Captain S. Nielsen and Captain O. Thue; 1913-1914; Norges geografiske oppmåling; available from Kartverket). (b) Modern-styled version in the design of the 1912 survey instructions (1:50,000; surveyed by Captain O. B. Getz and Captain S. Nielsen; 1913-1914; Norges geografiske oppmåling; available from Kartverket). Note the outlet glacier flowing down from Meraftesfjellet to Snøvatnet, which is not mapped in (a). Also, the group of ice patches to the west of the lake appears as only two ice bodies in (a). Panels (c) and (d) show ice cover to the south of the

Blåisen (Beajojiekŋa) glacier, as mapped in 1900-1901 on survey map N9 sö/4 (c) (1:50,000; surveyed by Captain F. Abrahamson; 1900-1901; Norges geografiske oppmåling; available from Kartverket) and in 1916 on survey map N10 nö/4 (d) (1:50,000; surveyed by Captain T. Nummedal and First Lieutenant E. Bjørstad; 1915-1916; Norges geografiske oppmåling; available from Kartverket). Dashed line links the same lake in both maps. The 1916 ice extent depicted in (d) is visibly more restricted than it was in 1900-1901 (c).

Each digitised glacier polygon, including its extent and any nunataks, was also compared and validated against the original survey maps. This showed generally good agreement for almost all mapped glaciers. However, we found 21 surveyed ice bodies, with an average size of only 0.04 km^2, that were not included on the maps, and which we subsequently added to our data set. For some of the excluded glaciers, a likely reason for their omission may be that they are in locations covered by map labels on the final maps. In a few other instances, very small glacier patches that had originally been surveyed as two adjacent ice bodies appeared as one glacier on the maps. We suspect this is the result of generalisation during upscaling of the 1:50,000 survey maps to the 100,000 maps, and thus digitised them as separate ice bodies. In a third case, two versions of the same survey map (M10 sö/4; surveyed 1913-1914), one in the classic design of the 1905 survey instructions, and the other in the more modern design of the 1912 instructions, display differing ice cover in the western part of the Meraftesfjellet massif to the south of Frostisen (Fig. 3-6a and b). The classic version was the basis for the final map sheet M10 Tysfjord. The more modern-styled version of the survey map shows an outlet glacier descending from Meraftesfjellet down to the Snøvatnet lake, in addition to a group of small ice patches to the west of the lake (Fig. 3-6b). By contrast, only two ice patches are present on the classic version of the survey map, whilst the outlet glacier is absent (Fig. 3-6a). Hoel (1907), who investigated and described the Frostisen and Meraftesfjellet icefields in detail, does not report the existence of an outlet in this location, so we regard the modern-styled survey map as incorrect. Lastly, we discovered one case where the same glacier-covered area at the boundary between two survey maps (N9 sö/4; N9 Narvik and N10 nö/4; N10 Skjomen) had been surveyed twice at different dates (1900-1901 and 1916, respectively) by different topographers (Fig. 3-6c and d). A clear reduction in local ice cover is observable in the 15 years between the surveys, which may either represent a true glacier retreat, or may just be due to a more selective mapping approach of the later topographer. The glacier extent on the final N10 map sheet is based on the 1916 survey map, which is the year we have assigned to the inventoried outlines.

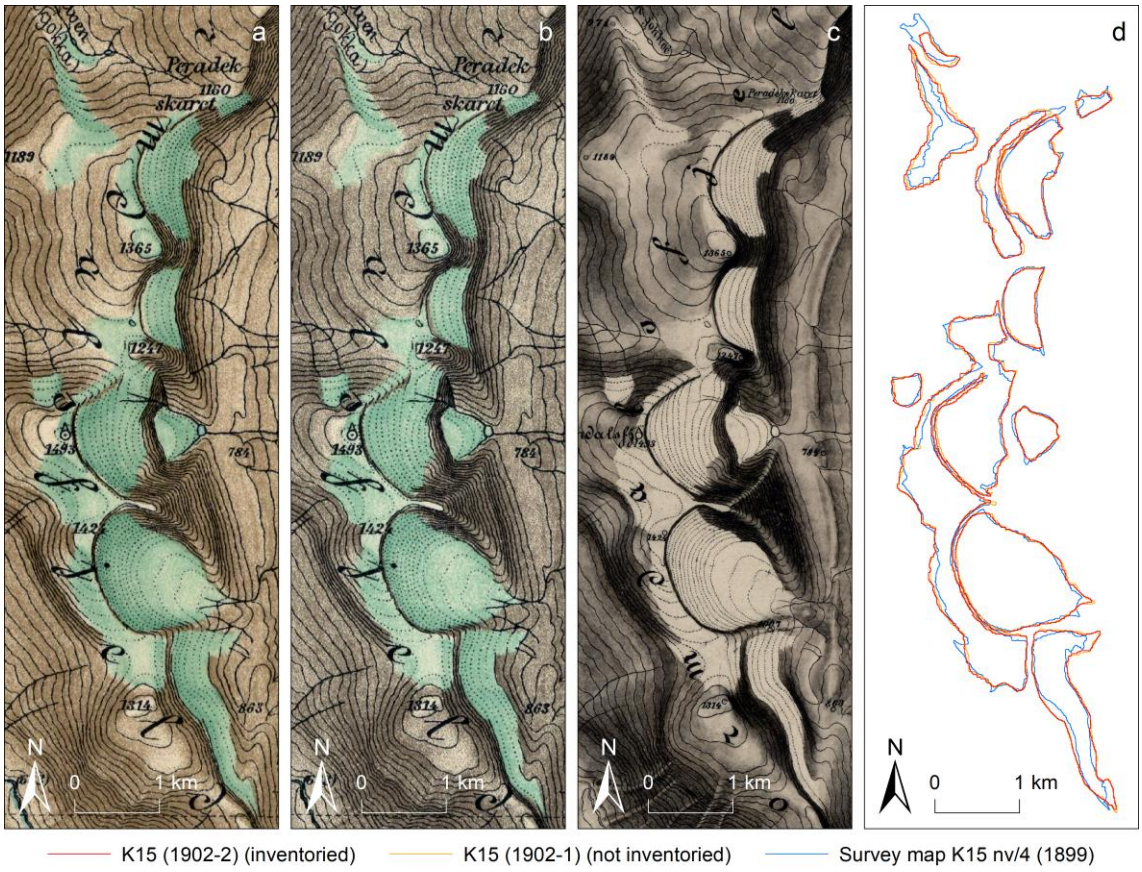

Fig. 3-7. Comparison of glacier area in the Stormdalsfjellet mountain range. (a) Print version 1902-2 (printed 06/1919) of map sheet K15 Dunderlandsdalen (1:100,000; produced by O. Tolstad and O. Engh; published in 1902; Norges geografiske oppmåling; available from Kartverket); this print version was used for the 1899 inventory; (b) K15 print version 1902-1; and (c) survey map K15 nv/4 (1:50,000; surveyed by Captain V. H. L. von Munthe af Morgenstierne, Captain C. M. N. Havig and Captain O. H. Paulsen; 1894, 1896 and 1899; Norges geografiske oppmåling; available from Kartverket). (d) Comparison of the 1899 glacier area as digitised from (a), (b) and (c).

In order to quantify the potential differences in glacier extent that may have resulted from the multistep map (re-)production process between (1) the survey maps and the final maps; and (2) the printed copies of the same map sheets, we examined survey map K15 nv/4 and two prints of the corresponding map sheet K15 Dunderlandsdalen more closely. The survey map and a second print version of the K15 map (one had already been georectified along with the rest of the map sheets) were georeferenced and transformed using second-order polynomials (Table 3-2). We then digitised a chain of cirque glaciers in the Stormdalsfjellet mountain range to the east of Østre Svartisen in a pixel-accurate fashion from all three map sources and compared the polygon area of these data sets (Fig. 3-7). The difference in size between the selected glaciers of the two K15 prints is only 0.02 km^2 and thus negligible. There is, however, a marked difference of 7 % (0.45 km^2) between the survey map (6.7 km^2) and each of the printed copies of the final map (7.1 km^2) (Fig. 3-7d). We take this number as a representative

estimate of the map (re-)production error (e_{MR}) caused by the complex workflow involved in creating the final map sheets (see Section 3.3.).

The final step in digitising the glacier outlines in the raster graphics editor was to turn each map sheet into a stencil-like, monochromatic image, where only the digitised glacier polygons were visible in black on an otherwise white background (Fig. 3-5e). These monochromes were then used to overwrite the original GeoTIFF map files.

3.4.3. Geodatabase and polygon merge correction

After reapplying the geospatial information to the monochrome rasters (i.e. the former GeoTIFF map files), they were converted into GIS polygons in ArcGIS. These polygons were then compiled into a geodatabase, creating the 1899 glacier inventory. We clipped the data set to the present-day outline of Norway to account for localised changes in the position of the border with Sweden (which did not affect boundary markers used in the georeferencing). Key metadata, including the original survey year/period of each glacier along with the surveyor(s), was extracted from the survey maps and linked to each glacier polygon in our geodatabase.

A number of glaciers extend across more than one map sheet, particularly Nordland's large plateau icefields such as Østre and Vestre Svartisen, Blåmannsisen, Okstindbreen and Frostisen (Table 3-3). Their separate polygons had to be manually merged into one continuous glacier outline for each of these ice bodies (Fig. 3-8). However, the georectified raster map sheets did not align seamlessly; both minor overlaps and narrow gaps occurred. This, in turn, translated into small misalignments between the digitised glacier parts (Fig. 3-8), so that the merging of polygons either meant glacier area was lost or gained. For our entire Nordland inventory, the overlapping (i.e. deleted) polygon area is 2 km^2, whilst an additional polygon area of 1 km^2 had to be created in order to connect glacier polygons separated by gaps (see Table 3-3). As a result, a correction of 1 km^2 has to be added to the total glacier area of our inventory to compensate for the area deficit.

Table 3-3. Overview of glacier area loss and/or gain due to the merging of separate icefield polygons and comparison of area change at the nine largest Nordland ice masses between 1899 and 2000 (Andreassen and others, 2012a).

Glacier	Original polygons (*n*)	Area (km²)								Area change (%) 1899-2000
		1899 polygons (Σ)	Created (+)	Deleted (-)	Merged 1899 glacier outline	± 17 % e_T	2000*	Change 1899-2000	± 17 % e_T	
Vestre Svartisen	5	267.62		-0.65	266.97	45	223.1	-43.9	7	-16
Østre Svartisen	3	200.61		-0.68	199.93	34	153.3	-46.6	8	-23
Blåmannsisen (Ålmåjalosjiegŋa)	5	115.94	0.003	-0.23	115.71	20	88.9	-26.8	5	-23
Okstindbreen	5	65.39	0.17	-0.23	65.33	11	49.4	-15.9	3	-24
Sulitjelmaisen (Sallajiegŋa)	1				37.81	6	29.5	-8.3	1	-22
Frostisen (Ruostajiekŋa)	2	31.98	0.11		32.09	5	25.4	-6.7	1	-21
Gihtsejiegŋa	2	40.67		-0.20	40.47	7	25.2	-15.3	3	-38
Høgtuvbreen	1				36.27	6	22.6	-13.7	2	-38
Simlebreen	1				33.14	6	22.1	-11.0	2	-33
Mean										**-27**

* Note that the 2000 icefield extents include the main 2000 icefield polygons and all additional 2000 ice bodies that lie within the respective 1899 polygon boundaries; the resulting area values can differ from those published in Andreassen and others (2012a, p. 51).

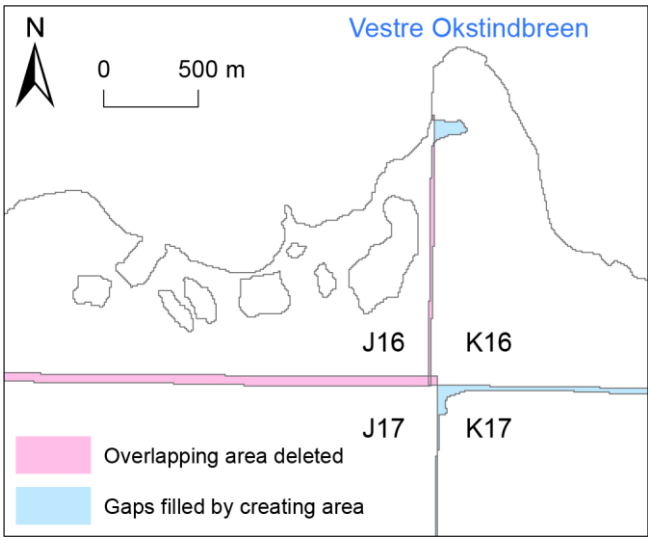

Fig. 3-8. Example of Okstindbreen extending across four map sheets. The merging of the separate polygons of the plateau icefield into one continuous outline resulted in both the loss of overlapping polygon area and the creation of additional glacier area.

3.4.4. Snow-related error and total inventory uncertainty

Other inventories of Norwegian glaciers have shown that the digitised extent and area of the mostly debris-free glaciers in Norway is particularly prone to errors that arise from difficulties in differentiating between glacier ice and perennial/seasonal snow (e.g. Andreassen and others,

2008; Paul and Andreassen, 2009). For the Svartisen–Blåmannsisen region, Paul and Andreassen (2009) estimated that this uncertainty might be 5-10 % for glaciers over 5 km^2 in size and as much as 25 % for ice bodies smaller than 1 km^2. Although our qualitative analysis of old survey reports and photographs suggests that seasonal snow was not included in the mapping (see Section 3.3.1.), we suggest an error value in the range of that given by Paul and Andreassen (2009) is also reasonable for our data set. To differentiate between glaciers and snowfields was probably as challenging in the field at the turn of the 19th century as it is today based on high-resolution remote sensing data. We take the median of Paul and Andreassen's (2009) uncertainty range (15 %) as a realistic value for the snow-related error (e_S). This value is substantiated by long-term snow depth observations in Nordland (the first measurements began in 1895). These observations show that the period up to the 1920s was characterised by both large maximum snow depths and long durations of winter snow cover, particularly in the years 1904 and 1905 when values where as high as > 1.5 m (Theakstone, 2013). The deep-snow winter of 1905 was also noted by the surveyor First Lieutenant K. M. Leewy in his topographic description (Leewy, 1905; see Section 3.3.1.). This allows us to calculate the total error (e_T) associated with the 1899 glacier area, using the equation:

$$e_T = \sqrt{({e_D}^2 + {e_{MR}}^2 + {e_S}^2)} \quad (1)$$

where the digitising error e_D = ±4 %; the map (re-)production error e_{MR} = ±7 %; and the snow-related error e_S = ±15 %; which brings e_T to ±17 %.

3.4.5. 1899 glacier inventory

Our 1899 inventory contains a total of 1,587 glaciers with a combined area of 1,736 ± 295 km^2 (including the 1 km^2-area correction; see Section 3.4.3.). A breakdown of the number of glaciers by Norwegian glacier region, as defined by Andreassen and others (2012a), is given in Table 3-4. Nearly half of all inventoried glaciers (47 %) are smaller than 0.1 km^2; and 89 % of the 1899 glaciers are below 1 km^2 in area. Table 3-3 lists the 1899 area of Nordland's nine largest ice masses. The plateau icefields Vestre Svartisen, Østre Svartisen and Blåmannsisen were 267 ± 45 km^2, 200 ± 34 km^2 and 116 ± 20 km^2 in size, respectively. The number of glaciers within the present-day county boundaries of Nordland is 1,540 with a total area of 1,713 ± 291 km^2.

Equation (1) allows other researchers interested in using the Nordland inventory to re-calculate and adjust the total error based on uncertainty values they deem more appropriate. For

example, almost 90 % of the ice masses in the inventory are < 1 km^2 in area, for which Paul and Andreassen (2009) estimate an uncertainty of up to 25 %. So, in order to obtain a more conservative total error, Equation (1) can be solved using a snow-related error e_S of ±25 %, which would bring the total error e_T to ±26 %. This would give an overall area uncertainty of ±451 km^2 for the entire 1899 inventory and ±445 km^2 for the 1899 glacier area in Nordland county.

Table 3-4. Breakdown of the number of 1899 glaciers by Norwegian glacier region, as defined by Andreassen and others (2012a).

Norwegian glacier region[1]	Name	Glaciers in 1899 (*n*)[3]	Area (km^2)	Mean size (km^2)[3]
8	Troms - South[2]	53	30	0.6
9	Skjomen	107	128	1.2
10	Frostisen	69	118	1.7
11	Hamarøy - Vestfjorden	288	110	0.4
12	Blåmannsisen	218	277	1.3
13	Saltfjellet	184	96	0.5
14	Svartisen - West	42	342	8.1
15	Svartisen - East	178	399	2.2
16	Helgeland - Inner	106	42	0.4
17	Okstindbreen	18	80	4.4
18	Vefsn	131	38	0.3
19	Børgefjell	143	62	0.4
Outliers		50	13	0.3
Complete 1899 inventory[4]		1587	1735	1.1

[1] Defined by Andreassen and others (2012a)

[2] Region only partly covered by the historical maps used in this study

[3] Not separated into glacier-hydrological units

[4] A 1 km^2-area correction has to be added

3.5. Independent quality assessment of glacier outline accuracy

In order to independently assess the accuracy of the 1899 glacier outlines, we developed a validation test using the post-LIA glacial history of Nordland (see Section 3.2.). Following the LIA maximum in the mid-18th century, glacier retreat was initially slow, but accelerated dramatically between ~1930-70 (e.g. Theakstone, 1965), after a brief period of renewed glacier advance at the beginning of the 20th century. Our test compared the historical 1899 outlines of selected glaciers in the Svartisen area with the glacier extent of the LIA maximum and to that of 1945 during the period of accelerated recession. In the context of the regional glacial history, the 1899 outlines had to lie between the LIA limit (1899 < LIA) and the 1945 glacier extent (1899 > 1945) to pass as not inaccurate. The Svartisen glaciers selected for our test are considered a representative subset of the glacier types to be found in Nordland. These ranged

from differently sized icefield outlet glaciers (Vestre Svartisen: Fonndalsbreen–Engabreen–Litlbreen, and outlets along the Vesterdalen valley, including Flatisen as an example of a glacier that exhibited post-LIA calving retreat; Østre Svartisen: Fingerbreen) to small mountain and valley glaciers adjacent to the northern sector of Østre Svartisen.

We used geomorphological mapping (e.g. Chandler and others, 2018) and the approach outlined in Weber and others (2019) to reconstruct the maximum LIA extent of the selected glaciers, primarily from ice-marginal moraines, glacial drift limits, trimlines and identifiable erosion and weathering boundaries. Field mapping was carried out in summer 2016 and 2017 and was underpinned by remote mapping from high-resolution digital colour aerial photographs captured in 2007-2014 (acquired from http://norgeibilder.no/). The 1945 glacier extent in these areas was extracted from post-WWII aerial reconnaissance photographs taken by the British Royal Air Force (RAF), which is the earliest available vertical aerial imagery of Svartisen. The scanned images were georeferenced and the 1945 outlines were manually digitised.

There are, of course, elements of uncertainty with the data sets we use in the independent assessment of accuracy. For example, in Norway, the former maximum LIA extent is often clearly imprinted and readily discernible in the form of moraines, trimlines and a stark difference in vegetation density between the glacier forelands exposed since the LIA and the area beyond (e.g. Erikstad and Sollid, 1986; Baumann and others, 2009; Stokes and others, 2018; Weber and others, 2019). In particular, Weber and others (2019) found that nearly 60 % of the Hardangerjøkulen icefield's LIA extent could be established from geomorphological evidence. Nonetheless, geomorphological mapping is not an objective practice, and both mapping errors and landform misinterpretation may occur (Chandler and others, 2018). The black-and-white RAF air photos contain geometric distortions (relief displacement) and have low contrast, particularly over and around ice masses. In addition, a major portion of many photographs shows glacier- and snow-covered terrain without identifiable landscape features, which made georeferencing challenging, especially in icefield summit areas without nunataks. The snowy, featureless icefield areas combined with the low contrast give rise to the risk of snow being included in the digitised 1945 glacier outlines.

With these caveats, our validation revealed that the selected icefield outlet glaciers and many of the larger valley glaciers generally meet the test criteria, and are therefore not inaccurate. Their ice fronts can be seen to have terminated not far behind the outer LIA limit by the end of the 19th century (Fig. 3-9). This suggests that the topographers realistically delineated the extent of outlet and valley glaciers. These ice masses typically descend to areas of lower ground where summer ablation removes the snow cover and exposes bare ice, providing ideal survey conditions (see Fig. 3-3c). A few minor, local-scale violations of both criteria are, however, present, which mainly occur in the icefield summit areas. In instances where parts of the 1945 glacier outlines are slightly more extensive than their 1899 counterparts, the most

likely explanations are relief displacement or ice-marginal snow in the RAF photographs, which were passed on to the digitised 1945 glacier extents. In those instances where the 1899 glacier outlines slightly extend beyond the reconstructed LIA limit, map georeferencing may be a factor because our georeferencing approach (see Section 3.4.1.) favoured geolocation accuracy of an entire map sheet over local accuracy around individual ice masses.

For the 1899 outlines of the small mountain and valley glaciers to the north of Fingerbreen (Østre Svartisen), we found evidence of both over- and underestimated ice masses (Fig. 3-9c). The most notable example is the small valley glacier (glacier ID 1300) to the northwest of the Bogvatnet (Tjoamodisjávrre) lake. Moraine ridges and a pronounced trimline mark the glacier's maximum LIA position, which is located approximately 450 m from the lakeshore (Fig. 3-9d). An extensive glaciofluvial outwash plain occupies the intervening area. The valley sides above the LIA trimline are gullied and well vegetated, suggesting prolonged ice-free conditions. Despite this strong evidence for the glacier's LIA maximum, the 1899 outline is shown on the historical maps to have extended all the way down to the lake and laterally up the northern valley side (Fig. 3-9c), which constitutes a clear mapping error. Geomorphological evidence also indicates an exaggerated 1899 glacier extent in the neighbouring valley to the south (glacier ID 1306) (Fig. 3-9c). By contrast, when the 1899 outline of glacier 1300 is compared to the 1945 extent, a marked underestimation of the accumulation area is evident (Fig. 3-9c). This also applies to the accumulation areas of the small ice masses occupying the Spidstinden massif, some of which were not mapped at all by the topographers (Fig. 3-9c). We speculate that the complex, mountainous topography hindered the precise mapping of these glaciers. Underestimation of glacier accumulation areas was probably amplified by the conservative mapping approach of the surveyors in snow-covered terrain (see Section 3.3.1).

Based on the sample of glaciers included in our test, it seems that over- and underestimation of small ice masses on the historical maps is present to an approximately equal degree and more or less balance each other out. Icefield outlet glaciers and larger ice masses, on the other hand, appear to have been realistically mapped. Overall, we judge that this does not affect our calculated inventory uncertainty. Our test approach would benefit from spatially more extensive validation data sets, particularly of digital outlines of the maximum LIA glacier extent, to provide a significant baseline for inventory comparisons.

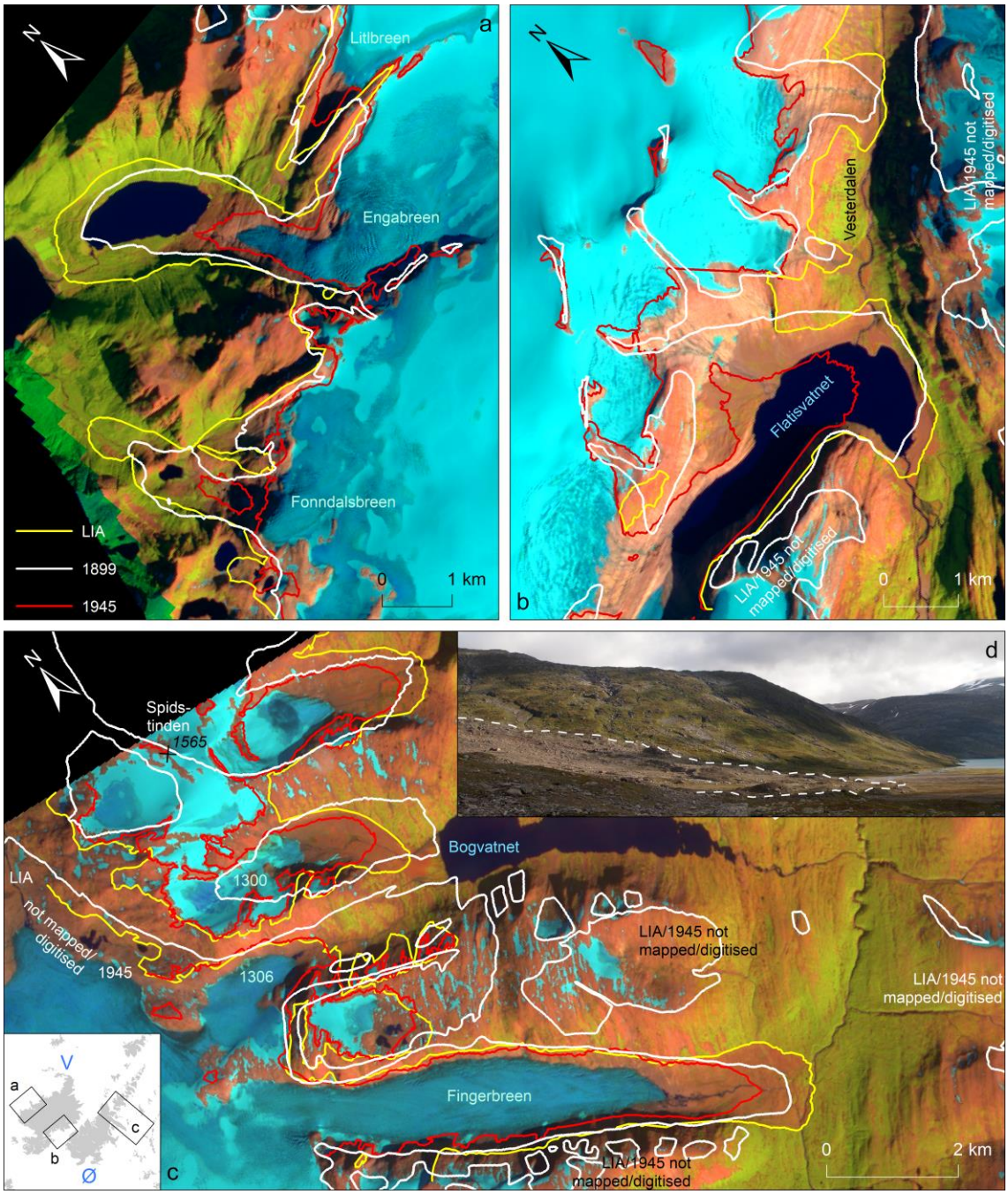

Fig. 3-9. LIA, 1899 and 1945 extent of (a) Vestre Svartisen's western outlet glaciers Fonndalsbreen, Engabreen and Litlbreen; (b) Vestre Svartisen's eastern outlet glacier Flatisen and smaller icefield outlets along the Vesterdalen valley; and (c) Østre Svartisen's eastern outlet glacier Fingerbreen and small mountain glaciers to the north. Background images are a Sentinel-2A scene (bands 11, 8, 2) from 26 August 2016 (acquired from the Copernicus Open Access Hub). The inset map shows the locations of the three areas. The 1899 glacier outlines can be deemed accurate and reliable if they fall within the LIA and 1945 glacier extent (LIA > 1899 > 1945). (d) Photograph showing the foreland of glacier 1300, as viewed to the north. The maximum LIA extent is defined by moraine ridges and a clear trimline along the valley side (indicated by white dashed line), without vegetation cover inside the LIA limit. A proglacial outwash plain has accumulated beyond the LIA maximum moraines and extends to the Bogvatnet (Tjoamodisjávrre) lake.

3.6. Quantifying 20th-century glacier recession in Nordland

We performed a glacier area change assessment by comparing our 1899 glacier inventory to the inventories for 1976 and 1988 (Winsvold and others, 2014) and 2000 (Andreassen and others, 2012a). Since the Andreassen and others (2012a) inventory was created from what is now ~20-year old Landsat data, our change analysis used the full, unprocessed inventory area in the calculations, without separating the glaciers into glacier-hydrological units (as is the norm; cf. Racoviteanu and others, 2009). Once new inventories of the present-day glacier extent are available, our data set can be used as a baseline for a more extensive and thorough analysis of individual drainage basins. For such an analysis, it would be important to use the survey date for individual glaciers, rather than the overall inventory median date of 1899 that we use here. In this way, the results of glacier change assessments will not be influenced by a potential systematic change in the survey date, as the Nordland surveys spanned 34 years in total. All inventories were clipped to the county boundaries of Nordland, which excluded from our analysis a small number of 1899 glaciers located in the border regions of the neighbouring counties. Also omitted from the analysis were ice masses smaller than 0.01 km^2 in area, for consistency with Andreassen and others (2012a). We calculated absolute and relative glacier area change for each time step between the successive inventories, as well as for the entire ~100-year period. Decadal rates of area change were computed using compound interest calculation (Andreassen and others, 2008; Zemp and others, 2014).

Excluding 65 ice bodies smaller than 0.01 km^2, the glaciers within the county boundaries of Nordland covered 1,712 ± 291 km^2 in 1899 (n = 1,475). Changes in glacier area between the four inventories are summarised in Table 3-5. From 1899 to 1976, the glacier area change in Nordland was -39 % (-660 ± 112 km^2), which equates to a decadal rate of area loss of 6 % $10a^{-1}$ (86 ± 15 km^2 $10a^{-1}$). Areal shrinkage continued in the period 1976-1988 (23 %; 240 ± 36 km^2), albeit at a significantly faster rate of 21 % $10a^{-1}$ (200 ± 30 km^2 $10a^{-1}$). In the final period 1988-2000, Nordland's glaciers grew by 11 % (93 ± 14 km^2), which translates into a decadal rate of area growth of 9 % $10a^{-1}$ (78 ± 12 km^2 $10a^{-1}$). Over the total ~100-year period up to 2000, the glaciers in Nordland lost almost half of their original 1899 area (47 %; 807 ± 137 km^2), with a decadal rate of recession of 6 % $10a^{-1}$ (80 ± 14 km^2 $10a^{-1}$). Total area change was lower for the nine largest icefields, which receded by 27 % on average between 1899 and 2000, with the lowest recession recorded at Vestre Svartisen (16 %) (Fig. 3-10), whilst the three smallest icefields in this group retreated in excess of 30 % (Table 3-3).

Here, we discuss our results in the context of existing estimates of centennial-scale glacier change from historical maps both in Norway and elsewhere. Winsvold and others (2014)

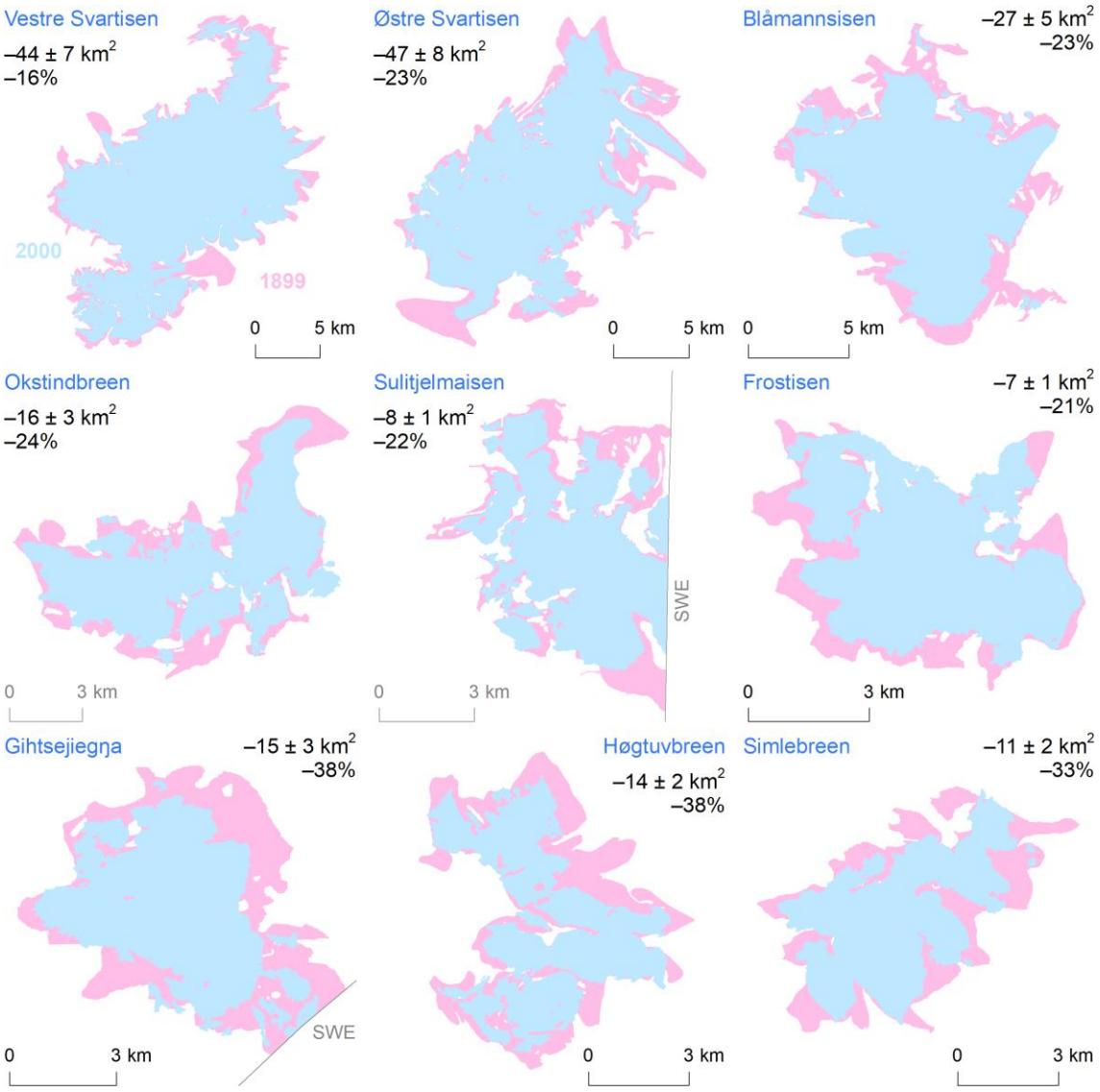

Fig. 3-10. Glacier area change at the nine largest Nordland ice masses between 1899 and 2000 (Andreassen and others, 2012a). See Fig. 3-1 for locations.

Table 3-5. Comparison of rates of glacier area change in Nordland for each measurement period.

Period*	1899-1976 (1882-1916 / 1967-85)	± 17 % e_T	1976-88 (1967-85 / 1988)	± 15 % e_S	1988-2000 (1988 / 1999-2001)	± 15 % e_S	1899-2000 (1882-1916 / 1999-2001)	± 17 % e_T
Total area change (km^2)	-660	112	-240	36	+93	14	-807	137
Total area change (%)	-39		-23		+11		-47	
Rate of change (km^2 $10a^{-1}$)	-86	15	-200	30	+78	12	-80	14
Rate of change (% $10a^{-1}$)	-6		-21		+9		-6	

* Median of each time interval; used as basis for calculations

assessed 20th-century glacier change from three gradteigskart map sheets of Finnmark, northernmost Arctic Norway (Fig. 3-1). They found that the five major plateau icefields

Langfjordjøkelen (Bártnatvuonjiehkki), Øksfjordjøkelen (Ákšovuonjiehkki), Svartfjelljøkelen, Seilandsjøkelen (Nuortageašjiehkki) and Nordmannsjøkelen (Dáččavuonjiehkki) had receded by an average of 53 % (7 % $10a^{-1}$; 74 km^2) in the period 1895-2006 (decadal rate calculated from data given in Winsvold and others, 2014). These values compare well with total 20th-century glacier change across Nordland (-47 %; -6 % $10a^{-1}$). However, when considering icefield-type glaciers alone, mean glacier area loss at the nine largest Nordland icefields (27 %; 3 % $10a^{-1}$; Table 3-3) represents only half of the change that Winsvold and others (2014) reconstructed for Finnmark. This indicates that plateau icefields in northernmost Arctic Norway experienced particularly severe recession in the 20th century, which is supported by surface mass balance modelling and geodetic mass balance measurements at Langfjordjøkelen (Andreassen and others, 2012b).

Two studies have calculated long-term glacier change in southern Norway from gradteigskart maps: an area loss of 23 % (~4 % $10a^{-1}$; ~30 km^2) between 1931-1934 and 2003 in the Jotunheimen mountains (Andreassen and others, 2008); and a decrease of 24 % (~4 % $10a^{-1}$; ~22 km^2) in the period 1926-2003 at the Hardangerjøkulen icefield (Weber and others, 2019) (Fig. 3-1). Percentage area change at Hardangerjøkulen is comparable with average icefield recession in Nordland (Table 3-3), although we note the later date of the historical survey and thus the shorter time step between the two Hardangerjøkulen inventories (< 80 years). By contrast, there is less agreement between Nordland and percentage change of the more continental mountain glaciers in Jotunheimen, but, again, the measurement interval between the Jotunheimen inventories is considerably shorter (~70 years). Taken together, the four Norwegian regions for which 20th-century glacier area change has been quantified from historical gradteigskart maps experienced a total area loss of ~942 km^2 between ~1900 and ~2000. These four regions still contained 1,142 km^2 of glacier area in the 2003 inventory by Andreassen and others (2012a).

In the Canadian Rocky Mountains, Tennant and others (2012) documented a 40 ± 5 % (590 ± 70 km^2) reduction in ice cover between 1919 and 2006, at a decadal rate of 5 ± 1 % $10a^{-1}$. Tielidze (2016) reported an area loss of 42 ± 2 % (7 ± 0.2 % $10a^{-1}$; 258 ± 7 km^2) for the glaciers in the Caucasus Mountains of Georgia in the period 1911-2014. Glacier area in the Swiss Alps shrank by 47 % (6 % $10a^{-1}$; 831 km^2) between ~1900 and 2010 (~1900-2003: 41 %; 6 % $10a^{-1}$; 732 km^2), based on data provided by Freudiger and others (2018) (however, note that this study used the publication date of the historical maps as timestamps). The results of these studies show consistency with the 47 % (6 % $10a^{-1}$) relative glacier area decline in Nordland between 1899 and 2000.

Overall, the few glacier inventories based on historical map analysis suggest that mountain glaciers in western Eurasia and western Canada have substantially decreased in area over the course of the 20th century, and that this recession was similar in terms of both the

percentage area lost and the relative rate of shrinkage. Conversely, 20th-century retreat of the tropical Kilimanjaro icefields was approximately twice that of the Northern Hemisphere examples (1912-2003: 78 %; 17 % $10a^{-1}$; ~9 km^2; 1912-2011: 85 %; 19 % $10a^{-1}$; ~10 km^2; calculated using data from Cullen and others, 2013).

3.7. Conclusions and recommendations

We present an inventory of the ~1899 glacier extent in Nordland county, northern Norway, from historical gradteigskart maps. The maps are based on topographic field surveys that took place between 1882 and 1916. Although the survey duration of 34 years is not comparable to the temporal coverage and revisit time of modern satellite platforms used in contemporary glacier monitoring, the uniform, systematic and continuous mapping programme ensured that the maps are of high quality and consistent in both form and content. Historical survey reports and photographs suggest that glacier mapping was carried out accurately and in a careful and conservative manner in areas of snow-covered terrain that could be erroneously mapped as glacier ice. Thus, the maps can serve as a basis for a glacier inventory. We digitised glacier outlines from georectified scans of 33 Nordland map sheets in a raster graphics editor employing a semi-automated procedure. The outlines were then compiled and inventoried in a GIS. Errors relating to glacier outline digitisation, map (re-)production and ice-marginal snow amount to a total inventory uncertainty of ±17 %. In an additional independent validation of the accuracy of the historical glacier extent, we compared the 1899 outlines of selected glaciers in the Svartisen area with the maximum LIA glacier extent (established from geomorphological evidence) and the 1945 glacier extent (extracted from RAF vertical aerial photographs). For the 1899 glacier outlines to be not inaccurate, their extent had to be smaller than at the LIA maximum, but larger than that of 1945 (LIA > 1899 > 1945). The test shows that both underestimated and exaggerated outlines are present, with misestimation more of a problem for small glaciers and ice masses in complex alpine terrain, but less of an issue for larger valley glaciers and icefield outlets.

Our 1899 inventory contains 1,475 glaciers (≥ 0.01 km^2) within the county boundaries of Nordland, with a combined area of 1,712 ± 291 km^2. Since the end of the 19th century, substantial changes in the areal extent of Nordland's glaciers have occurred. Between 1899 and 2000, the total glacier cover decreased by 47 % (807 ± 137 km^2) at a decadal rate of 6 % $10a^{-1}$ (80 ± 14 km^2 $10a^{-1}$). This demonstrates the value of historical maps for improving understanding of 20th-century glacier change. A more detailed assessment of change in comparison to an updated 21st century glacier inventory, and at an individual glacier-unit level, should be a priority for future work.

Based on our research, we recommend that future studies of glacier inventories from old maps should first assess the overall quality of the historical map source and, in particular, the mapping approach and accuracy of ice masses depicted on the maps. For instance, this could include examining historical survey instructions, reports, photographs or other available historical observations. Second, detected mapping errors/inconsistencies as well as uncertainties relating to the GIS-based production of the glacier inventory should be reported, quantified and, most crucially, combined into a total inventory uncertainty, with corresponding error terms for all calculated glacier area values. Third, where possible, the inventoried glacier outlines should be independently validated against separate data sets, for example other available glacier inventories or the maximum LIA extent. Observed occurrences of over- or underestimation should be reported in the inventory metadata, and, if significant, incorporated into the total inventory uncertainty. Finally, in order to employ the inventory in glacier change assessments, it is important to establish the actual *survey* date of each inventoried glacier polygon. Using the publication date of the maps, which may have been much later than the original map surveys, precludes glacier change from being compared to other glacier regions and from being linked to (sub-)decadal variations in climate. Ideally, glacier change should be calculated for each individual ice body and its respective change period before computing the mean change (Winsvold and others, 2014). Following these general guidelines will ensure that historical maps can be utilised to their full potential, whilst gaining a realistic picture of the uncertainties (and possible shortcomings) associated with historical map-based glacier inventories.

Data availability

The 1899 glacier inventory can be viewed online and downloaded from NVE's web mapping service *Breatlas* ('Glacier Atlas'), and is also available for download at https://www.nve.no/hydrology/glaciers/glacier-data/.
All historical maps can be freely accessed via Kartverket's online database of historical maps of Norway; https://kartverket.no/Kart/Historiske-kart/.

Acknowledgements

Thanks are due to Nasjonalbiblioteket (National Library of Norway) for providing high-resolution scans of selected gradteigskart survey photographs. We also thank Benjamin M. P. Chandler for fieldwork assistance at Østre Svartisen in 2016. PW gratefully acknowledges funding from the EU's Erasmus+ programme and the University of Portsmouth's Placement Scheme for Postgraduate Researchers, enabling invaluable research stays at NVE. PW's fieldwork in the Vesterdalen valley was funded by a Mount Everest Foundation (MEF) expedition grant (Reference 17-36). A British Society for Geomorphology ECR grant awarded to CMB aided in ground truthing LIA limits at Østre Svartisen. This work is also a contribution to the Norwegian Copernicus Glacier Service project.

Author contributions

PW: Conceptualisation, methodology, GIS and field investigation, archival research, analysis, writing – original draft, figure preparation

LMA, CMB, HL, SK: Conceptualisation (LMA), field investigation (CMB, HL), archival research (SK), writing – review and editing, supervision (LMA, CMB, HL)

References

Aasbø K (2016) Landmålerliv – Topografenes fotografier fra Hauglandet. *Haugaledningen – Årbok for Haugalandmuseene,* **2015-2016**, 64–77.

Andreassen LM, KjølImoen B, Knudsen NT, Whalley WB and Fjellanger J (2000) *Regional change of glaciers in northern Norway.* NVE Report 1 2000, NVE, Oslo.

Andreassen LM, Elvehøy H, Kjøllmoen B, Engeset RV and Haakensen N (2005) Glacier mass-balance and length variation in Norway. *Annals of Glaciology*, **42**, 317–325 (doi: 10.3189/172756405781812826).

Andreassen LM, Paul F, Kääb A and Hausberg JE (2008) Landsat-derived glacier inventory for Jotunheimen, Norway, and deduced glacier changes since the 1930s. *The Cryosphere*, **2**(2), 131–145 (doi: 10.5194/tc-2-131-2008).

Andreassen LM, Winsvold SH, Paul F and Hausberg JE (2012a) *Inventory of Norwegian glaciers.* NVE, Oslo.

Andreassen LM, Kjøllmoen B, Rasmussen A, Melvold K and Nordli Ø (2012b) Langfjordjøkelen, a rapidly shrinking glacier in northern Norway. *Journal of Glaciology*, **58**(209), 581–593 (doi: 10.3189/2012JoG11J014).

Bahr DB, Meier MF and Peckham SD (1997) The physical basis of glacier volume-area scaling. *Journal of Geophysical Research: Solid Earth*, **102**(B9), 20355–20362 (doi: 10.1029/97JB01696).

Bahr DB, Dyurgerov M and Meier MF (2009) Sea-level rise from glaciers and ice caps: A lower bound. *Geophysical Research Letters*, **36**(3), L03501 (doi: 10.1029/2008GL036309).

Bakke J, Dahl SO, Paasche Ø, Simonsen JR, Kvisvik B, Bakke K and Nesje A (2010) A complete record of Holocene glacier variability at Austre Okstindbreen, northern Norway: an integrated approach. *Quaternary Science Reviews*, **29**(9–10), 1246–1262 (doi: 10.1016/j.quascirev.2010.02.012).

Baumann S, Winkler S and Andreassen LM (2009) Mapping glaciers in Jotunheimen, South-Norway, during the "Little Ice Age" maximum. *The Cryosphere*, **3**(2), 231–243 (doi: 10.5194/tc-3-231-2009).

Chandler BMP, Lovell H, Boston CM, Lukas S, Barr ID, Benediktsson ÍÖ, Benn DI, Clark CD, Darvill CM, Evans DJA, Ewertowski MW, Loibl D, Margold M, Otto J-C, Roberts DH, Stokes CR, Storrar RD and Stroeven AP (2018) Glacial geomorphological mapping: A review of approaches and frameworks for best practice. *Earth-Science Reviews*, **185**, 806–846 (doi: 10.1016/j.earscirev.2018.07.015).

Cullen NJ, Sirguey P, Mölg T, Kaser G, Winkler M and Fitzsimons SJ (2013) A century of ice retreat on Kilimanjaro: the mapping reloaded. *The Cryosphere*, **7**(2), 419–431 (doi: 10.5194/tc-7-419-2013).

de Seue C (1876) Undersøgelse af Svartisen og temperaturforhold i enkelte af de Nordlandske fjorde. *Nyt magazin for naturvidenskaberne*, **21**(3), 229–270.

Engeset RV, Schuler TV and Jackson M (2005) Analysis of the first jökulhlaup at Blåmannsisen, northern Norway, and implications for future events. *Annals of Glaciology*, **42**, 35–41 (doi: 10.3189/172756405781812600).

Erikstad L and Sollid JL (1986) Neoglaciation in South Norway using lichenometric methods. *Norsk Geografisk Tidsskrift - Norwegian Journal of Geography*, **40**(2), 85–105 (doi: 10.1080/00291958608552159).

Farinotti D, Huss M, Bauder A, Funk M and Truffer M (2009) A method to estimate the ice volume and ice-thickness distribution of alpine glaciers. *Journal of Glaciology*, **55**(191), 422–430 (doi: https://doi.org/10.3189/002214309788816759).

Fischer M, Huss M, Barboux C and Hoelzle M (2014) The New Swiss Glacier Inventory SGI2010: Relevance of Using High-Resolution Source Data in Areas Dominated by

Very Small Glaciers. *Arctic, Antarctic, and Alpine Research*, **46**(4), 933–945 (doi: https://doi.org/10.1657/1938-4246-46.4.933).

Freudiger D, Mennekes D, Seibert J and Weiler M (2018) Historical glacier outlines from digitized topographic maps of the Swiss Alps. *Earth System Science Data*, **10**(2), 805–814 (doi: 10.5194/essd-10-805-2018).

Fægri K (1935) *Forandringer ved norske breer 1933–34*. (Bergens Museums Årbok 1934, Naturvidenskapelig rekke, Nr. 11). Bergens museum, Bergen, 1–10.

Gardent M, Rabatel A, Dedieu J-P and Deline P (2014) Multitemporal glacier inventory of the French Alps from the late 1960s to the late 2000s. *Global and Planetary Change*, **120**, 24–37 (doi: https://doi.org/10.1016/j.gloplacha.2014.05.004).

Georges C (2004) 20th-Century Glacier Fluctuations in the Tropical Cordillera Blanca, Perú. *Arctic, Antarctic, and Alpine Research*, **36**(1), 100–107 (doi: 10.1657/1523-0430(2004)036[0100:TGFITT]2.0.CO;2).

Griffey NJ (1977) A lichenometric study of the Neoglacial end moraines of the Okstindan Glaciers, North Norway, and comparisons with similar recent Scandinavian studies. *Norsk Geografisk Tidsskrift - Norwegian Journal of Geography*, **31**(4), 163–172 (doi: 10.1080/00291957708552019).

Griffey NJ and Worsley P (1978) The pattern of Neoglacial glacier variations in the Okstindan region of northern Norway during the last three millennia. *Boreas*, **7**(1), 1–17 (doi: 10.1111/j.1502-3885.1978.tb00046.x).

Grove JM (2004) *Little Ice Ages: Ancient and Modern.* Routledge, London, New York.

Harsson BG (2009) Historien bak Statens kartverk og kartleggingens historie. *Lokalhistorisk magasin*, **01/2009**, 4–9.

Harsson BG and Aanrud R (2016) *Med kart skal landet bygges: oppmåling og kartlegging av Norge 1773-2016.* Kartverket, Ringerike.

Hoel A (1907) Frostisen. *Det Norske Geografiske Selskabs Aarbok*, **18, 1906–1907**, 127–151.

Hoel A and Werenskiold W (1962) Glaciers and Snowfields in Norway. *Norsk Polarinstitutt skrifter*, **114**.

Holmsen G (1948) En ny bredemt sjø i Svartisen. *Norsk Geografisk Tidsskrift - Norwegian Journal of Geography*, **12**(4), 153–167 (doi: 10.1080/00291954808551660).

Howarth P and Ommanney C (1986) The Use of Landsat Digital Data For Glacier Inventories. *Annals of Glaciology*, **8**, 90–92 (doi: 10.3189/S0260305500001208).

Huss M (2011) Present and future contribution of glacier storage change to runoff from macroscale drainage basins in Europe. *Water Resources Research*, **47**(7), W07511 (doi: 10.1029/2010WR010299).

IPCC (2014) *Climate Change 2014: Synthesis Report. Contribution of Working Groups I, II and III to the Fifth Assessment Report of the Intergovernmental Panel on Climate Change* [Core Writing Team, Pachauri RK and Meyer LA eds.]. IPCC, Geneva.

Jackson M and Ragulina G (2014) *Inventory of glacier-related hazardous events in Norway.* NVE Report 83 2014, NVE, Oslo.

Jansen HL, Simonsen JR, Dahl SO, Bakke J and Nielsen PR (2016) Holocene glacier and climate fluctuations of the maritime ice cap Høgtuvbreen, northern Norway. *The Holocene,* **26**(5), 736–755 (doi: 10.1177/0959683615618265).

Jansen HL, Dahl SO and Nielsen PR (2018) An inverse approach to the course of the 'Little Ice Age' glacier advance and the following deglaciation at Austerdalsisen, eastern Svartisen, northern Norway. *The Holocene,* **28**(7), 1041–1056 (doi: 10.1177/0959683618761539).

Kennett M, Rolstad C, Elvehoy H and Ruud E (1997) Calculation of drainage divides beneath the Svartisen ice-cap using GIS hydrologic tools. *Norsk Geografisk Tidsskrift - Norwegian Journal of Geography,* **51**(1), 23–28 (doi: 10.1080/00291959708552360).

Kjøllmoen B, Andreassen LM, Elvehøy H and Jackson M (2018) *Glaciological investigations in Norway in 2017.* NVE Report 82 2018, NVE, Oslo.

Knudsen NT and Theakstone WH (1984) Recent Changes of Some Glaciers of East Svartisen, Norway. *Geografiska Annaler: Series A, Physical Geography,* **66**(4), 367–380 (doi: 10.1080/04353676.1984.11880122).

Knudsen NT and Theakstone WH (1988) Drainage of the Austre Okstindbreen Ice-dammed Lake, Okstindan, Norway. *Journal of Glaciology,* **34**(116), 87–94 (doi: 10.3189/S0022143000009102).

Kvarteig S, Hansen U and Lillethun A (2009) Statens kartverks arkiver for landkart. *Lokalhistorisk magasin,* **01/2009**, 20–22.

Leewy KM (1905) *Topografisk beskrivelse L13 nö/4 1905*. Norges geografiske Opmaaling, Kristiania.

Linsbauer A, Paul F and Haeberli W (2012) Modeling glacier thickness distribution and bed topography over entire mountain ranges with GlabTop: Application of a fast and robust approach. *Journal of Geophysical Research: Earth Surface,* **117**(F3), F03007 (doi: 10.1029/2011JF002313).

Liestøl O (1956) Glacier Dammed Lakes in Norway. *Norsk Geografisk Tidsskrift - Norwegian Journal of Geography,* **15**(3–4), 122–149 (doi: 10.1080/00291955608542772).

Lund OG (1908) *Topografisk beskrivelse L12 sv/4 1908*. Norges geografiske Opmaaling, Kristiania.

Marstrander R (1910) Svartisen. Strøgets morfologi og bræerne. *Archiv for Mathematik og Naturvidenskab,* **31**(8), 1–40.

Marstrander R (1911) Svartisen, dens geologi. In Reusch H ed. *Aarbok for 1911. Norges Geologiske Undersøkelse 59,* I kommission hos H. Aschehoug & Co., Kristiania, 1–31.

Marzeion B, Jarosch AH and Hofer M (2012) Past and future sea-level change from the surface mass balance of glaciers. *The Cryosphere,* **6**(6), 1295–1322 (https://doi.org/10.5194/tc-6-1295-2012).

Nesje A, Bakke J, Dahl SO, Lie Ø and Matthews JA (2008) Norwegian mountain glaciers in the past, present and future. *Global and Planetary Change,* **60**(1–2), 10–27 (doi: 10.1016/j.gloplacha.2006.08.004).

Norges Geografiske Opmåling (1905) *Instruks for detaljemåling*. Norges Geografiske Opmåling, Kristiania.

Nuth C, Kohler J, König M, von Deschwanden A, Hagen JO, Kääb A, Moholdt G and Pettersson R (2013) Decadal changes from a multi-temporal glacier inventory of Svalbard. *The Cryosphere,* **7**(5), 1603-1621 (doi: https://doi.org/10.5194/tc-7-1603-2013).

Parkes D and Marzeion B (2018) Twentieth-century contribution to sea-level rise from uncharted glaciers. *Nature,* **563**, 551–554 (doi: 10.1038/s41586-018-0687-9).

Paul F and Andreassen LM (2009) A new glacier inventory for the Svartisen region, Norway, from Landsat ETM data: Challenges and change assessment. *Journal of Glaciology,* **55**(192), 607–618 (doi: 10.3189/002214309789471003).

Paul F, Andreassen LM and Winsvold S (2011a) A new glacier inventory for the Jostedalsbreen region, Norway, from Landsat TM scenes of 2006 and changes since 1966. *Annals of Glaciology,* **52**(59), 153–162 (doi: 10.3189/172756411799096169).

Paul F, Frey H and Le Bris R (2011b) A new glacier inventory for the European Alps from Landsat TM scenes of 2003: Challenges and results. *Annals of Glaciology,* **52**(59), 144–152 (doi: 10.3189/172756411799096295).

Paulsen OH (1898) *Topografisk beskrivelse J15 nö/4 1898*. Norges geografiske Opmaaling, Kristiania.

Pfeffer WT, Arendt AA, Bliss A, Bolch T, Cogley JG, Gardner AS, Hagen JO, Hock R, Kaser G, Kienholz C, Miles ES, Moholdt G, Mölg N, Paul F, Radić V, Rastner P, Raup BH, Rich J and Sharp M (2014) The Randolph Glacier Inventory: A globally complete inventory of glaciers. *Journal of Glaciology,* **60**(221), 537–552 (doi: 10.3189/2014JoG13J176).

Rabot C. (1899) Les variations de longueur des glaciers dans les régions arctiques et boréales. *Archives des sciences physiques et naturelles,* **per. 4 v. 8**, p. 321–343.

Racoviteanu AE, Paul F, Raup B, Khalsa SJS and Armstrong R (2009) Challenges and recommendations in mapping of glacier parameters from space: Results of the 2008

Global Land Ice Measurements from Space (GLIMS) workshop, Boulder, Colorado, USA. *Annals of Glaciology,* **50**(53), 53–69 (doi: 10.3189/172756410790595804).

Radić V and Hock R (2010) Regional and global volumes of glaciers derived from statistical upscaling of glacier inventory data. *Journal of Geophysical Research: Earth Surface,* **115**(F1), F01010 (doi: 10.1029/2009JF001373).

Radić V, Bliss A, Beedlow AC, Hock R, Miles ES and Cogley JG (2014) Regional and global projections of twenty-first century glacier mass changes in response to climate scenarios from global climate models. *Clim. Dyn.,* **42**(1–2), 37–58 (doi: https://doi.org/10.1007/s00382-013-1719-7).

Rastner P, Joerg PC, Huss M and Zemp M (2016) Historical analysis and visualization of the retreat of Findelengletscher, Switzerland, 1859–2010. *Global and Planetary Change,* **145**, 67–77 (doi: 10.1016/j.gloplacha.2016.07.005).

Rekstad J (1892) Om Svartisen og dens gletschere. *Det Norske Geografiske Selskabs Årbog,* **3, 1891–1892**, 71–86.

Rekstad J (1893) Beretning om en undersøgelse af Svartisen, foretagen i somrene 1890 og 1891. *Archiv for Mathematik og Naturvidenskab,* **16**, 266–321.

Rekstad J (1900) Om periodiske forandringer hos norske bræer. In Reusch H ed. *Aarbog for 1896 til 99. Norges Geologiske Undersøgelse 28,* I kommission hos H. Aschehoug & Co., Kristiania, 1–15.

Rekstad J (1910) *Forandringer ved norske bræer i aaret 1908–09.* (Bergens Museums Aarbok 1910, Nr. 4). Bergens museum, Bergen, 1–8.

Rekstad J (1912) Die Ausfüllung eines Sees vor dem Engabrä, dem größten Ausläufer des Svartisen, als Maß der Gletschererosion. *Zeitschrift für Gletscherkunde,* **6**, 212–214.

Rekstad J (1914) *Forandringer ved norske bræer i aaret 1913–14.* (Bergens Museums Aarbok 1914–1915, Nr. 7). Bergens museum, Bergen, 1–5.

Rundquist DC, Collins SG, Barnes RB, Bussom DE, Samson SA and Peake JS (1980) The use of Landsat digital information for assessing glacier inventory parameters. *International Association of Hydrological Sciences,* **126**, 321–331.

Stokes CR, Andreassen LM, Champion MR and Corner GD (2018) Widespread and accelerating glacier retreat on the Lyngen Peninsula, northern Norway, since their 'Little Ice Age' maximum. *Journal of Glaciology,* **64**(243), 100–118 (doi: 10.1017/jog.2018.3).

Tennant C, Menounos B, Wheate R and Clague JJ (2012) Area change of glaciers in the Canadian Rocky Mountains, 1919 to 2006. *The Cryosphere,* **6**(6), 1541–1552 (doi: 10.5194/tc-6-1541-2012).

Theakstone WH (1965) Recent Changes in the Glaciers of Svartisen. *Journal of Glaciology,* **5**(40), 411–431 (doi: 10.3189/S0022143000018402).

Theakstone WH (1990) Twentieth-Century Glacier Change at Svartisen, Norway: The Influence of Climate, Glacier Geometry and Glacier Dynamics. *Annals of Glaciology*, **14**, 283–287 (doi: 10.3189/S0260305500008764).

Theakstone WH (2010) Glacier changes at Svartisen, northern Norway, during the last 125 years: Influence of climate and other factors. *Journal of Earth Science*, **21**(2), 123–136 (doi: 10.1007/s12583-010-0011-6).

Theakstone WH (2013) Long-term variations of the seasonal snow cover in Nordland, Norway: The influence of the North Atlantic Oscillation. *Annals of Glaciology*, **54**(62), 25–34 (doi: 10.3189/2013AoG62A300).

Theakstone WH (2018) Flatisen, Svartisen: A Norwegian glacier in decline. *Norsk Geografisk Tidsskrift - Norwegian Journal of Geography*, **72**(5), 305–312 (doi: 10.1080/00291951.2018.1547789).

Tielidze LG (2016) Glacier change over the last century, Caucasus Mountains, Georgia, observed from old topographical maps, Landsat and ASTER satellite imagery. *The Cryosphere*, **10**(2), 713–725 (doi: 10.5194/tc-10-713-2016).

Vaughan DG, Comiso JC, Allison I, Carrasco J, Kaser G, Kwok R, Mote P, Murray T, Paul F, Ren J, Rignot E, Solomina O, Steffen K and Zhang T (2013) Observations: Cryosphere.

In Stocker TF, Qin D, Plattner G-K, Tignor M, Allen SK, Boschung J, Nauels A, Xia Y, Bex V and Midgley PM eds. *Climate Change 2013: The Physical Science Basis. Contribution of Working Group I to the Fifth Assessment Report of the Intergovernmental Panel on Climate Change*, Cambridge University Press, Cambridge, United Kingdom and New York, NY, USA, 317–382.

Weber P, Boston CM, Lovell H and Andreassen LM (2019) Evolution of the Norwegian plateau icefield Hardangerjøkulen since the 'Little Ice Age'. *The Holocene*, (doi: 10.1177/0959683619865601).

Winkler S (2003) A new interpretation of the date of the 'Little Ice Age' glacier maximum at Svartisen and Okstindan, northern Norway. *The Holocene*, **13**(1), 83–95 (doi: 10.1191/0959683603hl573rp).

Winsvold SH, Andreassen LM and Kienholz C (2014) Glacier area and length changes in Norway from repeat inventories. *The Cryosphere*, **8**(5), 1885–1903 (doi: 10.5194/tc-8-1885-2014).

Worsley P and Alexander MJ (1976) Glacier and Environmental Changes—Neoglacial Data From the Outermost Moraine Ridges at Engabreen, Northern Norway. *Geografiska Annaler: Series A, Physical Geography*, **58**(1–2), 55–69 (doi: 10.1080/04353676.1976.11879924).

Zemp M, Armstrong R, Gärtner-Roer I, Haeberli W, Hoelzle M, Kääb A, Kargel JS, Khalsa SJS, Leonard GJ, Paul F and Raup, BH (2014) Introduction: Global Glacier

Monitoring—a Long-Term Task Integrating in Situ Observations and Remote Sensing. In Kargel J, Leonard G, Bishop M, Kääb A and Raup B eds. *Global Land Ice Measurements from Space*, Springer, Berlin, Heidelberg, 1–21 (doi: 10.1007/978-3-540-79818-7_1).

Chapter 4

Paper III – Manuscript for submission to Norsk Geografisk Tidsskrift - Norwegian Journal of Geography

A substantially improved, peer-reviewed and revised version of this manuscript has been published under the title

'Reconstructing the Little Ice Age extent of Langfjordjøkelen, Arctic mainland Norway, as a baseline for assessing centennial-scale icefield recession'

in

*Polar Research, **39**, 2020, 4304*

https://doi.org/10.33265/polar.v39.4304

All external readers should refer to the published version. The following version of the original manuscript has been amended according to the examiners' comments.

Nearly a century of rapid icefield recession at Langfjordjøkelen, northernmost Arctic Norway, since the Little Ice Age

Paul Weber[1,*], Liss M. Andreassen[2], Clare M. Boston[1], Harold Lovell[1], Bjarne Kjøllmoen[2]

[1]University of Portsmouth, Department of Geography, Buckingham Building, Lion Terrace, Portsmouth, PO1 3HE, United Kingdom, *paul.weber@port.ac.uk

[2]Norwegian Water Resources and Energy Directorate (NVE)

Abstract

Current warming in the Arctic is occurring at a rate two to three times higher than that of the rest of the world, leading to rapid glacier wastage. Surface mass balance measurements show that the plateau icefield Langfjordjøkelen in Arctic mainland Norway has experienced the greatest mass loss of all monitored glaciers in Norway in recent decades. Here, we examine this decline in a centennial-scale context through geomorphological mapping and the analysis of historical aerial photographs and maps. This allows Langfjordjøkelen's maximum Little Ice Age (LIA) extent (~1925) to be reconstructed, providing an important baseline for a long-term assessment of icefield change. At the LIA maximum, Langfjordjøkelen covered an area of 14.9 km^2. A comparison of the LIA dimensions with the icefield extent in 1891/1902, as

displayed on a historical map, reveals a substantial overestimation of the map-based glacier outline. The post-LIA evolution of Langfjordjøkelen has been characterised by sustained high rates of glacier recession. By 2018, the icefield had lost 57 % (8.5 km^2) of its original LIA area, at a rate of 9 % $10a^{-1}$, and its outlet glaciers had reduced in average length by 42 % (1 km), at a rate of 11 m a^{-1}. Langfjordjøkelen's percentage area decline has been greater than that of Norwegian ice masses at lower latitudes where comparable long-term glacier change data is available. This indicates that there is a significant latitudinal variation in Norwegian glacier response to 20th century warming.

Keywords: Langfjordjøkelen, plateau icefield, Arctic Norway, Little Ice Age (LIA), glacier reconstruction, glacier change

4.1. Introduction

Since the pre-industrial era (1850-1900), the global mean annual temperature has risen by ~1°C (Allen et al., 2018; World Meteorological Organization (WMO), 2019), causing rapid glacier recession accompanied by a rise in sea level (e.g. Vaughan et al., 2013; Zemp et al., 2015, 2019). This warming is amplified in the Arctic, largely because of a reduction in sea ice cover and resulting feedback effects (Serreze et al., 2009). Here, air temperatures are currently rising at two to three times the global rate (Allen et al., 2018; Box et al., 2019). In northern Canada, the mean annual temperature has increased by 2.3°C since 1948, which is 0.6°C above the Canada-wide average (Bush and Lemmen, 2019). On Svalbard, the mean annual temperature (as measured at Svalbard Airport, Longyear) has risen by 3.7°C since 1900 (Hanssen-Bauer et al., 2019). Parts of northern Norway have experienced an above-average increase in mean annual temperature of 0.11°C $10a^{-1}$ since 1900 compared to the rest of Norway (0.09°C $10a^{-1}$) (Hanssen-Bauer et al., 2015). As a result, Arctic ice masses are receding rapidly and are currently the largest contributor to global sea-level rise (Box et al., 2018).

In northernmost Arctic Norway, the maritime plateau icefield Langfjordjøkelen (Bártnatvuonjiehkki) (70º10'N, 21º45'E; Fig. 4-1) has been in sustained decline since the late 1940s (Andreassen et al., 2012a). Direct mass balance measurements carried out on the icefield's major eastern outlet glacier (Langfjordjøkelen East; informal name) since 1989 show that the icefield underwent the strongest mass loss of all Norwegian glaciers with mass balance records in the period 1989-2008 (Andreassen et al., 2012a). In situ length change measurements at Langfjordjøkelen East since 1998 document a cumulative frontal retreat of 618 m (Data: NVE). In 2018, the icefield was 6.4 km^2 in area and spanned an elevation range from 1,042 m a.s.l. on the icefield summit to 338 m a.s.l. at the front of the eastern outlet (Data: NVE). The

last major expansion of the icefield occurred during the Little Ice Age (LIA), dated to ~1925 at Langfjordjøkelen, with an uncertainty of ±20 years (Wittmeier et al., 2015). However, its exact maximum extent is largely unknown and has not been mapped systematically to date. A historical gradteigskart map shows the icefield extent in 1891/1902, presumably in a state of advance to its maximum limits. Winsvold et al. (2014) used the mapped outline to calculate glacier change to the year 2006 and found that Langfjordjøkelen had diminished in area and length by 62 % and 43 %, respectively. In this study, we reconstruct the icefield's dimensions at the LIA maximum, which can then serve as a baseline both to determine the accuracy of the old map and to examine icefield change over the last ~100 years in greater detail. The latter allows the magnitude of Langfjordjøkelen's recent rapid decline to be placed in a centennial-scale context, with the potential to detect a signal of amplified glacier retreat in Arctic Norway. The objectives of this research are thus threefold: (1) to establish Langfjordjøkelen's maximum LIA extent from the glacial landform record preserved around the icefield; (2) to compare our reconstructed LIA outline with the map-based 1891/1902 glacier extent; and (3) to quantify and discuss icefield area and length change since the LIA maximum.

4.2. Methods

Following a standard approach outlined in Chandler et al. (2018), glacial landforms were mapped remotely in ArcGIS from high-resolution (0.25 m) digital colour vertical aerial photographs captured on 20-21 August 2015 (acquired from http://norgeibilder.no/; Table 4-1) and ground-truthed during a three-week field campaign in summer 2017. The landform features identified at Langfjordjøkelen include ice-marginal moraines, glacial trimlines, glacial drift limits (boundary between a surface composed of fresh and sparsely vegetated glacially derived material (assumed LIA) and drift-free (assumed older) terrain beyond), and erosional/weathering boundaries (boundary between freshly ice-moulded (assumed LIA) and more weathered (assumed older) bedrock). Field mapping took place around the entire icefield except for the relatively inaccessible northeastern sector (Nordmanndalen and Trolldalen (Skuonasvággi) valleys). Moraine positions were recorded using a handheld GPS unit that provided maximum accuracy of 4 m. The results of the geomorphological mapping are presented in Fig. 4-1).

The historical gradteigskart map shows evidence of mismapped topographic features, in both their shape and geographical location (described in more detail in Section 4.4.). In an attempt to rectify these inaccuracies, we georeferenced the map sheet again, using an Adjust Transformation with a total number of 127 control points in the immediate surroundings of the icefield. Many of the control points were placed in a way to drag landscape features such as lake

shorelines or mountaintops to their correct geographical location. We then manually re-digitised the icefield outline from the georectified map.

We used our reconstructed LIA outline together with other available outlines of Langfjordjøkelen since 1945 (Table 4-1) to examine rates of glacier area and length change in the period ~1925-2018. All icefield outlines were subdivided into glacier units along the drainage divides established by Andreassen et al. (2012b), which had to be slightly adjusted to the LIA icefield dimensions. Glacier area change per glacier unit and for the icefield as a whole was calculated for each time interval and for the overall measurement period. We used compound interest calculation (Andreassen et al., 2008; Zemp et al., 2014) to compute decadal rates of area change. Cumulative length change and rates of length change were measured along glacier centrelines. Guided by the 1966, 1988 and 2006 centrelines previously created for Langfjordjøkelen by Winsvold et al. (2014), we digitised one principal centreline per icefield unit by connecting the glacier head with the most downvalley point of each glacier outline's terminus. Ice-marginal snow included in remotely sensed glacier outlines can introduce glacier area uncertainties of 5-10 % for larger (>5 km^2) ice masses and up to 25% for smaller (<1 km^2) glaciers (Paul & Andreassen, 2009). Although not quantified here, these values are a realistic error estimate for our change assessment.

Table 4-1. Overview of remotely-sensed icefield outlines of Langfjordjøkelen.

Date/ Year	Source	Scale/ resolution	Produced/ published by	Reference/Comment
1891/1902	Topographic map (*gradteigskart*) based on ground surveys carried out in 1891 and 1902; published in 1907	1:100,000	Norwegian Mapping Authority (Norges geografiske opmaaling)	Map georectified (127 control points; total RMSE: 17.5; Adjust Transformation) and outline digitised on-screen by author
15/08/1945	Analogue vertical aerial photographs	1:40,000	British Royal Air Force (RAF)	Two photographs scanned and georectified (82/85 control points; Spline Transformation); outline digitised on-screen by author
11/07/1966	Topographic map (N50) based on vertical aerial photographs; published in 1979	1:50,000	Norwegian Mapping Authority (Norges geografiske oppmåling)	Winsvold et al. (2014)
11/07/1966	Vertical aerial photographs	Unknown	Fjellanger Widerøe AS	Andreassen et al. (2012a)
03/09/1988	Landsat 4 TM	30 m	Landsat	Winsvold et al. (2014)
01/08/1994	Vertical aerial photographs	Unknown	Fjellanger Widerøe AS	Andreassen et al. (2012a)
28/08/2006	Landsat 5 TM	30 m	Landsat	Andreassen et al. (2012b)
20.-21.08.2015	Digital vertical aerial photographs	0.25 m	Blom Geomatics AS; available from http://norgeibilder.no/	Outline digitised on-screen by author
01/09/2018	Pléiades	0.5 m PAN; 2 m MS	Pléiades	Outline digitised on-screen by NVE

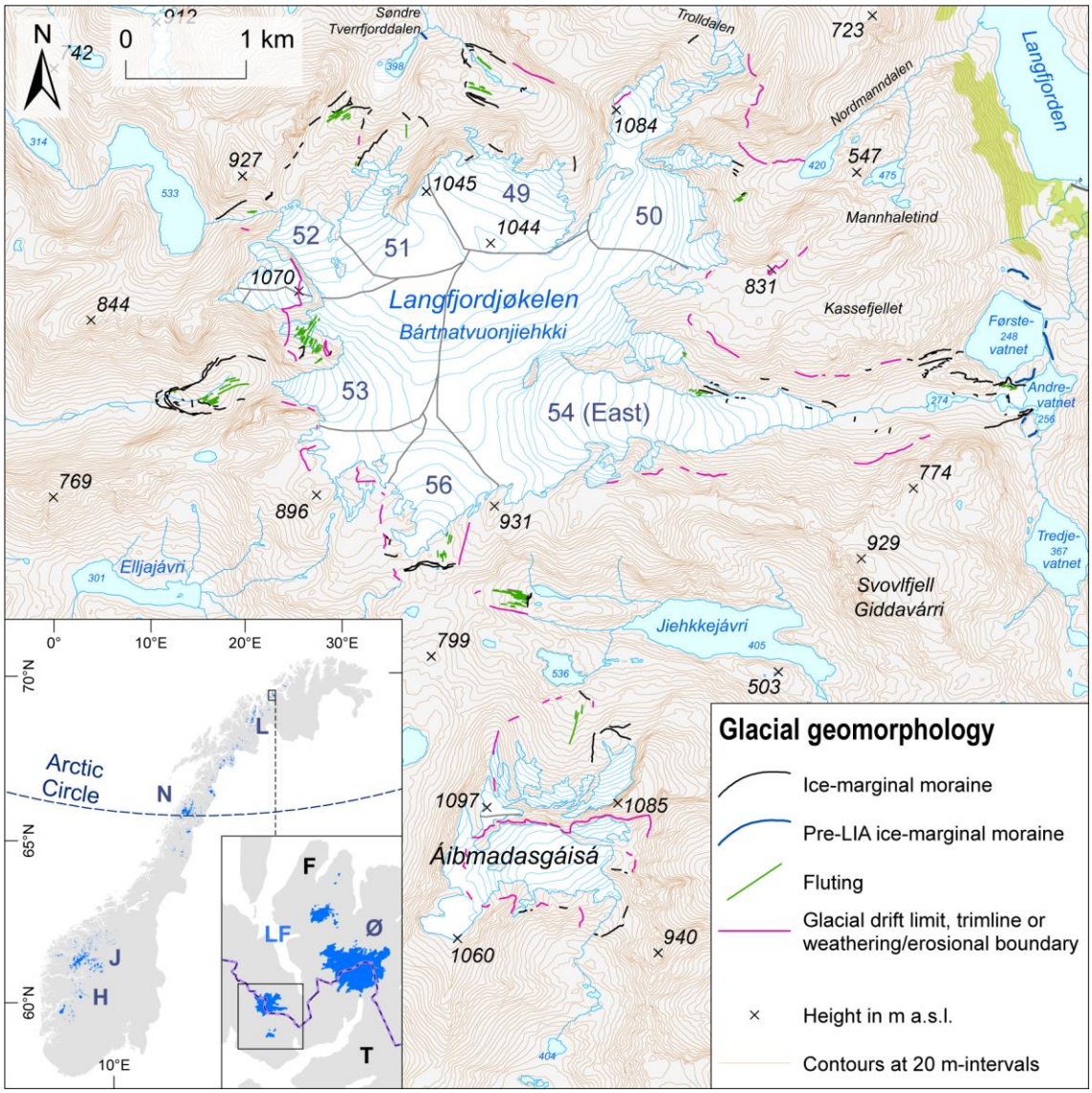

Fig. 4-1. Topographic map of Langfjordjøkelen including glacial geomorphological landform features mapped at the margins of the icefield (Coordinate System: ETRS 1989 UTM Zone 33N; Projection: Transverse Mercator; Map data from Kartverket – Norwegian Mapping Authority). The inset shows the location of Langfjordjøkelen in Norway, along with other ice masses. H: Hardangerjøkulen; J: Jotunheimen glaciers; N: Nordland glaciers; L: Glaciers on the Lyngen Peninsula; Ø: Øksfjordjøkelen. LF: Langfjorden; T: Troms county; F: Finnmark county.

4.3. Geomorphological evidence and identification of LIA limit

Langfjordjøkelen's maximum LIA extent is typically delineated by major, well-defined, sparsely vegetated and often bouldery moraine ridges in the valleys radiating from the glacier-covered plateau. These valleys are narrow, steep-sided and dominated by mass movement processes. Active talus and debris flow deposits cover the sides and base of the valleys so that there is little glacial landform evidence between the outer LIA moraines and the present-day ice margin. The talus outside the LIA limit often appears more stable and vegetated, providing an

indication of the maximum LIA extent. Also occurring outside the LIA limit in many of the valleys are suits of mature, round-crested and well-vegetated moraines (Fig. 4-1), which presumably outline the Younger Dryas icefield extent (cf. Evans et al., 2002).

At Langfjordjøkelen East, the lateral margins of the glacier tongue are mantled in debris, and ice-cored morainic mounds are present along the northern part of the terminus. Glaciofluvial outwash deposits occupy large parts of the valley floor down to the Andrevatnet lake. Here, prominent, sharp-crested, sparsely to moderately vegetated lateral moraine ridges mark the outlet's maximum LIA position. An enormous, more than 20 m high lateral moraine was deposited on the southern side of the valley mouth. The height of its crest gradually reduces towards the lake where the ridge terminates in a small cluster of lateral moraines. The LIA lateral moraine on the northern side of the valley mouth attains heights of up to 10 m and forms a small lobe in front of the Førstevatnet lake. A handful of discontinuous moraines occur immediately inside the ridge on a narrow patch of distinctly fluted drift. On the sandur fan in the middle of the LIA foreland, approximately 150 m from the lakeshore, lies a round-topped, slightly winding recessional end moraine composed of sands with gravel and pebble clasts and a few boulders incorporated in its flanks, reflecting an episode of post-LIA ice front stability or minor glacier advance. The northern LIA lateral moraine meanders up the crest of a prominent foothill that projects from the northern base of the plateau and extends halfway across the valley. In the narrow, debris-choked gorge between this foothill and the plateau flank that rises towards the Kassefjellet peak, a series of latero-frontal recessional moraines demonstrates that the LIA glacier tongue split around this semi-detached peak and sent a small side tongue down the gorge towards Førstevatnet. On the plateau flank above the gorge, a distinct trimline, interspersed by lateral moraines, runs along the entire length of the valley side onto the plateau summit, rising from ~357 m a.s.l. at the valley mouth to ~722 m a.s.l. on the plateau.

Fig. 4-2. Langfjordjøkelen's northern flank photographed on 31 July 1952 (National Library of Norway).

In the valleys along the northeastern icefield sector, sparse glacial landform evidence in the form of drift limits, erosional boundaries and ice-marginal moraines (identified from aerial photograph interpretation) tentatively indicates the maximum LIA extent. This evidence is strongest in the Nordmanndalen valley, where a relatively continuous drift limit along the northern valley side suggests that the LIA ice front advanced to the unnamed lake (420 m a.s.l.) currently occupying the valley floor.

The northern icefield sector overlooks the head of the presently ice-free Søndre Tverrfjorddalen (Bártnatvuonvággi) valley system. Here, three outlet glaciers are reconstructed to have extended from the plateau during the LIA maximum, which can still be seen on historical aerial photographs (Fig. 4-2 and 4-3). The easternmost outlet (originating from drainage basin 49) flowed down a U-shaped trough to ~485 m a.s.l. (Fig. 4-1), as evidenced by predominantly openwork, clast-supported, bouldery outer latero-frontal moraines with up to two sets of inset moraine ridges. Exposed bedrock on the valley floor is ice-moulded, contrasting with the weathered bedrock outside the LIA limit. The LIA lateral moraine on the northeastern valley side links up with a sharp glacial trimline that leads onto the plateau. A former LIA outlet issuing from drainage basin 51 (Fig. 4-2) deposited major, sharp-crested to round-topped outer moraine ridges down to an elevation of ~513 m a.s.l. Heavily ice-moulded bedrock occurs inside this limit. A third outlet glacier was fed by ice from drainage basin 52 in the northwest of Langfjordjøkelen (confluent with outlet 51 in the upper part of the glacier trunk). Ice from this basin flows in a northwesterly direction through a low saddle into a perpendicularly-oriented, chute-like stretch of the valley (the 2018 Pléiades imagery shows that the remaining ice in the saddle has become detached from the icefield). Down in the valley, the former outlet split into two branches, producing a double moraine ridge on the northwestern valley side. A short, west-flowing branch extended down to, but did not quite reach, the unnamed lake (533 m a.s.l.) to the northwest of Langfjordjøkelen, as indicated by a well-defined lateral moraine ridge on the northern valley side above the lake (Fig. 4-3). The main branch of the outlet trended in a northeasterly direction to the edge of a steep, debris-covered slope, forming bench-like lateral moraine segments along the northwestern valley side during outlet recession. At the edge of the slope, the outlet terminus split further into two tongues around an intervening bedrock protrusion. This created an extremely sharp-crested bifurcating moraine complex in the middle of the debris-choked, fluted valley floor. The northwestern tongue ended at the upper slope edge at ~520 m a.s.l., which is documented by a major lateral moraine paralleling the bifurcating ridge complex along the northwestern valley side. By contrast, the southeastern tongue descended halfway down the slope to ~460 m a.s.l., depositing sharp- to round-crested lateral moraines. Both tongues appear to have sent large quantities of debris down the slope.

The LIA icefield limit along the western edge of the plateau summit is often clearly delineated by glacial drift limits. Flutings and moraine fragments on the plateau edge show that

ice flow out of drainage basin 53 was funnelled entirely into the U-shaped valley stretching to the west, which hosted a sizeable LIA outlet glacier. The maximum extent and subsequent ice front fluctuations of this LIA outlet are marked by a system of nested bouldery latero-frontal moraines that can be traced almost continuously around the inner valley (Fig. 4-3). Today, only a minor ice tongue is occupying the upper valley headwall below the plateau edge.

In the south of the icefield (drainage basin 56), a multi-crested end moraine complex along with single moraine ridges, sharp drift limits and flutings define the maximum LIA extent of a sheet-like glacier lobe that spread across, but did not descend from, the southern plateau summit area. The oblique aerial photograph in Fig. 4-3 shows that the outlet lobe still stood at the moraine complex in 1936-1939. Just to the southeast, a small ice patch of presumed LIA age existed on the plateau flank above the Jiehkkejávri lake, as signified by a well-delimited sheet of fluted drift with a sequence of frontal moraine ridges at its downvalley end. The LIA extent of the two cirque glaciers of the Áibmadasgáisá massif is demarcated by ice-marginal moraines and erosional boundaries.

Fig. 4-3. Langfjordjøkelen's western flank photographed between 1936 and 1939 (National Library of Norway).

Following the approach developed by Weber et al. (2019), we used the outermost LIA glacial landforms as a framework to reconstruct Langfjordjøkelen's outline at the LIA maximum. The gaps between the landform-based sections of the outline were then filled by interpolation (Fig. 4-4). Our reconstructed LIA outline has a total length of 33.4 km. Just over one-third (36.5 %; 12.2 km) of this length is based on unambiguous landform evidence and can thus be classed as certain. Guided by the topography of the terrain and historical aerial

photographs, approximately half of the length (53.7 %; 17.9 km) was reliably interpolated between the evidence-based sections of the outline and can be classified as fairly certain. Most of the icefield's outlet glaciers fall into these two categories as ice-marginal landforms preferentially form at the glacier snout, where they are often abundant and closely spaced. An exception is the southern LIA margin of Langfjordjøkelen East, which was established by mirroring the reconstructed LIA margin along the northern valley side, due to a paucity of glacial landforms. Only a tenth of the outline (9.9 %; 3.3 km) is less certain and had to be inferred from the topography alone, representing a 'best-guess' interpolation. This is particularly the case for the LIA extent in drainage basin 50 where landform evidence on the plateau summit is sparse, leaving the possibility that the LIA ice in the Trolldalen valley was not connected to the main icefield (however, this would have only a minor effect on the area of the reconstructed LIA outline because the icefield and Trolldalen are only separated by a narrow ridge). The results of our confidence assessment are summarised in Table 4-2, which also shows the estimates for the small ice masses outside the LIA icefield.

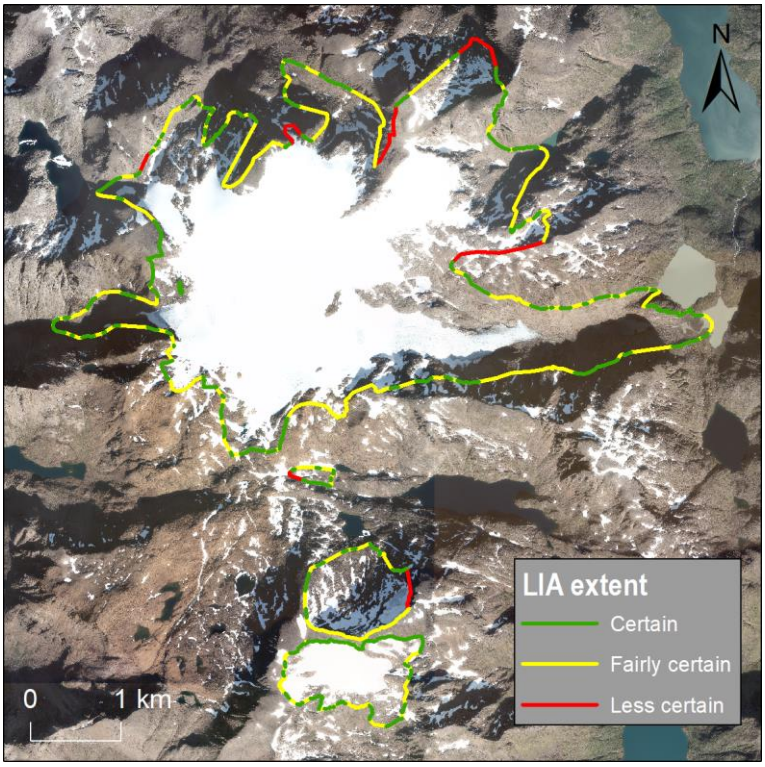

Fig. 4-4. Reconstructed maximum LIA extent of Langfjordjøkelen, classified into different levels of confidence. The vertical aerial photograph in the background shows the icefield between 20 and 21 August 2015 (available from http://norgeibilder.no/).

Table 4-2. Confidence estimates for the reconstructed LIA icefield.

	Length LIA outline (km)	Certain		Fairly certain		Less certain	
		km	%	km	%	km	%
LAJ icefield	33.4	12.2	36.5	17.9	53.7	3.3	9.9
Jiehkkejávri lake ice patch	1.2	0.5	38.7	0.5	42.7	0.2	18.6
Áibmadasgáisá North (ID 57-58)	3.8	0.8	21.4	2.5	65.5	0.5	13.1
Áibmadasgáisá South (ID 59)	5.2	3.1	59.2	2.1	40.8		
Total length	43.6	16.5		23.0		4.0	
Mean			38.9		50.7		13.9

4.4. Comparison with map-based 1891/1902 icefield extent

Langfjordjøkelen's reconstructed LIA outline has a total area of 14.9 km^2. This compares to an area of 20.6 km^2 calculated for the 1891/1902 icefield extent (based on historical field surveys), suggesting that the icefield was substantially larger in 1891/1902 than at its LIA maximum (dated to ~1925; Wittmeier et al., 2015). Particularly the southern icefield sector is more extensive than the maximum extent indicated by our reconstruction, including an additional outlet glacier in the east of the icefield (Fig. 4-5). On closer inspection, however, several map inaccuracies become apparent. The topography shown on the map appears smoothed, and a number of topographic features (or their geographical location) were mapped incorrectly, resulting in the georeferencing problems described in Section 4.2. A good example of this is the northern Áibmadasgáisá cirque, which was mapped as a convex mountain flank. Entirely missing from the map are the two prominent lakes Elljajávri and Jiehkkejávri to the southwest and southeast of Langfjordjøkelen, respectively (Fig. 4-5). The Jiehkkejávri lake basin is instead occupied by the additional eastern outlet glacier (for which there is no geomorphological evidence). These lakes are situated in high mountain valleys and are difficult to see unless one is close to them or at a higher elevation. Their absence from the map, therefore, implies that the field surveyors did not visit the area around the southern sector of Langfjordjøkelen directly, but carried out the mapping from a distance. As a result, seasonal or perennial snow present on the plateau summit at the time of the surveys may have been mistaken for glacier ice and included in the icefield outline. Consequently, we suspect the 1891/1902 icefield extent to be overestimated, and we will not use it in the following glacier change assessment.

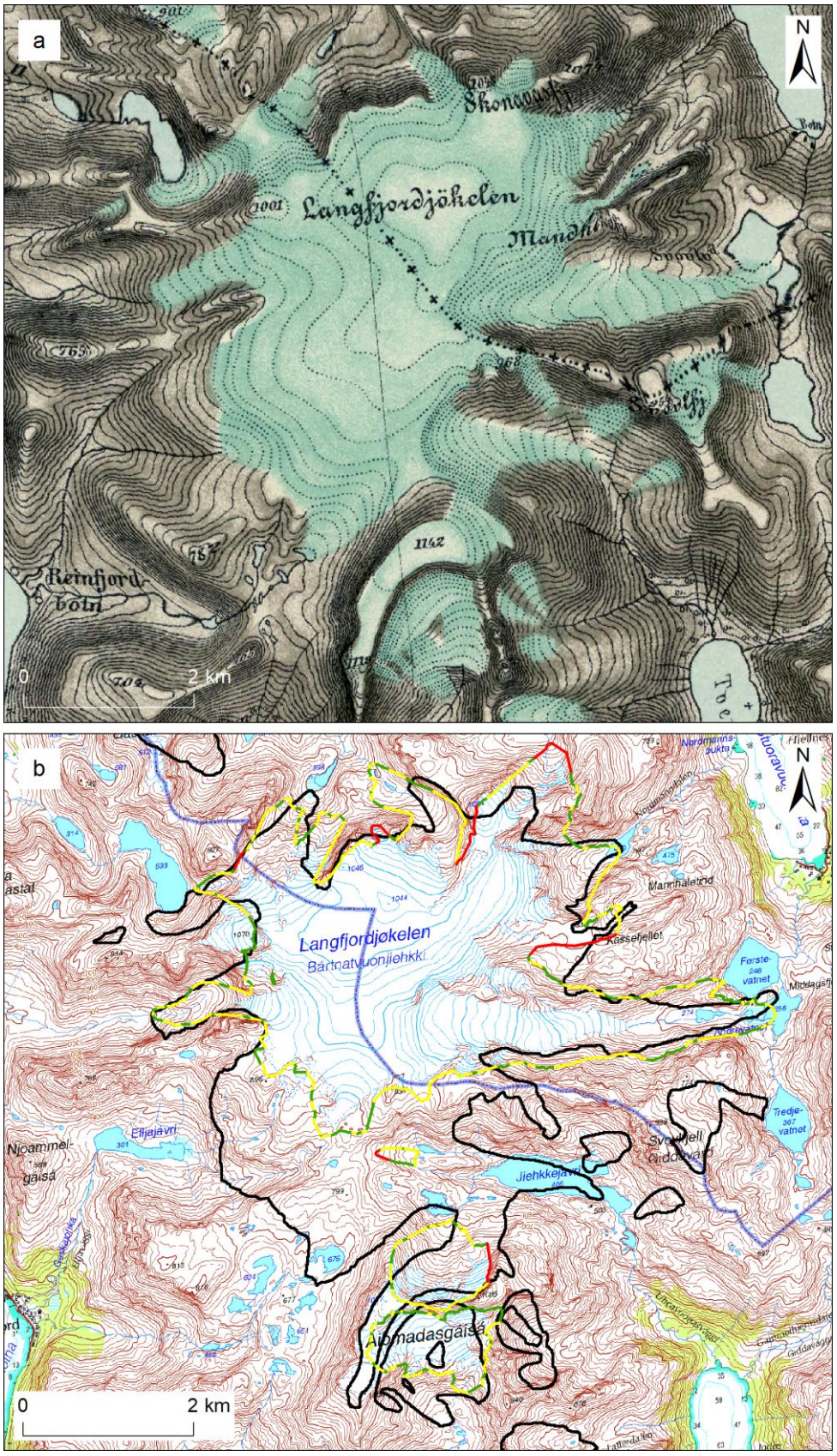

Fig. 4-5. (a) Gradteigskart map sheet S4 Bergsfjorden (Published: 1907; 1:100,000; Cartographers: Torgrim Lundtvedt, Carl Christian Olberg; available from Kartverket). (b) Comparison of historical (1891/1902) and reconstructed LIA icefield extent.

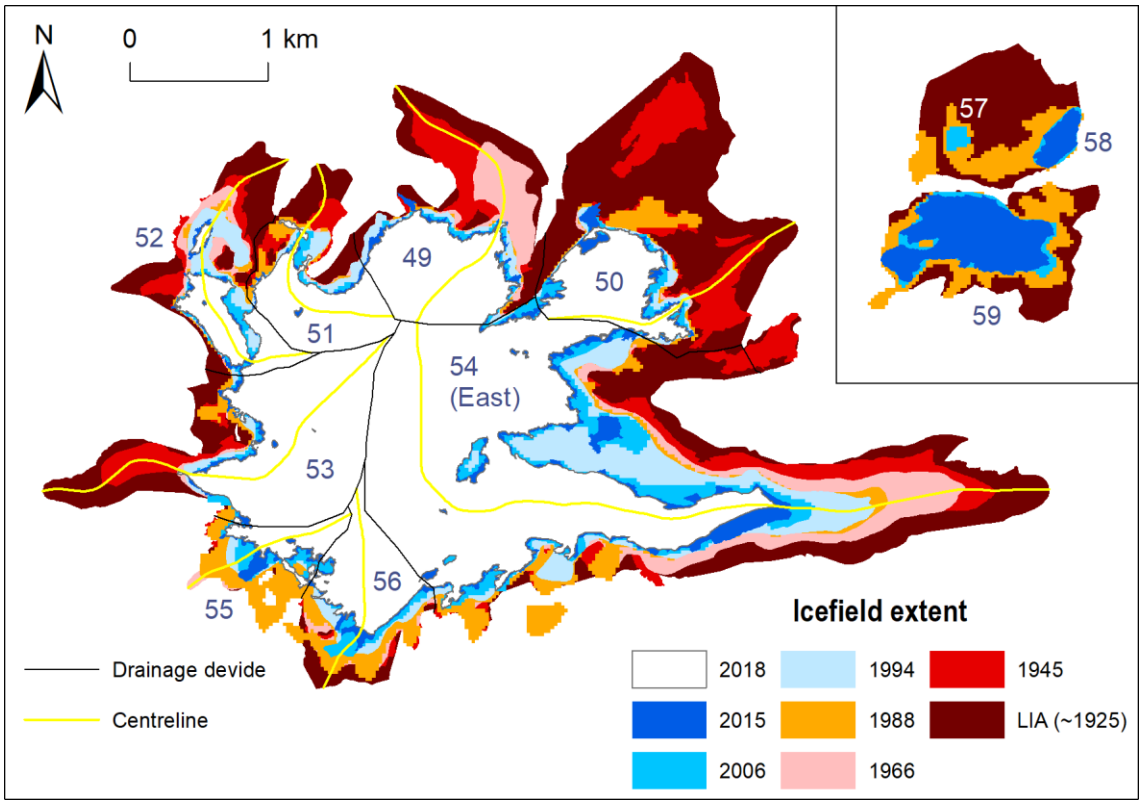

Fig. 4-6. Icefield recession from the LIA maximum to present using glacier outlines from successive time points. Glacier centrelines used for assessing glacier length change are shown for all icefield units.

Table 4-3. Glacier area of Langfjordjøkelen and its glacier units since the LIA (1925). Aspect data from Andreassen et al. (2012b).

Glacier unit ID	Informal glacier unit name	Aspect	LIA	1945	1966 [a]	1966 [b]	1988	1994	2006	2015	2018
49	LAJ NE	NE	1.5	1.2	1.3	1.0	0.8	0.8	0.7	0.7	0.6
50		E	2.5	1.2	2.2	0.6	0.7	0.6	0.6	0.5	0.5
51		NW	0.8	0.7	0.8	0.6	0.6	0.6	0.5	0.5	0.5
52	LAJ NW	NW	1.0	0.7	0.9	0.6	0.5	0.5	0.3	0.3	0.3
53	LAJ West	SW	1.7	1.4	1.4	1.2	1.3	1.2	1.2	1.2	1.1
54	LAJ East	SE	6.1	4.9	5.6	4.7	4.3	4.1	3.5	3.1	2.8
55		W	0.4	0.4	0.6	0.4	0.5	0.3	0.3	0.2	0.2
56		S	0.8	0.7	0.9	0.7	0.7	0.6	0.5	0.5	0.4
LAJ	**Langfjordjøkelen**		**14.9**	**11.2**	**13.5**	**9.8**	**9.4**	**8.6**	**7.5**	**7.0**	**6.4**
57	Áibmadasgáisá North (ID 57)	NE					0.1		0.02	0	
58	Áibmadasgáisá North (ID 58)	N	0.9		0.6		0.3		0.1	0.1	
59	Áibmadasgáisá South	SE	1.0		1.1		0.8		0.5	0.5	
	Jiehkkejávri lake ice patch		0.1								

[a] Winsvold et al. (2014) outline

[b] Andreassen et al. (2012a) outline

4.5. Glacier change assessment

Here, we describe glacier change at Langfjordjøkelen between the LIA icefield maximum (~1925) and 2018 (Fig. 4-6; Table 4-1). These changes are discussed in the context of the available mass balance data (Fig. 4-7) (Andreassen et al., 2012a; Kjøllmoen et al., 2018), which is useful because annual surface mass balance represents the undelayed, combined signal of, primarily, air temperature (mass loss) and solid precipitation (mass gain) across the glacier surface. A breakdown of the total glacier area of the icefield and its glacier units for each time point is given in Table 4-3. Rates of icefield area and length change are summarised in Table 4-4 and 4-5, respectively. Table 4-6 shows cumulative length change at Langfjordjøkelen since the LIA.

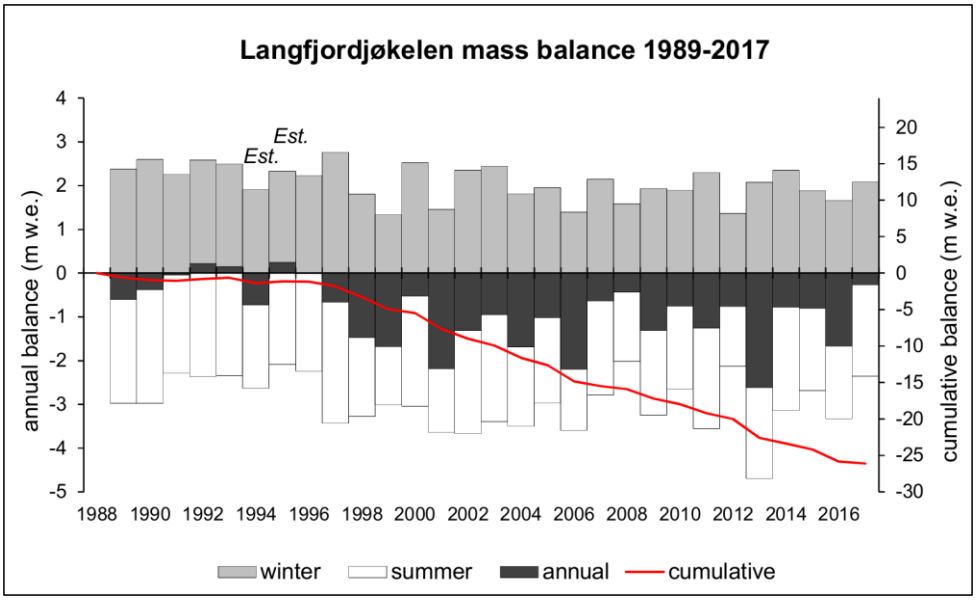

Fig.4-7. Mass balance at Langfjordjøkelen for the period 1989-2017 (taken from Kjøllmoen et al., 2018). *Est.*: Values modelled by Andreassen et al. (2012a).

In the 20 years between the LIA maximum and 1945, Langfjordjøkelen's area shrank by a quarter (3.7 km^2; 24.9 %) at a rate of 1.9 km^2 $10a^{-1}$ (14.2 % $10a^{-1}$), whilst length changes averaged -12.1 m a^{-1}. Over the next ~40 years, total area loss as well as the rate of loss decreased, with an areal reduction of 1.3 km^2 (11.9 %) in the period 1945-1966 (0.6 km^2 $10a^{-1}$; 6.0 % $10a^{-1}$) and a further reduction of 0.5 km^2 (4.8 %) in the period 1966-1988 (0.2 km^2 $10a^{-1}$; 2.3 % $10a^{-1}$). By contrast, the rate of frontal retreat increased by almost 2 m a^{-1} after 1945 (13.9 m a^{-1}), before falling to 7.7 m a^{-1} from 1966 to 1988. Andreassen et al. (2012a) modelled a cumulative mass balance of -24.4 m water equivalent (w.e.) between 1948/1949 and 1988/1989

(annual balance of -0.61 m w.e.) (The water equivalent is the amount of water contained within a layer of ice/firn/snow and is calculated by multiplying the ice/firn/snow depth by their respective density; snow/firn density: measured in the field; ice density: estimated at 900 kg m^{-3}; Kjøllmoen et al., 2018). We hypothesise that strong icefield recession in the 1925-1945 period (and continued strong frontal retreat between 1945 and 1966) can be attributed to the distinct global Early Twentieth Century Warming (ETCW) episode, which was particularly pronounced in the Arctic, and specifically in the European Arctic (Hegerl et al., 2018). In coastal Arctic Norway and the Langfjordjøkelen region, the ETCW culminated in the mid-1930s, with annual mean temperatures of up to ~0.6°C above the 1961-1990 average (Hanssen-Bauer, 2005).

Table 4-4. Comparison of rates of glacier area change at Langfjordjøkelen for each measurement period.

	Total area change (km^2)	Total area change (%)	Rate of change (km^2 $10a^{-1}$)	Rate of change (% $10a^{-1}$)
LIA[a]-1945	-3.7	-24.9	-1.9	-14.2
1945-1966[b]	-1.3	-11.9	-0.6	-6.0
1966-1988[b]	-0.5	-4.8	-0.2	-2.3
1988-1994	-0.8	-8.5	-1.3	-14.6
1994-2006	-1.1	-12.6	-0.9	-11.1
2006-2015	-0.5	-6.8	-0.6	-7.8
2015-2018	-0.6	-8.4	-2.0	-28.8
LIA[a]-2018	-8.5	-57.0	-0.9	-9.0

[a] Assuming 1925 as the timing of the icefield-wide LIA maximum

[b] Using the 1966 outline from Andreassen et al. (2012a)

Table 4-5. Comparison of mean length changes of Langfjordjøkelen's icefield units for each measurement period.

	LIA[a]-1945	1945-66[b]	1966-88[b]	1988-94	1994-2006	2006-15	2015-18	LIA-2018[c]
Mean total change (m)	-242	-293	-170	-80	-128	-73	-122	-1108
Mean rate of change (m a^{-1})	-12.1	-13.9	-7.7	-13.4	-10.7	-8.1	-40.7	-11.9

[a] Assuming 1925 as the timing of the icefield-wide LIA maximum

[b] Using the 1966 outline from Andreassen et al. (2012a)

[c] Using the mean cumulative change (Table X)

The 1966 icefield extent highlights the effect of snow included in remotely sensed glacier outlines. Two outlines are available for that year, both based on the same vertical aerial photographs from 11 July 1966 (Table 4-1). One outline was directly produced by the aerial photography contractor and used in the study by Andreassen et al. (2012a) as well as this study,

whilst the other was produced by the Norwegian Mapping Authority (Kartverket) for a 1:50,000 topographic map sheet. Winsvold et al. (2014) digitised and included the latter outline in their ~1960 inventory of Norwegian glaciers. The Winsvold et al. (2014) icefield outline features a number of uncharacteristic, tentacle-shaped branches (Fig. 4-8). Visual inspection of the original aerial photographs revealed these branches to be ice-marginal snow. The inclusion of the snow in this outline leads to an overestimation of the 1966 glacier area by 38 % compared to the Andreassen et al. (2012a) outline (Table 4-3). This is significantly higher than the reference error estimates obtained by Paul and Andreassen (2009) (5-10 % for glaciers with an area of >5 km^2; see Section 4.2.). Calculating icefield change using this outline would yield an unrealistic area increase of 22.0 % (2.4 km^2) between 1945 and 1966, followed by an abrupt area loss of 30.8 % (4.2 km^2) in the period 1966-1988. This example demonstrates the need to rigorously examine the quality of digital glacier outlines prior to glacier change assessments.

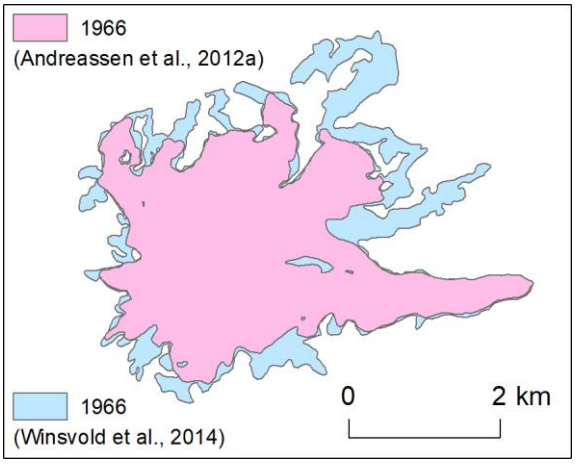

Fig. 4-8. Comparison of the two versions of the 1966 icefield extent.

In the following two measurement periods, rates of icefield shrinkage increased to 14.6 % $10a^{-1}$ (1.3 km^2 $10a^{-1}$) between 1988 and 1994 (exceeding the values reached during the ETCW episode) and 11.1 % $10a^{-1}$ (0.9 km^2 $10a^{-1}$) between 1994 and 2006. Absolute and percentage area change was -0.8 km^2 (-8.5 %) in the 1988-1994 period and -1.1 km^2 (-12.6 %) in the 1994-2006 period. Rates of frontal retreat accelerated to 13.4 m a^{-1} after 1988, only to decrease slightly to 10.7 m a^{-1} from 1994 to 2006. This contrasts sharply with many other maritime glaciers along the Norwegian coast, which exhibited a pronounced readvance in the 1990s in response to increased winter precipitation in the late 1980s/early 1990s (Andreassen et al., 2005; Nesje et al., 2008). The advance of these glaciers was associated with a considerable mass surplus (Andreassen et al., 2005, 2016; Kjøllmoen et al., 2018). Although the mass balance record of Langfjordjøkelen also shows high annual winter balances between 1989 and

1994, and even slightly positive balance years in 1991/1992 (0.22 m w.e.) and 1992/1993 (0.15 m w.e.), summer ablation was often slightly higher (Fig. 4-7). This resulted in negative annual balances between 1989 and 1991, and a cumulative mass balance of -1.38 m w.e. in the period 1989-1994. Nonetheless, these values cannot satisfactorily explain Langfjordjøkelen's excessive retreat in the 1988-1994 period, which remains a question for further investigation (see also discussion in Andreassen et al., 2012a). By contrast, the strong recession in the 1994-2006 period is well reflected in the mass balance record, which is characterised by consistently highly negative balance years between 1997 and 2006 (Fig. 4-7). By 2006, the cumulative mass balance decreased to -14.83 m w.e. An analysis of icefield elevation change for the period 1994-2008 (Andreassen et al., 2012a) reveals that virtually the entire icefield surface (97 %) lowered by more than 2 m, and half of the icefield even thinned by 10-20 m, equating to a geodetic mass balance of -13.5 m w.e. (Thinning is the change in elevation of the glacier surface derived from DEM differencing). Thinning was particularly severe in the lower part of Langfjordjøkelen East (up to 73 m) (Andreassen et al., 2012a).

Table 4-6. Cumulative glacier length changes at Langfjordjøkelen since the LIA (1925).

Glacier unit ID	Informal glacier unit name	LIA centreline length (m)	Cumulative length change (m)							Cumulative length change LIA-2018 (%)
			1945	1966[a]	1988	1994	2006	2015	2018	
49	LAJ NE	2354	-144	-784	-1363	-1355	-1363	-1356	-1367	-58.1
50		2046	-235	-944	-963	-953	-990	-999	-1036	-50.6
51		1817	-260	-494	-472	-515	-541	-607	-539	-29.7
52	LAJ NW	2325	-307	-444	-545	-640	-1095	-1133	-1906	-82.0
53	LAJ West	3082	-455	-1064	-1110	-1114	-1188	-1161	-1147	-37.2
54	LAJ East	5836	-391	-620	-1191	-1293	-1726	-1896	-2014	-34.5
55		1070	+4	+248	+117	-94	-139	-313	-337	-31.5
56		1544	-148	-174	-112	-316	-265	-425	-520	-33.7
Mean	**Langfjord-jøkelen**	2509	-242	-535	-705	-785	-913	-986	-1108	-44.2

[a] Using the 1966 outline from Andreassen et al. (2012a)

After 2006, icefield recession continued at a slightly lower rate of 7.8 % $10a^{-1}$ (0.6 km^2 $10a^{-1}$), with an areal reduction of 0.5 km^2 (6.8 %) and a change in average length of -8.1 m a^{-1} between 2006 and 2015. Since then, Langfjordjøkelen's decline has increased dramatically to 28.8 % $10a^{-1}$ (2.0 km^2 $10a^{-1}$), resulting in an area loss of 0.6 km^2 (8.4 %) in the final measurement period 2015-2018. The rate of frontal retreat has risen sharply to 40.7 m a^{-1} since 2015. The varying pace of 21st-century icefield retreat is not mirrored in Langfjordjøkelen's cumulative mass balance record, which has displayed a steady, and steep, downward trend since 1997, decreasing to -27.48 m w.e. in 2017/2018 (Fig. 4-7). Nonetheless, the unprecedented

magnitude of recent icefield recession is a reflection of accelerated global and regional glacier wastage since the end of the 20th century (Vaughan et al., 2013; Zemp et al., 2015; Stokes et al., 2018; Weber et al., 2019).

Over the total measurement period from the LIA (~1925) to 2018, Langfjordjøkelen lost an area of 8.5 km^2 (57.0 %) at a rate of 0.9 km^2 $10a^{-1}$ (9.0 % $10a^{-1}$). The icefield's glacier units decreased in cumulative length by 1.1 km (44.2 %; 11.9 m a^{-1}) on average, and Langfjordjøkelen East retreated by 2.0 km (34.5 %) (Fig. 4-9). We did not observe aspect to have a noticeable influence on icefield area or length change. Assuming a LIA maximum in 1905 (based on the uncertainty of ±20 a associated with the Wittmeier et al. (2015) LIA age) yields slightly lower rates of icefield change over the total period LIA-2018, with areal shrinkage of 0.7 km^2 $10a^{-1}$ (7 % $10a^{-1}$) and a frontal retreat of 9.3 m a^{-1} (17.8 m a^{-1} at Langfjordjøkelen East).

Glacier area change of the two cirque glaciers of the Áibmadasgáisá massif was assessed for the period 1925-2015, revealing a total area loss of 0.6 km^2 (53.7 %) at the southern cirque (ID 59) and 0.8 km^2 (91.5 %) at the northern cirque (ID 57/58). Both ice masses receded at an absolute rate of 0.1 km^2 $10a^{-1}$, which corresponds to a relative rate of 8.5 % $10a^{-1}$ at the southern cirque (consistent with the icefield) and 27.0 % $10a^{-1}$ at the northern cirque.

We compare icefield change at Langfjordjøkelen to existing estimates of long-term glacier change along a latitudinal transect across Norway. At Hardangerjøkulen in southern Norway (Fig. 4-1), data from Weber et al. (2019) shows a total reduction in icefield area and average length of 26.5 % and 18.0 %, respectively, between 1923-1929 and 2013. By contrast, data from Langfjordjøkelen reveals a substantially greater loss in icefield area and average length of 53.1 % and 39.3 %, respectively, in the same period (1925-2015). In Jotunheimen, approximately 125 km to the north-northeast of Hardangerjøkulen (Fig. 4-1), available glacier inventory data from Andreassen et al. (2008) indicates areal shrinkage of 22.6 % between 1931-1934 and 2003, which can be compared to a much greater value of 49.7 % in the 1925-2006 period at Langfjordjøkelen. Our comparison suggests that the relative magnitude of long-term glacier change in northernmost Arctic Norway was twice that of southern Norwegian glaciers.

Glacier inventory data from Nordland county, northern central Norway (Fig. 4-1), indicates that the glaciers across that region receded in area by 47.1 % between ~1899 and 2000 (Weber et al., submitted). This value is similar to Langfjordjøkelen's 49.7 % area reduction between 1925 and 2006, but reflects a considerably longer measurement interval. In other words, the same percentage change occurred at Langfjordjøkelen over a much shorter time span, implying that 20th-century glacier change was more severe in northernmost Arctic Norway. When comparing icefield-type glaciers alone, the nine largest Nordland icefields decreased in area by only 26.5 % in the period 1899-2000 (Weber et al., submitted), emphasising the intensity of glacier decline in northernmost Norway even more.

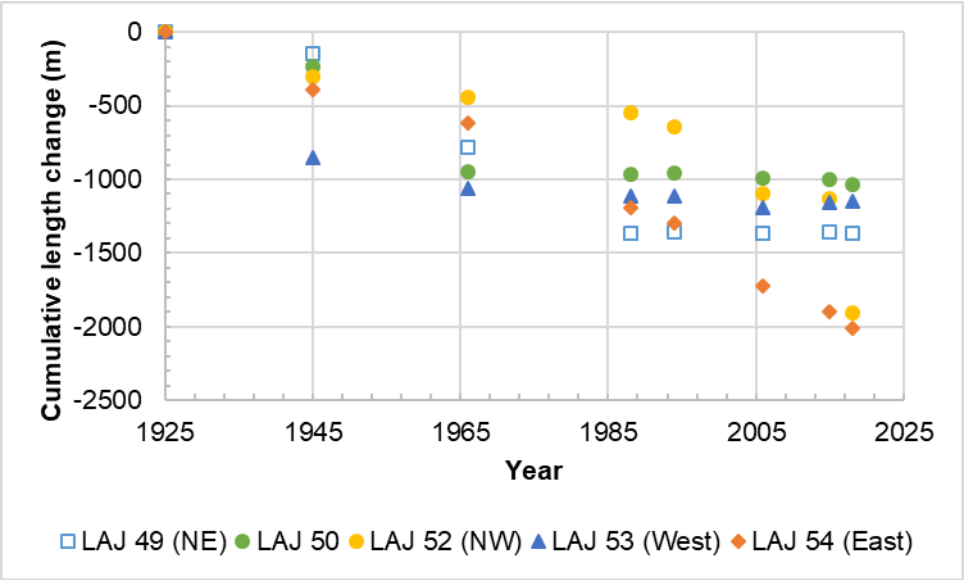

Fig. 4-9. Cumulative centreline length change of Langfjordjøkelen' icefield units since the LIA maximum.

Table 4-7. Comparison of percentage area change in Lyngen (Stokes et al. 2018) and at Langfjordjøkelen (this study). The measurement periods at Langfjordjøkelen were adjusted (originally: 1925–1945–1966–1988–1994–2006–2015–2018) to match the Stokes et al. (2018) intervals.

Lyngen (Stokes et al., 2018)		Langfjordjøkelen (this study)		Difference factor[a]
Period	Area change (%)	Period	Area change (%)	
1915-53	-11.0	1925-45	-24.9	2.3
1953-88	-10.3	1945-88	-16.2	1.6
1988-2001	+4.3	1988-2006	-20.0	4.6
2001-14	-12.8	2006-15	-6.8	0.5

[a] Calculated by dividing percentage area change at Langfjordjøkelen by percentage area change in Lyngen

Stokes et al. (2018) assessed long-term glacier change on the Lyngen Peninsula, approximately 90 km to the southwest of Langfjordjøkelen (Fig. 4-1), since the local LIA maxima in 1750 and 1915. They quantified glacier change for several measurement intervals (1750-1915-1953-1988-2001-2014), but did not calculate overall change from the local LIA to present. In order to allow a general comparison with Langfjordjøkelen, we re-calculated our data to match the Stokes et al. (2018) intervals as closely as possible (1925-1945-1988-2006-2015) (Table 4-7). Whilst the re-calculated Langfjordjøkelen values for the 20th century are considerably more negative (by factors of between ~1.5 to ~4.5) than those calculated for Lyngen, initial 21st-century glacier recession was twice as high in Lyngen (but has accelerated dramatically at Langfjordjøkelen since 2015; Table 4-4).

Based on the available data, we conclude that centennial-scale glacier recession in Norway since the early 20th century has nowhere been as substantial as in northernmost Arctic

Norway, supporting the results of Andreassen et al. (2012a). We speculate that the over-proportionate warming in this part of Norway (Hanssen-Bauer et al., 2015), possibly influenced by Arctic Amplification, has been a factor in the observed strong retreat. An additional factor might be the area and volume distribution of Langfjordjøkelen, specifically of its eastern outlet glacier, which contains a significant amount of mass at critically low altitudes (Andreassen et al., 2012a).

4.6. Concluding remarks

We presented a reconstruction of the ~1925 maximum LIA extent of Langfjordjøkelen, a plateau icefield in northernmost Arctic Norway. In addition to Langfjordjøkelen's main eastern outlet glacier, which was considerably more extensive at the LIA maximum, major icefield outlets also existed in the north and west of the plateau. These have completely disappeared since the LIA. A historical map of Langfjordjøkelen overestimates the southern icefield extent and cannot be employed in glacier change assessments. Since the LIA, the icefield has been in continuous retreat, at variable, but highly negative rates. By 2018, Langfjordjøkelen had lost 57.0 % (8.5 km^2) of its original LIA area, at a rate of 9.0 % $10a^{-1}$. This loss is greater than that of any other Norwegian ice mass with available long-term glacier change data, and may be ascribed to amplified glacier decline at high latitude.

References

Allen, M.R., Dube, O.P., Solecki, W., Aragón-Durand, F., Cramer, W., Humphreys, S., Kainuma, M., Kala, J., Mahowald, N., Mulugetta, Y., Perez, R., Wairiu, M. & Zickfeld, K. 2018. Framing and Context. Masson-Delmotte, V., Zhai, P., Pörtner, H.-O., Roberts, D., Skea, J., Shukla, P.R., Pirani, A., Moufouma-Okia, W., Péan, C., Pidcock, R., Connors, S., Matthews, J.B.R., Chen, Y., Zhou, X., Gomis, M.I., Lonnoy, E., Maycock, T., Tignor, M. & Waterfield, T. (eds.) *Global Warming of 1.5°C. An IPCC Special Report on the impacts of global warming of 1.5°C above pre-industrial levels and related global greenhouse gas emission pathways, in the context of strengthening the global response to the threat of climate change, sustainable development, and efforts to eradicate poverty.* In Press.

Andreassen, L.M., Elvehøy, H., Kjøllmoen, B. & Engeset, R.V. 2005. Glacier mass-balance and length variation in Norway. *Annals of Glaciology* 42, 317–325.

Andreassen, L.M., Paul, F., Kääb, A. & Hausberg, J.E. 2008. Landsat-derived glacier inventory for Jotunheimen, Norway, and deduced glacier changes since the 1930s. *The Cryosphere* 2, 131–145.

Andreassen, L.M., Kjøllmoen, B., Rasmussen, A., Melvold, K. & Nordli, Ø. 2012a. Langfjordjøkelen, a rapidly shrinking glacier in northern Norway. *Journal of Glaciology* 58, 581–593.

Andreassen, L.M., Winsvold, S.H., Paul, F. & Hausberg, J.E. 2012b. *Inventory of Norwegian Glaciers*. NVE Rapport 38. Oslo: Norwegian Water Resources and Energy Directorate.

Andreassen, L.M., Elvehøy, H., Kjøllmoen, B. & Engeset, R.V. 2016. Reanalysis of long-term series of glaciological and geodetic mass balance for 10 Norwegian glaciers. *The Cryosphere* 10, 535–552.

Bush, E. & Lemmen, D.S. (eds.) 2019. *Canada's Changing Climate Report*. Ottawa: Government of Canada.

Box, J.E., Colgan, W.T., Wouters, B., Burgess, D.O., O'Neel, S., Thomson, L.I. & Mernild, S.H. 2018. Global sea-level contribution from Arctic land ice: 1971–2017. *Environmental Research Letters* 13, 125012.

Box, J.E., Colgan, W.T., Christensen, T.R., Schmidt, N.M., Lund, M., Parmentier, F.-J.W., Brown, R., Bhatt, U.S., Euskirchen, E.S., Romanovsky, V.E., Walsh, J.E., Overland, J.E., Wang, M., Corell, R.W., Meier, W.N., Wouters, B., Mernild, S., Mård, J., Pawlak, J. & Skovgård Olsen, M. 2019. Key indicators of Arctic climate change: 1971–2017. *Environmental Research Letters* 14, 045010.

Chandler, B.M.P., Lovell, H., Boston, C.M., Lukas, S., Barr, I.D., Benediktsson, Í.Ö., Benn, D.I., Clark, C.D., Darvill, C.M., Evans, D.J.A., Ewertowski, M.W., Loibl, D., Margold, M., Otto, J.-C., Roberts, D.H., Stokes, C.R., Storrar, R.D. & Stroeven, A.P. 2018. Glacial geomorphological mapping: A review of approaches and frameworks for best practice. Earth-Science Reviews 185, 806–846.

Evans, D.J., Rea, B.R., Hansom, J.D. & Whalley, W.B. 2002. Geomorphology and style of plateau icefield deglaciation in fjord terrains: the example of Troms-Finnmark, north Norway. *Journal of Quaternary Science* 17, 221–239.

Hanssen-Bauer, I. 2005. *Regional Temperature and Precipitation Series for Norway: Analyses of Time-Series Updated to 2004.* MET report no. 15/2005. Oslo: Meteorologisk institutt.

Hanssen-Bauer, I., Førland, E.J., Haddeland, I., Hisdal, H., Mayer, S., Nesje, A., Nilsen, J.E.Ø., Sandven, S., Sandø, A.B., Sorteberg, A. & Ådlandsvik, B. (eds.) 2015. *Klima i Norge 2100*. NCCS report no. 2/2015. Oslo: Miljødirektoratet.

Hanssen-Bauer, I., Førland, E.J., Hisdal, H., Mayer, S., Sandø, A.B. & Sorteberg, A. 2019. *Climate in Svalbard 2100*. NCCS report no. 1/2019. Oslo: Miljødirektoratet.

Hegerl, G.C., Brönnimann, S., Schurer, A. & Cowan, T. 2018. The early 20th century warming: Anomalies, causes, and consequences. *WIREs Climate Change* 9, e522.

Kjøllmoen, B., Andreassen, L.M., Elvehøy, H. & Jackson, M. 2018. *Glaciological investigations in Norway in 2017*. NVE Report 82. Oslo: Norwegian Water Resources and Energy Directorate.

Nesje A., Bakke J., Dahl S.O., Lie, Ø. & Matthews, J.A. 2008. Norwegian mountain glaciers in the past, present and future. *Global and Planetary Change* 60, 10–27.

Paul, F. & Andreassen, L.M. 2009. A new glacier inventory for the Svartisen region, Norway, from Landsat ETM+ data: Challenges and change assessment. *Journal of Glaciology* 55, 607–618.

Serreze, M.C., Barrett, A.P., Stroeve, J.C., Kindig, D.N. & Holland, M.M. 2009. The emergence of surface-based Arctic amplification. *The Cryosphere* 3, 11–19.

Stokes, C.R., Andreassen, L.M., Champion, M.R. & Corner, G.D. 2018. Widespread and accelerating glacier retreat on the Lyngen Peninsula, northern Norway, since their 'Little Ice Age' maximum. *Journal of Glaciology* 64, 100–118.

Vaughan, D.G., Comiso, J.C., Allison, I., Carrasco, J., Kaser, G., Kwok, R., Mote, P., Murray, T., Paul, F., Ren, J., Rignot, E., Solomina, O., Steffen, K. & Zhang, T. 2013. Observations: Cryosphere. In: Climate Change 2013: The Physical Science Basis. Contribution of Working Group I to the Fifth Assessment Report of the Intergovernmental Panel on Climate Change. Stocker, T.F., Qin, D., Plattner, G.-K., Tignor, M., Allen, S.K., Boschung, J., Nauels, A., Xia, Y., Bex, V. & Midgley, P.M. (eds.) Cambridge, New York: Cambridge University Press.

Weber, P., Boston, C.M., Lovell, H. & Andreassen, L.M. 2019. Evolution of the Norwegian plateau icefield Hardangerjøkulen since the 'Little Ice Age.' *The Holocene* 29, 1885–1905.

Weber, P., Andreassen, L.M., Boston, C.M., Lovell, H. & Kvarteig, S. submitted. An ~1899 glacier inventory for Nordland, northern Norway, produced from historical maps. Submitted to *Journal of Glaciology*.

Winsvold, S.H., Andreassen, L.M. & Kienholz, C. 2014. Glacier area and length changes in Norway from repeat inventories. *The Cryosphere* 8, 1885–1903.

Wittmeier, H.E., Bakke, J., Vasskog, K. & Trachseld, M. 2015. Reconstructing Holocene glacier activity at Langfjordjøkelen, Arctic Norway, using multi-proxy fingerprinting of distal glacier-fed lake sediments. *Quaternary Science Reviews* 114, 78–99.

World Meteorological Organization (WMO) 2019. *WMO Statement on the state of the global climate in 2018*. Geneva: Switzerland.

Zemp, M., Armstrong, R., Gärtner-Roer, I., Haeberli, W., Hoelzle, M., Kääb, A., Kargel, J.S., Khalsa, S.J.S., Leonard, G.J., Paul, F. & Raup, B.H. 2014. Introduction: Global Glacier

Monitoring—a Long-Term Task Integrating in Situ Observations and Remote Sensing. Kargel, J., Leonard, G., Bishop, M., Kääb, A. & Raup, B. (eds.) *Global Land Ice Measurements from Space*, 1–21. Berlin, Heidelberg: Springer.

Zemp, M., Frey, H., Gärtner-Roer, I., Nussbaumer, S.U., Hoelzle, M., Paul, F., Haeberli, W., Denzinger, F., Ahlstrøm, A.P., Anderson, B., Bajracharya, S., Baroni, C., Braun, L.N., Cáceres, B.E., Casassa, G., Cobos, G., Dávila, L.R., Granados, H.D., Demuth, M.N., Espizua, L., Fischer, A., Fujita, K., Gadek, B., Ghazanfar, A., Hagen, J.O., Holmlund, P., Karimi, N., Li, Z., Pelto, M., Pitte, P., Popovnin, V.V., Portocarrero, C.A., Prinz, R., Sangewar C.V., Severskiy, I., Sigurđsson, O., Soruco, A., Usubaliev, R. & Vincent, C. 2015. Historically unprecedented global glacier decline in the early 21st century. *Journal of Glaciology* 61, 745–762.

Zemp, M., Huss, M., Thibert, E., Eckert, N., McNabb, R., Huber, J., Barandun, M., Machguth, H., Nussbaumer, S. U., Gärtner-Roer, I., Thomson, L., Paul, F., Maussion, F., Kutuzov, S. & Cogley, J.G. 2019. Global glacier mass changes and their contributions to sea-level rise from 1961 to 2016. *Nature* 568, 382–386.

Chapter 5

Discussion

Here, the main themes connecting the three result chapters (Papers I, II and III) in this doctoral thesis are drawn out and discussed in order to synthesise the key findings of this work. These themes are (1) detailed Little Ice Age (LIA) glacier reconstructions based on mapped geomorphological evidence, and (2) the quantification of centennial-scale glacier change from the LIA to present based on digital glacier outlines from successive time points. For each of the two themes, potential sources of uncertainty are discussed and the wider implications of the results are explored, before outlining potential future work in these areas.

The production of digital glacier outlines from historical maps is an important overarching aspect of this thesis too, but this topic is discussed at length in Chapters 2, 3 and 4. It has been shown that old maps can be used to derive inventories of the historical glacier extent, but that it is crucial to assess the accuracy of the map sources rigorously. In some areas (for example at Langfjordjøkelen; Chapter 4), the maps contained clear errors (distorted terrain topography, snow likely mapped as glacier ice) and were thus less suitable for reconstructing former glacier dimensions.

Another important research topic of this thesis is the role of topography in influencing the formation of ice-marginal moraines at the outlet glaciers of plateau icefields. This question has only been investigated at Hardangerjøkulen (Chapter 2) and is discussed in Section 2.8. Moraine production was shown to be asynchronous across the individual icefield outlet glaciers and is tentatively linked to sediment abundance on reverse bed slopes due to inefficient meltwater drainage and limited sediment evacuation in these locations.

At Svartisen (Chapter 3), such an investigation was beyond the scope of the chapter because the research focus there was on using the LIA moraine record for historical map validation. At Langfjordjøkelen (Chapter 4), where the steep plateau flanks and valley slopes are dominated by mass movement processes, no suitable moraine sequences were either formed or preserved to allow such an investigation. Nonetheless, the Hardangerjøkulen results raise two interesting points for discussion and future research, echoing the conclusions of Chapter 2:

First, Chapter 2 draws the tentative conclusion that the slope topography of the glacier foreland determines the degree of coupling between the ice margin and the glaciofluvial system, and thus sediment availability (reverse slope) or non-availability (forward slope) for moraine production. This adds to the growing body of evidence that topographic factors, in particular bed slope, influence the distribution of moraine ridges (e.g. Barr & Lovell, 2014; Boston & Lukas, 2019). However, further research is needed to confirm that the mechanism proposed here operates at Hardangerjøkulen. In a first step, multiple series of vertical aerial photographs

should be used to track the evolution of the glaciofluvial system and its coupling with the ice margin (e.g. meltwater ponding versus unobstructed drainage) at each outlet through time, and then relate this to the presence or absence of moraines at each time point. In a second step, a combination of geomorphometrical and spatial statistical analysis should be carried out to correlate moraine distribution with the topographic parameters (e.g. slope gradient, surface curvature, etc.) of the outlet forelands.

Second, the finding that moraine formation at Hardangerjøkulen occurs at different times (presumably mainly whenever the outlet termini are located on a poorly drained, debris-charged reverse bed slope) has implications for how moraine records are interpreted and utilised to make (palaeo-)climatic inferences. There is the general notion that moraine ridges represent climatically-induced episodes of glacier advance or standstill (cf. Kirkbride & Winkler, 2012). However, applying such reasoning to the differential moraine patterns at, for example, Midtdalsbreen and Blåisen would yield a different climate history at each of the two icefield outlets. More specifically, direct observations at Midtdalsbreen (Andersen & Sollid, 1971) show that moraine ridges are being produced annually during overall glacier recession (Section 2.5.1), and the dense moraine spacing in parts of the Blåisen (Section 2.5.2) and Rembesdalskåka (Section 2.5.7) forelands suggests that this is also true for these outlets. Previous studies have used dated sequences of annual moraines, and in particular the distance between individual ridges, as a proxy for glacier terminus (length) change and to calculate annual rates of frontal retreat, which they then linked to climate data and specific climatic conditions (Bradwell, 2004; Beedle et al., 2009; Lukas, 2012; Bradwell et al., 2013; Chandler et al., 2016a, b). However, this may be questionable if the formation and distribution of annual moraines, and therefore moraine spacing, is also influenced by non-climatic factors (here presumed to be slope topography) (cf. Lukas, 2012).

5.1. Establishing a means for quantifying uncertainty in LIA glacier reconstructions

This thesis has developed a novel quantitative GIS approach to measure and visualise the uncertainties associated with glacier and icefield reconstructions in a robust and transparent way. The first step of this approach involved conventional geomorphological mapping of glacial landform features (Chandler et al., 2018), both in the outlet glacier forelands and on the plateau summits around the icefields' accumulation areas, in order to identify the LIA limit. The outermost LIA glacial landforms then provided the basic structure from which complete digital GIS outlines of the LIA icefields could be interpolated. The sections of the outlines based directly on landform evidence were classed as certain. Outline segments that only needed to be interpolated over short distances, or where the terrain topography dictated the shape of the

outline (e.g. along steep valley sides), were classed as fairly certain. Outline segments were classed as less certain when the interpolated line could have also been drawn either closer to the present-day glacier margin (resulting in a smaller icefield outline) or extending further away (indicating an even larger outline). By calculating the percentage that each of the three classes represents of the total perimeter length of a reconstructed LIA outline, the *geomorphological confidence* in the glacier reconstruction was quantified. This is illustrated in Fig. 5-1 for Vestre Svartisen's three western outlets Litlbreen, Engabreen and Fonndalsbreen (only the LIA extent of these outlets but not the corresponding confidence classification was presented in Chapter 3, because the focus there was to use the LIA limit to validate the glacier extent extracted from historical maps. Chapter 3 also established the LIA extent of the Svartisen outlets in the Vesterdalen valley and Fingerbreen area, but no confidence classification is available as it proved difficult to delineate the exact LIA drainage basins). The outer margin of these three icefield units was reconstructed to have a combined perimeter length of 30.7 km at the LIA maximum. Based on the criteria outlined above, just over two-fifths (42.5 %; 13.0 km) of this length can be considered certain, whilst the major portion (55.7 %; 17.1 km) of the LIA ice margin is assessed to be fairly certain, and only a fraction (1.8 %; 0.6 km) of the total length is less certain (Table 5-1).

The approach and classification system presented here provide a significantly higher level of detail and clarity than many previous studies reconstructing the former extent of past or present ice masses. In palaeo-glacier reconstructions, in particular, it is often not common to specify the exact approach used to link the mapped landform evidence in order to produce complete outlines of the former glacier extent by inter- and/or extrapolation (e.g. McDougall, 2001, 2013; Benn & Ballantyne, 2005; Finlayson, 2006; Lukas & Bradwell, 2010; Finlayson et al., 2011; Jones et al., 2017). This vagueness can occasionally also be found in LIA glacier reconstructions (e.g. Paul & Kääb, 2005; Martín-Moreno et al., 2017), where it is unclear exactly how the maximum LIA extent was digitised in areas where LIA landform evidence was absent or sparse (for example in areas between ice cap/icefield outlet glaciers). Many other LIA glacier reconstructions use a method that extends the glacier front of more recent outlet or valley glacier outlines down to the outermost LIA moraines, without appearing to consider changes in the upglacier parts, and are technically minimum reconstructions of the maximum LIA extent (e.g. Baumann et al., 2009; Way et al., 2015; Meier et al., 2018; Stokes et al., 2018; Leigh et al., 2020). This technique may work well when applied to cirque glaciers, or valley glaciers with high-altitude source areas, where changes since the LIA are typically restricted to the downglacier part, whilst the extent of the upglacier part can be expected to have remained more or less unchanged. However, the technique may be less suitable for separate ice masses that have possibly formed by the disintegration of continuous ice caps/plateau icefields since the LIA. In this regard, Leigh et al. (2020) mentioned that they also reconnected fragmented ice

bodies to produce glacier outlines of the former LIA extent, but without going into detail on the process. By contrast, the advantage of the approach developed in this thesis is that equal care and attention is given to establishing the LIA limit around the upglacier parts (accumulation areas) of the ice masses investigated here.

Only a small minority of previous studies assess the uncertainties surrounding the identification of the LIA limits (e.g. Meier et al., 2018; Martin-Mikle & Fagre, 2019). This is achieved mainly through several investigators independently digitising the same ice masses and quantifying any differences in the resulting glacier outlines, a process that is labour-intensive and time-consuming.

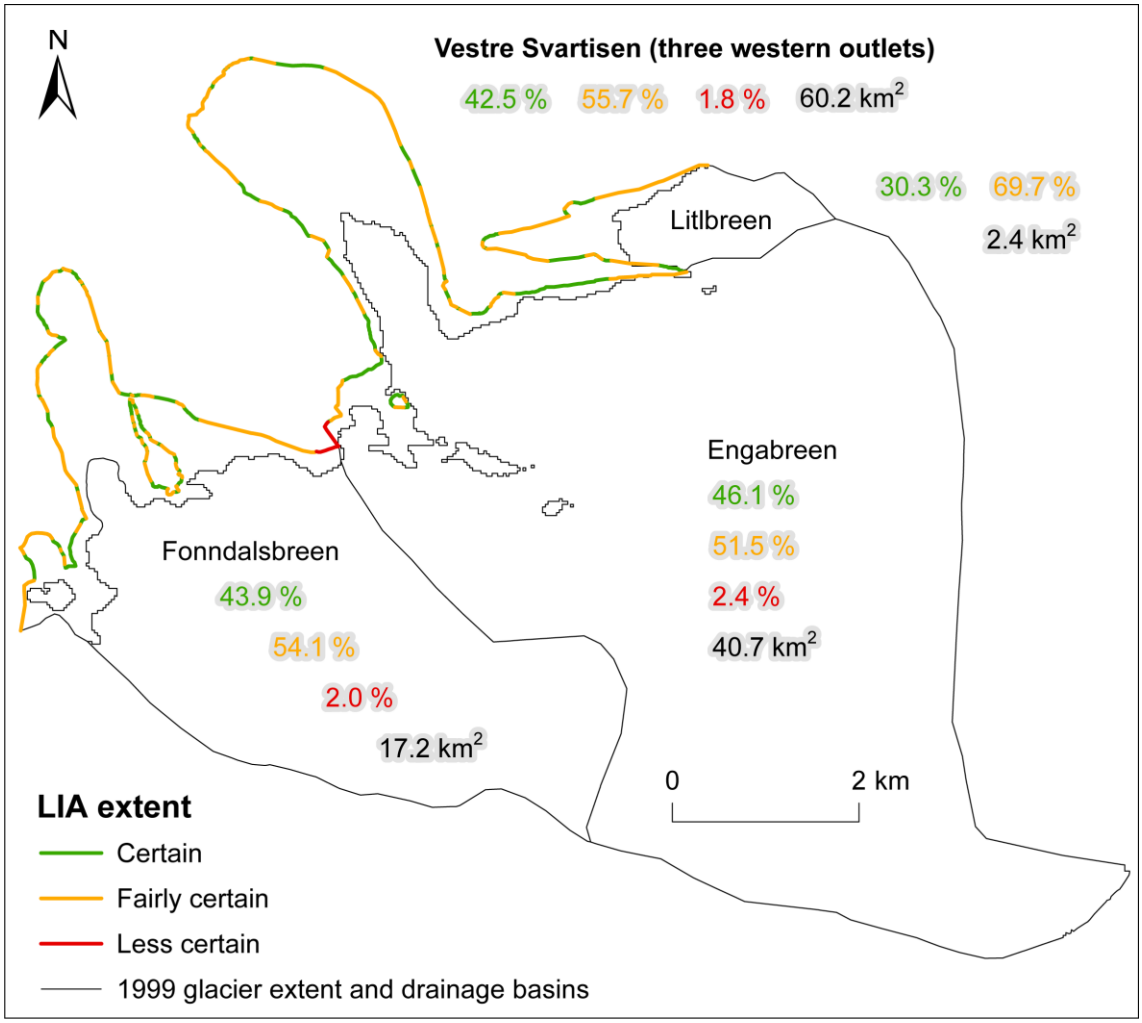

Fig. 5-1. Reconstructed maximum LIA extent and drainage basins of the three Vestre Svartisen outlet glaciers Litlbreen, Engabreen and Fonndalsbreen. The reconstruction is classified into different levels of confidence (in green, orange and red), with the green sections of the outline (certain) representing mapped glacial landform features. The 1999 glacier extent (Andreassen et al., 2012a) is shown for comparison.

The complete icefield outlines reconstructed in this thesis allow the former area of an ice mass to be quantified and to be used as a baseline in long-term glacier change assessments. They can also serve as a validation data set for numerical glacier models (see Section 2.6). However, researchers examining glacier change might not only be interested in the LIA glacier area alone, but also in a corresponding error term (± km^2), which the geomorphological confidence assessment introduced here does not provide in its current form. Furthermore, glacier modellers might be more interested in having an uncertainty range (± m) to match their modelled ice margin positions to, rather than a fixed geomorphological limit or outline (even though the geomorphological imprint of the LIA limit at the locations studied in this thesis is often so clear that defining an uncertainty range is misleading; see Fig. 2-4). In order to satisfy both needs (i.e. an error term for the LIA area; uncertainty ranges for the LIA ice margin position), a *probability uncertainty* approach can be taken.

This uncertainty is a probabilistic measure of how likely it is that a reconstructed LIA glacier outline (including its area) and the terminus position of its outlet(s) are accurate. It is *not* a geomorphological uncertainty, but based on the geomorphologically-derived confidence classification described above (see Fig. 5-1). The probability uncertainty is calculated by multiplying the percentage values of the geomorphological confidence (certain, fairly certain, less certain; expressed in decimal form) by predefined confidence levels (also in decimal form), and then computing the sum. The confidence levels can be chosen as appropriate (however, it should be noted that the chosen confidence levels largely determine the results of this calculation). Here, sensible, but somewhat arbitrary, values are applied: LIA outline segments classed as certain are assigned a 99 % (0.99) confidence; there is a 99 % chance that the outline segments are correct, and a 1 % chance that some of the landform evidence has been interpreted incorrectly, for example, that they are not glacial in origin or that they belong to an ice advance other than the LIA maximum (i.e. pre- or post-LIA). Outline segments classed as fairly certain are given a 90 % (0.90) confidence. Lastly, a 50 % (0.50) confidence is assigned to outline segments classified as less certain, because there is a fifty-fifty chance that the LIA outline segments are either accurate (i.e. a realistic representation of the LIA ice limit) or inaccurate (i.e. over- or underestimated). This allows the probability uncertainty (PU) to be computed, using the equation:

$$PU = 1 - ((C * 0.99) + (FC * 0.90) + (LC * 0.50)) \quad (1)$$

where C, FC and LC denote the portions of the reconstructed outline that are certain (C), fairly certain (FC) and less certain (LC).

Using the Vestre Svartisen values as an example (Fig. 5-1), Eqn. (1) can be solved as follows:

$$PU = 1 - ((0.425 * 0.99) + (0.557 * 0.90) + (0.018 * 0.50)) \quad (2)$$

This yields a PU of 1 – 0.931 (100 % – 93.1 %) = 0.069 (6.9 %). In other words, this means that there is a 93.1 % probability that the reconstructed LIA outline of Vestre Svartisen is accurate, and only a 6.9 % probability that it is not, as determined on the basis of the geomorphological confidence classification. The PU of 6.9 % (7 %; rounded to the nearest integer) can now be used to calculate the error term for the LIA glacier area. Vestre Svartisen's three western outlets had a combined area of 60.2 km^2 at the LIA maximum (Fig. 5-1). A 7 % PU gives an error of ± 4.2 km^2.

In the same way, PU values can be established for Hardangerjøkulen and Langfjordjøkelen (as well as the two neighbouring Áibmadasgáisá cirque glaciers to the south) (Table 5-1). At Hardangerjøkulen, the percentages of the geomorphological confidence for the certain, fairly certain and less certain classes are 59.7 % (0.597), 31.5 % (0.315) and 8.8 % (0.088), respectively, which gives a PU of 1 – 0.919 (100 % – 91.9 %) = 0.081 (8.1 %; rounded to 8 %). At Langfjordjøkelen, the confidence percentages for certain, fairly certain and less certain are 36.5 % (0.365), 53.7 % (0.537) and 9.9 % (0.099), respectively, resulting in a PU of 1 – 0.894 (100 % – 89.4 %) = 0.106 (10.6 %; rounded to 11 %). These values suggest that there is a slightly higher, although generally low, chance that the reconstructed LIA outline of Langfjordjøkelen is inaccurate (11 %) as compared to the outlines of Vestre Svartisen (7 %; its three western outlets) and Hardangerjøkulen (8 %). An 11 % PU at Langfjordjøkelen adds an error of ± 1.6 km^2 to the LIA icefield area of 14.9 km^2, whilst the 8 % PU at Hardangerjøkulen translates into an error of ± 8.8 km^2 associated with the LIA area of 109.7 km^2. The respective PU values and error terms for the Áibmadasgáisá glaciers (south of Langfjordjøkelen) are 13 % and ± 0.1 km^2 for the northern cirque (LIA area of 0.9 km^2), and 5 % and ± 0.05 km^2 for the southern cirque (LIA area of 1.0 km^2).

PU values can also be calculated for the individual units of an icefield. In order to do so, the reconstructed icefield outline consisting of the three geomorphological confidence classes has to be split along the icefield's drainage divides (Fig. 5-1). The advantage of having an individual PU for each icefield unit is that the number of outer LIA landforms and the resulting reliability of the glacier reconstruction, both of which may vary spatially, can be combined into a single value per glacier unit and compared across the icefield. For example, Table 5-1 lists the PUs and the corresponding LIA area errors for the selected icefield units (outlet glaciers) of Hardangerjøkulen (clockwise from north) Ramnabergbreen (7 %; ± 1.1 km^2), Midtdalsbreen (3 %; ± 0.3 km^2), Blåisen (5 %; ± 0.5 km^2), Vestra Leirebottsskåka (7 %; ± 0.8 km^2), Isdøleskåka (24 %; ± 2.0 km^2), and Rembesdalskåka (7 %; ± 1.4 km^2). The high values for Isdøleskåka reflect the relative scarcity of LIA glacial landforms at this outlet (see Section 2.5.6), and hence the medium confidence placed in the reconstructed outline of this icefield unit

(38.0 % certain; 19.2 % fairly certain; 42.8 % less certain). Conversely, the low values for Midtdalsbreen are a direct result of the LIA landform abundance (see Section 2.5.1), enabling a very reliable and robust outlet reconstruction (83.1 % certain; 16.9 % fairly certain; no outline segments classed as less certain). The individual PUs show large outlet-to-outlet variations, and are particularly useful in local-scale studies of single ice masses to highlight spatial differences in the robustness of the geomorphological glacier reconstruction. Icefield-wide PU values, on the other hand, can be employed in regional-scale studies comparing reconstructions of different ice masses, but may be of limited use in single-glacier studies, because a whole icefield value can mask any glacier units that are very well constrained, such as Midtdalsbreen, where the outlet PU of 3 % is obscured by the icefield-wide PU of 8 %.

Table 5-1. Confidence classification and probability uncertainty (PU) of the reconstructed LIA glacier outlines.

Glacier/*Glacier unit*	Certain	Fairly certain	Less certain	Overall confidence	PU (rounded)	LIA area	Error term (±)
			%			km²	
Langfjordjøkelen	36.5	53.7	9.9	89.4	10.6 (11)	14.9	1.6
Áibmadasgáisá North	21.4	65.5	13.1	86.7	13.3 (13)	0.9	0.1
Áibmadasgáisá South	59.2	40.8	0.0	95.3	4.7 (5)	1.0	0.05
Vestre Svartisen (Litlbreen-Engabreen-Fonndalsbreen)	42.5	55.7	1.8	93.1	6.9 (7)	60.2	4.2
Hardangerjøkulen	59.7	31.5	8.8	91.9	8.1 (8)	109.7	8.8
Ramnabergbreen	49.9	46.0	4.1	92.9	7.1 (7)	15.8	1.1
Midtdalsbreen	83.1	16.9	0.0	97.5	2.5 (3)	10.9	0.3
Blåisen	59.6	40.4	0.0	95.4	4.6 (5)	10.9	0.5
Vestra Leirebottsskåka	58.4	37.1	4.5	93.5	6.5 (7)	11.9	0.8
Isdøleskåka	38.0	19.2	42.8	76.3	23.7 (24)	8.3	2.0
Rembesdalskåka	61.9	32.6	5.5	93.4	6.6 (7)	20.7	1.4

The calculated PU values and corresponding area uncertainties are based on the positions of the outline segments as shown in the icefield reconstructions in Fig. 2-6 (Hardangerjøkulen), Fig. 4-4 (Langfjordjøkelen) and Fig. 5-1 (Vestre Svartisen). As noted above, the criterion for classifying glacier outline segments as less certain is that these segments could have also been drawn further in or out either side of the current outline position. For example, in Chapter 2, a negative 100-metre buffer is applied to a section of Hardangerjøkulen's reconstructed LIA outline that contains a significant number of segments classed as less certain (see Fig. 2-6). This reduces the area of the reconstructed icefield outline by 0.9 % (1.0 km^2). It should be noted, however, that the resulting numbers depend on the size of the icefield. Applying a ± 100-metre buffer to a hypothetical ice mass with a radius of 5000 m translates to

glacier outlines with radii of 4900/5100 m (glacier outline areas of 75.4 and 81.7 km^2, respectively). The difference in area between the two outlines is 7.7 % (6.3 km^2). For an ice mass with a 500-metre radius, the same ± 100-metre buffer translates to glacier outlines with radii of 400/600 m (glacier outline areas of 0.5 and 1.1 km^2, respectively), with a difference in area between the two outlines of 55.6 % (0.6 km^2). Thus, depending on the size of the glacier, the same change in distance in the position of a glacier outline can produce large differences in area uncertainty.

Next, the calculated error terms (± km^2) for the LIA area of the individual icefield units can be used to provide glacier modellers with an uncertainty range (± m) to compare their modelled ice extents to. Using GIS, the error terms can be laid as a buffer around their respective glacier units (i.e. each glacier unit is buffered by the specified area of its error term). The width of the resulting buffers can be measured and taken as uncertainty ranges. For example, the uncertainty ranges (buffer widths) for the six selected icefield units of Hardangerjøkulen vary between a minimum of ± 19 m at Midtdalsbreen (buffer area of ± 0.3 km^2) and a maximum of ± 105 m at Isdøleskåka (buffer area of ± 2.0 km^2) (Fig. 5-2). The relatively narrow ranges measured at the six icefield units can be regarded as reasonable given that the typically well-defined LIA limit does not necessarily imply the need for uncertainty ranges. These ranges can now be compared to the ice margin positions of the Åkesson et al. (2017) LIA model of Hardangerjøkulen. Åkesson et al. (2017) underestimated the glacier extent of Blåisen, Vestra Leirebottsskåka and Rembesdalskåka by ~370-~1060 ± 100-250 m (see Section 2.6), which is too large to overlap with the uncertainty ranges produced here based on the geomorphological record. Glacier modellers may use the PU-derived uncertainty ranges in the future to get an indication of the fit between modelled and empirical ice limits.

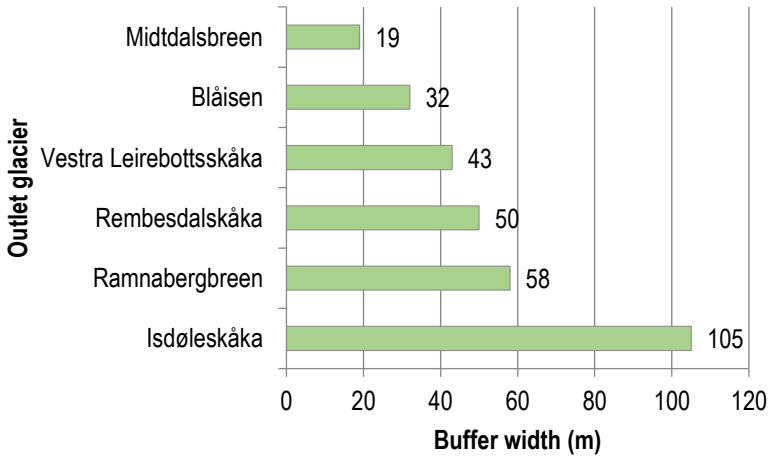

Fig. 5-2. Width of the buffers created around selected icefield units of Hardangerjøkulen from the calculated error terms (± km^2) for the LIA area.

In conclusion, the novel geomorphological confidence classification and the concept of the probability uncertainty presented in this thesis allow the quality and reliability of reconstructions of different ice masses, or individual glacier units of the same ice mass, to be quantitated and compared. This has not been possible to date and brings a hitherto unprecedented degree of both transparency and scrutiny in the field of geomorphologically-derived glacier reconstructions.

5.2. Quantifying glacier change

In Chapters 2, 3 and 4, glacier change is shown in absolute (square kilometre) and relative (percentage) terms. The latter is predominantly used to compare glacier change across different ice masses or glacier units. This allowed Chapter 4 (Paper III) to conclude that the Langfjordjøkelen icefield has experienced the greatest percentage area loss of all Norwegian ice masses with available long-term data since the beginning of the 20th century. There is, however, a tendency at small ice masses/glacier units that even minor absolute area changes will translate into large percentage changes (Winsvold et al., 2014). This systematic effect will increase over time as the small ice masses/glacier units decrease further in size during glacier recession. Given the inherent problem with percentage values, this section reassesses glacier change in Norway since the LIA using normalised values.

Winsvold et al. (2014; and references therein) normalised glacier change by dividing the measured area change between two time points (GAC) by the square root of the initial glacier area at time point 1 (A_i):

$$\text{Normalised GAC} = \text{GAC} / \text{root}(A_i) \quad (3)$$

Eqn. (3) can be used to normalise glacier area change between the LIA maximum and the present day. This has been done here for the ice masses studied in this thesis (Hardangerjøkulen, the three Vestre Svartisen outlets, Langfjordjøkelen, Áibmadasgáisá cirques) as well as other Norwegian ice masses with available LIA glacier outlines: the Jotunheimen glaciers (Baumann et al., 2009), the glaciers on the Lyngen Peninsula (Stokes et al., 2018), and the glaciers to the east of the Lyngen (Ivguvuotna) fjord (Leigh et al., 2020) (Table 5-2). In a further step, the normalised glacier change values have to be scaled to a common duration (i.e. rates of normalised change in the same time interval). This is necessary because both the timing of the maximum LIA extent and the timestamp for the most recent glacier outlines vary between the examined ice masses, resulting in change intervals of different lengths that cannot be compared (Table 5-2). Here, all normalised values were scaled to a reference period of 90 years ($90a^{-1}$),

which is the shortest post-LIA change interval among the investigated ice masses (at the Áibmadasgáisá glaciers; using the Langfjordjøkelen LIA date of 1925 established by Wittmeier et al., 2015).

The normalised glacier change values range from a minimum of -0.4 $90a^{-1}$ at the three Vestre Svartisen outlets to a maximum of -2.1 $90a^{-1}$ at Langfjordjøkelen, the glaciers on the Lyngen Peninsula and in Jotunheimen (Table 5-2). Intermediate values were calculated for Hardangerjøkulen (-1.3 $90a^{-1}$), the glaciers to the east of the Lyngen fjord (-1.1 $90a^{-1}$) and the Áibmadasgáisá cirques (-0.9 $90a^{-1}$) (Table 5-2).

The data allows a comparison of glacier change since the LIA across Norway. Normalised glacier recession in Jotunheimen was more than five orders of magnitude greater than that of the three outlet glaciers of Vestre Svartisen, suggesting that continental glaciers in Norway experienced a much greater post-LIA areal decline than maritime ice masses. However, Langfjordjøkelen and the ice masses on the Lyngen Peninsula, both located in the maritime parts of northernmost mainland Norway, show the same high magnitude of areal change as the Jotunheimen glaciers. The implication of this is that there is also a latitudinal factor controlling glacier area change in Norway, with glaciers in the northernmost parts of the Norwegian mainland receding fastest. This statement has to be qualified somewhat, however, as glacier change has not been uniformly high across this northernmost region: the glaciers to the east of the Lyngen fjord and the Áibmadasgáisá cirques display only moderate areal shrinkage.

Available glaciological and geodetic mass balance data as well as glacier front position records can be used to check whether or not the normalised area changes reflect true recession patterns. The average annual balance of the ten glaciers with continuous long-term surface mass balance data (see Section 1.3) is -0.36 m w.e. a^{-1} (calculated using data from NVE, 2019). Langfjordjøkelen's annual balance of -0.91 m w.e. a^{-1} (each glacier's annual balance was calculated by dividing the total cumulative balance by the number of measurement years) is the most negative of the ten series and lends support to a pattern of amplified glacier shrinkage in northernmost Norway (with the caveat that Langfjordjøkelen is the only monitored glacier in this region). By contrast, the data does not substantiate a pattern of stronger-than-average recession of continental glaciers: the mass balance of the three Jotunheimen glaciers Storbreen, Hellstugubreen and Gråsubreen is only minimally above average (-0.38 to -0.43 m w.e. a^{-1}), whilst some maritime glaciers in southern Norway exhibit more negative rates (Austdalsbreen: -0.52 m w.e. a^{-1}; Hansebreen: -0.76 m w.e. a^{-1}). A balance loss of -0.12 m w.e. a^{-1} at Rembesdalskåka may be regarded as consistent with the moderate areal decline observed at Hardangerjøkulen.

Andreassen et al. (2020) determined the geodetic mass balance of 137 Norwegian glaciers grouped into 15 glacier regions and found an average balance loss of -0.27 ± 0.05 m w.e. a^{-1} between ~1960 and ~2010. The measured Langfjordjøkelen value of -0.50 ± 0.04 m w.e.

a^{-1} is the most negative balance for any of the investigated glacier regions and double the Norway-wide average, again corroborating a pattern of above-average areal decline in northernmost Norway. However, this is not directly supported by the average balance value of -0.31 ± 0.09 m w.e. a^{-1} obtained for the Lyngen and northern Troms region. By contrast, Andreassen et al. (2020) produced a below-average balance rate of -0.21 ± 0.04 m w.e. a^{-1} for Jotunheimen, which is a further argument against a pattern of accelerated continental glacier shrinkage. Hardangerjøkulen's geodetic balance of -0.23 ± 0.06 m w.e. a^{-1} is slightly lower than the Norway-wide average too, which seems to agree with the icefield's moderate areal change values.

The eleven Norwegian (outlet) glaciers with continuous or near-continuous front position records since 1899-1905 have retreated at an average rate of -13 m a^{-1}, with the highest annual rates of retreat of -22 to -25 m a^{-1} observed at Nigardsbreen, Fåbergstølsbreen (both outlet glaciers of Jostedalsbreen) and Engabreen (calculated using data from NVE, 2019) (see Section 1.4.2). Andreassen et al. (2020) calculated a similar rate of -12 m a^{-1} on average for a subset of 30 Norwegian glaciers in the period between the 1960s and 2018. The annual retreat rates of Rembesdalskåka (-14 m a^{-1}; NVE, 2019), Hardangerjøkulen (remotely sensed icefield average of -15 m a^{-1}; Weber et al., 2019), the Lyngen Peninsula (-10 m a^{-1}; calculated by averaging the retreat rates for the change intervals 1915-53-88-2001-14; Stokes et al., 2018) and Langfjordjøkelen (remotely sensed icefield average of -11 m a^{-1}; Weber et al., 2020) vary around the two averages. Only the remotely sensed retreat rate of the eastern outlet glacier of Langfjordjøkelen (Langfjordjøkelen East) of -22 m a^{-1} (Weber et al., 2020) fits with the proposed pattern of amplified glacier recession in northernmost Norway, making the outlet one of the most rapidly retreating glaciers in Norway with available long-term observations. The annual retreat rate of the three continental Jotunheimen glaciers Styggedalsbreen, Hellstugubreen and Storbreen (-5 to -10 m a^{-1}) is lower than average.

Based on the data outlined above, there is no supporting evidence to confirm a pattern of accelerated recession of continental glaciers, and an explanation for the high values of normalised area loss in Jotunheimen remains elusive. By contrast, there is moderate to strong supporting evidence for a pattern of amplified glacier area change in northernmost mainland Norway, specifically at Langfjordjøkelen (cf. Andreassen et al., 2012b). Two possible explanations are explored: (1) that the glacier area in northern Norway generally has a lower elevation range (1,000-1,300 m a.s.l.) than the glacier area in southern Norway (1,400-1,600 m a.s.l.) (Andreassen et al., 2012a; see Section 1.1); and (2) that the coastal areas of Arctic mainland Norway have warmed faster since 1900 (0.11°C $10a^{-1}$) compared to the rest of Norway (0.09°C $10a^{-1}$) (Hanssen-Bauer et al., 2015; see Section 1.2).

The first factor appears to have a significant impact on the strong areal decline of Langfjordjøkelen, which is situated entirely at altitudes below 1,050 m a.s.l. (Kjøllmoen, 2019).

The icefield surface lowered by 30.5 m in the period 1966-2008 (Andreassen et al., 2012b, 2020). Surface lowering was particularly severe across the glacier tongue of Langfjordjøkelen East, which thinned by more than 100 m between 1966 and 1994, by up to 73 m until 2008 and by up to 70 m until 2018 (Andreassen et al., 2012b; Kjøllmoen, 2019), explaining its extreme backwasting (-22 m a^{-1}) at twice the icefield's mean frontal retreat rate (-11 m a^{-1}). The mean accumulation-area ratio at Langfjordjøkelen East has dropped sharply from 45 % in the period 1989-99 (already significantly below the ~60 % threshold to be in balance) to 16 % since 2000 (up to and including the year 2018) (Andreassen et al., 2012b; NVE 2019). This shows that a major factor in the strong recession observed at Langfjordjøkelen is that the icefield, and particularly its eastern outlet glacier, lies at altitudes too low to build up any mass (Andreassen et al., 2012b; Kjøllmoen 2019).

However, this is not the case on the Lyngen Peninsula, where the glacier area in the alpine terrain is distributed over altitudes of up to 1,834 m a.s.l., making the second factor the most likely explanation. Stokes et al. (2018) found that the decadal mean annual temperature in nearby Tromsø was >1.5°C higher in the 2000s than in the 1900s-10s, with climate warming governing overall glacier change. Therefore, it is speculated that the disproportionate warming in these parts of the Norwegian mainland (Hanssen-Bauer et al., 2015), possibly influenced by Arctic amplification (e.g. Serreze et al., 2009), controls the high rates of glacier area loss in northernmost Norway, which is compounded at Langfjordjøkelen by its low-altitude hypsometry.

Table 5-2. Glacier area change since the LIA for all Norwegian glaciers with available data.

Glacier/ glacier region[a]	LIA glacier extent		Present-day glacier outline		Change interval (years)	Glacier area change LIA-present				
	Timing[b]	Area (km^2)	Time point	Area (km^2)		km^2	Normalised	Normalised $90a^{-1}$	%	% $90a^{-1}$
Hardangerjøkulen	1750	109.7	2010	68.9	260	-40.8	-3.9	-1.4	-37.2	-12.9
Jotunheimen	1753	290	2003	190	250	-100	-5.9	-2.1	-34.5	-12.4
Vestre Svartisen (Litlbreen-Engabreen-Fonndalsbreen)	1750	60.2	1999	51.7	249	-8.5	-1.1	-0.4	-14.2	-5.1
Lyngen Peninsula	1918	119.7	2014	95.5	96	-24.2	-2.2	-2.1	-20.2	-19.0
To the east of the Lyngen fjord	1846	10.0	2018	3.1	172	-6.9	-2.2	-1.2	-69.0	-36.1
Langfjordjøkelen	1925	14.9	2018	6.4	93	-8.5	-2.2	-2.1	-57.0	-55.2
Áibmadasgáisá cirque glaciers	1925	1.9	2015	0.6	90	-1.3	-0.9	-0.9	-68.4	-68.4

[a] See text for references

[b] See Section 1.4.1 for details

There is no apparent explanation why this trend is not mirrored in the moderate normalised area change seen to the east of the Lyngen fjord and at the Áibmadasgáisá cirques. However, when post-LIA glacier change is expressed in percentage values (Table 5-2) the pattern of accelerated areal shrinkage in northernmost mainland Norway becomes obvious across all ice masses in this region. The four groups of northern Norwegian glaciers exhibit percentage area losses of -19.0 to -68.4 % $90a^{-1}$, which compares to lower values of -12.9 and -12.4 % $90a^{-1}$ at Hardangerjøkulen and in Jotunheimen, respectively, and -5.1 % $90a^{-1}$ at the three Vestre Svartisen outlets. This example demonstrates the need for more systematic research and general guidelines on how to best present and compare glacier change.

5.3. Future work

A key task for future work is the production of a complete (or as complete as possible) inventory of the maximum LIA glacier extent in Norway (or possibly even Scandinavia). The glacier reconstructions carried out to compile this inventory have to be based on a transparent methodology and submitted to a rigorous confidence assessment. Such an inventory is not only important to quantify centennial-scale glacier area and length change, but will also help to better and more correctly identify the patterns of post-LIA glacier change across Norway. A glacier change assessment that also includes LIA inventory data from Svalbard (Martín-Moreno et al., 2017) could help determine with higher certainty the extent to which glacier recession in northernmost mainland Norway is amplified. Moreover, a complete LIA inventory for Norway (Scandinavia) can be used as a validation data set for numerical glacier models (see Section 2.6) as well as the glacier extent displayed on historical maps (see Section 3.5). Finally, it might also help reveal older moraines outside the LIA limit in an easier and more systematic way, leading to an improved understanding of Holocene glacier (and climate) fluctuations.

References

Andersen, JL & Sollid, JL (1971): Glacial chronology and glacial geomorphology in the marginal zones of the glaciers, Midtdalsbreen and Nigardsbreen, south Norway. *Norsk Geografisk Tidsskrift - Norwegian Journal of Geography* 25, 1–38.

Andreassen, LM, Winsvold, SH, Paul, F & Hausberg, JE (2012a): *Inventory of Norwegian Glaciers*. NVE Rapport 38. Norwegian Water Resources and Energy Directorate (NVE), Oslo, pp. 236.

Andreassen, LM, Kjøllmoen, B, Rasmussen, A, Melvold, K & Nordli, Ø (2012b): Langfjordjøkelen, a rapidly shrinking glacier in northern Norway. *Journal of Glaciology* 58, 581–593.

Andreassen, LM, Elvehøy, H, Kjøllmoen, B & Belart, J (2020): Glacier change in Norway since the 1960s – an overview of mass balance, area, length and surface elevation changes. *Journal of Glaciology* 66, 313–328.

Barr, ID & Lovell, H (2014): A review of topographic controls on moraine distribution. *Geomorphology* 226, 44–64.

Baumann, S, Winkler, S & Andreassen, LM (2009): Mapping glaciers in Jotunheimen, South-Norway, during the "Little Ice Age" maximum. *The Cryosphere* 3, 231–243.

Beedle, MJ, Menounos, B, Luckman, BH & Wheate, R (2009): Annual push moraines as climate proxy. *Geophysical Research Letters* 36, L20501.

Benn, DI & Ballantyne, CK (2005): Palaeoclimatic reconstruction from Loch Lomond Readvance glaciers in the West Drumochter Hills, Scotland. *Journal of Quaternary Science* 20, 577–592.

Boston, CM & Lukas, S (2019): Topographic controls on plateau icefield recession: insights from the Younger Dryas Monadhliath Icefield, Scotland. *Journal of Quaternary Science* 34, 433–451.

Bradwell, T (2004): Annual Moraines and Summer Temperatures at Lambatungnajökull, Iceland. *Arctic, Antarctic, and Alpine Research* 36, 502–508.

Bradwell, T, Sigurđsson, O & Everest, J (2013): Rapid retreat of a temperate glacier, SE Iceland. *Boreas* 42, 959–973.

Chandler, BMP, Evans, DJA & Roberts, DH (2016a): Characteristics of recessional moraines at a temperate glacier in SE Iceland: Insights into patterns, rates and drivers of glacier retreat. *Quaternary Science Reviews* 135, 171–205.

Chandler, BMP, Evans, DJA & Roberts, DH (2016b): Recent retreat at a temperate Icelandic glacier in the context of the last ~80 years of climate change in the North Atlantic region. *Arktos* 2, 24.

Chandler, BMP, Lovell, H, Boston, CM, Lukas, S, Barr, ID, Benediktsson, ÍÖ, Benn, DI, Clark, CD, Darvill, CM, Evans, DJA, Ewertowski, MW, Loibl, D, Margold, M, Otto, J-C, Roberts, DH, Stokes, CR, Storrar, RD & Stroeven, AP (2018): Glacial geomorphological mapping: A review of approaches and frameworks for best practice. *Earth-Science Reviews* 185, 806–846.

Finlayson, A (2006): Glacial geomorphology of the Creag Meagaidh Massif, Western Grampian Highlands: Implications for local glaciation and palaeoclimate during the Loch Lomond Stadial. *Scottish Geographical Journal* 122, 293–307.

Finlayson, A, Golledge, N, Bradwell, T & Fabel, D (2011): Evolution of a Lateglacial mountain icecap in northern Scotland. *Boreas* 40, 536–554.

Hanssen-Bauer, I, Førland, EJ, Haddeland, I, Hisdal, H, Mayer, S, Nesje, A, Nilsen, JEØ, Sandven, S, Sandø, AB, Sorteberg, A & Ådlandsvik, B (eds.) (2015): *Klima i Norge 2100*. NCCS report 2/2015. Miljødirektoratet, Oslo, 203 pp.

Jones, RS, Lowe, JJ, Palmer, AP, Eaves, SR & Golledge, NR (2017): Dynamics and palaeoclimatic significance of a Loch Lomond Stadial glacier: Coire Ardair, Creag Meagaidh, Western Highlands, Scotland. *Proceedings of the Geologists' Association* 128, 54–66.

Kirkbride, MP & Winkler, S (2012): Correlation of Late Quaternary moraines: impact of climate variability, glacier response, and chronological resolution. *Quaternary Science Reviews* 46, 1–29.

Kjøllmoen, B (2019): *Reanalysing a glacier mass balance measurement series—Langfjordjøkelen 2008–2018*. NVE Rapport 2019:48. Norwegian Water Resources and Energy Directorate (NVE), Oslo, pp. 28.

Leigh, JR, Stokes, CR, Evans, DJA, Carr, RJ & Andreassen, LM (2020): Timing of Little Ice Age maxima and subsequent glacier retreat in northern Troms and western Finnmark, northern Norway. *Arctic, Antarctic, and Alpine Research* 52, 281–311.

Lukas, S (2012): Processes of annual moraine formation at a temperate alpine valley glacier: Insights into glacier dynamics and climatic controls. *Boreas* 41, 463–480.

Lukas, S & Bradwell, T (2010): Reconstruction of a Lateglacial (Younger Dryas) mountain ice field in Sutherland, northwestern Scotland, and its palaeoclimatic implications. *Journal of Quaternary Science* 25, 567–580.

Martin-Mikle, CJ & Fagre, DB (2019): Glacier recession since the Little Ice Age: Implications for water storage in a Rocky Mountain landscape. *Arctic, Antarctic, and Alpine Research* 51, 280–289.

Martín-Moreno, R, Allende Álvarez, F & Hagen JO (2017): 'Little Ice Age' glacier extent and subsequent retreat in Svalbard archipelago. *The Holocene* 27, 1379–1390.

McDougall, DA (2001): The geomorphological impact of Loch Lomond (Younger Dryas) Stadial plateau icefields in the central Lake District, northwest England. *Journal of Quaternary Science* 16, 531–543.

McDougall, DA (2013): Glaciation style and the geomorphological record: evidence for Younger Dryas glaciers in the eastern Lake District, northwest England. *Quaternary Science Reviews* 73, 48–58.

Meier, WJ-H, Grießinger, J, Hochreuther, P & Braun, MH (2018): An Updated Multi-Temporal Glacier Inventory for the Patagonian Andes With Changes Between the Little Ice Age and 2016. *Frontiers in Earth Science* 6, 62.

NVE (2019): *Climate indicator products*. Retrieved from the Norwegian Water Resources and Energy Directorate (NVE) website: http://glacier.nve.no/glacier/viewer/ci/en/.

Paul, F & Kääb, A (2005): Perspectives on the production of a glacier inventory from multispectral satellite data in Arctic Canada: Cumberland Peninsula, Baffin Island. *Annals of Glaciology* 42, 59–66.

Serreze, MC, Barrett, AP, Stroeve, JC, Kindig, DN & Holland, MM (2009): The emergence of surface-based Arctic amplification. *The Cryosphere* 3, 11–19.

Stokes, CR, Andreassen, LM, Champion, MR & Corner, GD (2018): Widespread and accelerating glacier retreat on the Lyngen Peninsula, northern Norway, since their 'Little Ice Age' maximum. *Journal of Glaciology* 64, 100–118.

Way, RG, Bell, T & Barrand, NE (2015): Glacier change from the early Little Ice Age to 2005 in the Torngat Mountains, northern Labrador, Canada. *Geomorphology* 246, 558–569.

Weber, P, Boston, CM, Lovell, H & Andreassen, LM (2019): Evolution of the Norwegian plateau icefield Hardangerjøkulen since the 'Little Ice Age'. *The Holocene* 29, 1885–1905.

Weber, P, Lovell, H, Andreassen, LM & Boston, CM (2020): Reconstructing the Little Ice Age extent of Langfjordjøkelen, Arctic mainland Norway, as a baseline for assessing centennial-scale icefield recession. *Polar Research* 39, 4304.

Winsvold, SH, Andreassen, LM & Kienholz, C (2014): Glacier area and length changes in Norway from repeat inventories. *The Cryosphere* 8, 1885–1903.

Wittmeier, HE, Bakke, J, Vasskog, K & Trachseld, M (2015): Reconstructing Holocene glacier activity at Langfjordjøkelen, Arctic Norway, using multi-proxy fingerprinting of distal glacier-fed lake sediments. *Quaternary Science Reviews* 114, 78–99.

Åkesson, H, Nisancioglu, KH, Giesen, RH & Morlighem, M (2017): Simulating the evolution of Hardangerjøkulen ice cap in southern Norway since the mid-Holocene and its sensitivity to climate change. *The Cryosphere* 11, 281–302.

Chapter 6

Conclusions

In the context of the four knowledge gaps and research aims that this doctoral thesis set out to address (see Chapter 1), the following conclusions can be drawn:

(1) *Identification and reconstruction of the maximum Little Ice Age (LIA) extent at Norwegian plateau icefields.* The thesis has mapped the landform record associated with the maximum LIA glacier expansion (the timing of which varies between ~1750 and 1925) and subsequent recession of the three Norwegian plateau icefields (from south to north) Hardangerjøkulen (Chapter 2), Vestre and Østre Svartisen (selected icefield sectors) (Chapter 3) and Langfjordjøkelen (Bártnatvuonjiehkki) (Chapter 4). The landforms identified include ice-marginal moraines, trimlines, glacial drift limits, and erosional/weathering boundaries, of which the two latter also commonly occur in the plateau summit areas. These three icefield examples add to the understanding of the LIA (and post-LIA) landform signature and recession patterns of Norwegian glaciers, which have yet to be studied in a systematic way.

(2) *Glacier recession patterns and style since the LIA.* A novel relative dating technique employed at Hardangerjøkulen (Chapter 2) revealed that moraines were formed in an asynchronous fashion across the icefield's outlet glaciers. The relative moraine age was established through remote sensing by placing a series of digital icefield outlines from known time points since the early 20th century over the ridge sequences inside the LIA limit and assigning the respective age brackets to the ridges that lie between any two successive outlines. Episodes of moraine formation are thought to be associated with the availability of sediments where outlet glaciers retreat across reverse bed slopes with poorly developed surface meltwater drainage and sediment deposition. The asynchrony in moraine formation implies that moraine ridges may be an unreliable indicator of climatically-controlled glacier advances or standstills. Further research attention to how glacier foreland topography modulates moraine production and preservation is desirable.

(3) *Quantifying errors in glacier reconstructions from geomorphological data.* The outermost LIA landforms at all three locations provided the framework for a full reconstruction of the LIA extents of the Hardangerjøkulen and Langfjordjøkelen icefields, and of selected outlet glaciers of Vestre Svartisen. The reconstructed LIA extents were classed into certain (landform-based), fairly certain (reliably interpolated) and less certain (inferred from the terrain

topography alone) segments, allowing the *geomorphological confidence* in the reconstructions to be assessed. Between 37 and 60 % of the perimeter length of the icefield outlines were represented by glacial landforms, and thus certain, whilst 32 to 56 % were fairly certain, and only <10 % less certain. A comparison of the reconstructed Hardangerjøkulen outline with a recent model simulation of the icefield extent in 1750 (LIA) (Chapter 2) showed that the model underestimated the terminus position of several key outlet glaciers by up to 1060 m. The classification system introduced in this thesis provides a more transparent means to assess the robustness of geomorphological glacier reconstructions.

(4) *Quantifying centennial-scale glacier change since the LIA using GIS-based glacier outlines derived from geomorphological evidence, historical maps, vertical aerial photographs, and satellite imagery.* The reconstructed LIA icefield outlines indicated a LIA area of 109.7 ± 9 km^2 at Hardangerjøkulen, 60.2 ± 7 km^2 at Vestre Svartisen's three western outlets Litlbreen, Engabreen and Fonndalsbreen, and 14.9 ± 2 km^2 at Langfjordjøkelen. In addition, the ~1900 extent of the icefields was extracted from historical maps: Hardangerjøkulen covered an area of 94.4 ± 16 km^2 in 1923-29. Vestre and Østre Svartisen were 267 ± 45 km^2 (1896-99) and 200 ± 34 km^2 (1894-1905) in size, respectively. The combined glacier area in Nordland, northern Norway, was 1712 ± 291 km^2 in 1882-1916 (Chapter 3). A historical map of Langfjordjøkelen contained clear mapping errors and could not be used. Chapter 3 gave a detailed description of the steps carried out in order to produce a digital glacier inventory from historical maps and to assess the uncertainties associated with the mapped glacier extent. The procedure presented in the chapter can serve as a blueprint for other researchers interested in employing historical maps in glacier change assessments.

Until present, glacier area decreased to 68.9 km^2 (2010) at Hardangerjøkulen, to 51.7 km^2 (1999) at the three Vestre Svartisen outlets, and to 6.4 km^2 (2018) at Langfjordjøkelen. Ice cover in Nordland had shrunk to 907 km^2 by 1999-2001. Percentage area loss since the LIA has been greatest in the Langfjordjøkelen area in northernmost mainland Norway, with rates of areal shrinkage of 55 to 68 % $90a^{-1}$. By comparison, areal decline has only been moderate at Hardangerjøkulen (13 % $90a^{-1}$), and low at the three Vestre Svartisen outlets (5 % $90a^{-1}$). Based on the available data, the results of this change analysis suggest that the magnitude of post-LIA glacier recession in mainland Norway varies latitudinally, being strongest in the far north, which may be related to a greater-than-average temperature rise in the coastal areas of northern Norway. The presence of a pattern that sees glaciers in northernmost mainland Norway to have receded fastest since the LIA should be confirmed by producing a complete inventory of the LIA extent of Norwegian glaciers and employing this to reassess glacier change in Norway.

Glacial geomorphology and surficial geology of the plateau icefield Hardangerjøkulen, southern Norway

Paul Weber[1], Clare M. Boston[1], Harold Lovell[1], Liss M. Andreassen[2]

[1] Department of Geography, University of Portsmouth, UK
[2] Norwegian Water Resources and Energy Directorate (NVE), Norway

0 0.5 1 2 3 4 5 km

1:20 000

Surficial geology

- Bedrock - Relatively weathered, often vegetated, moss- and/or lichen-covered, with patches of diamictic sediment (till) of varying thickness
- Bedrock - Freshly ice-moulded, predominantly unweathered and unvegetated
- Glacial drift - Stable cover of diamictic sediment (till), often with well-established vegetation, varying thickness
- Glacial drift - Substantial and thick cover of diamictic sediment (till), predominantly fresh-looking and unvegetated
- Glacial drift - Discontinuous and/or thin veneer of diamictic sediment (till) draped over predominantly ice-moulded bedrock, in places only glacial erratics and boulders strewn across bedrock surface, predominantly fresh-looking and unvegetated
- Debris-covered glacier
- Glaciofluvial deposits
- Boulder blanket
- Scree

Glacial geomorphology

- Glacial drift limit, trimline or weathering/erosional boundary
- Ice-marginal moraine
- Controlled moraine
- Esker
- Fluting
- Former meltwater channel
- Raised palaeo-shoreline

Mapping and icefield extent based on digital colour aerial photographs from 20.-22.07.2013 (http://norgeibilder.no/)
Coordinate System: ETRS 1989 UTM Zone 32N; Projection: Transverse Mercator; Datum: ETRS 1989
Contour interval: 50 m
(Shaded relief and contour lines based on the national DEM of Norway with elevation data from 1994/97; Source: Kartverket - Norwegian Mapping Authority)

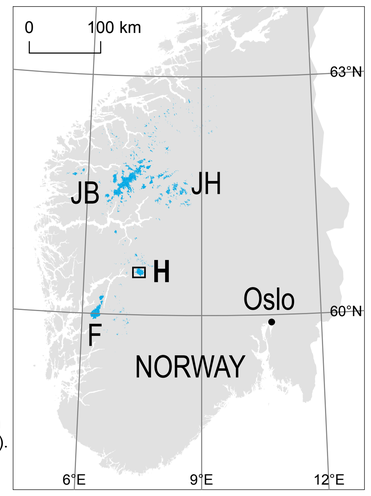

Location of Hardangerjøkulen (H) along with other ice masses in southern Norway (in blue).
F: Folgefonna; JB: Jostedalsbreen;
JH: Jotunheimen glaciers (Source: NVE).

FORM UPR16

Research Ethics Review Checklist

Please include this completed form as an appendix to your thesis (see the Research Degrees Operational Handbook for more information

UNIVERSITY OF PORTSMOUTH

Postgraduate Research Student (PGRS) Information				**Student ID:**	UP795385
PGRS Name:	Paul Weber				
Department:	SEGG	**First Supervisor:**	Dr Harold Lovell		
Start Date: (or progression date for Prof Doc students)		**October 2015**			
Study Mode and Route:	Part-time ☐	MPhil ☐	MD ☐		
	Full-time ☒	PhD ☒	Professional Doctorate ☐		

Title of Thesis:	Ice-marginal processes and retreat dynamics of Norwegian plateau icefields
Thesis Word Count: (excluding ancillary data)	50537

If you are unsure about any of the following, please contact the local representative on your Faculty Ethics Committee for advice. Please note that it is your responsibility to follow the University's Ethics Policy and any relevant University, academic or professional guidelines in the conduct of your study

Although the Ethics Committee may have given your study a favourable opinion, the final responsibility for the ethical conduct of this work lies with the researcher(s).

UKRIO Finished Research Checklist:
(If you would like to know more about the checklist, please see your Faculty or Departmental Ethics Committee rep or see the online version of the full checklist at: http://www.ukrio.org/what-we-do/code-of-practice-for-research/)

a)	Have all of your research and findings been reported accurately, honestly and within a reasonable time frame?	YES ☒ NO ☐
b)	Have all contributions to knowledge been acknowledged?	YES ☒ NO ☐
c)	Have you complied with all agreements relating to intellectual property, publication and authorship?	YES ☒ NO ☐
d)	Has your research data been retained in a secure and accessible form and will it remain so for the required duration?	YES ☒ NO ☐
e)	Does your research comply with all legal, ethical, and contractual requirements?	YES ☒ NO ☐

Candidate Statement:

I have considered the ethical dimensions of the above named research project, and have successfully obtained the necessary ethical approval(s)

Ethical review number(s) from Faculty Ethics Committee (or from NRES/SCREC):	SFEC 2016 - 049

If you have *not* submitted your work for ethical review, and/or you have answered 'No' to one or more of questions a) to e), please explain below why this is so:

Signed *(PGRS)*:		**Date:** 08.10.2020